

Microperoxidase-8

Tuning of its catalysis and reactivity

Promotoren: prof. dr. C. Veeger

Emeritus hoogleraar, Laboratorium voor Biochemie

prof. dr. R. Weiss

Emeritus hoogleraar, Laboratorium voor Cristallochemie en Structurele
Chemie

prof. dr. I.M.C.M. Rietjens

Persoonlijk hoogleraar bij de Leerstoelgroep Biochemie en Toxicologie

Statements

1. The importance of metal (hydro)peroxo species for heme-based oxygen transfer is generally highly underestimated.
This thesis.
2. The involvement of high-valent iron-oxo porphyrin radical cation species in cytochrome P450 chemistry is not based on direct experimental characterisation. Available evidences point to a high-valent iron-oxo protein radical.
Schünemann et al., (2000) FEBS Lett. 179, 149-154, this thesis.
3. In contrast to the statement of Low *et al.*, the pK_a values of manganese porphyrins aquo complexes are not generally lower than the pK_a values of the corresponding iron complexes.
Low et al., (1998) Inorg. Chem. 37, 1841-1843.
4. The interpretation of Baek *et al.* that a saturation curve for the description of the observed rate of breakdown of a chemical complex is evidence for a fast reversible step, is not correct.
Baek et al., (1989) Biochemistry 28, 5714-5719.
5. Fundamental research is a quest for convergence and unity.
6. "En vertu de la qualité et des propriétés biologiques de la Pensée, nous nous trouvons placés en un point singulier, sur un nœud, qui commande la fraction entière du Cosmos actuellement ouvert à notre expérience."
Teilhard de Chardin (1955) Le phénomène humain, Seuil (Ed) p. 21.

7. In contrast to bureaucratic believes, the fact that the future of science lies in multidisciplinary research does not guarantee excellent quality of the scientific outcomes.
8. George Orwell's vision of the world of "Big Brother" which is described in his novel *1984*, was a good prophecy on all aspects but the time.
9. Hope and motivation are going hand in hand. Hope is the tiny fragment of non-rationality which stimulates the motivation required to turn hope into reality.
This thesis.

Statements being part of the thesis entitled

Microperoxidase-8; tuning of its catalysis and reactivity

Jean-Louis Primus

Wageningen University, December 8th 2000

NN08201, 2905

Microperoxidase-8

Tuning of its catalysis and reactivity

Jean-Louis Armand Primus

Proefschrift

ter verkrijging van de graad van doctor
op gezag van de rector magnificus
van Wageningen Universiteit, dr. ir. L. Speelman,
en van Université Louis Pasteur, Strasbourg, dr. J.Y. Merindol,
in het openbaar te verdedigen
op vrijdag 8 december 2000
des namiddags te half twee in de Aula.

inn 982285

**BIBLIOTHEEK
LANDBOUWUNIVERSITEIT
WAGENINGEN**

The research described in this thesis was carried out at the laboratory of Biochemistry, Wageningen University, Wageningen, The Netherlands and at the laboratory of Cristallogenesis and Structural Chemistry, Université Louis Pasteur, Strasbourg, France. This work was supported by the Dutch Organisation for Scientific Research (NWO).

ISBN 90-5808-341-1

*A mon père, à ma mère,
A Soph,*

A tous mes amis.

Table of Contents

1	Introduction	1
2	Reversible formation of high-valent-iron-oxo porphyrin intermediates in heme-based catalysis: Revising the kinetic model for horseradish peroxidase.	29
3	A mechanism for oxygen exchange between ligated oxometalloporphyrinates and bulk water.	47
4	Heme-(hydro)peroxide mediated O- and N-dealkylation; A study with microperoxidase.	57
5	The effect of iron to manganese substitution on microperoxidase-8 catalysed peroxidase and cytochrome P450 type of catalysis.	71
6	Isolation and characterisation of a microperoxidase-8 with a modified histidine axial ligand; Implications for the nature of activated heme-oxo intermediates.	93
7	The nature of the intermediates in the reactions of Fe(III)- and Mn(III)-microperoxidase-8 with H₂O₂; A rapid kinetics study.	111
8	Summary and Discussion	133
	French Summary	143
	Dutch Summary	145
	Abbreviations	147
	References	149
	List of Publications	169
	Acknowledgements	171
	Curriculum Vitae	173

1

General Introduction

1.1 Hemoproteins

The family of heme-containing proteins is a versatile class of macromolecules encountered in all type of living organisms from bacteria to plants and mammals. Hemoproteins all have in common a porphyrin-based prosthetic group chelating an iron atom. Four types of heme groups are commonly found in biological systems, heme-a, heme-b, heme-c and heme-d1 (Figure 1.1). The reactivity of hemoproteins is based on the ability of the metal centre to switch from low oxidation states (Fe^{II} , Fe^{III}) to higher oxidation states (Fe^{III} , Fe^{IV}) and vice-versa, essentially upon binding of exogenous ligands. The combination of the reactivity of the heme group with different types of protein frameworks leads to many different possible biological functions for a quite similar prosthetic group. Hemoproteins transfer electrons (b- and c-cytochromes of the respiratory chain), transport and store oxygen (hemoglobin and myoglobin), reduce oxygen or peroxides to water (cytochrome oxidase and catalase), oxygenate organic substrates (cytochrome P450) or abstract electrons (heme-peroxidases) (Chapman *et al.*, 97).

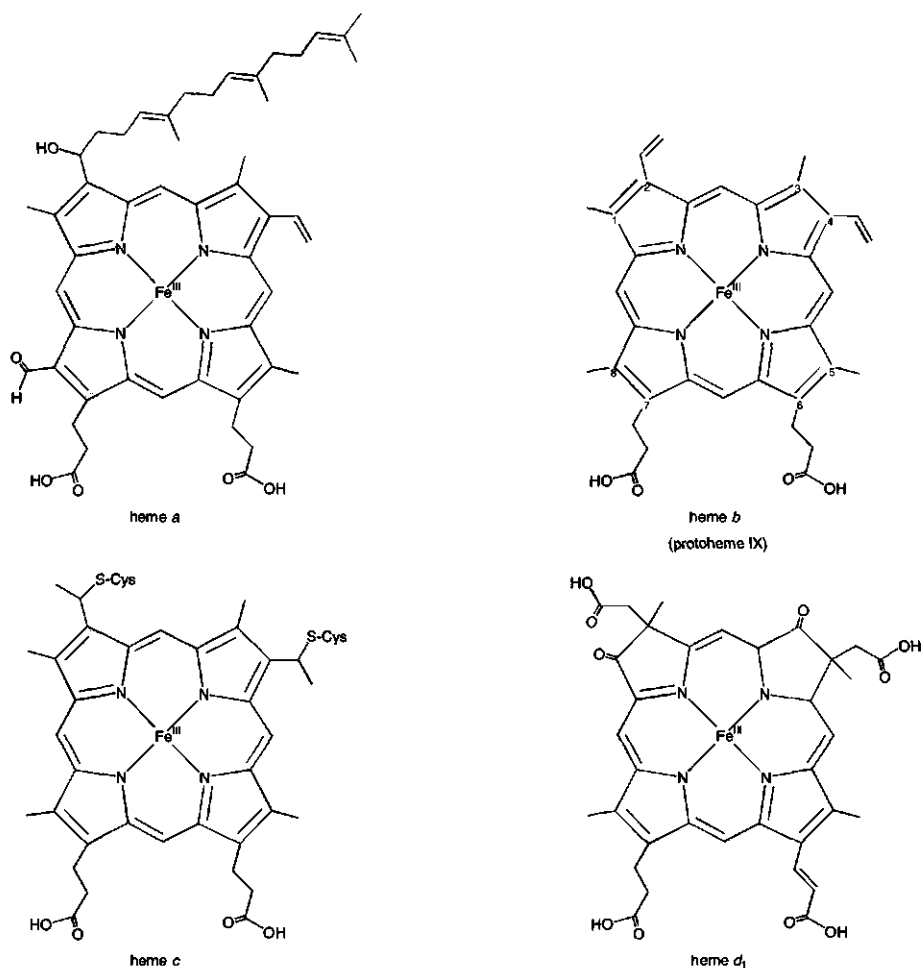


Figure 1.1 Heme groups commonly encountered in biological systems. Protoheme IX is by far the most commonly found heme group in heme-enzymes and is the prosthetic group of heme-peroxidases and cytochromes P450. Figure adapted from Chapman *et al.* (Chapman *et al.*, 97).

Most heme-peroxidases have a b-type of heme prosthetic group. They catalyse the oxidation of organic substrates at the costs of the $2 e^-$ reduction of hydroperoxide to water (Colonna *et al.*, 99). Cytochromes P450 which also contain a protoheme IX are monooxygenases performing an extremely diverse variety of reactions (Mansuy and Battioni, 2000). Monooxygenation of substrates occurs concomitantly with the reduction of molecular oxygen to water, the two electrons required for the overall reaction originating

from a NAD(P)H reductase partner protein. For both enzymes, high-valent oxidation states of the iron (Fe^{IV}), stabilised by the (oxidised) protoporphyrin IX ligand, are proposed to be responsible for the oxidation of organic substrates or for oxygen transfer (Ortiz de Montellano 92; Coon *et al.*, 98). Using the heme prosthetic group, both heme-peroxidases and cytochromes P450 take advantage of oxidation equivalents stored in hydroperoxides or molecular oxygen for converting organic substrates into oxidised or oxygenated products. However, these enzymes differ in their catalytic reactivity which may be related to the structure of their active sites and the type of intermediates formed during their catalytic cycle. This introduction will focus on these aspects: heme-peroxidases (termed peroxidase in the following text of this introduction), will be compared to cytochromes P450 (termed P450s in the following text of this introduction) with special emphasis on their catalytic conversions, the formation and the reactivity of their intermediate species and the structure of their active sites. This will be followed by a general presentation of the biomimetic approach of heme systems, and a modelling strategy suitable for studying the reactivity of peroxidases and P450s will be proposed.

1.2 Heme-based catalysis: the peroxidase mode

Peroxidases are found ubiquitously in living organisms. The superfamily of heme-peroxidases can be divided in three superfamilies: i) an indistinct group containing the particular di-heme cytochrome c peroxidase and, based on its reactivity, chloroperoxidase (CPO), even though the heme-thiolate structure of the active site of CPO resembles more P450 enzymes; ii) the group of mammalian peroxidases including enzymes such as lactoperoxidase, myeloperoxidase and prostaglandin H synthase; and iii) the group of plant peroxidases with peroxidases originating from plants, fungi and bacteria (Smith and Veitch, 98). Peroxidases catalyse the oxidation of organic substrates at the expense of hydroperoxide reduction. The catalytic activity of peroxidases can be grouped into five categories of reactions (Colonna *et al.*, 99): electron transfer, performed by cytochrome c peroxidase (CcP), oxidative dehydrogenations, essentially performed by horseradish peroxidase (HRP), oxidative halogenations, catalysed by CPO, hydrogen peroxide dismutation, performed by catalase but also a side reaction of many peroxidases, and oxygen transfer reactions (Figure 1.2).

In the present description of the peroxidase-catalysed conversions, only electron transfer, oxidative dehydrogenations and oxygen transfer will be considered.

1) Electron transfer by peroxidase is catalysed by CcP and results in the oxidation of Fe^{II} cytochrome c back to Fe^{III} cytochrome c (Yonetani, 76; Huyett *et al.*, 95). Cytochrome c is believed to transfer electrons to CcP from the γ -meso edge side of the heme (Poulos and Kraut, 80b) *via* a unique binding site (Miller, 96).

2) Oxidative dehydrogenations consist of the abstraction of one electron per molecule of substrate which is generally accompanied by the loss of a proton. The oxidation of substrates has been shown to occur at the δ -meso edge of the heme (Ator and Ortiz de Montellano, 87a; Ortiz de Montellano, 87). The oxidised substrates are transformed into a mixture of oligomeric oxidative products *via* polymerisation.

3) Oxygen transfer reactions are by far the most industrially relevant category of conversions which peroxidases can catalyse. In the case where the oxygen directly originates from H₂O₂, they consist of the enantioselective introduction of an oxygen atom in an organic substrate. This is an interesting process for the fine chemical and pharmaceutical industry. In that respect peroxidases resemble monooxygenase enzymes like the P450s. Five types of monooxygenase reactions were shown to be catalysed by peroxidases: heteroatom oxidation (sulphur and nitrogen), epoxidation, benzylic/allylic hydroxylation, alcohol hydroxylation and indole oxidation. With the exception of sulphur oxidation, which has been shown to be catalysed by HRP (Kobayashi *et al.*, 87), all these reactions are catalysed by CPO (Colonna *et al.*, 1999). The fact that in this enzyme the heme iron is coordinated on the proximal site by a thiolate ligand and not by a histidine ligand like for other peroxidases, may account for the high monooxygenase activity of CPO. The enzyme has an open active site allowing substrate binding near the metal centre (Sundaramoorthy *et al.*, 95). In fact CPO can be considered as a heme-thiolate enzyme structurally and catalytically close to P450s but also catalytically close to peroxidases. As will be discussed in § 1.2.2, HRP and CcP have no distal active site pocket allowing for substrate binding near the heme iron and have no tendency to transfer the peroxide oxygen to their substrates.

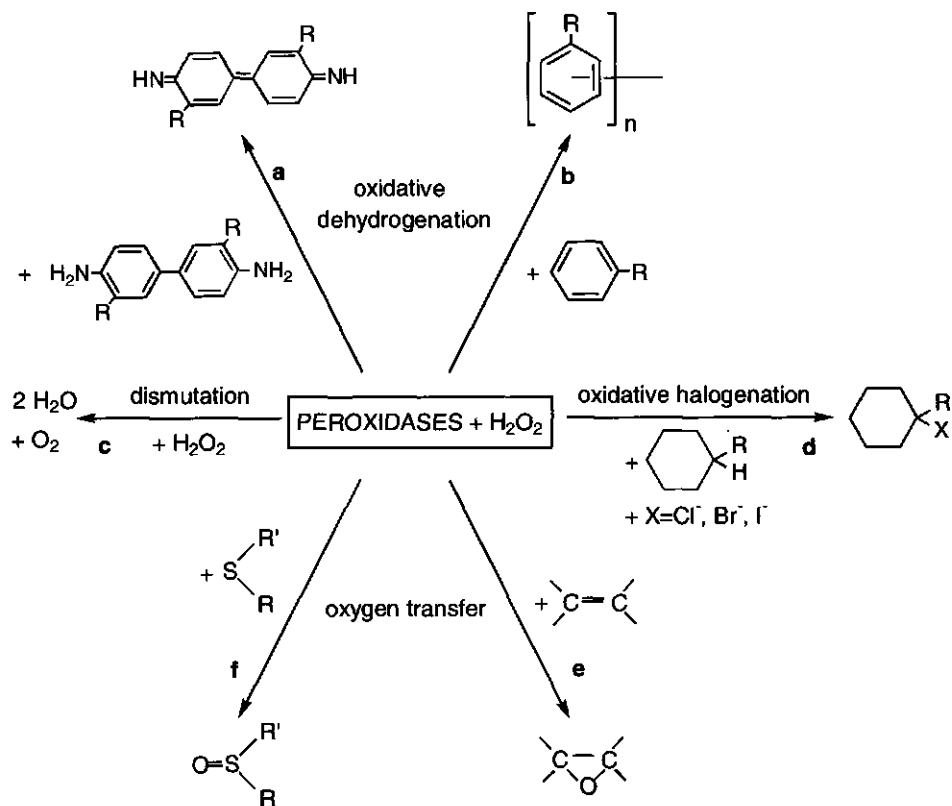


Figure 1.2 Overview of the reactions catalysed by peroxidases with two examples of oxidative dehydrogenation: (a) oxidative dehydrogenation of a benzidine and (b) formation of oligomeric oxidative products; (c) hydrogen peroxide dismutation; (d) oxidative halogenation and two examples of oxygen transfer: (e) epoxidation and (f) sulphur oxidation. Adapted from Colonna *et al.* (Colonna *et al.*, 99).

1.2.1 The catalytic cycle of the peroxidase mode

The reactive intermediates of the peroxidase type of chemistry are well characterised for many peroxidases. They are formed upon reaction of the enzyme with hydroperoxides. Figure 1.3 depicts the reaction cycle for peroxidase type of chemistry based on the reactivity of HRP-C and CcP (Ortiz de Montellano, 92, Poulos, 2000). Species between square brackets have not been yet directly characterised. Peroxidases in their resting state are activated by hydroperoxides leading to the various intermediates competent in catalysis.

(1) PorFe^{III} resting state: In the enzyme resting state, the heme-iron (Fe^{III}) is in a low-spin six-coordinated state. For peroxidases the proximal ligand is a histidine (His170 for HRP-C and His175 for CcP) and the distal coordination site is occupied by a water molecule. Site-directed mutagenesis of the distal histidine into alanine, leucine, glutamic acid or glutamine (Newmyer and Ortiz de Montellano, 96; Savenkova *et al.*, 96; Tanaka *et al.*, 97) or chemical alteration of the distal histidine (Bhattacharyya *et al.*, 92) have shown that the hydroperoxide molecule is probably deprotonated by the distal histidine (His42 in HRP and His52 in CcP). The consequence is that the iron-bound water molecule is exchanged for a deprotonated hydroperoxide molecule. The removed proton being shared between the Nε2 of the distal histidine and the two peroxide oxygens (Gajhede *et al.*, 97).

(2) PorFe^{III}-OOH state: The resulting PorFe^{III}-hydroperoxo intermediate which is formed is termed Compound 0 (Baek and van Wart, 89; Baek and van Wart, 92) and is generally not considered as an active species in peroxidase chemistry since no internal electron transfer between the metal and the porphyrin ligand has been shown to occur so far, in spite of being suggested by Baek and van Wart (Baek and van Wart, 89). In contrast this Compound 0 was proposed to be involved in electrophilic cytochrome P450 conversions (Coon *et al.*, 98) (see § 1.3). Replacement of the Arg38 at the distal site of the heme (Figure 1.3) by a leucine residue in HRP-C shows the accumulation of a transient species which can be regarded as Compound 0 (Rodriguez-Lopez *et al.*, 96) based on quantum theoretically simulated UV/visible spectra (Harris and Loew, 96)

(3) Por⁺⁺Fe^{IV}=O state: Two converging effects lead to the formation of this intermediate. The first one is the creation of a positive charge on the distal oxygen of the hydroperoxo intermediate through proton delivery by the distal histidine (Poulos and Kraut, 80a) and the polarisation of the peroxide bond by a distal arginine (Arg38 for HRP and Arg48 for CcP) resulting in a "pull" effect. The second one is the electron donation from the proximal histidine (His170 for HRP and His175 for CcP) to the peroxide through iron leading to an electron distribution in the antibonding orbitals of the peroxide O-O bond resulting in a pull effect (Yamaguchi *et al.*, 93). This "push-pull" step leads to the cleavage of the O-O peroxide bond. A water molecule is consequently released to generate an intermediate called Compound I being two oxidation equivalent above resting state. One electron is abstracted from the 3d shells of the iron atom leading to an Fe^{IV} oxidation state of the metal

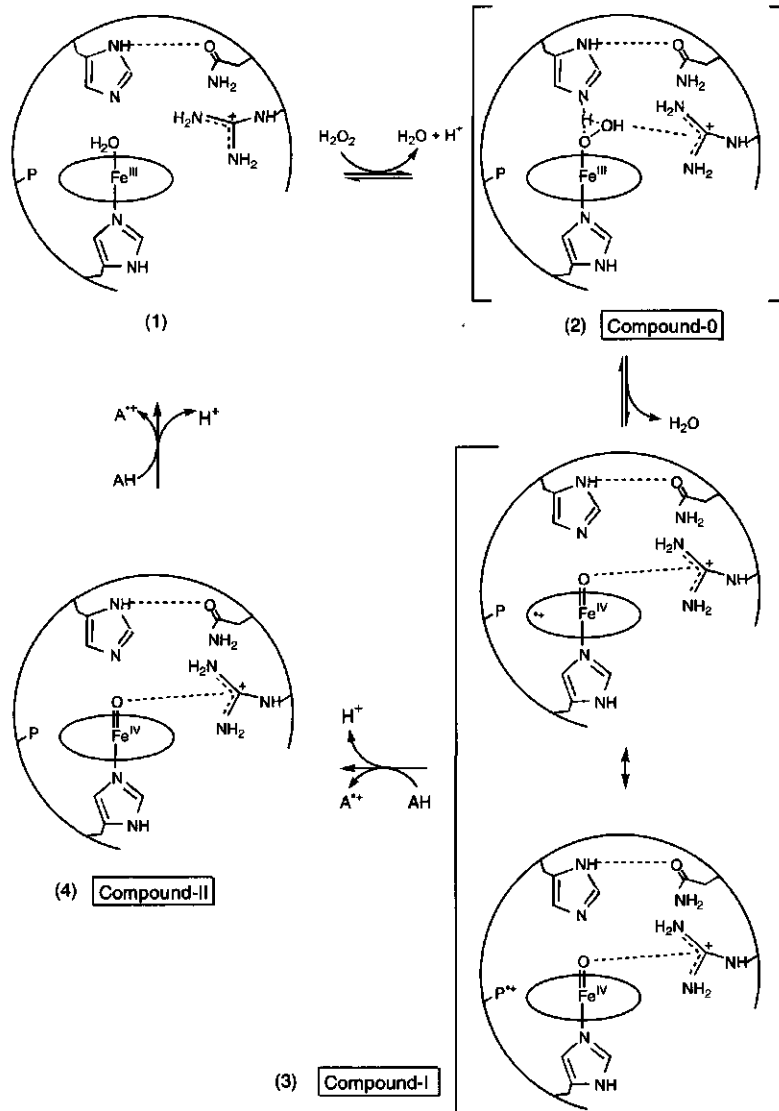


Figure 1.3 Typical reaction cycle for peroxidase-type of chemistry with H_2O_2 as hydroperoxide. The different reactive species are described and discussed in the text and square brackets indicate a non directly characterised species which structure is based on indirect evidence (essentially kinetics and catalytic studies). In the reaction cycle, Compound I, intermediate (3), is described as a porphyrin radical cation (HRP) or a protein radical symbolised by P (CcP). The oval symbolises the porphyrin ring with the four pyrrole nitrogens chelating the iron atom and AH an organic substrate molecule. Adapted from Ortiz de Montellano and from Poulos (Ortiz de Montellano, 92; Poulos, 2000).

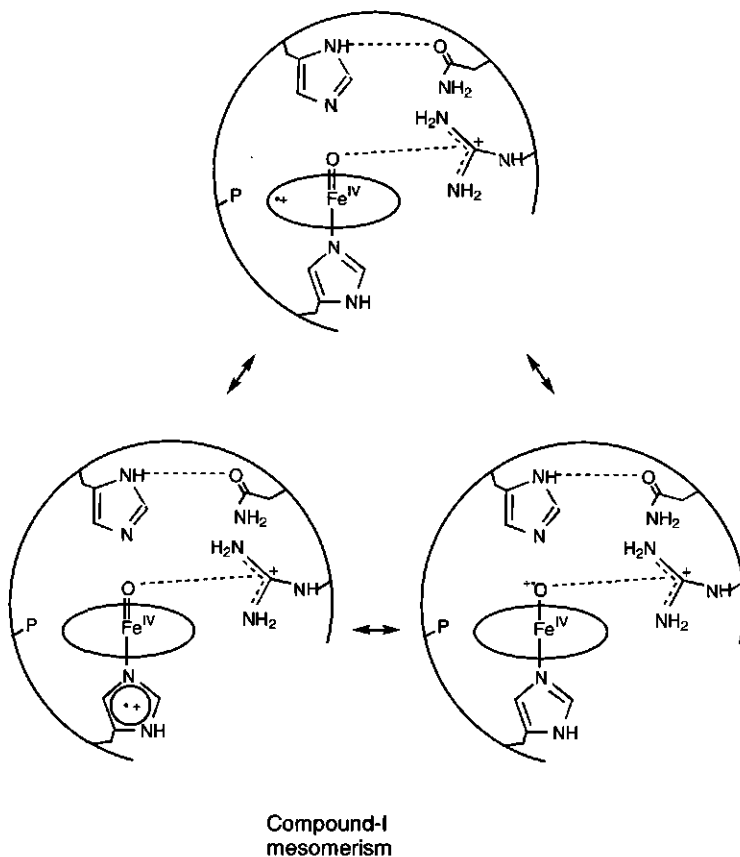


Figure 1.4 Different mesomeric contributions to the structure of Compound I. As already indicated, the oval symbolises the porphyrin ring. Adapted from Weiss *et al.* (Weiss *et al.*, 96).

and the other is generally abstracted from the π orbitals of the porphyrin macrocycle, for HRP, or an amino-acid residue, such as Trp191, for CcP, which is in the neighbourhood of the proximal His175 (Yonetani, 65; Yonetani, 76; Bonagura *et al.*, 96). Structurally the intermediate formed is a porphyrin high-valent iron-oxo radical cation species (Dolphin *et al.*, 71) also termed Compound I (Chance, 52; Rutter *et al.*, 83; Pond *et al.*, 98). The second oxidation equivalent is accepted to be stabilised by a mesomerism between the porphyrin ring, the ligand, and the oxo group (Weiss *et al.*, 96) (Figure 1.4). Compound I has a very high reduction potential, around 1-1.5 V, and hence it is highly reactive in abstracting electrons from substrates. The oxo group of Compound I was shown to be exchanged with oxygen atoms originating from the solvent in peroxidase and P450s models (Groves *et al.*, 81; MacDonald *et al.*, 82; Bernadou *et al.*, 98) but also in HRP (van Haandel *et al.*, 98).

(4) PorFe^{IV}=O state: Compound I is reduced into Compound II by one electron abstracted from a molecule of substrate. Compound II is an oxoferryl species having only one oxidation equivalent left. This intermediate is further reduced by a second molecule of substrate to the PorFe^{III} resting state of the enzyme (Pond *et al.*, 98). Both Compound I and Compound II have a similar reactivity in the way they both abstract electrons but Compound I is about 20-fold more reactive than Compound II (HRP) (Colonna *et al.*, 99). The high-valent iron-oxo group of Compound II has been shown to undergo oxygen exchange of the oxo group with bulk solvent by Raman spectroscopy for HRP (Hashimoto *et al.*, 86a) and CcP (Hashimoto *et al.*, 86b). However the validity of such exchange processes starting from Compound II remains questionable.

1.2.2 Structural determinants of the peroxidase mode reactivity

The formation of the reactive intermediates of the peroxidase chemistry is largely influenced and determined by the structure of the active site of the enzyme. The structure of the C isozyme of HRP has been solved at 2.15 Å resolution using a non-glycosylated recombinant enzyme (Gajhede, 97). A close-up on the active-site shows the key catalytic residues of the distal pocket (Figure 1.5). The distal His42 plays the role of an acid/base acceptor for the incoming hydroperoxide whereas Arg38 stabilises the PorFe^{III}hydroperoxo complex and polarises the peroxide bond before cleavage. A role for Asn70 is proposed in maintaining the good orientation and the good tautomeric form of the distal His42 in order to facilitate the acceptance of a proton from hydrogen peroxide by this residue (Nagano *et al.*, 96). The proximal His170 facilitates the cleavage of the iron-peroxide bond leading to the formation of Compound I by polarising the PorFe^{III}-hydroperoxo intermediate. Even though complexes of HRP with benzhydroxamic acid have been crystallised, HRP can not be considered as having a real distal pocket allowing the binding of organic substrate near the oxo group of Compound I which would facilitate oxygen transfer to the substrate. Only in the case of HRP with an engineered active site can the substrate directly bind near the heme oxo group (Ozaki and Ortiz de Montellano, 95). In the case of the native form of peroxidases, the substrate binds at the δ-heme edge (Ortiz de Montellano, 92).

In CcP the structure of the distal active site is similar to the one of HRP (Finzel *et al.*, 84). The heme iron is coordinated on the proximal site by His175 whereas the distal residues His52 and Arg48 act as bases favouring a heterolytic cleavage of the peroxide

bond. On the proximal site, the residue bearing the second oxidation equivalent of Compound I, Trp191, is localised close to the proximal His175 ligand, and parallel to the imidazole moiety of His175 (Bonagura *et al.*, 96). It has been shown that for CcP, Trp191 plays a central role in transferring electrons to the cytochrome *c* via Gly192, Ala193 and Ala194 (Pelletier, 92; Pappa, 96). Like for HRP, there is no clear distal heme pocket which could allow for organic substrate binding near the heme oxo group of Compound I which would facilitate oxygen transfer to substrates.

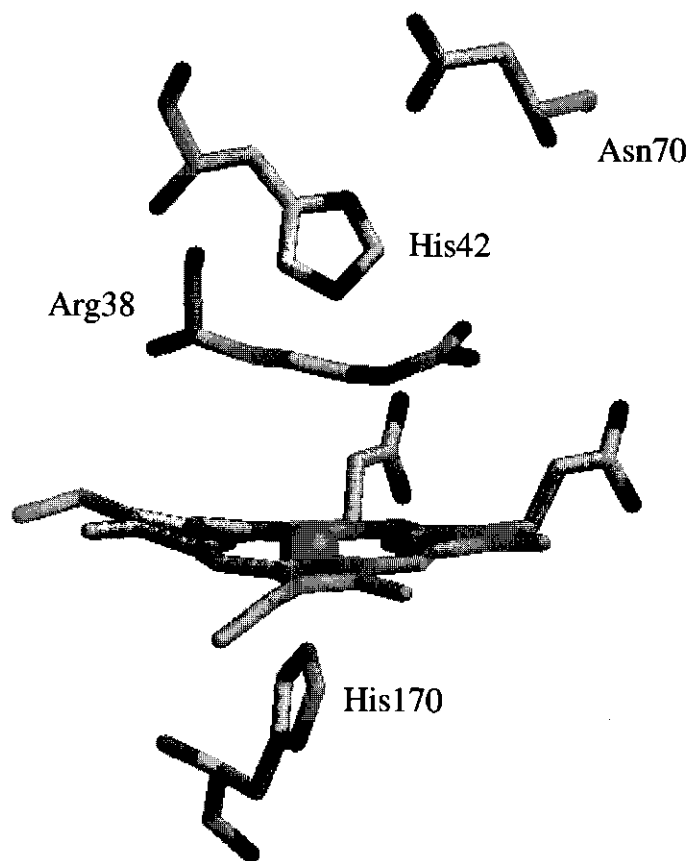


Figure 1.5 Structure of the active site of HRP-C (Gajhede *et al.*, 97) depicting the heme-b group and the residues which are important for the catalysis. The proximal His170 ligand is shown and the residues participating in the acid/base catalysis, leading to the formation of Compound I, namely Arg38, His42 and Asn70 are also shown. Note that the carboxylate group of Asn70 is hydrogen bonded to the N δ 1 of His42 thereby maintaining the tautomeric form of the imidazole ring of His42 favourable for proton acceptance. See text of § 1.2.2 for details.

1.3 Heme-based catalysis: the P450 mode

Members of the P450 family are monooxygenases whose reactivities are also based on the protoheme IX prosthetic group. They are found ubiquitously in living organisms and the production of eukaryotic and bacterial P450s can generally be induced by the presence of the substrate to be converted. Subtle variations of the amino-acid environment around the heme give rise to a huge diversity in the type of reactions catalysed (Chapman *et al.*, 97). The major group of reactions catalysed by P450s are monooxygenations which involve the transfer of an oxygen atom from O₂ to the substrate. Another group of oxidation reactions catalysed by P450s which do not result in oxygen transfer to the substrate are P450 catalysed dehydrogenations, and oxidative carbon-carbon or carbon-oxygen coupling. A last group of conversions supported by P450s are non oxidative reactions such as isomerisations and dehydrations and do not generally necessitate the activation of the P450 enzyme by oxygen. For the present description of the reactivity of P450s only oxygen transfer reactions will be considered. Monooxygenations performed by P450s include a great variety of reactions which can be differentiated in two groups according to the fact that there is a bond cleavage or not in the substrate (Mansuy and Battioni, 2000) (Figure 1.6).

- 1) Oxygen transfer reactions without bond cleavage in the substrate. This type of oxygen transfer reactions typically consists of N-hydroxylation, epoxidation, N- and S-oxidations.
- 2) Oxygen transfer reactions resulting in a bond cleavage in the substrate. This type of oxygen transfer reactions proceeds through the cleavage of a C-H bond in the substrate like for secondary amine N-hydroxylation, alkane hydroxylation and aromatic hydroxylation. However they essentially result in a C-X bond cleavage, where X represents a heteroatom, for oxidative N- and O-dealkylation and nitrile oxidative bond cleavage. This latter reaction is typical of the nitric oxide synthase (NOS) which catalyses the formation of NO from L-arginine. The oxidative deformylation of aldehydes proceeds *via* a C-C bond cleavage.

As specified in § 1.2, CPO can be regarded as a member of the heme-thiolate group of enzymes and is structurally very close to P450s (Sundaramoorthy *et al.*, 95). Besides its peroxidase reactivity CPO catalyses some of the P450s reactions, especially oxygen transfer to substrates such as S-oxidations. As it will be discussed in § 1.2.2, both CPO and P450s share a common heme distal cavity sufficiently wide to allow the binding of substrate near the heme iron center and subsequent oxygen transfer.

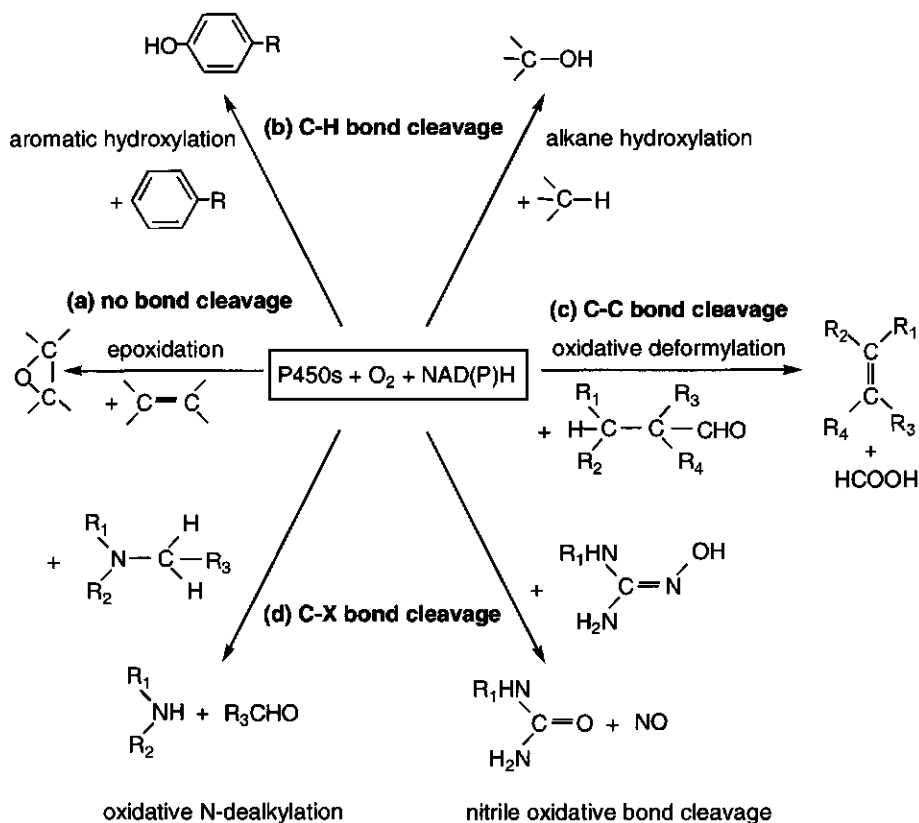


Figure 1.6 Overview of the oxygen transfer reactions catalysed by P450s with examples of reactions resulting in (a) no-bond cleavage (epoxidation); (b) C-H bond cleavage (alkane hydroxylation and aromatic hydroxylation); (c) C-C bond cleavage (oxidative deformylation of aldehydes); (d) C-X bond cleavage (N-dealkylation and nitrile oxidative bond cleavage). Adapted from Mansuy *et al.* (Mansuy *et al.*, 2000).

1.3.1 The catalytic cycle of the P450 mode

In contrast to peroxidases the reactive intermediates of P450s are not all fully characterised yet. They are formed upon reaction of the enzyme with molecular oxygen and two reduction equivalents or upon reaction of the enzyme with a molecule of hydroperoxide. The catalytic cycle of P450s heme-thiolate proteins is depicted in Figure 1.7 (Mansuy *et al.*, 2000; Poulos, 2000). P450s in their resting state are activated by molecular oxygen together with two reducing equivalents after the organic substrate is bound to the active site.

(1) PorFe^{III} state (S = 1/2): In the resting state the heme iron is in a ferric (Fe^{III}) low spin (S = 1/2) state. It is axially coordinated on the 5th position by a cysteine residue in the thiolate form. The 6th coordination position is occupied by a water molecule.

(2) PorFe^{III} state (S = 5/2): Upon substrate binding and displacement of bound water, the heme iron becomes high spin (S = 5/2) and for some P450s the redox potential of the heme is concomitantly increased; about 130 mV for P450_{cam} (Sligar, 76).

(3) PorFe^{II} state: The change in the P450 redox potential allows one electron to be transferred by the partner reductase to the ferric heme iron. Actually the transfer can only occur when the redox potential of the cytochrome P450 is sufficiently high. This means that substrate binding to the active site of P450s is necessary for the heme iron reduction to occur and the catalytical cycle to begin. This condition prevents the waste of reducing equivalents in the cell and plays a regulatory role.

(4) PorFe^{II}-O₂ state: The reduced ferrous iron binds an oxygen molecule forming a complex isoelectronic to a ferric superoxide PorFe^{III}-O₂⁻ (Sligar *et al.*, 74).

The following steps for the formation of the subsequent intermediates of the P450 reaction cycle are still a matter of debate. Their characterisation is rendered difficult by the fact that the transfer of a second electron to the ferrous oxygen complex is rate limiting. Therefore, all intermediates following intermediate (4) in the reaction cycle of Figure 1.7, were indicated between brackets in order to stress their transient nature.

(5) PorFe^{III}-O-O⁻ state: A second electron, originating from the partner reductase is transferred to the oxygen leading to a PorFe^{III}-peroxo intermediate isoelectronic to a ferrous superoxide complex, PorFe^{II}-O₂⁻. This intermediate corresponds to a deprotonated form of Compound 0 and is proposed to be active in electrophilic monooxygenations (Coon *et al.*, 98; Dorovska-Taran *et al.*, 98) which is supported by MO-calculations (Zakharieva *et al.*, 2000).

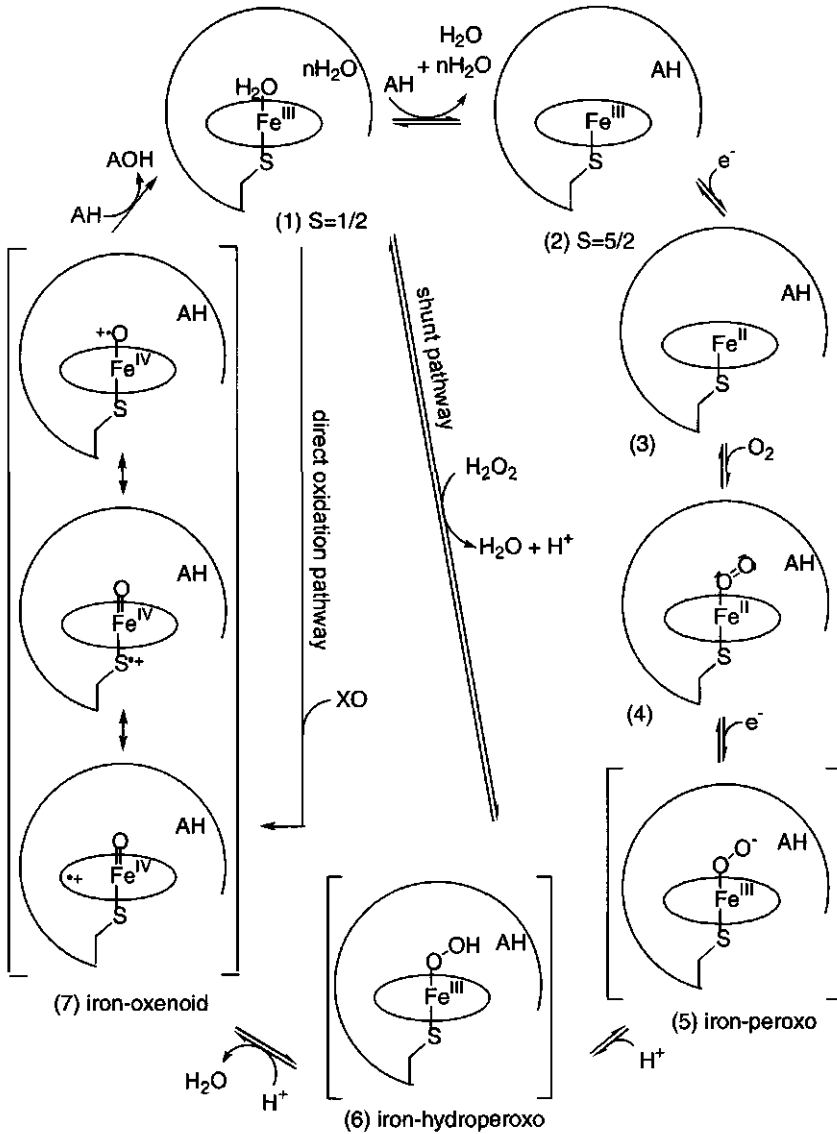


Figure 1.7 Typical reaction cycle for P450-type of chemistry. The different reactive species are described and discussed in the text and square brackets indicate a non-directly characterised species which structure is based on indirect evidence (essentially kinetics and catalytic studies). Activation by hydroperoxides such as H₂O₂ is depicted as the shunt pathway and direct oxidation of the heme iron by other type of oxidants, where XO can be an inorganic high-valent salt (KHSO₃) or a hypochloric acid (HOCl), is also indicated. The oval symbolises the porphyrin ring with the four pyrrole nitrogens chelating the iron atom and AH an organic substrate molecule. Adapted from Mansuy *et al.* and Poulos (Mansuy *et al.*, 2000; Poulos, 2000).

(6) PorFe^{III}-OOH state: The PorFe^{III}-peroxo intermediate group is subsequently protonated leading to the PorFe^{III}hydroperoxo species, Compound 0. This species can also be obtained upon reaction of an hydroperoxide with the resting state enzyme *via* the “peroxide shunt” pathway (Nordblom *et al.*, 76). This is relevant for investigations on P450 biomimics since no reducing equivalents are required to form the reactive oxidative species. Compound 0 is considered as a reactive intermediate for P450 catalysis (Vaz *et al.*, 96; Coon *et al.*, 96; Dorovska-Taran *et al.*, 98). High-level *ab initio* MO-calculations on a model reaction suggests that oxygen transfer to substrates from a Fe^{III}-hydroperoxo intermediate could occur before the formation of the ferryl intermediate (Bach *et al.*, 93). On the other hand, recent MO-calculations indicate that this species is not reactive in catalysis (Zakharieva *et al.*, 2000).

(7) Por⁺Fe^{IV}=O state: A subsequent protonation of the distal oxygen of the PorFe^{III}-hydroperoxo complex increases the positive charge on the distal oxygen making it easily eliminated as a water molecule. This heterolytic cleavage step leads to the formation of what is best described as a transient high-valent iron-oxo species isoelectronic to the Compound I of the peroxidase chemistry. In the P450 chemistry this intermediate is often termed iron-oxenoid (Coon *et al.*, 98). This species has two oxidation equivalents above the enzyme resting state. Like for peroxidases, one oxidation equivalent is localised on the iron center and the other is thought to be delocalised on the porphyrin macrocycle as a radical cation. However a delocalisation of the radical on the sulphur of the thiolate ligand or, more likely, on the oxo group has also been suggested (Champion, 89; Bernadou *et al.*, 94). It is proposed that the oxygen radical configuration of the P450 porphyrin high-valent iron-oxo intermediate is favoured because of the strong π -electron donating effects of the thiolate ligand (Urano *et al.*, 97). In contrast to the peroxidase Compound I, no characterisations of this high-valent intermediate have appeared yet in the literature. Only indirect evidences are provided for cytochrome P450 and some characterisations for resembling enzymes such as chloroperoxidase (Egawa *et al.*, 92).

Oxygen atom transfer to substrate

Two general mechanisms are proposed to explain most of the oxygen transfer reactions: i) oxygen rebound which is the mechanism of alkane hydroxylation and heteroatom dealkylation and ii) sigma addition explaining the hydroxylation of aromatic substrates and the epoxidation of alkenes (Guengerich and MacDonald, 90).

i) The oxygen rebound mechanism is illustrated for alkane hydroxylation. The abstraction of a hydrogen atom from the substrate by the $\text{Por}^+\text{Fe}^{\text{IV}}=\text{O}$ intermediate, or more likely by the corresponding isoelectronic form, $\text{PorFe}^{\text{IV}}-\text{O}^+$, results in the formation of a substrate radical and a $\text{PorFe}^{\text{IV}}-\text{OH}$ intermediate which corresponds to a protonated Compound II (Figure 1.8a). Collapsing of the substrate radical with the hydroxy group of the enzyme intermediate via an "oxygen rebound" step (Groves and McClusky, 78; Groves, 85) leads to the formation of a hydroxylated product which is released from the enzyme active site leaving it in the initial ferric resting state. This two step mechanism has recently been reconsidered and suggested to proceed by a concerted oxygen insertion mechanism (Atkinson *et al.*, 94).

ii) The sigma addition mechanism is illustrated on the basis of an aromatic ring hydroxylation (Figure 1.8b) (Guengerich and MacDonald, 90). The reaction is initiated by σ -addition between, most likely, the $\text{PorFe}^{\text{IV}}=\text{O}^+$ form of the iron-oxenoid intermediate, and the π -system of the substrate to produce a radical σ -adduct. The formation of this σ -adduct can also proceed via σ -addition of a substrate π -cation radical, formed through initial one electron oxidation by the $\text{Por}^+\text{Fe}^{\text{IV}}=\text{O}$ intermediate, to the $\text{PorFe}^{\text{IV}}=\text{O}$ intermediate (peroxidase Compound II). This leads to the formation of a cation σ -adduct. Upon return of the enzyme to the $\text{PorFe}^{\text{III}}-\text{OH}_2$ resting state, an aromatic hydroxylated ring product is released from the active site.

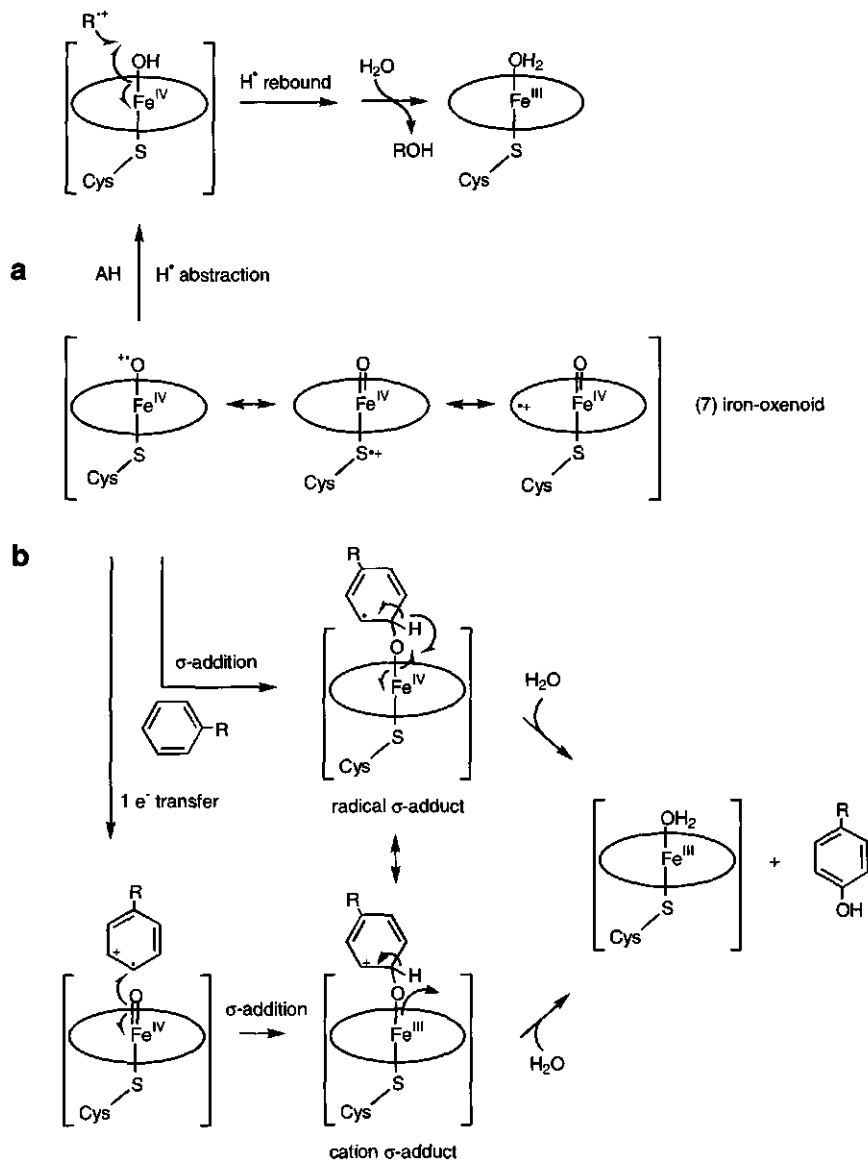


Figure 1.8 (a) Mechanism of oxygen rebound illustrated for alkane hydroxylation and (b) mechanism of sigma addition on π -bonded systems illustrated for aromatic ring hydroxylation. The square brackets stand for a non directly characterised species, the oval symbolises the porphyrin ring and AH an alkane molecule. Adapted from Mansuy *et al.* (Mansuy *et al.*, 2000) and from Guengerich and MacDonald (Guengerich and MacDonald, 90).

1.3.2 Structural determinants of the P450 mode reactivity

Until now, only five structures of P450s were solved owing to the difficulties of crystallising membrane bound proteins. Early site-directed mutagenesis studies have provided information on the structural determinants controlling the catalysis, such as for instance the binding of substrate and heme ligation. Furthermore the different structures can be compared by sequence homology. The structure of the following P450s is known: P450_{cam}, P450_{BM-3}, P450_{terp}, P450_{eryF} and P450_{nor} (Poulos, 2000). In all cases the fact that the 5th ligand is a conserved cysteinate is confirmed, so is the involvement of the residues stabilising the heme group and the heme proximal ligand (Figure 1.9) (Sligar *et al.*, 91; Munro *et al.*, 94). In P450_{cam} the thiolate group of Cys357 is shielded from the external environment by an ensemble of three hydrophobic residues (Phe350, Leu358 and Gln360) which confers a high stability to the iron-thiolate bond. From the structure of P450_{cam} it can be derived that two weak hydrogen bonds between the sulphur atom of Cys357 and respectively the amide NHs of Gly359 and Gln360 play a role in the control of the redox potential of the heme-thiolate system by increasing the electron density on the sulphur atom thereby stabilising the thiolate form of the ligand (Ueyama *et al.*, 96).

In contrast to peroxidases, no clear clue for residues participating in the reaction steps leading to acid catalysis involved in oxygen activation has yet been found. There may be a role for the highly conserved Thr252 in catalysis (Figure 1.9). Thr252 participates in a H-bond network and might be part of a proton conduit transferring solvent protons to the active site for the protonation of the bound oxygen molecule. This step is followed by the subsequent cleavage of the O-O peroxide bond (Gerber and Sligar, 92). Thr252 may also favour the end-on orientation of iron-bound dioxygen which in contrast to the side-on orientation is not resistant to heterolytic cleavage. Site-directed mutagenesis of Thr252 in P450_{cam} leads to the "uncoupling" of the P450 catalysis where the reducing equivalents are transferred to the molecular oxygen generating peroxide rather than being used for the generation of iron-oxenoid. This may be due to additional water molecules in the active site leading to unrestricted protonation (Raag *et al.*, 91). The Asp251Asn mutant of P450_{cam} does show rate reduction without uncoupling (Gerber *et al.*, 92). Moreover this mutant accumulates the iron-peroxo intermediate (compound 5 in Figure 1.7) which can be studied by spectroscopy (Benson *et al.*, 97). More generally the residues of the distal pocket are

quite hydrophobic favouring the binding of apolar organic substrates to the active site. Clearly the fact that P450s do show monooxygenase activity can be related to the large hydrophobic binding cavity they have on the distal heme part allowing substrate binding close to the heme iron. This is not the case with peroxidases, where as mentioned, electrons are abstracted from the substrate through contact with the δ -meso heme edge of the porphyrin ring.

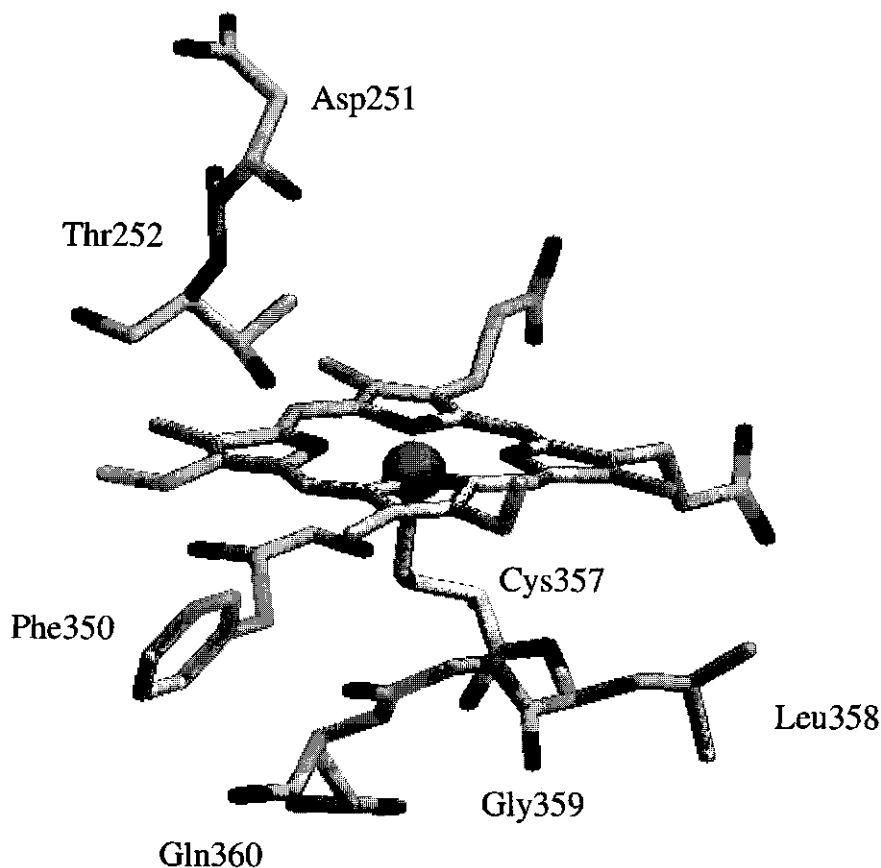


Figure 1.9 Structure of the active site of P450_{cam} (Poulos *et al.*, 85) depicting the heme-b group and the hydrophobic residues surrounding the proximal Cys357 ligand. Note that two hydrogen bonds participate in the control of the redox potential of the heme-thiolate: between the amide NHs of Gly359 and Gln360 and the sulphur of Cys357. Also Thr252 and Asp251 suggested to play a role in the acid/base catalysis leading to the formation of the iron-oxenoid intermediate are indicated. See text of § 1.3.2 for details.

1.4 Influence of the nature of the proximal axial ligand for peroxidase and P450 chemistry

The influence of the proximal cysteinate axial ligand of P450s was compared to the influence of the histidine axial ligand of peroxidases using local density functional quantum mechanical theoretical calculations (Zakharieva *et al.*, 96). It was demonstrated that aromatic hydroxylations promoted by a cysteinate Compound I analogue system are energetically favoured when compared to aromatic hydroxylations promoted by a histidyl Compound I analogue system. Additionally it was shown that oxygen transfer to the substrate for a cysteinate axial ligand system is based on a shift of the electron density from $\pi(\text{Fe-O})$ orbitals to $\pi(\text{Fe-S})$ orbitals whereas for a histidyl axial ligand system the oxygen transfer is explained by the breaking of the iron-oxo bond due to the population increase of $\pi^*(\text{Fe-O})$ orbitals. An electron flow from the Fe-O bond to the Fe-S bond may be considered favourable over an electron transfer *via* an antibonding orbital. Moreover, in the case of the cysteinate ligand, a mixing of the sulphur orbitals with the a_{2u} cationic state of the porphyrin macrocycle is observed along the reaction pathway, whereas it is not observed for the histidine ligand (Zakharieva *et al.*, 96; Rietjens *et al.*, 96). When O-demethylation catalysis of *para*-dimethoxybenzene by heme-systems with either a histidine or a thiolate ligand are compared, it was shown that the porphyrin high-valent iron-oxo intermediate of a thiolate-ligated iron model porphyrin has a stronger hydrogen atom-abstracting ability than that of imidazole-ligated iron model porphyrins (Urano *et al.*, 97). Champion has proposed that the difference of reactivity between P450s and peroxidases might be ascribed to the different nature of the oxidative intermediates which might be based on the stronger π -donor effect of the thiolate ligand (see § 1.3.1).

From another point, the lower reduction potential of P450s with respect to peroxidases (see Table 1.1) can be ascribed to the presence of the negatively charged cysteinate ligand (Raphael and Gray, 91). Assuming that, differences in the reduction potential of $\text{Fe}^{\text{III}}/\text{Fe}^{\text{II}}$ pairs parallel differences in the reduction potential of $\text{Fe}^{\text{IV}}/\text{Fe}^{\text{III}}$ pairs and $\text{Fe}^{\text{IV}}\text{R}^{\text{**}}/\text{Fe}^{\text{IV}}$ pairs (Banci *et al.*, 96), the lower reduction potential of P450s might favour an oxygen transfer *to* substrates catalysed by an iron-oxenoid over an electron abstraction *from* substrates catalysed by peroxidase Compound I. Indeed the higher reduction potential of

peroxidases seems to be more adapted to an electron abstraction reactivity than to an oxygen transfer reactivity, for electrons have to be shared to make the σ -bond (Figure 8.1) instead of being fully abstracted.

Table 1.1 Selected reduction potentials of heme-thiolate systems and heme-peroxidase enzymes. The effect of the cysteinyl ligand on the heme reduction potential is particularly striking for the cytochrome c thiolate double mutant. Adapted from Raphael and Gray (Raphael and Gray, 91) and from Banci *et al.* (Banci *et al.* 96).

Heme Systems	Iron Axial Ligands	$E^{\circ} (\text{Fe}^{\text{III}}/\text{Fe}^{\text{II}})$ (mV)	References
Cyt c	His/Met	262	Taniguchi <i>et al.</i> , 82
Cyt c-His80	His/His	41	Raphael and Gray, 89
LiP	His/H ₂ O	-142	Millis <i>et al.</i> , 89
CcP	His/H ₂ O	-194	Conroy <i>et al.</i> , 78
HRP	His/His	-260	Mauro <i>et al.</i> , 88 Yamada <i>et al.</i> , 75
P450	Cys/H ₂ O	-360 to -170	Huang <i>et al.</i> 86
Cyt c-Cys80	Cys/Cys	-390	Raphael and Gray, 91

1.5 Synthetic model compounds

For both peroxidases and P450s, the formation of the reactive intermediates responsible for the catalytic properties of heme-based enzymes have been extensively studied using biomimetic models. The biomimetic strategy allows for a fine tuning of the environment around the metal centre and a good control of the coordination sphere of the metal. As a consequence, a detailed comprehension of the factors influencing the reactivity of heme-based enzymes can be derived from model work (Meunier, 92). Model compounds have contributed for a great deal in delineating the formation and the reactivity of intermediates based on the high-valent iron-oxo moiety (see § 1.2 and § 1.3). During the "golden age" of peroxidase and P450 model work, in the seventies and the eighties, many studies describing the characterisation of porphyrin high-valent iron-oxo or porphyrin high-valent iron-oxo radical cation species were published (Dolphin *et al.*, 71; Groves *et al.*, 81; Groves and Stern, 88; Dawson, 88; Sono *et al.*, 96; Weiss *et al.*, 2000 and refs therein).

The importance of biomimetic models for heme-based catalysis, will be illustrated by considering the example of the influence of the ring substituents for the reactivity of the porphyrin macrocycle. Electron withdrawing groups such as halogens or cyanide groups have been shown to increase the reduction potential of the metalloporphyrin thereby increasing the resistance of porphyrin high-valent iron-oxo radical cation intermediates toward destructive oxidation (Campestrini and Meunier, 92; Ozette *et al.*, 97) and their reactivity toward substrate oxygenation (Goh and Nam, 99). An increase in the electron withdrawing power of porphyrin substituents can be correlated with a decrease of the rate of exchange of the oxo group of porphyrin high-valent iron-oxo intermediates with bulk solvent. More precisely, a fine study of the influence of the position of the substituents on the porphyrin ring can provide useful information concerning the electronic nature of the high-valent iron-oxo radical cation (Fujii, 93). Furthermore the introduction of bulky substituents on the porphyrin scaffold is a way to control the catalytic reactivity of the model porphyrin and to prevent the formation of μ -oxo dimers by providing steric hindrance (Fleischer *et al.*, 71; Panicucci and Bruice, 90). This resulted in so-called model compounds of the third generation provided with steric hindrance and an increased reduction potential of their high-valent iron-oxo intermediate (Meunier, 92).

The solubility of model porphyrins in water, limited by the hydrophobicity of the porphyrin macrocycle and the apolar ring substituents, is hampering catalytic studies. In fact as described in § 1.2 and § 1.3, protons plays a major role in the acid-base catalysed formation of the high-valent iron-oxo intermediates but also in the coordination properties of the added axial ligands. The pH is an important variable to control model-based catalysis. These requirements have led the chemists to develop water-soluble models which were initially designed by substitution of polar groups such as sulfate anions or pyridinium cations on meso-phenyl substituents (Zipplies *et al.*, 86; Panicucci and Bruice, 90, Yang and Nam, 98). This approach is interesting because it combines the hydrophobic conditions of an heme-enzyme active site, provided by the meso-phenyl substituents, with access to the metalloporphyrin oxidation chemistry in water. More analogous to the native enzyme are peptide-based synthetic porphyrins consisting of constructs between peptides and metalloporphyrins. They form a real artificial family of heme-enzymes (Nastri *et al.*, 97; D'Auria *et al.*, 97; Nastri *et al.*, 98).

1.5.1 Iron microperoxidase-8

The use of water-soluble models derived from redox proteins like cytochrome *c* is an alternative possibility to study hydroperoxide dependent catalysis. This family of heme-peptides, or microperoxidases, are obtained by controlled proteolytic digestion of horse heart cytochrome *c*. They all consist of a heme-*c* connected to a peptide chain. The chain length of these microperoxidases can be adapted by changing the conditions of the digestion (Spee *et al.*, 96). The peptide part of microperoxidase-8, Fe^{III}MP-8, is eight residues long (Figure 1.10). Fe^{III}MP-8 is obtained by two subsequent steps of peptic and tryptic digestion (Tsou, 51a; Tsou, 51b; Aron *et al.*, 86).

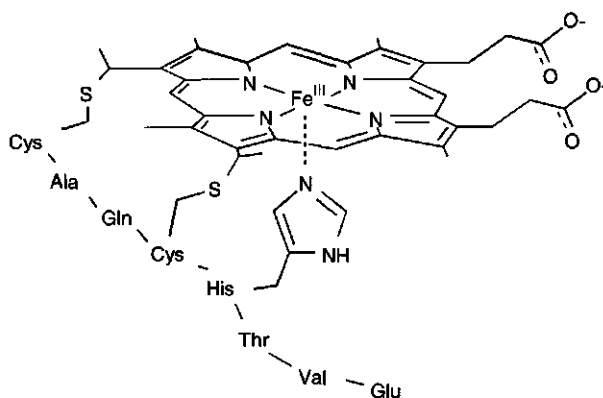


Figure 1.10 Chemical structure of microperoxidase-8, Fe^{III}MP-8, the heme-peptide obtained by controlled proteolytic digestion of horse heart cytochrome *c*.

The fact that Fe^{III}MP-8 retains the proximal axial histidine 18 ligand of cytochrome *c* justifies why this heme-peptide and other chain length derivatives were chosen as models for studying the general properties of hemoproteins. The presence of a proximal ligand makes microperoxidase an attractive model for studying heme-chemistry. Microperoxidases were used for coordination studies (Harbury and Loach, 60b; Harbury *et al.*, 65; Hamza and Pratt, 94), electrochemical studies (Harbury and Loach, 60a; Marques, 90), spectroscopical studies (Owens *et al.*, 88) or the formation of artificial hemoprotein constructs (Santucci *et al.*, 95). The fact that heme-peptides are able to act as peroxidase catalysts, gave them the name "microperoxidase", (Kraehenbuhl *et al.*, 74; Baldwin *et al.*, 85; Baldwin *et al.*, 87; Cunningham *et al.*, 91; Cunningham and Snare, 92; Cunningham *et al.*, 94; Adams, 90) and made them interesting models for studying the chemistry of the native peroxidase enzyme.

In addition, the non sterically hindered distal face of Fe^{III}MP-8 makes it a suitable model for studying P450 type of oxygen transfer reactions (Rusvai *et al.*, 88; Mashino *et al.*, 90; Nakamura *et al.*, 92; Okochi and Mochizuki, 95; Osman *et al.*, 96; Dorovska-Taran *et al.*, 98; Primus *et al.*, 99). Consecutively Fe^{III}MP-8 is considered as a good model for studying the differences and the similarities between peroxidase and P450 chemistry.

1.5.2 Objective of the thesis

The versatile reactivity of Fe^{III}MP-8 in peroxidase- and P450-type of reactions and the fact that this biocatalyst can be activated by a clean and cheap oxidant, H₂O₂, has attracted industrial interest. The Fe^{III}MP-8/H₂O₂ system offers, with virtually more than 300 000 compounds as potential substrates, a very broad substrate specificity due to its open distal heme environment. It also shows good stability toward pH variations (4-13) and temperature changes (up to 100°C). However the stability of this biocatalyst is very low under operational turnover conditions since the half-life is around $t_{1/2} = 10$ s for peroxidase and P450 chemistry (Spee *et al.*, 96). Providing this inactivation problem can be tackled, a role for Fe^{III}MP-8 can be foreseen in high-added value conversions like the transformation of raw chemicals into food additives or pharmaceutical compounds (Veeger *et al.*, 95). Thus the primary objective of the present work was to develop a new type of heme-based catalyst analogues to Fe^{III}MP-8 with an increased operational stability. One approach for solving this instability of microperoxidases under turnover conditions is to better understand their reactivity in peroxidase- and P450-type of conversions. A careful analysis and characterisation of the reactive intermediates involved in peroxidase- and P450-catalysis by direct methods, kinetics and spectroscopy, or indirect methods, product analysis, would provide essential information with respect to the reasons for the rapid inactivation of the catalyst.

At present little is known concerning the different porphyrin iron-hydroperoxo, porphyrin iron-peroxo and high-valent iron-oxo porphyrin radical cation intermediates involved in the Fe^{III}MP-8 supported catalysis. Direct evidence for the involvement of a Compound I analogue intermediate in catalysis by Fe^{III}MP-8 has been provided by low-temperature spectroscopy indicating a radical cation localised on the porphyrin macrocycle (Wang *et al.*, 91). A Compound I type of intermediate is indirectly suggested to

be the core reactive species in many of the catalytic conversions studied (Adams, 90). A Compound II analogue has already been characterised for Fe^{III}MP-8 by UV/visible spectroscopy and Raman (Low *et al.*, 96). An indirect involvement of Compound 0 is postulated for Fe^{III}MP-8 in P450-type of reactions (Dorovska-Taran *et al.*, 98). The existence of a porphyrin iron-hydroperoxo intermediate is supported by its involvement in the oxo/bulk water exchange chemistry (Dorovska-Taran *et al.*, 98) and direct spectroscopic evidence for the formation of Fe^{III}MP-8 Compound 0 at low temperature was also provided (Wang *et al.*, 91). There is a need to further explore the characterisation and the reactivity of the various intermediates involved in the catalysis in order to build up the knowledge necessary for initiating eventual industrial applications. This is the objective of the present work.

1.5.3 Manganese microperoxidase-8: a variant for studying the reactive intermediates of heme-based chemistry

A classical approach in studying the reactivity of enzymes in general, is to synthesise mutants in order to compare the native and the modified system for their corresponding reactivity toward the same substrate. For a model such as Fe^{III}MP-8 which represents a quasi minimal configuration for mimicking a peroxidase open active-site, (recently Fe^{III}MP-5 the minimal configuration of heme-peptide retaining a histidine axial ligand has been prepared; Chuang *et al.*, 99), the possibilities of mutating an amino-acid residue are quite limited. The most dramatic changes would probably be obtained by exchanging the histidine 18 ligand for a cysteine residue in order to mimick a P450 proximal pocket. But the stabilisation of a thiolate ligand in aqueous medium is a difficult task and so far, synthetic model porphyrins mimicking heme-thiolate proteins, are not water-soluble (Ueyama *et al.*, 96; Volz and Holzbecher, 97, Wagenknecht and Woggon, 97). Another approach is to replace the iron atom by a manganese atom in order to obtain a manganese substituted microperoxidase-8: Mn^{III}MP-8. Both metals are neighbours in the first transition series of the periodic table and show therefore a similar chemistry. The differences between iron porphyrin and manganese porphyrin systems essentially reside in a different reduction potential of the porphyrin complexes. It follows that the kinetics of formation of the corresponding porphyrin iron- or manganese-hydroperoxo and high-valent iron- or manganese-oxo complexes will be influenced as well as their rates of reaction with

substrates. This in turn will influence the catalysis and comparison of the catalytic reactivity for both systems will result in important information concerning which type of reactive intermediate is involved in catalysis. In other words, metal substitution provides a unique way of studying peroxidase- and P450-reaction intermediates without dramatic changes in the chemistry, *i.e.* by alteration of the protein active site.

Substituting a manganese atom for an iron in a porphyrin macrocycle can be achieved by a method already available for synthetic models and hemoproteins. For heme-b based hemoproteins, the procedure consists in exchanging a protoheme IX for a manganese porphyrin (Falk, 64). Using this method, manganese containing hemoglobin and myoglobin could be prepared and Yonetani *et al.* have also synthesised manganese substituted CcP and HRP for the purpose of optical and EPR studies (Hoffman *et al.*, 79; Waterman and Yonetani, 70; Yonetani, 70; Hori *et al.*, 87). Also manganese substituted P450_{cam} was prepared by this method (Gelb *et al.*, 82). In the case of heme-c based hemoproteins and models the substitution is a more difficult process due to the covalent linkage between the heme-c and the protein (Erecińska and Vanderkooi, 78). Low *et al.* have prepared the manganese complex of MP-8 by using a methodology designed for cytochrome c demetalation (Low *et al.*, 98). In the present thesis, the manganese variant of Fe^{III}MP-8 was prepared, using a different method than Low *et al.*, as an approach to gain information on the reactive intermediates involved in the Fe^{III}MP-8 and Mn^{III}MP-8 catalysed peroxidase and P450 reactions. In addition studies, on the process of oxygen exchange (Chapter 2 and 3), on substrate conversions (Chapter 4 and 5) on possible catalytic degradation products of Fe^{III}MP-8 (Chapter 6) and on detection of reactive MP-8 intermediates by transient kinetics and EPR (Chapter 7) have been performed to gain better insight in the tuning of the chemistry and the catalysis of Fe^{III}MP-8.

1.6 Detailed outline of the thesis

The first chapter of this thesis describes the catalytic reactivity of peroxidases and P450s and provides a detailed description of the reactive intermediates underlying the reactions catalysed by these enzymes. Peroxidases and P450s were shown to share similar reactive intermediates but peroxidases are mainly catalysing electron abstraction from substrates whereas P450s are mainly catalysing oxygen transfer to substrates. The structure

of the distal heme environment and the nature of the proximal axial ligand were compared for both enzymes. It is discussed that although peroxidases can bind hydroperoxides to the heme iron centre, the protein structures prevent efficient binding of organic substrates near the oxo group of Compound I. In P450s, both molecular oxygen and organic substrates can bind in the distal pocket near the heme iron. Moreover the negatively charged cysteinate ligand of P450s is shown to provide the heme iron with more electron density than the imidazole of the histidine.

Chapters 2 and 3 deal with the study of the oxygen exchange properties of the oxo group of high-valent metal-oxo intermediates of HRP, Fe^{III}MP-8, and water-soluble iron or manganese containing model porphyrins with bulk solvent. A better understanding of the exchange properties of high-valent heme or manganese porphyrin intermediates is of particular relevance for studying peroxidase and P450 chemistry, since ¹⁸O labelling experiments are generally used to discriminate between the peroxidase and the P450 chemistry. In Chapter 2 the kinetics of formation of HRP Compound I are reconsidered based on the results of oxygen exchange experiments. The formation of the heme-enzyme Compound I is shown to be reversible. Chapter 3 is an attempt in rationalising the mechanistic views in the field of metal-oxo/solvent exchange. The reversible formation of Compound I is proposed as a relevant mechanism to explain the exchange of the oxo group of axially ligated high-valent iron porphyrins but also of non ligated high-valent iron and manganese porphyrins with bulk solvent. It is shown that mechanisms proposed so far in the literature cannot account for the presented experimental data.

In Chapter 4 the Fe^{III}MP-8/H₂O₂ supported N- and O-dealkylation of aromatic substrates is studied. Fe^{III}MP-8/H₂O₂ supported dealkylation is shown to proceed *via* two modes. A peroxidase mode, *i.e.* in the absence of ascorbate, where the rate of conversion of the substrates is correlated to their calculated first ionisation potential and a P450 mode, in the presence of ascorbate. The involvement of a PorFe^{III}MP-8-OO(H) intermediate, Compound 0, for the N- and O-dealkylation in the P450 mode is pointed out.

In Chapter 5, the reactivity of Fe^{III}MP-8 and Mn^{III}MP-8 was compared during the conversion of peroxidase (oxidative dehydrogenation and oligomerisation) and P450 (aromatic hydroxylation) model substrates. The rate of conversions in the peroxidase mode,

i.e. in the absence of ascorbate, and the P450 mode, *i.e.* in the presence of ascorbate, were studied as function of the pH. Like in Chapter 4, a role played by the Compound 0 in the P450 mode conversions is proposed.

The high inactivation rate of Fe^{III}MP-8 under operational conditions is one of the major drawback of this biocatalyst for eventual industrial applications. In Chapter 6 the behaviour of Fe^{III}MP-8 was studied in the presence of H₂O₂. The isolation and the characterisation of a modified Fe^{III}MP-8 is described. This modified Fe^{III}MP-8 is proposed to originate from the solvent assisted decay of the Compound I analogue of Fe^{III}MP-8. This high-valent iron-oxo radical cation of iron MP-8 would have the second oxidation equivalent majorly delocalised on the histidine axial ligand.

Chapter 7 presents an analysis of the transient kinetics of the reaction of H₂O₂ with Fe^{III}MP-8 and Mn^{III}MP-8 as function of the pH. Evidence for the participation of metal-bound water in the hydrogen peroxide coordination to the metal is shown. Kinetic evidence for the formation of Fe^{III}MP-8 and Mn^{III}MP-8 Compound 0 is given. The analysis of the UV/visible transient spectra of the reaction with Fe^{III}MP-8 and Mn^{III}MP-8 again suggests the formation of an analogue of Compound I having the second equivalent of oxidation majorly delocalised on the peptide part of the molecule. This is corroborated by the analysis of the EPR transient spectra of the reaction product of Mn^{III}MP-8 with H₂O₂.

Finally, the results of the present thesis are summarised in Chapter 8. The importance of using Fe^{III}MP-8 and Mn^{III}MP-8 as relevant models for peroxidase and P450 reactions is discussed. In particular, the fact that Fe^{III}MP-8 and Mn^{III}MP-8 allow to study the porphyrin iron-hydroperoxo and porphyrin iron-peroxo intermediates, preceding Compound I analogue in the reaction cycle of the heme-enzymes, and active in P450 chemistry is pointed out.

2

Reversible formation of high-valent-iron-oxo porphyrin intermediates in heme-based catalysis: Revisiting the kinetic model for horseradish peroxidase.

Marijon J.H. van Haandel, Jean-Louis Primus, Cees Teunis, Marelle G. Boersma,
Ahmed M. Osmane, Cees Veeger, and Ivonne M.C.M. Rietjens

Inorganica Chimica Acta (1998) **275-276**, 98-105.

Abstract

Many heme-containing biocatalysts, exert their catalytic action through the initial formation of so-called high-valent-iron-oxo porphyrin intermediates. For horseradish peroxidase the initial intermediate formed has been identified as a high-valent-iron-oxo porphyrin π -radical cation, called compound I. A strongly hold concept in the field of peroxidase-type of catalysis is the irreversible character of the reaction leading to formation of this compound I. Results of the present paper, however, point at reversibility of formation of the high-valent-iron-oxo porphyrin intermediate for various heme containing catalysts, including horseradish peroxidase. This results in heme-catalysed exchange of the oxygens of H_2O_2 with those of H_2O . The existence of this heme-catalysed oxygen exchange follows from the observation that upon incubation of ^{18}O labelled $\text{H}_2^{18}\text{O}_2$ with heme-containing biocatalysts significant loss of the ^{18}O label from the $\text{H}_2^{18}\text{O}_2$, accompanied by the formation of unlabelled H_2O_2 , is observed. Thus, for the heme biocatalysts studied, exchange of the oxygen of their high-valent-iron-oxo intermediate with that of water occurs rapidly. This observation implies the need for an update of the kinetic model for horseradish peroxidase. Revaluation and extension of the previous kinetic model showed the necessity to include several additional reaction steps, taking both reversible compound I formation and formation of enzyme-substrate complexes into account.

2.1 Introduction

Heme-containing peroxidases and cytochromes P450 are generally considered to exert their catalytic activity through the intermediate formation of so-called high-valent-iron-oxo porphyrin complexes (Groves *et al.*, 81; Chance, 52; Low *et al.*, 96). However, the exact nature and reactivity of these high-valent-iron-oxo porphyrin intermediates is far from being fully understood. For horseradish peroxidase and chloroperoxidase the nature of the initial high-valent-iron-oxo species formed upon reaction with H_2O_2 has been characterised as an iron(IV)-porphyrin π -cation radical, generally referred to as compound I (Chance, 52; Low *et al.*, 96; Thomas *et al.*, 70; Dolphin *et al.*, 71; Palcic *et al.*, 80). In contrast, the high-valent-iron-oxo intermediate of cytochrome c peroxidase has unpaired electron density on a protein residue instead of on the porphyrin (Hoffman *et al.*, 79), whereas the reactive iron-oxo species of cytochromes P450, up to now, could not be detected.

In spite of this uncertainty about the exact nature of the reactive porphyrin species in heme-based peroxidases and cytochromes P450, many studies have focused on the kinetics and reaction mechanisms of these multi-functional enzymes. In general the reactions catalysed proceed through an initial electrophilic attack by the high-valent-iron-oxo porphyrin intermediate on the substrate eventually leading to either one-electron substrate oxidation and/or to a so-called monooxygenation reaction in which the oxygen of the high-valent-iron-oxo intermediate is transferred to the substrate. Peroxidases are thought to preferentially catalyse one electron substrate oxidations, maybe due to their axial histidine ligand and, especially, the supposed inaccessibility of the oxygen atom in their high-valent-iron-oxo porphyrin form (Ortiz de Montellano *et al.*, 92; Ozaki and Ortiz de Montellano, 95). Cytochromes P450, on the other hand, might prefer oxygen transfer reactions due to the involvement of their cysteinate proximal Fe ligand, stabilising oxygen transfer reaction pathways (Zakharieva *et al.*, 96; Rietjens *et al.*, 96).

A strongly held general concept in the field of peroxidase catalysis refers to the irreversible character of the reactions leading to formation of the reactive high-valent-iron-oxo porphyrin intermediate. Dunford (Dunford, 91) described the kinetic model for horseradish peroxidase as a modified ping-pong mechanism in which no K_m -values would

be obtained due to the irreversible nature of the reactions leading to compound I formation (Figure 2.1a). Recently, however, this model has been corrected at least to some extent, taking into account the reversible formation of an intermediate enzyme-H₂O₂ complex, preceding the formation of the compound I reaction intermediate (Jones and Suggett, 68a; Jones and Suggett, 68b; Rodriguez-Lopez *et al.*, 96a; Rodriguez-Lopez *et al.*, 96b; Adams, 90) (Figure 2.1b). The existence of such a H₂O₂ intermediate is well accepted nowadays, although the intermediate has never been directly observed. Theoretical quantum physical calculations on the exact nature of this intermediate have been performed (Loew and Dupuis, 96; Harris and Loew, 96). Nevertheless in spite of the assumed reversibility of the formation of the (porphyrin-Fe- H₂O₂)³⁺ intermediate, its subsequent conversion into H₂O and the high-valent-iron-oxo compound I intermediate is still generally assumed to be irreversible (Rodriguez-Lopez *et al.*, 96a; Rodriguez-Lopez *et al.*, 96b; Adams, 90) (Figure 2.1b).

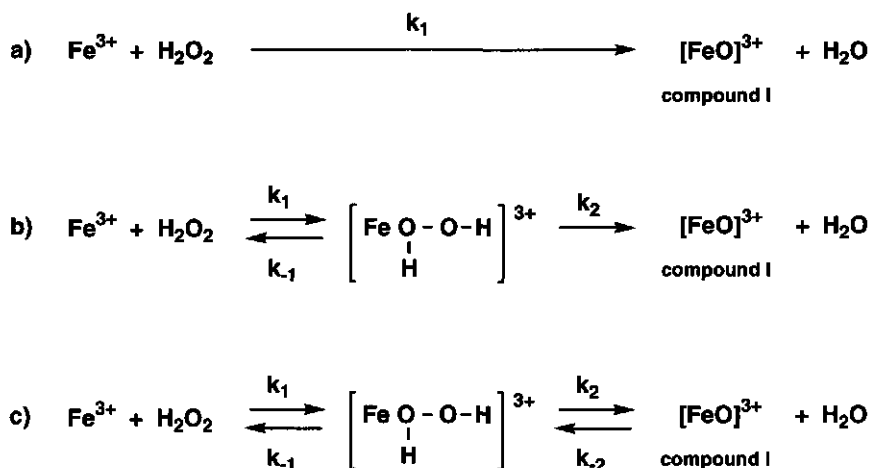


Figure 2.1 Reaction schemes for the compound I formation from the Fe-porphyrin and H₂O₂. (a) Generally both steps (Dunford, 91) or (b) only the second step is taken as essentially irreversible (i.e. k_2 and/or k_{-1} are neglected and are much smaller than k_2 and k_1 respectively) (Rodriguez-Lopez *et al.*, 96a; Rodriguez-Lopez *et al.*, 96b) c) Compound I formation from the Fe-porphyrin and H₂O₂ through reversible formation of an intermediate porphyrin-H₂O₂ adduct and reversible compound I formation, investigated in more detail in the present study. The notation of the H₂O₂ adduct in figure 2.1b and 2.1c is based on quantum chemical calculations (Loew and Dupuis, 96; Harris and Loew, 96).

The present study supports the existence of an enzyme-H₂O₂ intermediate and focuses on the concept of the (ir)reversibility of compound I formation in heme-based catalysis. Results are presented that point at the reversibility of not only the first reaction

step, leading to formation of the enzyme-H₂O₂ complex, but also the reversibility of the second reaction step in which the enzyme-H₂O₂ complex is converted to compound I and H₂O (Figure 2.1c). An evaluation of the consequences of such a reversible compound I formation and formation of enzyme-substrate complexes for the kinetic models for horseradish peroxidase catalysed reactions is presented.

2.2 Materials and methods

Chemicals

Horseradish peroxidase, cytochrome c from horseheart and catalase were obtained from Boehringer (Mannheim, Germany). Hematin (hydroxyprotoporphyrin IX iron(III)) and hemin (chloroporphyrin IX iron(III)) were purchased from Aldrich (Milwaukee, WI). Microperoxidase-8 was prepared by the proteolytic digestion of horseheart cytochrome c essentially as described previously (Kraehenbuhl *et al.*, 74; Aron *et al.*, 86). Heme concentrations were determined by the pyridine-chromogen method (Aron *et al.*, 86). ¹⁸O labelled H₂¹⁸O₂ (91% enriched) was obtained as a 2% solution from ICON, Sunnit (New Jersey, USA). Aniline and 4-aminophenol were obtained from Janssen (Beerse, Belgium). L-Ascorbic acid, Fe(II)sulphate and unlabelled hydrogen peroxide (30%) were from Merck (Darmstadt, Germany). Fe(III)chloride was obtained from Sigma (St Louis, USA).

Oxygen exchange experiments

Exchange experiments generally consisted of two subsequent incubations. First a so-called preincubation was performed. In this preincubation the iron-containing catalyst (150 μM, final concentration) was incubated in 0.1 M potassium phosphate pH 7.6 in the presence of 6.7 mM H₂¹⁸O₂ for 5 minutes at 37 °C. During this preincubation the iron-containing catalyst can react with H₂O₂ resulting in formation of its H₂O₂ adduct and subsequently its high-valent-iron-oxo intermediate and H₂O (Figure 2.1b and 2.1c). In case this reaction is reversible (Figure 2.1c) the reverse reaction will lead to incorporation of the unlabelled O from H₂O into the H₂¹⁸O₂, resulting in a gradual loss of the ¹⁸O label from H₂¹⁸O₂.

The preincubation was followed by a detection assay, carried out to quantify the residual extent of ¹⁸O labelling in the H₂¹⁸O₂. This detection assay was started by adding 6 mM of ascorbic acid, followed by 0.1 M aniline and 150 μM of microperoxidase-8 (final concentrations). Ascorbic acid was added to inhibit any peroxidase-type of chemistry by

microperoxidase-8 and/or the heme catalyst of the preincubation during the detection assay. Since P450-type of oxygen transfer reactions are not inhibited by ascorbic acid (Rietjens *et al.*, 96; Osman *et al.*, 96), microperoxidase-8, in the presence of ascorbic acid, converts aniline to 4-aminophenol with full transfer of the oxygen from $\text{H}_2^{18}\text{O}_2$ to the aminophenol formed (Osman *et al.*, 96). Thus, this incubation will result in formation of 4-aminophenol reflecting the amount of ^{18}O in the $\text{H}_2^{18}\text{O}_2$, providing a possibility to quantify the extent of (residual) ^{18}O in the $\text{H}_2^{18}\text{O}_2$ at the end of the preincubation period. After 2 minutes of incubation catalase was added (32,500 units) to convert all residual H_2O_2 . The reaction mixture was then extracted four times with 1 ml ethyl acetate. The collected ethyl acetate fractions were concentrated by evaporation to about 20 μl and the sample obtained was analysed by MS to detect the percentage of ^{18}O labelling of the 4-aminophenol.

Analysis by mass-spectrometry (MS)

MS analysis was performed with a Finnigan MAT 95 mass spectrometer on flat topped peaks at a resolution of 2000. At this resolution the sample peaks are well separated from hydrocarbon impurities. A correction for ^{13}C -content was made by calculation, as the resolution needed to resolve isobaric ^{18}O - and ^{13}C -peaks should be at least 80000. Sample introduction was via a direct probe. The mass spectrometer was operated in the 70 eV EI-ionisation mode, while scanning from mass 24 to 340 at a speed of 4 sec/deg. Labelling results obtained were corrected for the fact that the $\text{H}_2^{18}\text{O}_2$ was only 91% labelled with ^{18}O .

Chemical detection of 4-aminophenol

For the chemical determination of 4-aminophenol, the reaction was terminated by adding 0.8 ml reaction mixture to 0.24 ml 20% (mass/vol) trichloroacetic acid. After centrifugation for 5 min at 13,000 rpm, the supernatant was used for determination of the concentration of 4-aminophenol following the procedure described by Brodie and Axelrod (Brodies and Axelrod, 48). It is important to notice that the presence of ascorbic acid in the reaction mixtures retarded the normal time of colour development. For this reason, the absorbance at 630 nm was measured after 18-23 h instead of 1 h incubation at room temperature. A calibration curve of 4-aminophenol in the presence of ascorbic acid demonstrated that the absorption coefficient of the indophenol was not affected by the addition of ascorbic acid (the ϵ value at 630 nm is $30.5 \text{ mM}^{-1} \cdot \text{cm}^{-1}$).

2.3 Results and Discussion

Labelling of aminophenol in the control incubation

Figure 2.2 presents the representative part of the MS spectrum of 4-aminophenol formed in a control sample in which the preincubation mixture contained no heme-protein to catalyse the ^{18}O exchange between $\text{H}_2^{18}\text{O}_2$ and H_2O . From the relative intensities of the peaks at $M_z = 111.057$ (^{18}O labelled 4-aminophenol) and at $M_z = 109.053$ (^{16}O containing 4-aminophenol) it can be concluded that, taking into account the necessary correction for the 91% ^{18}O labelling of the $\text{H}_2^{18}\text{O}_2$, all 4-aminophenol formed contains the ^{18}O label derived from the $\text{H}_2^{18}\text{O}_2$. This result is in accordance with previous data (Osman *et al.*, 96). The oxygen transfer from the H_2O_2 via the histidine co-ordinated microperoxidase-8 to aniline creating 4-aminophenol, is indicative for so-called cytochrome P450- instead of peroxidase-type of reaction chemistry. This microperoxidase-8/ H_2O_2 -driven 4-hydroxylation of aniline is especially observed under conditions where the presence of ascorbic acid prevents peroxidase-type of product formation but does not affect the P450-type of conversions also catalysed (Osman *et al.*, 96; Kobayashi *et al.*, 87; Rusvai *et al.*, 88; Nakamura *et al.*, 92; Dorovska-Taran *et al.*, 98).

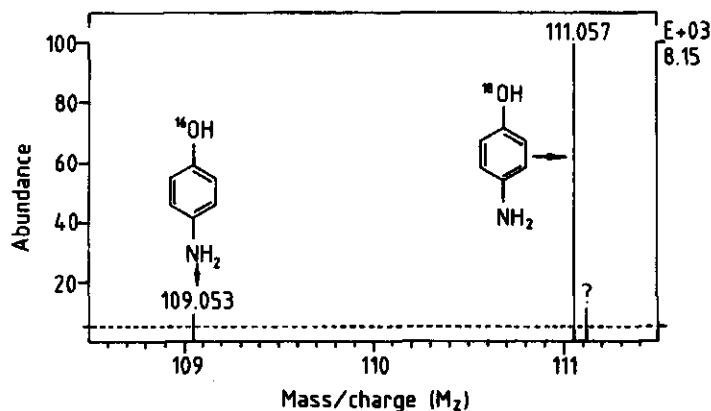


Figure 2.2 The mass spectrum of the molecular region of 4-aminophenol obtained from the extraction of an incubation of aniline with microperoxidase-8 with $\text{H}_2^{18}\text{O}_2$ resulting from 5 minutes preincubation without a heme protein. The unidentified peak is probably a contamination. Only the peaks with an abundance higher than 5% (dotted line) are presented.

Oxygen exchange by different heme-containing proteins

Table 2.1 presents the extent of ^{18}O labelling of 4-aminophenol formed in incubations in which the conversion of aniline by microperoxidase-8/ $\text{H}_2^{18}\text{O}_2$ was preceded by a 5 minutes preincubation of the $\text{H}_2^{18}\text{O}_2$ with either no iron sample, with iron(II)sulphate or iron(III)chloride, with different types of model porphyrins, or with different heme-proteins. The percentages of oxygen exchange present the % of the $\text{H}_2^{16}\text{O}_2$ as compared to $\text{H}_2^{18}\text{O}_2$ in the residual H_2O_2 fraction still available at the end of the preincubation, since this H_2O_2 population is used for the detection of ^{16}O : ^{18}O labelling.

As outlined above, in the control incubation with no heme-protein present during the preincubation, the 4-aminophenol formed in the subsequent detection assay, was fully labelled (Table 2.1, Figure 2.2). This also holds for the samples in which the preincubation was carried out in the presence of either Fe(II)sulphate or Fe(III)chloride (Table 2.1). This result indicates that neither ferro- nor ferric cations are capable of catalysing the loss of ^{18}O label from $\text{H}_2^{18}\text{O}_2$. This result excludes that the phenomena observed with the model porphyrins and heme-proteins are due to traces of iron cations in the samples liberated from the heme cofactor upon its inactivation and also implies that Fenton-type of chemistry is not involved in the oxygen exchange observed.

Table 2.1 Heme-protein catalysed oxygen exchange between $\text{H}_2^{18}\text{O}_2$ and H_2O , represented by the percentage of residual ^{18}O labelling in 4-aminophenol formed from aniline by microperoxidase-8 in the presence of 6 mM ascorbic acid, taken into account the necessary correction for the 91 % ^{18}O labelling of the $\text{H}_2^{18}\text{O}_2$. The percentages of oxygen exchange present the % of $\text{H}_2^{16}\text{O}_2$ as compared to $\text{H}_2^{18}\text{O}_2$ in the residual H_2O_2 fraction still available at the end of the preincubation. The preincubation time was 5 minutes unless indicated otherwise. The mechanism proposed for the exchange is schematically presented in Figure 2.1c.

heme protein present in pre-incubation	% of ^{18}O in 4-aminophenol (n=2 or 3)	% of O exchange (n=2 or 3)
none (control)	100 / 100	0 / 0
iron(II)sulphate	100 / 97	0 / 3
iron(III)chloride	100 / 95	0 / 5
hemin (chloroproporphyrin IX iron(III))	69 / 65	31 / 35
hematin (hydroxyproporphyrin IX iron(III))	80 / 67	20 / 33
microperoxidase-8	30 / 23 / 27	70 / 77 / 73
horseradish peroxidase	0 / 0	100 / 100
horseradish peroxidase (1 min)	18 / 18	82 / 82

The data presented in Table 2.1 also demonstrate that the model porphyrins hemin or hematin (chloro- and hydroxy-protoporphyrin IX iron(III) respectively) catalyse a partial exchange of the ^{18}O label in $\text{H}_2^{18}\text{O}_2$ resulting in 31/35 % and 20/33 % loss of label respectively, detected as the formation of respectively 31/35 % and 20/33 % unlabelled 4-aminophenol. In cases where the preincubation contained one of the heme-proteins tested, namely microperoxidase-8, or horseradish peroxidase, an even larger loss of label is observed. The extent of loss of ^{18}O labelling in the 4-aminophenol formed varies from about 73 % for microperoxidase-8 to full (100 %) loss of the ^{18}O label in the case of horseradish peroxidase. For horseradish peroxidase, a shorter preincubation period, i.e. 1 minute instead of 5 minutes, results in a smaller loss of label (Table 2.1). In addition, Figure 2.3a shows the time dependence of the loss of label from $\text{H}_2^{18}\text{O}_2$ during the preincubation with microperoxidase-8.

The results demonstrate a fast decay in the rate of ^{18}O exchange as catalysed by microperoxidase-8. This observation can be ascribed to three phenomena. First, to the inactivation of the catalyst, in a way comparable to the inactivation observed previously for microperoxidase-8 catalysed peroxidase- and/or aniline-4-hydroxylating activities (Figure 2.3b). Second, after initial exchange of the first of the two ^{18}O atoms of $\text{H}_2^{18}\text{O}_2$ a statistic reduction of the ^{18}O exchange rate can be expected, due to the formation of $\text{H}_2^{18}\text{O}^{16}\text{O}$ which can react in two ways: one leading to exchange and the other not leading to exchange. Third, due to full reversibility of the exchange, the accumulation of $\text{H}_2^{16}\text{O}_2$ and $\text{H}_2^{18}\text{O}^{16}\text{O}$ results in time-dependent formation of competitive inhibitors, a phenomenon also contributing to a decrease of the rate of ^{18}O exchange in time.

Moreover, comparison of Figure 2.3a to Figure 2.3b leads to the conclusion that, although formation of 4-aminophenol by microperoxidase-8 stops after one minute, still a slow microperoxidase-8 catalysed ^{18}O loss from $\text{H}_2^{18}\text{O}_2$ is observed. This phenomenon could be explained by the hypothesis that microperoxidase-8 loses its aniline 4-hydroxylating activity due to a loss of its axial histidin ligand. However, in spite of this loss in possibilities for oxygen transfer, possibilities for a reaction of the compound I derivative with H_2O leading to ^{18}O exchange may not be affected to the same extent upon loss of the axial histidine ligand. This hypothesis is supported by the observations reported here for hemin and hematin. These porphyrin models also lack the axial histidin ligand and show very limited activity for H_2O_2 -driven aniline 4-hydroxylation. In contrast, they appeared to be able to catalyse significant ^{18}O exchange (Table 2.1).

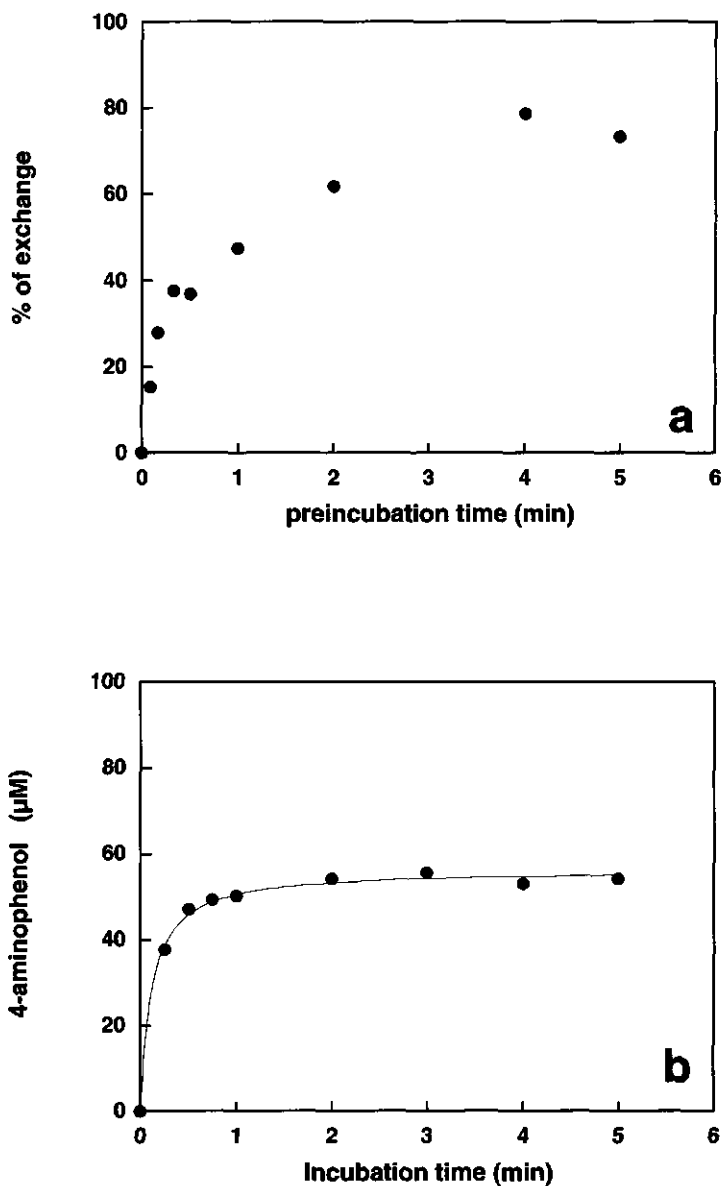


Figure 2.3 (a) Time-dependent microperoxidase-8 catalysed oxygen exchange between $\text{H}_2^{18}\text{O}_2$ and H_2O as derived from the residual amount of ^{18}O labelled 4-aminophenol formed in the detection assay described in materials and methods. (b) Time-dependent conversion of aniline to 4-aminophenol by microperoxidase-8 in the presence of ascorbic acid. Data points in Figure 2.3a were not fitted to a kinetic model since, as explained in the text, the mechanism is complex.

The decline in ^{18}O label incorporation upon preincubation of the $\text{H}_2^{18}\text{O}_2$ with horseradish peroxidase or microperoxidase-8, indicates that, during the preincubation, the $\text{H}_2^{18}\text{O}_2$ loses its ^{18}O label. Since the results obtained under anaerobic conditions were similar (data not shown) it can be concluded that the ^{18}O oxygens in the $\text{H}_2^{18}\text{O}_2$ are exchanged with unlabelled oxygens from H_2O . This could be expected when the reaction between the heme protein and H_2O_2 to form compound I and H_2O , that is, the compound I formation, is reversible (Figure 2.1c). Despite the high driving force of the formation of compound I from the resting enzyme, the reverse reaction is driven by 55.5 M H_2O , which is 10,000 fold in excess of H_2O_2 .

The role of Fenton chemistry in the 4-hydroxylation of aniline during the detection assay

Additional experiments were performed in order to exclude a role for Fenton-type of reaction chemistry in the 4-hydroxylation of aniline during the detection assay. Incubation of aniline with 3 or 300 μM of Fe(II) sulphate or 3 or 300 μM Fe(III) chloride, in the presence or absence of ascorbic acid, did not result in formation of 4-aminophenol. Thus, 4-aminophenol formation in the detection assay does not result from Fenton-type of reactions.

H_2O_2 present at the end of the preincubation period is the oxygen donor in the detection assay

Table 2.2 provides the evidence that H_2O_2 is present at the end of the preincubation periods and needed for the incorporation of oxygen into 4-aminophenol in the detection assay, even in the cases of full loss of ^{18}O -label. This can be concluded from the observation (Table 2.2) that in all cases the addition of catalase at the end of the preincubation period fully inhibits the formation of 4-aminophenol in the subsequent detection assay.

From the data presented in Table 2.2 it also follows that the amount of 4-aminophenol formed varies with the type of heme compound present in the preincubation. This can best be ascribed to varying levels of catalase activity of the heme proteins during the preincubation. Using a Clark electrode, N_2 instead of air saturated buffer and concentrations of all reagents 15 times lower than used in the preincubations, the conversion of H_2O_2 to O_2 could be observed for all heme compounds tested, indicating the possibility for catalase-type of H_2O_2 degradation during the preincubations. Since the

H₂O₂/microperoxidase-8 catalysed 4-hydroxylation of aniline is dependent on the H₂O₂ concentration (Osman *et al.*, 96), a partial reduction of the amount of H₂O₂ in the preincubation, due to catalase activity of the heme catalyst tested, can explain the differences in 4-aminophenol formation in the subsequent detection assay as following from the data depicted in Table 2.2. Catalase activity appears to be present especially in the incubation with horseradish peroxidase. It is low when compared to the peroxidase activity of the enzyme with for example ortho-dianisidine (*i.e.* < 1%), but it becomes relevant since our preincubations are performed with relatively high concentrations (150 μM) of the enzyme. Catalase activity of horseradish peroxidase has also been reported by Nakajima and Yamazaki (Nakajima and Yamazaki, 87) and Arnao *et al.* (Arnao *et al.*, 90).

Table 2.2 Effect of catalase on the formation of 4-aminophenol by microperoxidase-8 driven by the H₂O₂ resulting from preincubation with different heme biocatalysts. Preincubation time was 5 minutes unless indicated otherwise. 100 % = formation of 4-aminophenol in the control (*i.e.* without heme protein) without catalase.

heme protein present in pre-incubation	percentage (%) of 4-aminophenol formed	
	- catalase	+ catalase
none (control)	100	0
Fe(II)sulphate	96	0
Fe(III)chloride	99	0
hemin (chloroproporphyrin IX iron(III))	56	0
hematin (hydroxyproporphyrin IX iron(III))	80	0
microperoxidase-8	40	0
horseradish peroxidase	18	0
horseradish peroxidase (1min)	22	0

Rate of ¹⁸O exchange

In the present study heme-catalysed ¹⁸O exchange of the ¹⁸O in H₂¹⁸O₂ with that of H₂O was observed maybe via compound I as indicated in Figure 2.1c. However, irrespective of the mechanism of ¹⁸O exchange involved, the results of the present study also indicate that the rate of the exchange is fast. Especially when one takes into account that the t_{1/2} of inactivation of microperoxidase-8 under preincubation conditions is 10 seconds (Spee *et al.*, 96). Taking into account an exchange of 28 % of the oxygen atoms of 6.7 mM H₂¹⁸O₂ within the first 10 seconds (Figure 2.3a), catalysed by an amount of microperoxidase-8 decreasing from 150 μM to 75 μM in 10 seconds, a rate of exchange of > 100 min⁻¹ can be calculated from these data. Thus, the rate of the proposed ¹⁸O exchange

between the perferryl intermediate and H_2O is much faster than the rate of reaction of this intermediate with the substrate estimated to be about 23 min^{-1} (Rietjens *et al.*, 96; Osman *et al.*, 96) for 4-hydroxylation of aniline by microperoxidase-8. Data in the literature (Heimbrook and Sligar, 81; MacDonald *et al.*, 82; White and MacCarthy, 84) have reported on the exchange of oxygen between iodobenzene and water through the perferryl intermediate of cytochrome P450. The oxygen from water is incorporated into the substrate. Macdonald *et al.* (MacDonald *et al.*, 82) reported that the rate of oxygen exchange (170 min^{-1}) is much faster than the rate of oxygen incorporation (19 min^{-1}). A result in line with our data. However, Nam and Valentine (Nam and Valentine, 93) concluded from experiments with iodobenzene as oxygen donor that its mechanism of oxygen exchange does not involve metal-oxo intermediates. This, in contrast to the reaction with other oxygen donors for which the high-valent-metal-oxo compound is the suggested intermediate in ^{18}O exchange between (organic) peroxide and water (Nam and Valentine, 93).

However, at this point it also becomes relevant to question the identical nature of the reactive intermediate catalysing either oxygen exchange or aniline-4-hydroxylation. Especially taking into account the above calculated rates for the reaction with H_2O leading to oxygen exchange and that with aniline leading to formation of 4-aminophenol. When in both cases compound I would be involved it is difficult to foresee how 100 % ^{18}O transfer to aniline can ever occur when the reaction with H_2O leading to oxygen exchange and loss of ^{18}O label is much faster. Thus, these results could be explained by the reaction scheme already presented by Nam and Valentine (Nam and Valentine, 93). The scheme suggests that the possible heme species involved in oxygen transfer to substrates and in oxygen exchange are different. A definite hypothesis for the exact mechanism underlying the full labelling of 4-aminophenol in spite of the efficient ^{18}O exchange of the compound I with H_2O can at present not be provided.

Furthermore, it is of interest to point out that the observation of hemin and hematin catalysed oxygen transfer seems to be different from previous data reported by Nam and Valentine (Nam and Valentine, 93). Nam and Valentine reported for several model porphyrin catalysts the lack of ^{18}O -incorporation from H_2^{18}O into the products of olefin epoxidations, alkane hydroxylation and cyclohexene epoxidation. Since the ^{18}O transfer from H_2^{18}O into the monooxygenated products should proceed through exchange phenomena of the compound I-type intermediates, it was concluded that the porphyrin

compound I species did not exchange their oxygen atom with that of H₂O. Clearly this seems in contrast to the results of the present study. However, we would like to point out that such controversy may not exist at all, since our experiments were performed in 55.5 M H₂O instead of in 9 M H₂¹⁸O in 60 % CH₂Cl₂/40 % CH₃OH. This difference in conditions can affect the labelling in three ways. First, due to mass law the chances for a reaction between compound I and H₂O are 6 fold higher under our conditions. Second, the rate constants for exchange in organic solvents and in water may differ considerably. Third, the high concentration of methanol in the experiments of Nam and Valentine provides a well competing alternative for the reactions between water and compound I. The latter suggestion of a reaction between compound I and methanol is in accord with recent results (Osman *et al.*, 97a) indicating a role of the methanol in heme-based catalysis mediated through a reaction of compound I with methanol.

Reconsideration of the kinetic model for horseradish peroxidase

The results of the present study point at possibilities for a reaction between compound I and H₂O leading to oxygen exchange between H₂¹⁸O₂ and the solvent H₂O. This leads to the conclusion that formation of the high-valent-iron-oxo intermediate is a reversible reaction. This reversibility of the reaction leading to compound I and H₂O formation is in contrast to what is generally assumed for peroxidase reaction chemistry and kinetics (Dunford, 91; Jones and Suggett, 68a; Jones and Suggett, 68b; Rodriguez-Lopez *et al.*, 96a; Rodriguez-Lopez *et al.*, 96b; Adams, 90) and requires reconsideration of the kinetic models generally accepted for horseradish peroxidase.

Until now the irreversible character of the reaction leading to formation of compound I was a strongly hold concept in the field of peroxidase catalysis. Based on this concept, Dunford described the kinetic model for horseradish peroxidase as a modified ping-pong mechanism in which no K_m-values would be obtained due to the irreversible nature of the reactions leading to compound I (Figure 2.4a, Equation 1) (Dunford, 91).

$$\frac{2E_0}{v} = \frac{1}{k_1[\text{H}_2\text{O}_2]} + \frac{1}{k_3[\text{AH}_2]} \quad (2.1)$$

From this formula it follows that the rate constants k_1 and k_3 , but not k_2 , can be determined from steady-state kinetics.

Nowadays, the existence of an intermediate enzyme- H_2O_2 complex is well accepted (Jones and Suggett, 68a; Jones and Suggett, 68b; Rodriguez-Lopez *et al.*, 96a; Rodriguez-Lopez *et al.*, 96b; Adams, 90; Loew and Dupuis, 96; Harris and Loew, 96). This complex is thought to be converted irreversibly into the high-valent-iron-oxo species (Figure 2.1b). Figure 2.4b shows a modified form of Dunford's reaction scheme taking into account this intermediate enzyme- H_2O_2 complex. Furthermore, the reversibility of the formation of compound I, pointed out in the present study, is also taken into account. Based on this reaction scheme (Figure 2.4b) equation 2 can be derived using the schematic method of King and Altman (King and Altman, 56).

$$v = \frac{2k_2E_0}{1 + \frac{k_2+k_{-1}}{k_1[\text{H}_2\text{O}_2]} + \frac{k_2k_4+k_2k_3+k_{-2}k_4}{k_3k_4[\text{AH}_2]} + \frac{k_{-1}k_{-2}}{k_1k_3[\text{H}_2\text{O}_2][\text{AH}_2]}} \quad (2.2)$$

According to equation 2 the maximum catalytic activity ($k_{\text{cat}} = 2k_2$) is not dependent on the nature of the substrate. This is not in line with results previously reported (van Haandel *et al.*, 96; Sakurada *et al.*, 90) which do show dependence on the chemical characteristics of the substrate. To obtain a rate equation in which k_{cat} is dependent on the nature of the substrate a new reaction scheme is proposed taking into account the reversible formation and the existence of enzyme- AH_2 intermediates (Figure 2.4c), as Patel *et al.* (Patel *et al.*, 97) explained the saturation observed for oxidation of phenols by horseradish peroxidase compound II assuming such complex formation. In analogy to previous models, the reactions of compound I and compound II with substrate AH_2 are considered to be irreversible. Based on the reaction scheme in Figure 2.4c a new rate equation (Equation 3) can be derived for peroxidase-catalysed reactions using the schematic method of King and Altman (King and Altman, 56).

$$v = \frac{\left(\frac{2k_2k_4k_6}{k_2k_4+k_2k_6+k_4k_6}\right)E_0}{\frac{(k_{-1}+k_2)k_4k_6}{k_1(k_2k_4+k_2k_6+k_4k_6)[\text{H}_2\text{O}_2]} + \frac{(k_{-3}+k_4)k_{-1}k_{-2}k_6}{k_1k_3(k_2k_4+k_2k_6+k_4k_6)[\text{H}_2\text{O}_2][\text{AH}_2]} + \frac{(k_2+k_{-2})(k_{-3}+k_4)k_5k_6+k_2k_3k_4(k_{-5}+k_6)}{k_3k_5(k_2k_4+k_2k_6+k_4k_6)[\text{AH}_2]} + 1} \quad (2.3)$$

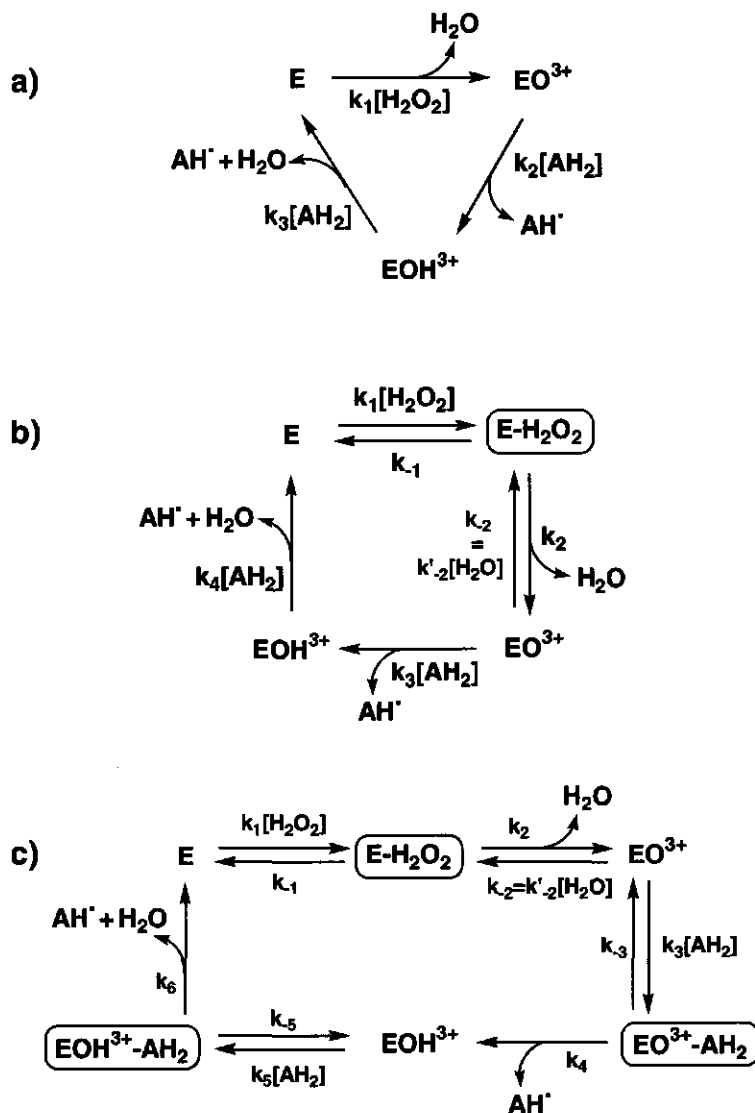


Figure 2.4 Three reaction schemes for peroxidase-type of conversion. (a) A reaction scheme for peroxidase-type of conversion as described by Dunford (Dunford, 91). (b) A modification of Dunford's model taking into account an intermediate enzyme-H₂O₂ complex (Jones and Suggett, 68a; Jones and Suggett, 68b; Rodriguez-Lopez *et al.*, 96a; Rodriguez-Lopez *et al.*, 96b; Adams, 90; Loew and Dupuis, 96; Harris et Loew, 96) and the reversibility of compound I formation as proposed in the present study. (c) The modified ping-pong-pang reaction mechanism for peroxidase-type of conversion as proposed in the present study taking into account the intermediate enzyme-H₂O₂ complex (Jones and Suggett, 68a; Jones and Suggett, 68b; Rodriguez-Lopez *et al.*, 96a; Rodriguez-Lopez *et al.*, 96b; Adams, 90; Loew and Dupuis, 96; Harris and Loew, 96) and the reversibility of compound I formation, as well as the existence of enzyme-AH₂ intermediates. E is the resting enzyme, E-H₂O₂ the enzyme-H₂O₂ intermediate, EO³⁺ compound I and EOH³⁺ the protonated compound II of horseradish peroxidase. EO³⁺-AH₂ and EOH³⁺-AH₂ are the enzyme-substrate intermediates.

Assuming that binding of the substrate AH_2 to the enzyme is irreversible (i.e. $k_3 = k_5 = 0$), that $k_2 \gg k_4$, and that $k_4 \sim 10 \cdot k_6$ (Chance, 52; Dunford, 91), equation 3 can be simplified to equation 4.

$$v = \frac{2k_6E_0}{1 + \frac{(k_{-1}+k_2)k_6}{k_1k_2[H_2O_2]} + \frac{(k_2+k_{-2})k_5k_6+k_2k_3k_6}{k_2k_3k_5[AH_2]} + \frac{k_{-1}k_{-2}k_6}{k_1k_2k_3[H_2O_2][AH_2]}} \quad (2.4)$$

From equation 4 it can be concluded that the maximum catalytic activity (k_{cat}) = $2k_6$. k_6 is the rate constant for the reaction of the $EOH^{3+}-AH_2$ complex to give product and native enzyme (E), i.e. the step for substrate oxidation by the so-called compound II. The fact that k_6 determines the maximum rate of conversion is in line with the previously reported observation that substrate oxidation by compound II is the rate limiting step in horseradish peroxidase catalysis (Chance, 52; Van Haandel *et al.*, 96; Sakurada *et al.*, 90; Georges, 53; Job and Dunford, 76; Yamazaki *et al.*, 81; Dunford and Adeniran, 86). The equation supports our previous conclusion (van Haandel *et al.*, 96) that the chemical characteristics (nucleophilicity) of the substrate determines its rate of oxidation. Furthermore, equation 4 indicates that plots of $1/v$ versus $1/[AH_2]$ at various $[H_2O_2]$ or plots of $1/v$ versus $1/[H_2O_2]$ at various $[AH_2]$ will not give parallel lines due the $[H_2O_2] \cdot [AH_2]$ term. The occurrence of this cross-term in the rate equation originates from the reversibility of the first half reaction, i.e. the contribution of $k_{-2} = k'_{-2}[H_2O_2]$. Since the reaction is performed in 55.5 M H_2O this backward reaction step can under no circumstances be ignored.

Altogether, we conclude that the reaction mechanism of horseradish peroxidase should not be described by the mechanisms previously proposed (Dunford, 91; Rodriguez-Lopez *et al.*, 96a; Rodriguez-Lopez *et al.*, 96b). Based on results of the present study the mechanism as depicted in Figure 2.4c provides an improved alternative. This reaction sequence involves three subsequent cycles of substrate binding followed by product release. This implies that it extends the so-called ping-pong or double displacement mechanism by one additional substrate binding-product release cycle. Therefore, we now suggest to name this revised mechanism for horseradish peroxidase a triple displacement, or, more tempting, a ping-pong-pang mechanism.

3.4 Conclusion

In the present study the (ir)reversibility of compound I formation in heme-based catalysis was investigated. Results are provided that support the existence of an enzyme- H_2O_2 intermediate. In addition, it could be concluded that the reaction between peroxidase-type heme catalysts and H_2O_2 , leading to formation of compound I and H_2O , is reversible. The results point at the reversibility of not only the first reaction step leading to formation of the enzyme- H_2O_2 complex but also of the consecutive reaction step in which the complex is converted to compound I and H_2O . Such oxygen exchange with H_2O by the high-valent-iron-oxo porphyrin complex of peroxidase-type heme catalysts seems to be in line with the results published previously by Macdonald *et al.* (MacDonald *et al.*, 82) for the, as yet unidentified, reactive high-valent-iron-oxo species of cytochromes P450. However, it has to be pointed out that the experiments of Macdonald *et al.* (MacDonald *et al.*, 82) were performed in the presence of iodosylbenzene.

Upon these findings and results reported previously (van Haandel *et al.*, 96; Sakurada *et al.*, 90) the kinetic model generally accepted for horseradish peroxidase had to be reconsidered. Thus, a possible reversible reaction of compound I formation could best be described using the modified ping-pong-pang type of mechanism described above in which binding of the substrate to compounds I and II is essential.

Acknowledgements

The authors gratefully acknowledge support from the EU BIOTECH programme (grant no. BIO2-CT942052), the TMR NMR large scale NMR facility (grant no. ERBCHGE-CT940061), the EU Copernicus programme (grant no. ERBIC15-CT961004), and from the SON/STW (project no. 349-3710) as well as IOP (grant no. IKA94045).

3

A mechanism for oxygen exchange between ligated oxometalloporphyrins and bulk water.

Jean-Louis Primus, Kees Teunis, Dominique Mandon, Cees Veeger and
Ivonne M.C.M. Rietjens

Biochemical and Biophysical Research Communications (2000) **272**, 551-556.

Abstract

Oxygen exchange between high-valent metal-oxo complexes and bulk water has been monitored for non-ligated model porphyrins (FeTDCPPS, MnTMPyP¹, hemin) and the axially ligated microperoxidase-8 (MP-8). Exchange extents up to 90 % were measured for MP-8 in spite of the presence of an axial histidine ligand, and accompanied by the formation of non-labelled H₂O₂ from H₂¹⁸O₂. These results point at the existence of a mechanism for oxygen exchange between the high-valent iron-oxo complex and the solvent different from the so-called "oxo-hydroxo tautomerism". Regeneration of the primary oxidant, H₂O₂, and oxygen exchange by axially ligated porphyrins can be explained by a mechanism involving the reversibility of Compound I formation.

¹ Abbreviations used: MnTMPyP, (*meso*-tetrakis-(4-*N*-methylpyridiniumyl)-porphyrinato)-manganese(III) and FeTDCPPS, (*meso*-tetrakis-(2, 6-dichloro-3-sulfonatophenyl)-porphyrinato)iron(III) both water soluble metalloporphyrins with two free axial ligand sites, for their synthesis see Bernadou *et al.*, 1994. Fe(F₂₀TPP)Cl, (*meso*-tetrakis-(pentafluorophenyl)-porphyrinato)iron(III); MnTMP, (*meso*-tetrakis-(mesityl)-porphyrinato)manganese(III) and MnTPP (*meso*-tetrakis-(phenyl)-porphyrinato)manganese(III) all three hydrophobic metallo-porphyrins with two free axial ligand sites.

3.1 Introduction

In the field of model porphyrins and/or hemoproteins the question of a mechanism for the oxygen exchange between bulk solvent, H₂O, and high-valent metal-oxo complexes has been raised frequently (Groves and Kruper, 79; Groves *et al.*, 80; Groves *et al.*, 81; Heimbrook and Sligar, 81; MacDonald *et al.*, 82; White and MacCarthy, 84; Nam and Valentine, 93; Bernadou *et al.*, 94; Pitié *et al.*, 95; Lee and Nam, 97; Groves *et al.*, 97; Bernadou and Meunier, 98; Goh and Nam, 99). A mechanism like “oxo-hydroxo tautomerism” can explain a 50 % oxygen exchange observed during MnTMPyP catalysed epoxidation of carbamazepine. Protonation/deprotonation equilibria of the two oxygen atoms ligated to the metal in a water coordinated high-valent metal-oxo complex leads to 50 % exchange between the oxygen atom of the high-valent metal-oxo porphyrin and that of its axially coordinated labelled water ligand (Figure 3.1a) (Bernadou *et al.*, 94; Pitié *et al.*, 95; Bernadou and Meunier, 98). Recently this model was extended, including possibilities for replacement of the coordinated water molecule by a solvent water molecule resulting in increased chances for the insertion of an oxygen atom originating from the solvent into the substrate and explaining oxygen exchange levels higher than 50 % (Figure 3.1a) (Lee and Nam, 97). However this so-called “oxo-hydroxo tautomerism” mechanism implies that when the axial position opposite to the oxo group is occupied by a non-water ligand, no oxygen exchange between the solvent water molecules and the oxygen atom of the high-valent metal-oxo species can occur (Meunier *et al.*, 84; Groves and Stern, 87; Groves and Stern, 88; Robert and Meunier, 88). In line with this, Lee *et al.* (Lee and Nam, 97) reported that no oxygen exchange was observed in the Fe(F₂₀TPP)Cl driven conversion of cyclooctene in the presence of an excess axial ligand such as 5-chloro-1-methylimidazole. Other studies reported that the addition of axial ligands such as pyridine (Groves and Stern, 87; Groves and Stern, 88), or substituted pyridines (Meunier *et al.*, 84; Robert and Meunier, 88) to a MnTMP/MnTPP driven catalytic system, prevented oxygen exchange during the conversion of various epoxides. These observations seem to corroborate that the occupancy of at least one axial ligand position of the metal centre in a porphyrin system prevents the oxygen exchange, which is in line with an “oxo-hydroxo tautomerism” type of mechanism. The present study reports oxygen exchange experiments with water soluble model porphyrins and microperoxidase-8 (MP-8), the latter being a model heme catalyst containing a histidine axially ligated to the iron centre (Aron *et al.*, 86). Oxygen exchange

between the solvent H_2O and the oxygen donor used for the generation of the high-valent iron-oxo intermediate, *i.e.* H_2O_2 , was observed to levels as high as 90 % for MP-8 in spite of the presence of the axial ligand. This result points at the existence of an alternative mechanism for oxygen exchange between the high-valent iron-oxo complex and the solvent.

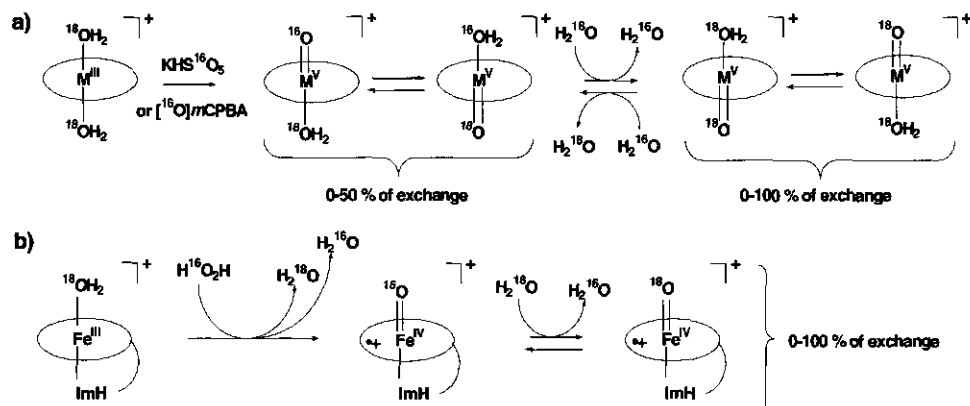


Figure 3.1: Mechanisms for metalloporphyrin catalysed oxygen exchange: (a) the mechanism called “oxo-hydroxo tautomerism” (Bernadou *et al.*, 94) and its modified version (Lee and Nam, 97) leading to respectively maximal 50 % and maximal 100 % of exchange, (b) direct oxygen exchange between Compound I and H_2^{18}O , leading to variable percentages of oxygen exchange. ImH stands for the imidazole moiety of the coordinated histidine from MP-8.

3.2 Materials and methods

Chemicals

Cytochrome c from horse heart and catalase were obtained from Boehringer (Mannheim, Germany). Hemin, chloroporphyrin IX iron(III), was purchased from Aldrich (Milwaukee, Wisconsin, USA). 90 % ^{18}O labelled $\text{H}_2^{18}\text{O}_2$ was obtained as a 2 % solution from ICON, (Sunlit, New Jersey, USA). Aniline and 4-aminophenol were obtained from Janssen (Beerse, Belgium). L-Ascorbic acid, Fe(II)sulphate and unlabelled hydrogen peroxide (30 %) were from Merck (Darmstadt, Germany). The concentration of unlabelled hydrogen peroxide solutions was always checked spectrophotometrically using $\epsilon_{240} = 39.4 \pm 0.2 \text{ M}^{-1}\cdot\text{cm}^{-1}$ (Nelson and Kiesow, 72). Fe(III)chloride was obtained from Sigma (St Louis, Missouri, USA).

Model porphyrins synthesis

MnTMPyP was synthesised according to previously published procedures (Longo *et al.*, 69; Bernadou *et al.*, 89). FeTDCPPS was prepared according to a published procedure (Campestrini and Meunier, 92) and purified following an adapted published procedure (Zippies *et al.*, 86). MP-8 was prepared by proteolytic digestion of horse heart cytochrome c essentially as described previously (Aron *et al.*, 86).

Oxygen exchange experiments

Exchange experiments consisted of two subsequent incubations (van Haandel *et al.*, 98). A pre-incubation step of variable time intervals was performed in the presence of (final concentrations) 150 mM of catalyst, 0.1 M potassium phosphate pH 7.6, 5.3 mM H₂¹⁸O₂ and 10 mM of DMSO as indicated. The pre-incubation step was followed by a detection step for which (final concentrations) 6 mM ascorbic acid, 0.1 M aniline (introduced as a 3 M stock solution in DMSO) and 150 mM MP-8 were added in the incubation mixture in the order indicated. Ascorbic acid was added to inhibit any peroxidase-type of chemistry by MP-8 and/or the catalyst of the pre-incubation during the detection assay. Since cytochrome P450 type of oxygen transfer to aniline is not inhibited by ascorbic acid, MP-8, in the presence of ascorbic acid, converts aniline to 4-aminophenol with *full* transfer of the oxygen from H₂O₂ to the 4-aminophenol formed (Rietjens *et al.*, 96; Osman *et al.*, 96; van Haandel *et al.*, 98; Primus *et al.*, 99). After 2 min of incubation, the reaction was stopped by adding 32,500 units of catalase. Both steps were carried out at 37 °C. The final volume of the incubations was 4 mL.

Analysis by mass spectrometry (MS)

The reaction mixture was extracted four times with 1 mL ethyl acetate and the collected fractions were concentrated by evaporation to about 20-100 ml. MS analysis was performed with a Finnigan MAT 95 instrument. Sample was introduced via a direct probe and the machine was operated in the 70 eV EI-ionisation mode. The percentage of ¹⁸O in 4-aminophenol was calculated from the relative intensities between the peaks at $m/z = 111.057$ and at $m/z = 109.053$ and corrected for the fact that the H₂¹⁸O₂ was only 90 % labelled with ¹⁸O.

Chemical detection of 4-aminophenol

Chemical determination of 4-aminophenol was performed following a published procedure (van Haandel *et al.*, 98).

3.3 Results and Discussion

In order to specifically monitor oxygen exchange, catalysed by MP-8 and model porphyrins, an alternative experimental approach was used. Experiments were performed in two independent steps and oxygen exchange and oxygen transfer were no longer measured simultaneously. This eliminated the problem that the extent of exchange is dependent upon the relative rates of the competing reactions of the high-valent metal-oxo complex with H_2O (leading to oxygen *exchange*) or with substrate (leading to oxygen *transfer*) (Nam and Valentine, 93; Lee and Nam, 97; Goh and Nam, 99). First an incubation was performed during which the MP-8 or model porphyrin catalysed exchange between the oxygens from $\text{H}_2^{18}\text{O}_2$ and that of unlabelled H_2O from the solvent can occur. Then, independently, the residual extent of ^{18}O label in the $\text{H}_2^{18/16}\text{O}_2$ remaining at the end of the exchange incubation was detected by using the $\text{H}_2^{18/16}\text{O}_2$ for conversion of aniline to 4-aminophenol (Rietjens *et al.*, 96; Osman *et al.*, 96; van Haandel *et al.*, 98; Primus *et al.*, 99). The extent of labelling of the 4-aminophenol, reflecting the extent of labelling of the H_2O_2 at the end of the exchange incubation (Osman *et al.*, 96; van Haandel *et al.*, 98), was determined by MS analysis after extraction of the 4-aminophenol with ethyl acetate.

Figure 3.2a presents the time-dependent MP-8 catalysed oxygen exchange between $\text{H}_2^{18}\text{O}_2$ and H_2O whereas Figure 3.2b presents the time-dependent hemin and MnTMPyP catalysed oxygen exchange. From both figures it is clear that the amount of ^{16}O incorporated in 4-aminophenol *increases* with the incubation time of the exchange step, ultimately resulting in a *loss* of more than 50 % of ^{18}O label from the $\text{H}_2^{18}\text{O}_2$ primary oxidant. To further evaluate the possible mechanism underlying this oxygen exchange phenomenon, additional control experiments were performed.

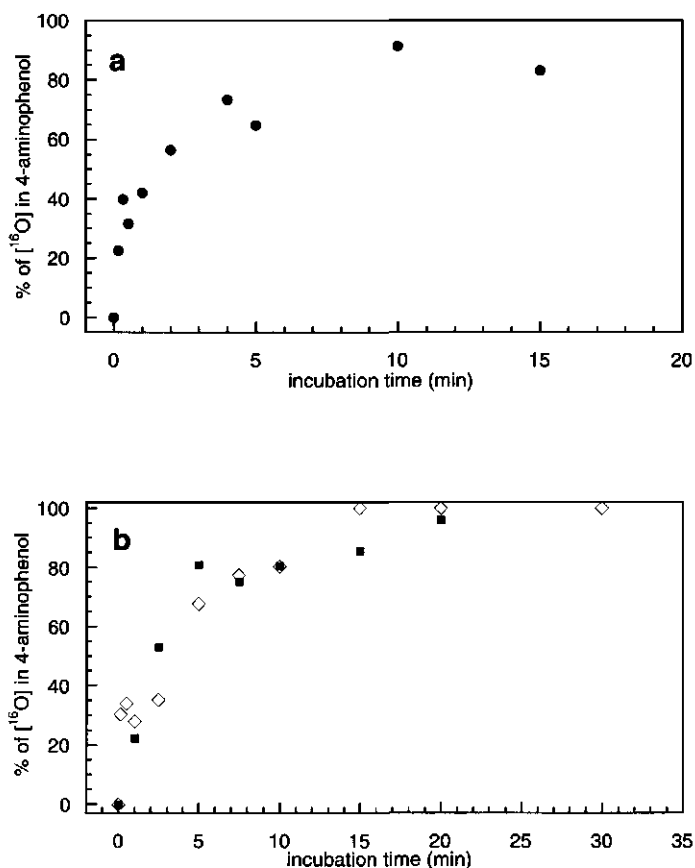


Figure 3.2: Time-dependent (a) MP-8 (●) and (b) hemin (◇) and MnTMPyP (■) catalysed oxygen exchange between $\text{H}_2^{18}\text{O}_2$ and H_2O as derived from the residual amount of ^{18}O labelled 4-aminophenol formed in the detection assay. Data were corrected for the 90 % ^{18}O labelling of $\text{H}_2^{18}\text{O}_2$.

Anaerobic incubations did show the same levels of oxygen exchange, as aerobic incubations which excludes a role played by O_2 in this exchange mechanism (data not shown). Incubations in which the pre-incubation was carried out in the presence of either iron(II) sulfate or iron(III) chloride indicate that neither ferrous nor ferric cations are capable of catalysing the loss of ^{18}O label from $\text{H}_2^{18}\text{O}_2$, ruling out the involvement of Fenton-type of chemistry (Table 3.1) (van Haandel *et al.*, 98).

Table 3.1 Effect of catalase on the MP-8/H₂O₂ driven conversion of 4-aminophenol and percentage of oxygen exchange, derived from the percentage of ¹⁸O labelling of residual 4-aminophenol, for the different catalysts.

Catalyst ^a	4-aminophenol formed (%)		¹⁸ O in 4-aminophenol (%)	O-exchange (%)
	- catalase	+ catalase		
None (control)	100	0	100	0
Fe(II) sulfate	96.2	0	98.5	1.5
Fe(III) chloride	96.5	0	97.5	2.5
Hemin	27.6	0	19.7	80.3
FeTDCPPS	22.2	0	11.7	88.3
MnTMPyP	90.0	0	19.5	80.5
MP-8	25.7	0	8.7	91.3

Note. ^a: type of catalyst present in the pre-incubation step. The percentages of oxygen exchange were corrected for the 90 % ¹⁸O labelling of H₂¹⁸O₂ and catalase was added at the end of a 10 min pre-incubation step. 100 % of 4-aminophenol formed corresponds to a control experiment where no catalyst was present in the pre-incubation step and no catalase was added before the detection step. Differences in the amounts of 4-aminophenol formed may be related to different levels of catalase activity of the catalysts involved.

A possible participation of hydroxyl radicals in the exchange process was also investigated. DMSO was chosen as a hydroxyl radicals trap since it is believed to be very efficient, its rate of reaction with hydroxyl radicals being almost diffusion limited (bimolecular rate constant = $7 \times 10^9 \text{ M}^{-1} \cdot \text{s}^{-1}$) (Cederbaum *et al.*, 78; Cederbaum and Coheng, 84; Czapski, 84). Experiments performed, in the presence or absence of 10 mM DMSO in the pre-incubation step, showed no significant difference in the extent of oxygen exchange (Table 3.2). Furthermore the detection step was performed in the presence of additional 0.34 M of DMSO since aniline was introduced as a 3 M solution in DMSO (see Experimental). These arguments and results corroborate the conclusion that hydroxyl radicals have no significant participation in the oxygen exchange process described in this study.

Table 3.2 Influence of the hydroxyl radical scavenger DMSO on the MP-8 catalysed oxygen exchange process.

	O-exchange (%)
No DMSO in the pre-incubation step (n = 3)	58.4 ± 5.2
+ 10 mM DMSO in the pre-incubation step (n = 3)	58.4 ± 4.6

Note. The percentage of oxygen exchange was measured in the presence or in the absence of DMSO in the pre-incubation step. Data were corrected for the 90 % ^{18}O labelling of $\text{H}_2^{18}\text{O}_2$ and represent the mean value of 3 independent measurements. In this experiment the pre-incubation time was 1 min (not 10 min as used in Table 3.1).

Altogether the results obtained indicate that the incorporation of ^{16}O from H_2O into $\text{H}_2^{18}\text{O}_2$ is catalysed by MP-8. Clearly this MP-8 catalysed oxygen exchange between $\text{H}_2^{18}\text{O}_2$ and H_2O cannot be explained by a mechanism like "oxo-hydroxo tautomerism" because the axial ligand present in MP-8 prevents such a mechanism. Obviously, for MP-8 having one of its axial ligand position blocked by a histidine, oxygen exchange should proceed directly at the other axial site. This could be either via a direct oxygen exchange between the oxo moiety of the high-valent iron-oxo complex and H_2O (Figure 3.1b) or via a process regenerating the primary oxidant, H_2O_2 , and involving the reversibility of Compound I formation (Figure 3.3) (van Haandel *et al.*, 98). Evidence for the latter mechanism can be found in the fact that non labelled H_2O_2 is present at the end of the pre-incubation period. The observation that the addition of 32,500 units of catalase to the incubation mixture at the end of the oxygen exchange incubation eliminates *all conversion* of aniline into 4-aminophenol during the subsequent detection assay (Table 3.1), corroborates that unlabelled H_2O_2 is the oxygen donor required for generation of the unlabelled 4-aminophenol in the detection assay. Clearly a mechanism of direct oxygen exchange between the high-valent iron-oxo intermediate and H_2O (Figure 3.1b) cannot account for the loss of ^{18}O label from the $\text{H}_2^{18}\text{O}_2$, since it would lead to exchange of the oxygen of Compound I/II without regenerating unlabelled H_2O_2 . It is therefore reasonable to postulate that the dilution of the $\text{H}_2^{18}\text{O}_2$ label can be explained by an exchange mechanism based on the reversible formation of Compound I.

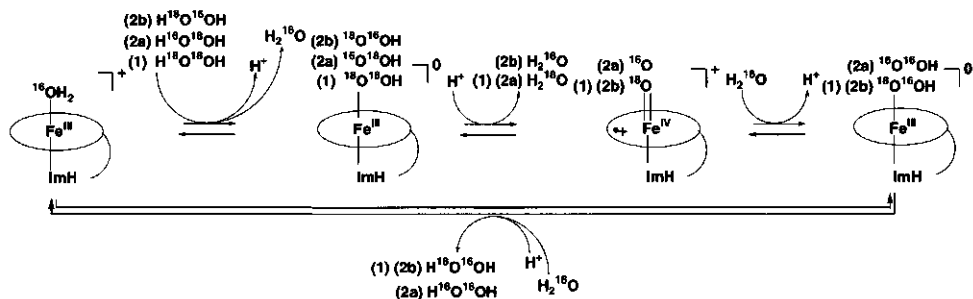


Figure 3.3: Reversible Compound I formation, leading to a maximum of 100 % of exchange in the primary oxidant and resulting in a maximum of 100 % of exchange in the product formed in the subsequent detection assay. Subsequent exchange cycles are numbered. ImH stands for the imidazole moiety of the coordinated histidine from MP-8.

Obviously such a mechanism can also account for the fast oxygen exchange observed by others for HRP (van Haandel *et al.*, 98) and *Arthromyces ramosus* peroxidase (ARP) (Proshlyakov *et al.*, 96). For both enzymes, the presence of a proximal histidine ligand rules out an “oxo-hydroxo tautomerism” explanation for oxygen exchange. However the mechanism of “reversible Compound I formation” can account for oxygen exchange with axially coordinated heme-based biocatalysts with only one open axial ligand position such as cytochromes P450, peroxidases or microperoxidases. Moreover this mechanism could in principle also be relevant for metalloporphyrins having both axial positions free for solvent ligands as it is the case for hemin, MnTMPyP and FeTDCPPS. Table 3.1 depicts the relative exchange extent observed with those model porphyrins. In all cases, oxygen exchange values higher than 50 % were observed which could be consistent with a modified “oxo-hydroxo tautomerism” as already explained. However, addition of catalase at the end of the exchange incubation again fully eliminates the formation of 4-aminophenol in the subsequent detection assay (Table 3.1). This proves that the formation of [¹⁶O]-4-aminophenol is dependent on H₂O₂ present at the end of the oxygen exchange incubation. This formation of [¹⁶O]-4-aminophenol reflects the generation of ¹⁶O containing H₂O₂ during the exchange incubation. Since control incubations without catalysts show no loss of label in H₂¹⁸O₂ (Table 3.1) this result indicates that also the model porphyrins of the present study, in spite of their two open axial ligand positions, are able to catalyse the conversion of H₂¹⁸O₂ into unlabelled and/or partially labelled H₂O₂.

Clearly this generation of unlabelled H_2O_2 , as the mechanism underlying the loss of label in 4-aminophenol, cannot be explained by “oxo-hydroxo tautomerism” and indicates that oxygen exchange through “reversible Compound I formation” may be a relevant mechanism for oxygen exchange between the high-valent metal-oxo species and bulk water in model porphyrins having two free axial positions. Since this reversible process is driven by 55.5 M H_2O , the lack of oxygen exchange observed with hydrophobic model porphyrins could be explained by the absence or a low concentration of H_2O under the conditions employed. The determination of the exchange extent as a function of the water concentration in the reaction medium, may be an interesting topic for further investigations.

Acknowledgments

The authors gratefully acknowledge support from the TMR NMR large scale NMR facility (grant no. ERBCHGE-CT940061), the EU Copernicus programme (grant no. ERBIC15-CT961004) and from the Dutch Foundation for Technical Research (SON/STW project no. 349-3710) as well as from the National Centre for Scientific Research (CNRS, France).

4

Heme-(hydro)peroxide mediated O- and N-dealkylation; A study with microperoxidase

Marelle G. Boersma, Jean-Louis Primus, Janneke Koerts, Cees Veeger and
Ivonne M. C. M. Rietjens

European Journal of Biochemistry (2000) **267**, 6673-6678.

Abstract

The mechanism of microperoxidase-8 (MP-8)¹ mediated O- and N-dealkylation was investigated. In the absence of ascorbate (peroxidase mode) many unidentified polymeric products are formed and the extent of substrate degradation correlates ($r = 0.94$) with the calculated substrate ionization potential, reflecting the formation of radical intermediates. In the presence of ascorbate (P450 mode) formation of polymeric products is largely prevented but, surprisingly, dealkylation is not affected. In addition, aromatic hydroxylation and oxidative dehalogenation is observed. The results exclude a radical mechanism and indicate the involvement of a (hydro)peroxo-iron heme intermediate in P450-type of heteroatom dealkylation.

¹ Abbreviations used: MP-8, microperoxidase 8; (hydro)peroxo-iron, Heme-(hydro)peroxide; oxenoid-iron, horseradish peroxidase compound I.

4.1 Introduction

Heme-based mini-enzymes, also called microperoxidases, form a new generation of biocatalysts and/or biomimics. They consist of a protoporphyrin IX heme cofactor covalently bound to an oligopeptide, which contains histidine acting as the axial ligand to the heme iron (Harbury *et al.*, 65). These heme-based mini-enzymes have been reported to catalyse peroxidase-type of one-electron oxidation (Wang and van Wart, 89; Wang *et al.*, 91) as well as cytochrome P450-type of oxygen transfer reactions (Osman *et al.*, 96). Of all the possible peroxidase- and cytochrome P450-type of reactions, N- and O-dealkylations are the subject of the present study. Cytochromes P450 and peroxidases have been reported to catalyse heteroatom dealkylations by a radical mechanism (Guengerich *et al.*, 96). In spite of this, both types of heme-based biocatalysts behave remarkably different in heteroatom dealkylations. Heteroatom dealkylation by cytochromes P450 is proposed to proceed by a radical type mechanism that is similar and equally efficient for both N- and O-dealkylations (Kedders and Hollenberg, 84; Meunier and Meunier, 85; Guengerich *et al.*, 96). It has been suggested to proceed by formation of an alkyl centered radical which, upon hydroxyl rebound, results in formation of an unstable carbinolamine which decomposes to give the dealkylated product and formaldehyde. The exact route leading to formation of the alkyl centered radical is still matter of debate and can be either direct hydrogen abstraction, or one electron oxidation followed by proton release (Guengerich *et al.*, 96). Nevertheless, this route results in O- and N-dealkylation by a similar radical-type of mechanism.

In contrast, peroxidase-mediated heteroatom dealkylation has been reported to be especially efficient for N- and not for O-dealkylations. Only a few reports demonstrate peroxidase-catalysed O-dealkylations (Meunier and Meunier, 85; Ross *et al.*, 85). Generally peroxidase mediated O-dealkylations are observed so far only for methoxybenzenes substituted with an additional amino (Meunier and Meunier, 85; Haim *et al.*, 87) or a methoxy group (Haim *et al.*, 87). This observation, together with the fact that experiments with ^{18}O -labeled H_2^{18}O have demonstrated that the oxygen of the hydroxyl group introduced in the O-dealkylated product originates from the solvent water rather than from the substrate itself (Meunier and Meunier, 85), has led to the conclusion that the mechanism of cytochrome P450 catalysed heteroatom dealkylations differs from that of peroxidase catalysed O-dealkylation. The latter is proposed to proceed by initial one-electron oxidation

of the substrate, which, upon a subsequent one-electron oxidation step, leads to a cation intermediate, which reacts with water to give the dealkylated product (Kedders and Hollenberg, 84; Meunier and Meunier, 85). Thus, although different, heme-based peroxidase and cytochrome P450 catalysed heteroatom dealkylation proceed by radical mechanisms. The present study shows evidence that in the presence of the radical scavenger ascorbate heteroatom dealkylation by the heme-based microperoxidase-8 (MP-8) proceeds by a non-radical-type of mechanism. The involvement of a (hydro)peroxo-iron heme in the mechanism for heme-based heteroatom dealkylation, similar to that for flavin containing mono-oxygenases, explains the results.

4.2 Materials and methods

Chemicals

N-methylaniline, p-anisidine, N-methyl-p-anisidine, anisol, 1,4-dimethoxybenzene, p-hydroxyanisol, hydroquinone and 4-fluoroaniline were obtained from Aldrich (Steinheim, Germany). Aniline, 4-fluoro-N-methylaniline, p-aminophenol and N-methyl-p-aminophenol were from Janssen Chimica (Beerse, Belgium), and phenol was purchased from Merck (Darmstadt, Germany). Horseradish peroxidase was obtained from Boehringer (Mannheim, Germany). Microperoxidase-8 was prepared by proteolytic digestion of horse heart cytochrome c (Boehringer) essentially as described previously (Aron *et al.*, 83). Hydrogen peroxide (30% v/v) was from Merck and was diluted in nanopure water to obtain the required 50 mM stock solution. The concentration of the latter solution was always checked spectrophotometrically using $\epsilon_{240} = 39.4 \text{ M}^{-1}\text{cm}^{-1}$ (Baldwin *et al.*, 87).

Incubation conditions

A typical assay contained in 1 ml volume (final concentration) 100 mM potassium phosphate pH 7.6, 5 mM of the alkylated substrate added as a 200 times concentrated stock in dimethylsulfoxide and 30 μM MP-8. Upon pre-incubation for 2 minutes at 37 °C in a shaking water bath, the reaction was started by the addition of H_2O_2 (final concentration 2.5 mM added as a 50 mM stock solution in water) and carried out at 37 °C for 60 seconds. Incubations were stopped by freezing the samples into liquid nitrogen until HPLC analysis was performed. When indicated ascorbic acid was added up to a final concentration of 4 mM.

HPLC

Reaction product analysis was performed using a Waters 600 pump equipped with a Waters 996 photodiode Array Detector. Analysis was done by injecting 10 μL on an Alltech LichrosSphere RP8 column (4.6 x 150 mm, 5 μm particle size). Elution was carried out at 1 mL/min starting with 50 mM potassium phosphate (pH 7.0) for 2 min, followed by a linear gradient to give 100 % of methanol in 30 min and kept constant at 100 % of methanol for 5 min. Products were identified by comparison of the retention time and UV/visible spectrum of the observed peaks to those of reference compounds and quantified by their peak area at 295 nm.

Quantum mechanical calculations

Quantum mechanical calculations were carried out on a Silicon Graphics Indigo2 using Spartan 5.0 (Wavefunction Inc. CA USA). A semi-empirical molecular orbital method applying the AM₁ Hamiltonian was used. Geometries were optimised for all bond lengths, bond angles and torsion angles. The calculated ionisation potentials are those for molecules in a vacuum.

4.3 Results

Microperoxidase-8 (MP-8) catalyses, in the absence of ascorbate (the so-called peroxidase mode), with H_2O_2 as substrate, one-electron abstraction reactions (Wang and van Wart, 89; Wang *et al.*, 91). However, in the presence of ascorbate (the so-called P450 mode) peroxidase activity is fully inhibited and, instead, the catalyst is able to perform reactions in the presence of H_2O_2 of the P450-type (Osman *et al.*, 96; Dorovska-Taran *et al.*, 98). Our results show that catalysis by MP-8 in both modes is totally different.

Heteroatom dealkylation in the peroxidase mode.

The HPLC chromatograms of incubations of the peroxidase-type of activity catalysed by MP-8 (figure 4.1a-d) show the results obtained with four different compounds. The compounds tested are N-methylaniline, methoxybenzene, p-anisidine, N-methyl-p-anisidine, 1,4-dimethoxybenzene and 4-fluoro-N-methylaniline. One result is obvious: in all

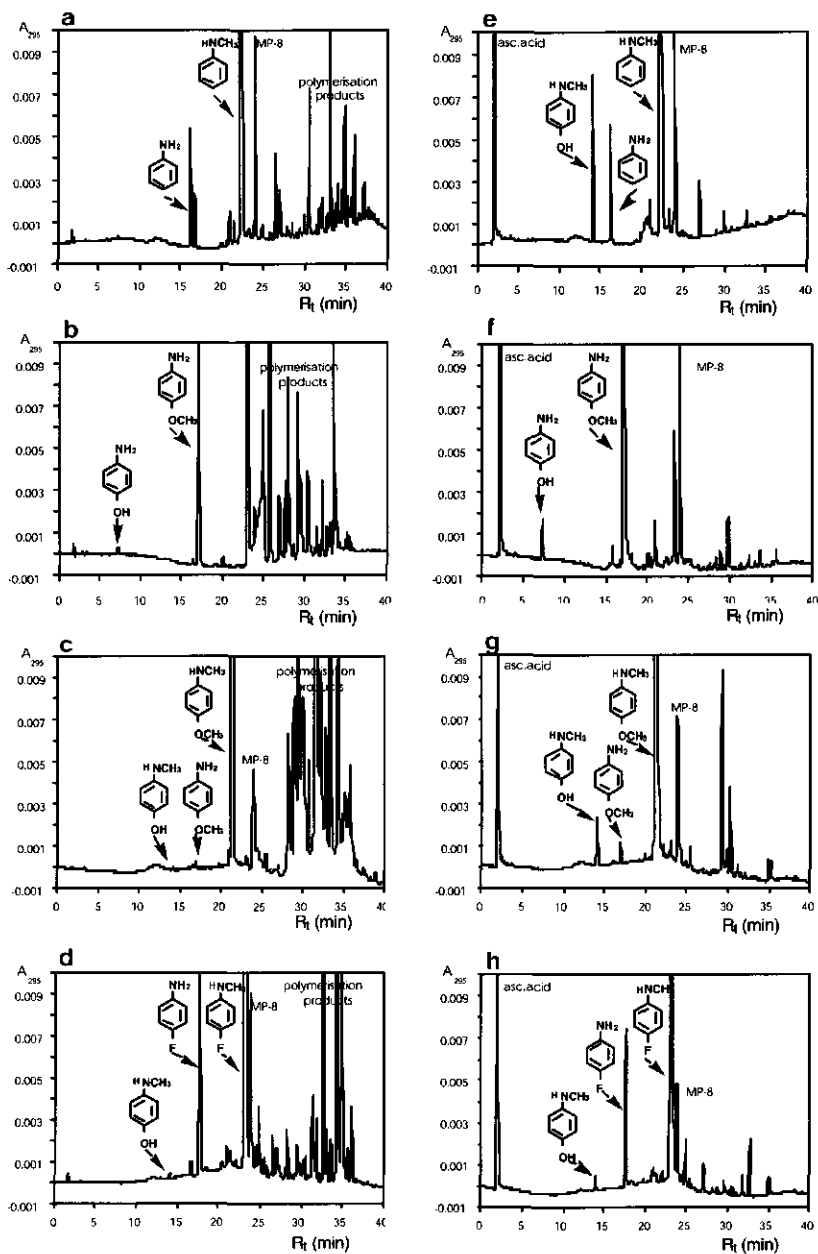


Figure 4.1. HPLC chromatograms of the MP-8/H₂O₂ incubations with different compounds. Figures 4.1a and 4.1e, *N*-methylaniline; figures 4.1b and 4.1f, *p*-anisidine; figures 4.1c and 4.1g, *N*-methyl-*p*-anisidine; figures 4.1d and 4.1h, 4-fluoro-*N*-methylaniline. For conditions see methods. Figures 4.1a-4.1d, incubations in the absence of ascorbate; figures 4.1e-4.1h, incubations in the presence of ascorbate.

cases that compounds are converted large amounts of di- and polymeric products are formed in addition to dealkylated products with N-methylaniline N-dealkylation is readily observed (figure 4.1a). On the other hand the chromatogram of incubations with methoxybenzene (not shown) reveals that this compound is not O-dealkylated and the chromatogram also shows that the MP-8 is efficiently degraded in the presence of an inefficient substrate (Osman *et al.*, 96). In contrast, the chromatogram of the incubation with N-methylaniline shows the presence of a significant amount of the catalyst at the end of the reaction, alike the chromatograms of incubations of the three other substrates that are efficiently converted (figure 4.1b-d).

The observation that MP-8/H₂O₂ efficiently catalyses N-dealkylation, but not O-dealkylation is in line with peroxidase-type and not with cytochrome P450-type of behaviour in these conversions. Previous studies showed that peroxidase-catalysed O-dealkylation was only observed with substrates containing an additional amino- or methoxy substituent (Kedders and Hollenberg, 85). Therefore, in addition to the two compounds mentioned also the O-dealkylation of p-anisidine, N-methyl-p-anisidine and 1,4-dimethoxybenzene catalysed by MP-8 was tested. 1,4-Dimethoxybenzene was not dealkylated, no polymeric products were observed and MP-8 was degraded fully (data not shown).

In incubations of MP-8/H₂O₂ with p-anisidine (figure 4.1b) and N-methyl-p-anisidine (figure 4.1c) the formation of small amounts of O-dealkylated products was observed, illustrating the need for an additional amino substituent for this conversion. N-methyl-p-anisidine is converted into small amounts of O-dealkylated, 4-hydroxy-N-methylamine, and N-dealkylated, p-anisidine, products. 4-Fluoro-N-methylaniline (figure 4.1d) was also included as a substrate in this study to investigate the importance of the role of the ionisation potential in these radical reactions by MP-8. In spite of the presence of the electronegative fluorine atom conversion of 4-fluoro-N-methylaniline leads to the formation of a large amount of the dealkylated product, 4-fluoroaniline, and, surprisingly, to a small amount of 4-hydroxy-N-methylaniline (figure 4.1d). To investigate the importance of one-electron substrate oxidation in MP-8/H₂O₂ driven conversions in the absence of ascorbate, the ionisation potentials of the different substrates were calculated using quantum mechanical calculations (Table 4.1). Comparison of these potentials with the extent of overall substrate conversion indicates that below a threshold potential of 8.6 eV (AM₁), a clear correlation (0.94) is observed (figure 4.2). These results indicate that in the absence of

ascorbate conversion of the N- and O-alkyl substrates results primarily in the formation of polymeric reaction products; this conversion is mainly determined by the ionisation potential of the compound. The absence of O-dealkylation for methoxybenzene and 1,4-dimethoxybenzene, as well as the occurrence of O-dealkylation upon the introduction of an amino moiety in the aromatic ring, can all be explained by the effects of the various substituent patterns on the ease of substrate oxidation. When the ionisation potential reaches the threshold value of 8.6 eV (AM_1 calculated) MP-8/ H_2O_2 is no longer capable to abstract an electron from the substrate and substrate conversion is no longer observed.

Table 4.1 Calculated ionisation potentials and percentage overall conversion of the model compounds studies.

Substrate	Ionisation potential (eV)	% conversion	
		ascorbic acid absent	ascorbic acid present
N-methylaniline	8.41	44	16
p-anisidine	8.20	96	1
N-methyl-p-anisidine	8.13	80	4
4-fluoro-N-methylaniline	8.45	41	14
anisol	9.0	0	0
1,4-dimethoxybenzene	8.57	0	0

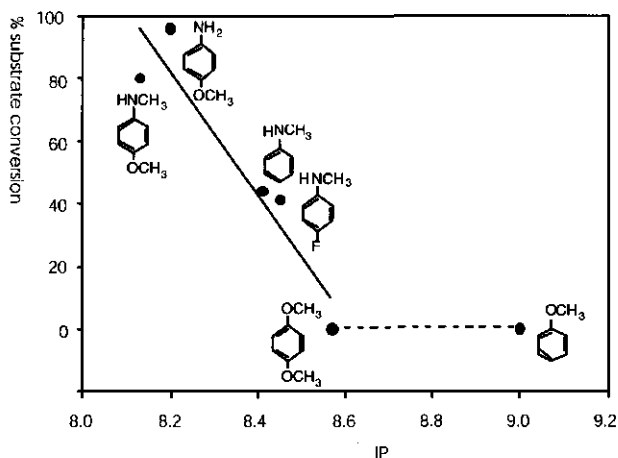


Figure 4.2 Relation between the overall peroxidase activity of microperoxidase-8 and the calculated ionisation potential of the substrate (see Table 4.1). The overall activity is defined as the decline in initial substrate concentration.

Heteroatom dealkylation in the P450 mode

In the presence of ascorbate substrate conversion is significantly reduced while no correlation between the level of substrate conversion and ionisation potential exists (Table 4.1). In line with what was expected, with all compounds tested formation of di- and polymerisation products is drastically reduced (figure 4.1e-h). On the other hand, in contrast to expectations reported in the literature (Wang and van Wart, 89), N-dealkylation is observed with N-methylaniline to an amount comparable with that in the absence of ascorbate (compare figures 4.1a and 4.1e). Additionally, however, appreciable amounts of the p-hydroxylated product, 4-hydroxy-N-methylaniline, is observed, a product not obtained in the absence of ascorbate. Para-hydroxylation of aniline derivatives by MP-8 has been reported before (Osman *et al.*, 96).

In the case of 4-methoxyaniline as substrate O-dealkylation is observed (figure 4.1f). With N-methyl-p-anisidine formation of the N-dealkylated product, p-anisidine, (figure 4.1g) is again observed, now in an amount considerably larger than in the absence of ascorbate (compare figures 4.1c and 4.1g). Another phenomenon visible in figure 4.1g is the considerable O-dealkylation catalysed in the presence of ascorbate; the product 4-hydroxy-N-methylaniline is hardly obtained in the absence of ascorbate (figure 4.1c). In these incubations the amount of O-dealkylated product, 4-hydroxy-N-methylaniline, even exceeds the amount of N-dealkylated product, 4-methoxyaniline. 1,4-Dimethoxybenzene is not O-dealkylated in the presence of ascorbate, alike in its absence. The presence of ascorbate seems to inhibit to some extent the N-dealkylation of 4-fluoro-N-methylaniline (figure 4.1h) in comparison with the amount produced in its absence. However, the amount of the dehalogenated product, 4-hydroxy-N-methylaniline is considerably higher. MP-8/H₂O₂ driven dehalogenation of halophenols was reported before (Osman *et al.*, 97b), but was only observed in the absence of ascorbate. When this reaction was performed in alcoholic solution, dehalogenation was accompanied by methoxylation at the same place (Osman *et al.*, 97a). Horseradish peroxidase is also fully inhibited by (higher) concentrations of ascorbate (Chance, 52), but is, in contrast to MP-8, under this condition neither able to perform P450-type of reactions nor heteroatom dealkylation (data not shown).

4.4 Discussion

The results presented here clearly show that O- and N-dealkylation as catalysed by MP-8 has two totally different aspects: 1. It converts in the peroxidase mode in a radical reaction substrates depending on their ionisation potentials (figure 4.2, $r = 0.94$) into di- and polymeric products; in addition heteroatom dealkylated products are detected. The correlation observed between the calculated ionisation potentials and the rate of degradation of substrates provides an explanation for the requirement of an extra amino moiety for the O-dealkylation of methoxy compounds. 2. The addition of ascorbate inhibits peroxidase-type of radical chemistry (Osman *et al.*, 96), confirmed by the drastically reduced amounts of polymerisation products. In addition it induces P450-type of chemistry (Osman *et al.*, 96; Dorovska-Taran *et al.*, 98), and, as the results show, O- and N-dealkylation as well. With p-anisidine and N-methyl-p-anisidine increased formation of dealkylated products is found. With N-methylaniline and 4-fluoro-N-methylaniline significant amounts of dealkylated products were still observed accompanied by an increase in para-hydroxylated products, resulting from either aromatic hydroxylation or from oxidative dehalogenation of the substrates. Together these results indicate that in the presence of ascorbate the reaction does not proceed through a radical mechanism and one-electron oxidised substrate intermediates.

Involvement of a (hydro)peroxo-iron intermediate, catalysing direct oxygen transfer (figure 4.3) is an alternative mechanism, based on previous studies and observations (Osman *et al.*, 96; Dorovska-Taran *et al.*, 98). This mechanism of N-dealkylation is comparable with that of N-dealkylation catalysed by a flavin-containing mono-oxygenase through the reactive flavin-(C4a)hydroxyperoxide intermediate (Boersma *et al.*, 93). The dualities which one encounters in designing a common mechanism for the reactions of the present study is not only which heme intermediate, (hydro)peroxo-iron or oxenoid-iron, catalyses such different conversions, but also is the reaction electrophilic or nucleophilic. Oxygen exchange studies with horseradish peroxidase, MP-8 and cytochrome P450 showed (MacDonald *et al.*, 82; Dorovska-Taran *et al.*, 98; van Haandel *et al.*, 98) that a (hydro)peroxide intermediate is formed prior to oxenoid-iron formation, a conclusion substantiated by rapid kinetic studies with the horseradish peroxidase mutant R38L (Rodriguez-Lopez *et al.*, 96).

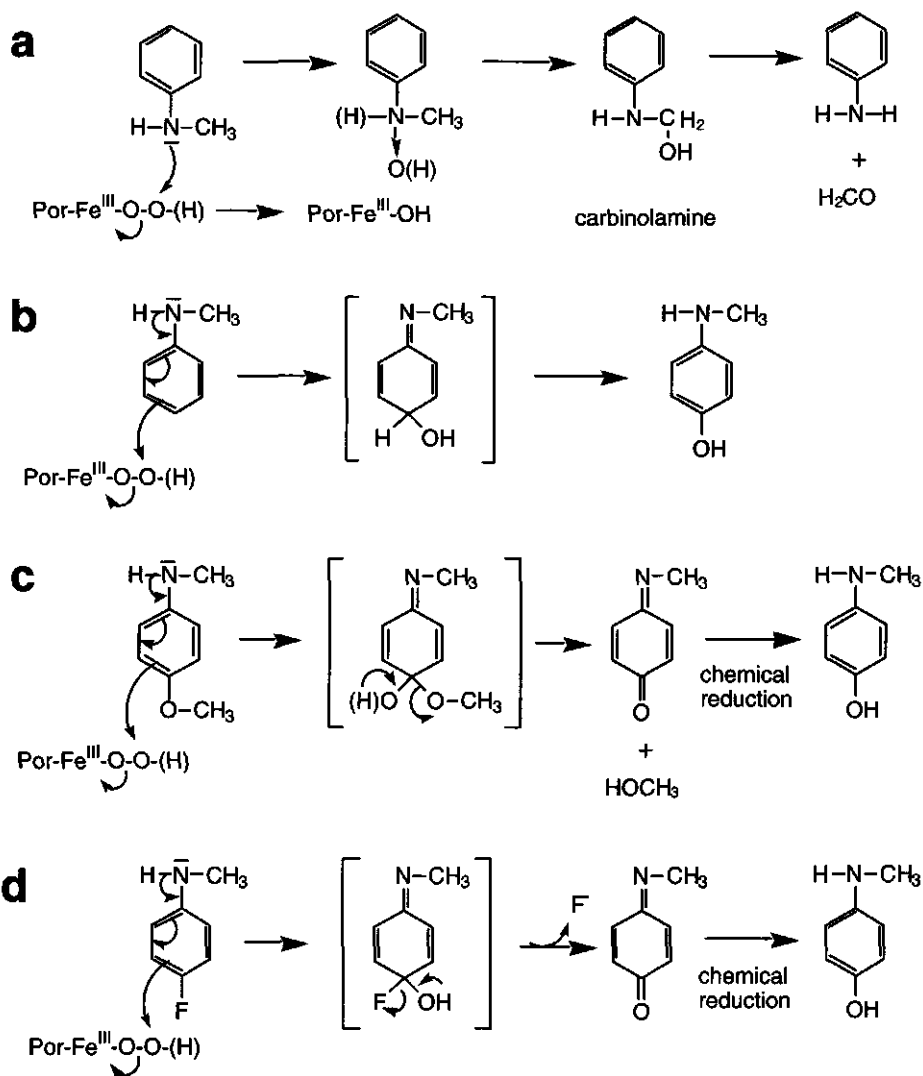


Figure 4.3. Proposed reaction mechanism of electrophilic (hydro)peroxy-iron catalysed reactions. N-dealkylation (figure 4.3a), aromatic hydroxylation (figure 4.3b), O-dealkylation (figure 4.3c) and dehalogenation (figure 4.3d). For explanation see text. At the present moment no distinction can be made which form, hydroperoxy-iron or peroxy-iron, is involved in these conversions.

The occurrence of a peroxo-iron species as intermediate in cytochrome P450 catalysed conversions was first proposed in the demethylation of androgens to estrogens (Akhtar *et al.*, 82). Evidence for a functional role of different (hydro)peroxo-iron species was presented by Vaz *et al.* (Vaz *et al.*, 98) to account for differences in rates of conversion of olefinic substrates by different cytochromes P450 as well as for the oxidative deformylation of aldehydes to olefines and formate (Vaz *et al.* 91; Roberts *et al.*, 91; Vaz *et al.*, 94; Vaz *et al.*, 96). Peroxo-iron was proposed as nucleophilic intermediate (aldehyde deformylation), hydroperoxo-iron as nucleophilic and electrophilic intermediate (aldehyde deformylation and epoxidation) and oxenoid-iron as electrophilic intermediate hydroxylation and epoxidation). A similar conclusion was derived from experimental results with MP-8 (Dorovska-Taran *et al.*, 98; Primus *et al.*, 99) demonstrating that oxygen from either H₂O₂ or from H₂O was incorporated in the hydroxylated product. In the case of oxidative deformylation of aldehydes (cf. reference 23 in Mansuy and Battioni, 2000) proposed schematically that initially peroxo-iron attacks the aldehyde as nucleophile, followed by what the authors call a polycyclic flow of electrons to the proximal oxygen and formation of the heme-ironhydroxide indicating electrophilic character of the peroxo-iron reactant. A similar indication comes from recent MO-calculations demonstrating peroxo-iron can act as an electrophilic reactant in aromatic hydroxylations; hydroperoxo-iron is chemically inert (Zakharieva *et al.*, 2000). In the present study the involvement of oxenoid-iron is excluded for the reactions performed in the presence of ascorbate. Figures 4.3a-4.3d present the reaction schemes, based on catalysis by an electrophilic (hydro)peroxo-iron intermediate. Demethylation and para-hydroxylation of N-methylaniline both proceed by electrophilic attack of (hydro)peroxo-iron on the substrate and the electron-flow leads to heme-ironhydroxide formation (figures 4.3a and 4.3b). One may argue about the existence of the tetrahedral intermediate as depicted in figure 4.3b or a concerted mechanism in which keto-enol tautomerisation accompanies the attack. Similarly one may visualise an electrophilic reaction in the O-demethylation of N-methyl-p-anisidine and oxidative dehalogenation of 4-fluoro-N-methylaniline (figures 4.3c and 4.3d) also leading to formation of heme-ironhydroxide. However, the product of the latter reactions is in a two-electron higher imino-quinoid form. Formation of this quinoid type of product in oxidative dehalogenation has been shown before for flavin-mediated catalysis (Husain *et al.*, 80; Boersma *et al.*, 93), cytochrome P450 (Rietjens and Vervoort, 91; Cnubben *et al.*, 95),

MP-8 (Osman *et al.*, 97) and model heme mediated conversions (Sorokin and Meunier, 94; Ohe *et al.*, 95). By chemical reduction (ascorbate) the hydroxylated aromate is formed.

The alternative for these electrophilic mechanisms in figures 4.3c and 4.3d is a nucleophilic attack by the (hydro)peroxo-iron on the C4-atom of the aromate leading to elimination of the halogen (F) ion or the methanolate (CH₃O⁻) ion (figure 4.4). In this case the catalyst is released as oxenoid-iron (compound I) form. Regeneration of the catalyst in its ferric form can be achieved: 1. Through reduction in the case of MP-8 by ascorbate; in cytochrome P450 most probably by the cytochrome P450 reductase; 2. Through the reversible reaction (MacDonald *et al.*, 82; Dorovska-Taran *et al.*, 98; van Haandel *et al.*, 98) between compound I with H₂O regenerating (hydro)peroxo-iron. In this case H₂O would be the driving force of the reaction as well as the oxygen-providing reagent.

It is of interest to notice in this context that plant P450's catalyse the dehydration of fatty acid hydroperoxides with formation of allene oxides (Song and Brash, 91; Lau *et al.*, 93) without the need for the enzyme NADPH-cytochrome P450 reductase or any additional substrate (NADPH, O₂ or H₂O₂). A mechanism as depicted in figure 4.4 could account for the oxygen transfer and other P450-type of chemistry without the requirement for reduction equivalents and would thus explain this observation as well. Such mechanism can also explain the direct addition of methanol to the oxenoid-iron leading to the formation of heme-iron methoxyperoxide. The latter can be replaced by nucleophilic attack on an aromatic halogen the halogen by a methoxy substituent (Osman *et al.*, 97a).

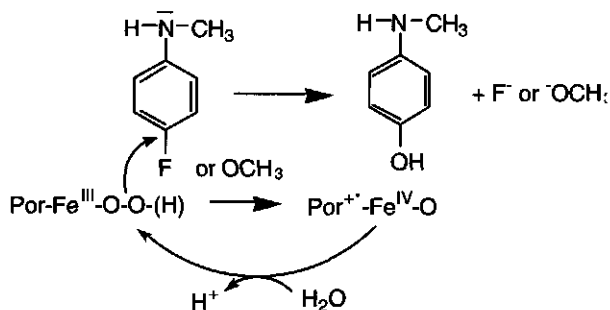


Figure 4.4. Proposed reaction mechanism for a nucleophilic dehalogenation and O-dealkylation reaction. See also figure 4.3.

The choice of mechanism in the case of O-demethylation and oxidative dehalogenation may seem trivial in the case of MP-8 catalysis. It is certainly not when these conversions are catalysed by cytochrome P450. The generation of products in the imino-quinoid state implies potentially harmful electrophiles and, thus, cellular damage (Haim *et al.*, 87), unless the cell contains a high level of reductant, like ascorbate or another anti-oxidant. On the other hand the nucleophilic reaction mechanism as depicted in figure 4.4 proceeds without generation of reactive products.

Acknowledgements

The authors gratefully acknowledge the support from the TMR large scale NMR facility (grant no. ERBFMGE-CT950066) and from the Dutch Foundation of Technical Research (SON/STW project no. 349-3710).

**The effect of iron to manganese substitution on microperoxidase-8
catalysed peroxidase and cytochrome P450 type of catalysis.**

Jean-Louis Primus, Marelle G. Boersma, Dominique Mandon, Sjef Boeren, Cees Veeger,
R. Weiss, and Ivonne M.C.M. Rietjens

Journal of Biological Inorganic Chemistry (1999) 3, 274-283.

Abstract

This study describes the catalytic properties of manganese microperoxidase-8 (Mn(III)MP-8), as compared to iron microperoxidase-8 (Fe(III)MP-8). The mini-enzymes were tested for pH dependent activity and operational stability in peroxidase type of conversions, using 2-methoxyphenol and 3,3'-dimethoxybenzidine, and in a cytochrome P450 like oxygen transfer reaction converting aniline to *para*-aminophenol. For the peroxidase type of conversions the Fe to Mn replacement resulted in a less than 10-fold decrease in the activity at optimal pH, whereas the aniline *para*-hydroxylation is reduced at least 30-fold. In addition it was observed that the peroxidase type of conversions are all fully blocked by ascorbate and that aniline *para*-hydroxylation by Fe(III)MP-8 is increased by ascorbate whereas aniline *para*-hydroxylation by Mn(III)MP-8 is inhibited by ascorbate. Altogether these results indicate that different types of reactive metal oxygen intermediates are involved in the various conversions. Compound I/II, scavenged by ascorbate, may be the reactive species responsible for the peroxidase reactions, the polymerisation of aniline and (part of) the oxygen transfer to aniline in the absence of ascorbate. The *para*-hydroxylation of aniline by Fe(III)MP-8, in the presence of ascorbate, must be mediated by another reactive iron-oxo species which could be the electrophilic metal(III) hydroperoxide anion of microperoxidase-8 (M(III)OOH MP-8). The lower oxidative potential of Mn, as compared to Fe, may affect the reactivity of both the Compound I/II and the metal(III) hydroperoxide anion intermediate, explaining the differential effect of the Fe to Mn substitution on the pH dependent behaviour, the rate of catalysis and the operational stability of MP-8.

5.1 Introduction

Hemoprotein models have been used during the last decades in order to obtain better understanding of heme-based catalysis. Most of the chemical and biochemical models show catalytic activities closely related to the activities of the proteins they mimic. Thus, metalloporphyrin models can act as oxygen binding and/or oxygen transport molecules, they can transfer electrons, and also catalyse peroxidase and/or monooxygenase reactions (Meunier, 92; Chorghade *et al.*, 96). Fe(III)MP-8¹ is a water-soluble hemoprotein model which has been extensively studied since its first description in the literature (Tsou, 51a; Tsou, 51b). Fe(III)MP-8 is obtained by controlled proteolytic digestion of horse heart cytochrome c (Tsou, 51a; Tsou, 51b; Aron *et al.*, 86) and consists of iron protoporphyrin IX to which a residual histidine containing octapeptide is connected in a heme c pattern. At pH > 3, the histidine residue remains axially coordinated to the iron centre (Wang *et al.*, 92). This hemoprotein fragment contains the almost minimal part of the protein polypeptidic chain necessary to mimic a catalytically active hemoprotein (Spee *et al.*, 96). It also undergoes less aggregation than other porphyrin models in aqueous solution (Aron *et al.*, 86). Fe(III)MP-8 has an open active site leading to broad substrate specificity in two types of catalytic reactions. First of all Fe(III)MP-8 shows peroxidase type of activities like oxidation of 3, 3'-dimethoxybenzidine (*o*-dianisidine) (Kraehenbuhl *et al.*, 74), 2-methoxyphenol (guaiacol) (Baldwin *et al.*, 85; Baldwin *et al.*, 87) or 2, 2'-azinobis-(3-ethylbenzothiazoline-6-sulphonate) (ABTS) (Adams, 90; Cunningham *et al.*, 91; Cunningham *et al.*, 92; Cunningham *et al.*, 94). Furthermore cytochrome P450 type of oxygen transfer reactions can be catalysed such as aniline hydroxylation (Rusvai *et al.*, 88; Osman *et al.*, 96), monooxygenation of polycyclic aromatics like naphthalene and anthracene (Dorovska-Taran *et al.*, 98), sulfide oxidation (Nakamura *et al.*, 92) and N-demethylations (Mashino *et al.*, 90; Nakamura *et al.*, 92; Okochi and Mochizuki, 95).

¹ **Abbreviations used:** ϵ_x , extinction coefficient at x nm; MP, microperoxidase; Fe(III)MP-8, Fe(III) containing microperoxidase-8; Mn(III)MP-8, Mn(III) containing microperoxidase-8; M(III)OOH MP-8, metal hydroperoxide anion microperoxidase-8; HPLC, high performance liquid chromatography; MALDI-TOF, Matrix-Assisted Laser Desorption/Ionization-Time Of Flight.

Many investigations suggested a key role played by so called high-valent-iron-oxo intermediates in both peroxidase and cytochrome P450 type MP-8 catalyzed reactions (Low *et al.*, 96; Low *et al.*, 98). But recently possible involvement of iron-hydroperoxo intermediates in cytochrome P450 type of reactions has also been suggested (Mansuy *et al.*, 89; Dorovska-Taran *et al.*, 98; Vaz *et al.*, 98). However the exact nature of the intermediate involved in each MP-8 catalysed process has not been clearly defined.

In spite of their wide substrate specificity and the different types of reactions catalysed, the use of those mini-catalysts is limited by their low operational stability in both peroxidase as well as cytochrome P450 type of conversions (Spee *et al.*, 96; Osman *et al.*, 96). This limited operational stability of model iron porphyrins is a well known phenomenon (O'Carra, 75). Although the exact mechanism underlying the inactivation remains poorly understood (Bonnett and McDonagh, 73; O'Carra, 75; Brown, 76), a role of a reactive iron-oxo or iron-hydroperoxo anion intermediate, formed during the catalytic cycle, seems to be generally agreed upon (Wilks and Ortiz de Montellano, 93). Since manganese-oxo porphyrins species are shown to be less reactive than the corresponding iron complexes (Yonetani and Asakura, 69; Gelb *et al.*, 82; Low *et al.*, 98), many different types of manganese model porphyrins have been studied in various catalytic systems in order to get insight into and/or to circumvent the operational instability of iron porphyrin models (Low *et al.*, 98) (for a review on Fe/Mn porphyrin catalytic potentialities see Meunier, 92). Nevertheless, iron and manganese porphyrins have hardly been tested in parallel for catalytic activity and operational stability.

Thus the objective of the present work was to study the effect of the iron to manganese substitution in MP-8 on the catalytic activity, the operational stability and the pH-dependent behaviour for model peroxidase and cytochrome P450 type of reactions. Additionally we present an alternative synthetic route leading to Mn(III)MP-8 avoiding the use of hazardous chemicals such as hydrogen fluoride.

5.2 Materials and methods

Materials

MP-8 was prepared by peptic and tryptic digestion of horse heart cytochrome c (Boehringer Mannheim, Germany) essentially as described previously (Aron *et al.*, 86). According to HPLC analysis using a detection wavelength of 395 nm (see below) the purity

of the MP-8 preparation used for catalytic studies is estimated to be over 95 % and about 85 % when used as a starting material for synthesis. Anhydrous iron(II) chloride was obtained from Strem Chemicals (Newburyport MA, USA). Aniline and 4-aminophenol were obtained from Janssen (Beerse, Belgium). Manganese(II) sulfate tetrahydrate, and L-ascorbic acid were from Merck ; 2-methoxyphenol, 3,3'-dimethoxybenzidine and alpha-cyano-4-hydroxycinnamic acid from Aldrich (Steinheim, Germany). All substrates were of 97-98 % purity. Hydrogen peroxide (30 % v/v) was from Merck and was diluted in nanopure water to obtain the required 50 mM stock solution. The concentration of the latter solution was always checked spectrophotometrically using $\epsilon_{240} = 39.4 \text{ M}^{-1} \cdot \text{cm}^{-1}$ (Baldwin *et al.*, 87). All HPLC solvents were of chromatographic grade. All others reagents used were of analytical grade.

Preparation of MP-8 free base by reductive demetalation

The demetalation procedure was adapted from previously published methods for the demetalation of model porphyrins (Hasegawa *et al.*, 91; and refs therein). During the process care was taken to avoid direct exposure to light (Low *et al.*, 98). Fe(III)MP-8 (230.5 mg, 153 μmol) was dissolved in 225 mL of glacial acetic acid and 3.8 mL of concentrated HCl (200 μM) were added. The reaction mixture was purged with argon by three freeze-thaw cycles. Using a syringe, 450 μL (1.8 mmol, 11.8 eqs) of a 0.5 g/mL aqueous, argon saturated, iron(II) chloride solution were added. The reaction mixture was stirred at room temperature for 5 min resulting in demetalation, reflected by a change in color from red to purple. The solvent was removed by evaporation under reduced pressure. The residue was dissolved in water and immediately reevaporated in order to completely remove residual HCl. This washing was repeated twice and the final residue was solubilized in a minimal volume of 50 mM NH_4HCO_3 pH 8 and desalted over a Biogel P6DG column. The supernatant thus obtained was lyophilized in the dark. Purity was 67 % according to HPLC analysis (see Results for characterization). The residue was used for metalation without further purification.

Preparation of MP-8 free base by hydrogen fluoride demetalation

Demetalation of 4 mg (2.6 μmol) of Fe(III)MP-8 was done according to a previously published procedure (Low *et al.*, 98).

Preparation of Mn(III)MP-8

The metalation procedure was adapted from the literature (Jiménez and Momenteau, 94). MP-8 free base (222 mg, 152.8 μmol) was dissolved in 220 mL of 50 mM potassium phosphate buffer pH 7.8. The reaction medium was purged with argon by three freeze-thaw cycles and manganese(II) sulfate (210 mg, 917 μmol) was added. The reaction mixture was incubated at 90°C and during the course of the reaction another 210 mg of manganese(II) sulfate were added. After 36 h of incubation, almost no free-base was left as judged by the disappearance of the free-base porphyrin Soret band ($\lambda = 403 \text{ nm}$) from the UV/visible absorption spectrum of the reaction mixture. The reaction medium was allowed to cool at room temperature and centrifuged 10 min at 24,000 g, the supernatant was lyophilized. The residue obtained was purified by preparative HPLC (see below) and characterized (see Results).

Analytical HPLC

Analytical HPLC of MP samples was performed using a Waters 600 pump equipped with a Waters 996 PhotoDiode Array Detector. Analysis was done with a Waters Delta-Pak C18 column (3.9 X 150 mm, 300 Å pore size, 5 μm particle size) and elution was carried out at a flow of 1 $\text{mL}\cdot\text{min}^{-1}$ with 0.1 % trifluoroacetic acid/ H_2O (eluent A) and 0.1 % trifluoroacetic acid/ CH_3CN (eluent B) using a linear gradient from 20 to 38 % B over 18 min. A 10 μL injection loop was used. Reaction product analysis by analytical HPLC was performed using an Alltech LichroSphere RP8 column (4.6 X 150 mm, 5 μm particle size), eluted either isocratically with 88 % 50mM potassium phosphate buffer pH 7 (eluent A) and 12 % MeOH (eluent B) at 1 $\text{mL}\cdot\text{min}^{-1}$ or using a linear gradient from 12 to 80 % B over 25 min at 1 $\text{mL}\cdot\text{min}^{-1}$. In a typical run, aliquots of the incubation mixture were injected using a 50 μL loop. Products were identified by comparison of observed peaks to the retention time and UV/visible spectrum of commercially available standards and quantified by their peak area at 295 nm.

Semi-preparative HPLC of MP samples

Semi-preparative HPLC was performed using two Isco Model 2300 HPLC pumps equipped with a Pye Unicam LC-UV Detector. Samples were prepared by dissolving the crude material in eluent A followed by centrifugation and the supernatant, typically 1 mL,

was loaded on a Waters Delta-Pak C18 column (25 X 200 mm, 300 Å pore size, 10 µm particle size). Elution was performed with a gradient of 0.1 % H₃PO₄/0.3 % triethylamine/H₂O (eluent A) and CH₃CN (eluent B) (Miller and Rivier, 96). For semi-preparative purification of Mn(III)MP-8, 26 % of B were first applied for 8 min followed by a linear gradient from 26 to 28 % B over 14 min at 8 mL.min⁻¹.

Cytochrome P450 incubation conditions using aniline as substrate

Incubations (200 µL volume) were performed essentially as previously described (Osman *et al.*, 96). In short, incubations contained (final concentrations) 100 mM buffer (prepared according to literature (Stoll and Blanchard, 90) for the pH values between 4.6 and 10.7 and by adjusting the pH of phosphate and carbonate solutions with a 3 M potassium hydroxide solution for the pH values above 10.7, variation of the ionic strength was checked to have no influence on the rate of substrate conversion), 2 mM ascorbate (as indicated), 10 mM aniline added as a 200 mM stock solution in 20 % dimethyl sulfoxide/80 % H₂O, 7.5 µM microperoxidase catalyst. Upon preincubation for 2 min at 37 °C in a shaking water bath, the reaction was started by addition of H₂O₂ (2.5 mM final concentration, added as a 50 mM stock solution in water) and carried out at 37°C for 5 s to 60 s as required. Incubations were stopped by directly injecting the sample on the column for HPLC analysis.

Peroxidase incubation conditions using 2-methoxyphenol as substrate

A typical assay (1 mL volume) contained (final concentrations) 100 mM buffer (prepared as described above ; variation of the ionic strength was checked to have no influence on the rate of substrate conversion), 3 mM 2-methoxyphenol added as a 0.3 M stock solution in dimethyl sulfoxide, 0.8 µM microperoxidase catalyst added as 80 µM stock solution in water. The reaction was started by addition of H₂O₂ (final concentration 0.26 mM, added as a 5.2 mM stock solution in water) and product formation was followed by monitoring the absorbance at 470 nm of the tetrameric oxidized 2-methoxyphenol ($\epsilon_{470} = 26.6 \cdot 10^3 \text{ M}^{-1} \cdot \text{cm}^{-1}$). Due to the time required for H₂O₂ addition and the consecutive mixing time within the cuvette, typically, a 7 s delay was added to the data points and the initial slope was extrapolated to the origin using the fit specified in the Results section. The initial rate was calculated taking into account the tetrameric structure of the oxidized

2-methoxyphenol (Baldwin *et al.*, 87) and checked to be proportional to the concentration of the mini-catalysts.

Peroxidase incubation conditions using 3,3'-dimethoxybenzidine as substrate

A typical assay (1 mL volume) contained (final concentrations) 100 mM buffer (prepared as described above; variation of the ionic strength was checked to have no influence on the rate of substrate conversion), 0.25 mM 3,3'-dimethoxybenzidine added as a 25 mM stock solution in dimethyl sulfoxide, 0.8 μ M microperoxidase catalyst added as a 80 μ M stock solution in water. The reaction was started by addition of H₂O₂ (final concentration 0.26 mM, added as a 5.2 mM stock solution in water) and product formation was followed by monitoring the absorbance at 460 nm ($\epsilon_{460} = 1.13 \cdot 10^4 \text{ M}^{-1} \cdot \text{cm}^{-1}$) (Kraehenbuhl *et al.*, 74). The initial rate was calculated the same way as described above for 2-methoxyphenol and conditions were chosen such that the rate was proportional to the amount of mini-catalyst added.

Mass spectrometry measurements

Alpha-cyano-4-hydroxycinnamic acid dissolved in 1 % trifluoroacetic acid/30 % CH₃CN/69 % H₂O at a concentration of 10 mg/mL was used as a matrix solution. MP samples were prepared by dilution into the matrix solution to a concentration of 1 mM. A 1 μ L volume of the sample-matrix solution was deposited directly on a well plate, air dried and introduced into the mass spectrometer. Spectra were obtained using a Voyager-DE spectrometer (PerSeptive Biosystems) in the positive reflector mode. The MALDI spectra were externally calibrated using protonated Fe(III)MP-8 (monomeric monoisotopic molecular mass 1506.52 g/mol) and one matrix peak (dimeric monoisotopic molecular mass of 379.09 g/mol for the alpha-cyano-4-hydroxycinnamic acid).

¹H NMR spectroscopy

¹H NMR measurements were performed at 500.14 MHz on an AMX 500 Bruker instrument. Spectra were recorded with presaturation of the water signal for 1.5 s. Experiments were carried on at 300 K and 1D spectra were acquired using a 100,000 Hz sweep width.

Cyclic voltammetry

Midpoint potentials of MP's were measured using a microscale direct voltammetry technique essentially as previously described (Hagen, 89). The working electrode was a glassy carbon disc pretreated for a few minutes with 65 % HNO₃. Potentials were measured via a platinum counter electrode using a saturated silver electrode (SSE) as reference at a scan rate of 5mV/s. Conversion of the measured potential to standard potentials against saturated calomel electrode (SCE) was done using $E_0(\text{SSE}) = + 197 \text{ mV}$ against SCE at 25°C.

5.3 Results

Demetalation

Figure 5.1a shows the HPLC chromatogram of the starting material Fe(III)MP-8 ($R_t = 13.2 \text{ min}$). Figure 5.1b presents the HPLC pattern of the sample obtained after demetalation. Figure 5.1c shows MP-8 free base resulting from the demetalation using hydrogen fluoride (HF) (Low *et al.*, 98). Comparison of Figure 5.1b to Figure 5.1c indicates that the purity of the MP-8 free base obtained with the present method is similar to the one obtained via HF demetalation although in the present method impurities are more clearly separated from the main product. Comparison of the HPLC trace from Figure 5.1b to the one presented in Figure 5.1a shows the complete absence of Fe(III)MP-8. The peak at $R_t = 19.8 \text{ min}$ was identified as MP-8 free base by its UV/visible absorption spectrum at pH 2 showing a Soret band at $\lambda_{\text{max}} = 403 \text{ nm}$ and two Q bands at $\lambda_{\text{max}} = 552 \text{ and } 595 \text{ nm}$ typical for a free base porphyrin di-cation (low pH conditions) (Smith, 75). Mass spectrometry was performed as additional characterization using MALDI-TOF (Figure 5.2a). The main product was detected at $m/e = 1453.65 \text{ g/mol}$ corresponding to MP-8 free base. In addition six unidentified minor byproducts are observed.

Further characterization of MP-8 free base was performed by doing large sweep width ^1H NMR spectroscopy measurements. The absence of iron exchange in this system excludes the possibility that as a result of this exchange, line broadening effects make the NMR signal becoming invisible. This makes it possible to use paramagnetically shifted signals as an indication for the presence of iron(III) still coordinated to the molecule (Bertini *et al.*, 89; Low *et al.*, 97). The ^1H NMR spectrum of MP-8 free base did not show any paramagnetic shifts (data not shown). This observation corroborates that no iron(III) is present in the tetrapyrrolic coordination site of the molecule. Thus MP-8 free base has been unambiguously characterized as a major product from Fe(III)MP-8 demetalation.

Remetalation

Remetalation with manganese was done using crude MP-8 free base. The Mn(III)MP-8 was then purified by semi-preparative HPLC. Figure 5.1d shows the HPLC chromatogram of the purified Mn(III)MP-8 obtained ($R_t = 12.6$ min). From this HPLC chromatogram the purity of the transmetalated compound was estimated to be over 95 %. The UV/visible absorption spectrum of Mn(III)MP-8 shows a split Soret pattern typical for Mn(III) porphyrins (Boucher, 68; Low *et al.*, 98), with two bands arising at 460 nm and 372 nm. The band at 460 nm has been ascribed to a ligand to metal charge transfer band for many Mn(III) porphyrins (Boucher, 68; Boucher, 69). MALDI-TOF mass spectrometry characterization of the purified remetalated material shows a main peak at $m/e = 1505.3$ g/mol corresponding to protonated Mn(III)MP-8 (Figure 5.2b).

Cyclic voltammetry

Figure 5.3 shows the cyclic voltammogram of Fe(III)MP-8 and Mn(III)MP-8. The Fe(III) to Mn(III) substitution results in a dramatic change in the redox potential of the MP-8. The value of $E_{0'} = -361$ mV found for the Mn(II)/Mn(III) transition is 154 mV lower than the value of $E_{0'} = -207$ mV found for the Fe(II)/Fe(III) transition, the latter being consistent with literature data (Harbury and Loach, 60a; Harbury and Loach, 60b; Harbury *et al.*, 65). Since the only difference between both systems is the nature of the metal centre, the lower oxidation potential of the manganese MP-8 can be ascribed to the Fe(III) to Mn(III) replacement.

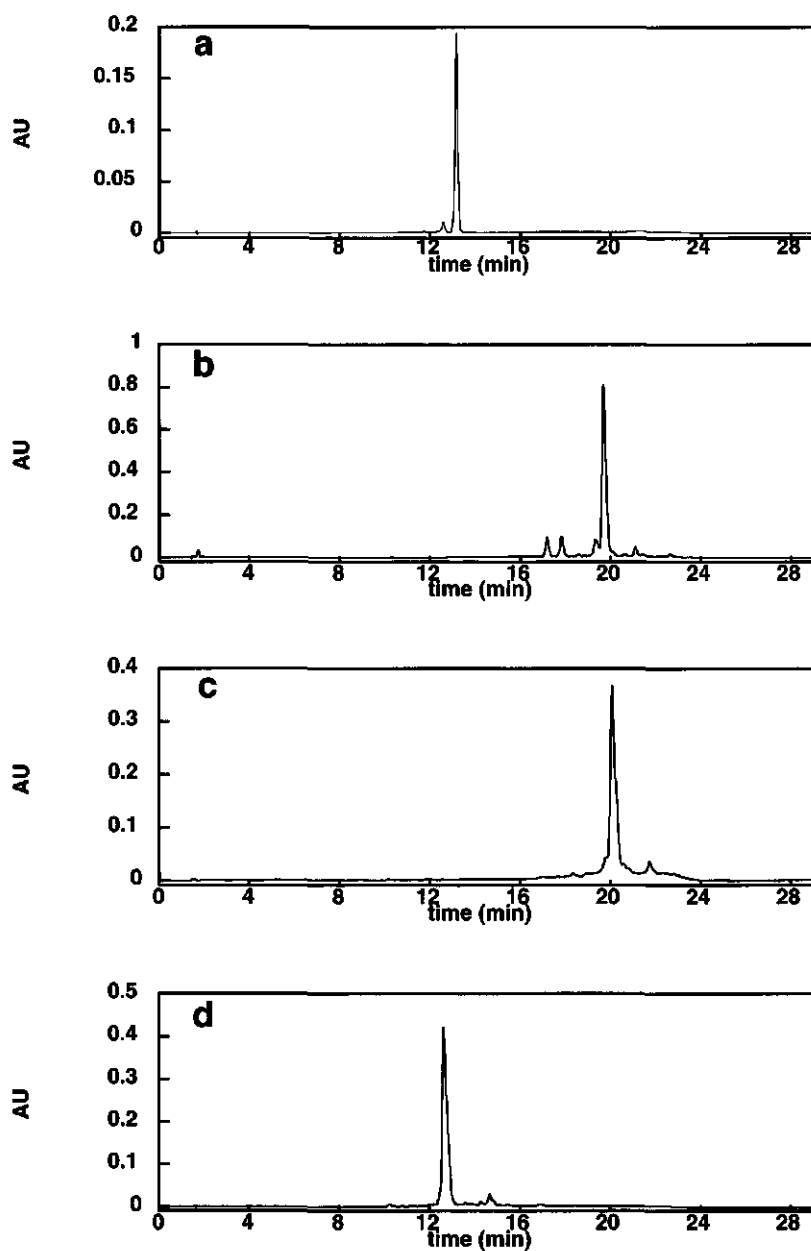


Figure 5.1. HPLC chromatograms of (a) Fe(III)MP-8 monitored at 395 nm, (b) MP-8 free base obtained by the reductive method monitored at 403 nm, (c) MP-8 free base obtained by the HF method monitored at 403 nm, (d) Mn(III)MP-8 monitored at 460 nm.

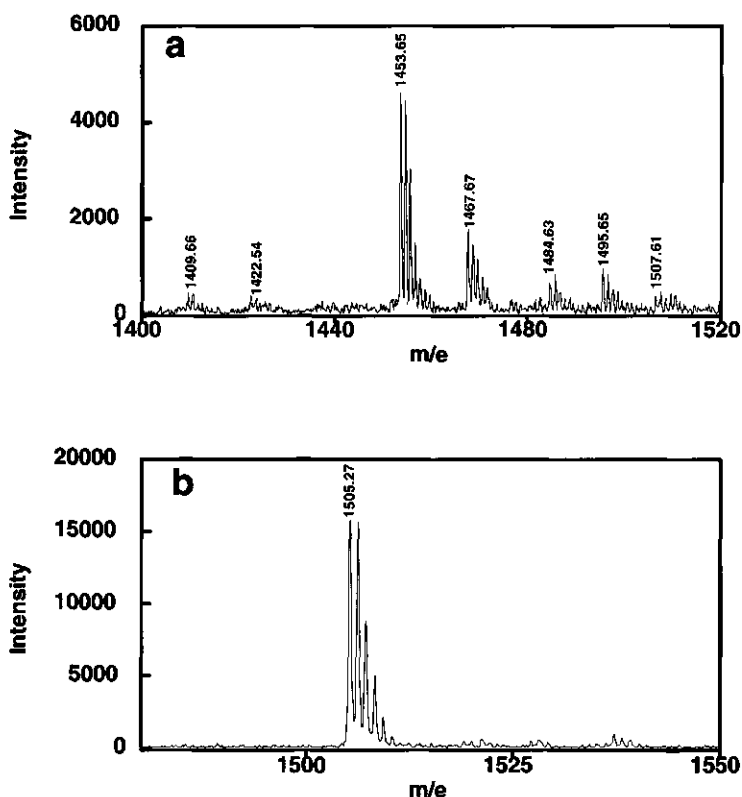


Figure 5.2. MALDI-TOF mass spectrum of (a) MP-8 free base mixture and (b) purified Mn(III)MP-8.

Peroxidase activity of Mn(III)MP-8

The activity as well as the operational stability of Mn(III)MP-8 as compared to Fe(III)MP-8 was investigated in peroxidase type of catalysis by using 2-methoxyphenol (guaiacol) (Baldwin *et al.*, 87) and 3,3'-dimethoxybenzidine (*o*-dianisidine) (Kraehenbuhl *et al.*, 74) as model substrates. Activity profiles as a function of the pH were determined for both catalysts in both assays (Figure 5.4). The results obtained indicate distinct differences in the pH dependent behaviour of Mn(III)MP-8 as compared to Fe(III)MP-8. Most striking is the difference in pH value at which the peroxidase activity starts to occur. Whereas Fe(III)MP-8 peroxidase activity starts around pH 6-7 (Figure 5.4) this value shifts to a 2-3 units higher pH for Mn(III)MP-8. As a result the optimal pH for both catalysts are separated by 2-3 pH units.

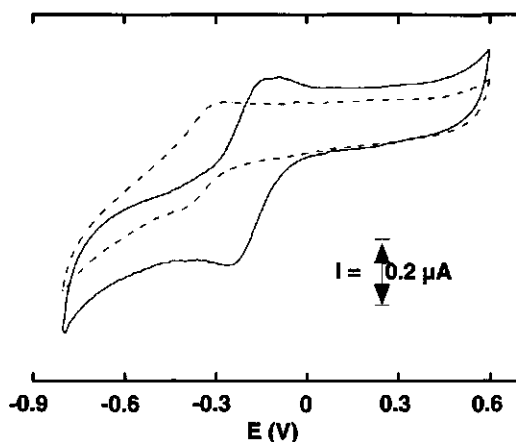


Figure 5.3. Cyclic voltammogram of Fe(III)MP-8 (50 μM) (solid line) and Mn(III)MP-8 (50 μM) (dotted line) in 20 mM KPi pH 7.6. Scan rate: 5 mV/s. The potential axis is defined versus the normal hydrogen electrode.

Maximal activity for peroxidase type of conversion is measured at pH 9 for Fe(III)MP-8 and pH 11 for Mn(III)MP-8. Very similar profiles are observed for the conversion of both substrates by Fe(III)MP-8 whereas the Mn(III)MP-8 corresponding profiles are quite different. The sharp decrease in the conversion of 2-methoxyphenol at pH > 10 is not observed for the 3,3'-dimethoxybenzidine and can be ascribed to the instability of the reaction product (Baldwin *et al.*, 87).

As a next step the operational stability for both catalysts was measured at their optimum pH values using 2-methoxyphenol as the model substrate (Figure 5.5). For a first approximation data were fitted assuming a pseudo-first order degradation of the catalyst with respect to H₂O₂ driven inactivation. Therefore conditions of the assay were chosen such that the 2-methoxyphenol concentration was much larger than the concentration of Mn(III)MP-8 and Fe(III)MP-8 (Spee *et al.*, 96). Inactivation constants obtained were as follows $k_i = 0.104 \pm 0.001 \text{ s}^{-1}$ for Fe(III)MP-8 and $k_i = 0.064 \pm 0.001 \text{ s}^{-1}$ for Mn(III)MP-8. Initial rate values determined from the fit were $k_{\text{cat}} = 21 \pm 0.1 \text{ s}^{-1}$ and $k_{\text{cat}} = 3.4 \pm 0.01 \text{ s}^{-1}$ for Fe(III)MP-8 and Mn(III)MP-8 respectively. Thus the values of the kinetic constants calculated in this way indicate that Mn(III)MP-8 has a 1.6 times higher operational stability than Fe(III)MP-8, and the initial rate of conversion of 2-methoxyphenol by Mn(III)MP-8 is

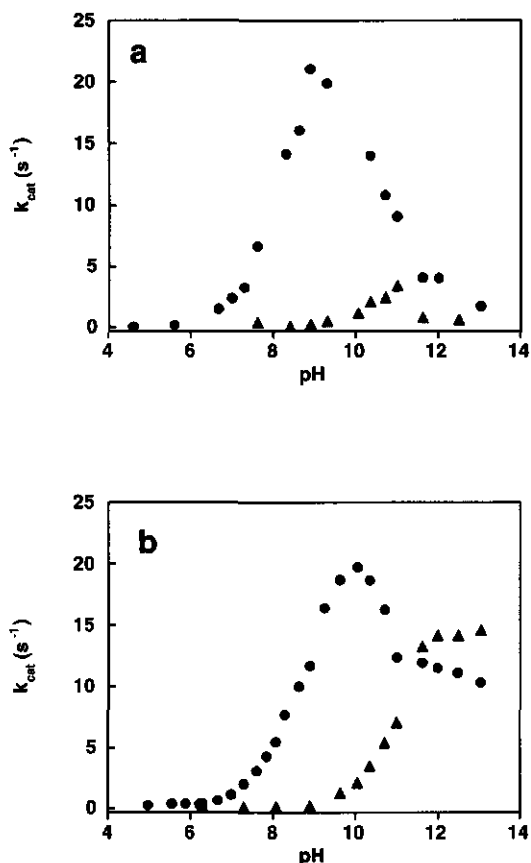


Figure 5.4. The pH profile of the oxidation of (a) 3 mM 2-methoxyphenol and (b) 0.25 mM 3,3'-dimethoxybenzidine catalysed by Fe(III)MP-8 (0.8 μ M) (closed circles) and Mn(III)MP-8 (0.8 μ M) (closed triangles). Hydrogen peroxide concentration was 0.26 mM.

lower as compared to Fe(III)MP-8. As a result, the final extent of conversion of 2-methoxyphenol upon full inactivation of the catalyst is 4 times lower for the Mn(III)MP-8 as compared to Fe(III)MP-8. The same relative changes in k_{cat} and k_i were detected when the experiments were performed at different mini-catalyst concentrations keeping the H₂O₂/MP-8 concentration ratio constant (data not shown). This implies that the difference in activity and inactivation between Fe(III)MP-8 and Mn(III)MP-8 is independent of the mini-catalyst concentration and mainly depends on the nature of the heme peptide.

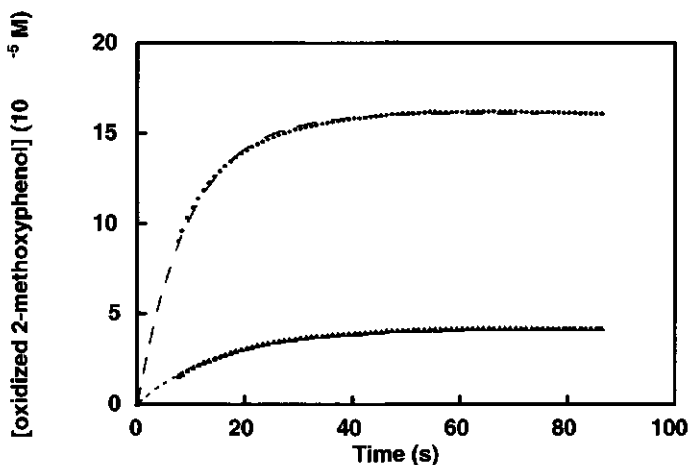


Figure 5.5. Time-dependent oxidation of 2-methoxyphenol (3 mM) catalysed by Fe(III)MP-8 (upper trace) and Mn(III)MP-8 (lower trace) at optimum pH (9.0 for Fe(III)MP-8 and 11.0 for Mn(III)MP-8). Mini-catalysts concentration was 0.8 μ M and hydrogen peroxide concentration 0.26 mM. Data were fitted according to the equation described in the Results section.

Cytochrome P450 activity of Mn(III)MP-8

Cytochrome P450 type of conversion was investigated using aniline *para*-hydroxylation as an oxygen transfer model reaction. Previous studies using ^{18}O labelled $\text{H}_2^{18}\text{O}_2$ proved that the oxygen incorporated into aniline by the Fe(III)MP-8/ $\text{H}_2^{18}\text{O}_2$ system in the presence of 2 mM ascorbate, fully derives from $\text{H}_2^{18}\text{O}_2$ (Osman *et al.*, 96). The assay was performed in the presence and the absence of 2 mM ascorbate. Ascorbate was shown to efficiently block the peroxidase pathway(s) for Fe(III)MP-8 (Osman *et al.*, 96). Results of the present study show that in the presence of 2 mM ascorbate also the Mn(III)MP-8 catalysed conversion of 2-methoxyphenol and 3,3'-dimethoxybenzidine are fully blocked (data not shown). Figure 5.6 presents the HPLC pattern of the incubations of H_2O_2 driven Fe(III)MP-8 and Mn(III)MP-8 conversions of aniline in both the absence and the presence of ascorbate. In the absence of ascorbate conversion by both catalysts results in the preferential formation of large amounts of unidentified polymeric reaction products eluting at a retention time higher than the parent compound (Osman *et al.*, 96) (Figure 5.6a and 5.6b). These polymers most likely result from the radical-type of products formed upon 1 electron oxidation of aniline by Compound I and/or II type of intermediates of the catalysts. In full analogy to the block of peroxidase type of conversions upon addition of 2 mM ascorbate, also the formation of

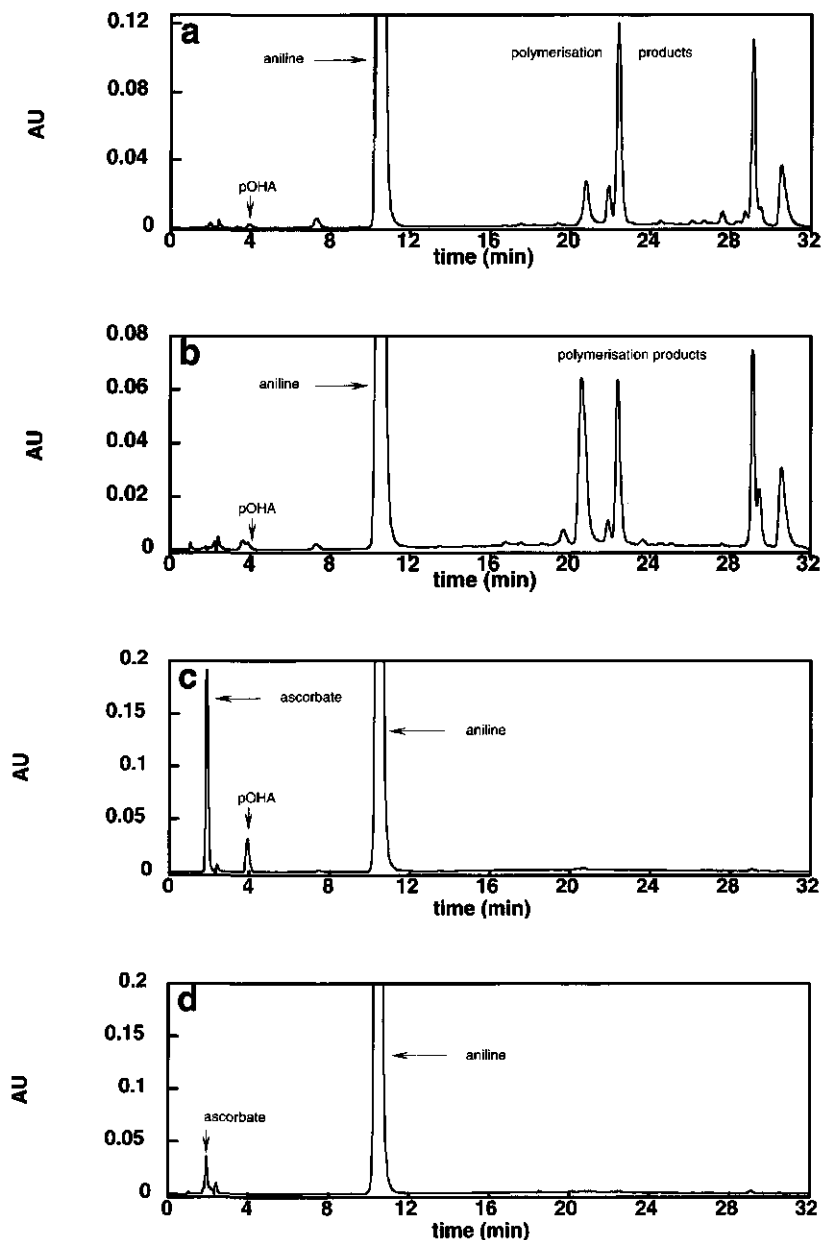


Figure 5.6. HPLC chromatograms monitored at 295 nm of H₂O₂ driven conversion of aniline (10 mM) at optimum pH (9.0 for Fe(III)MP-8 and 11.0 for Mn(III)MP-8) catalysed by (a) Fe(III)MP-8 (7.5 μM), (b) Mn(III)MP-8 (7.5 μM), (c) Fe(III)MP-8 (7.5 μM) in the presence of 2 mM ascorbate, (d) Mn(III)MP-8 (7.5 μM) in the presence of 2 mM ascorbate

these polymeric products is fully inhibited by the presence of 2 mM ascorbate (Figure 5.6c and 5.6d). The effect of the addition of ascorbate on the formation of 4-aminophenol is, however, opposite for the Fe(III)MP-8 and the Mn(III)MP-8. For the Fe(III)MP-8 there is a large increase in the amount of 4-aminophenol formed whereas for the Mn(III)MP-8 the addition of ascorbate decreases the amount of 4-aminophenol formed. Figure 5.7a shows the pH dependency of the 4-aminophenol formation as determined for both catalysts in the

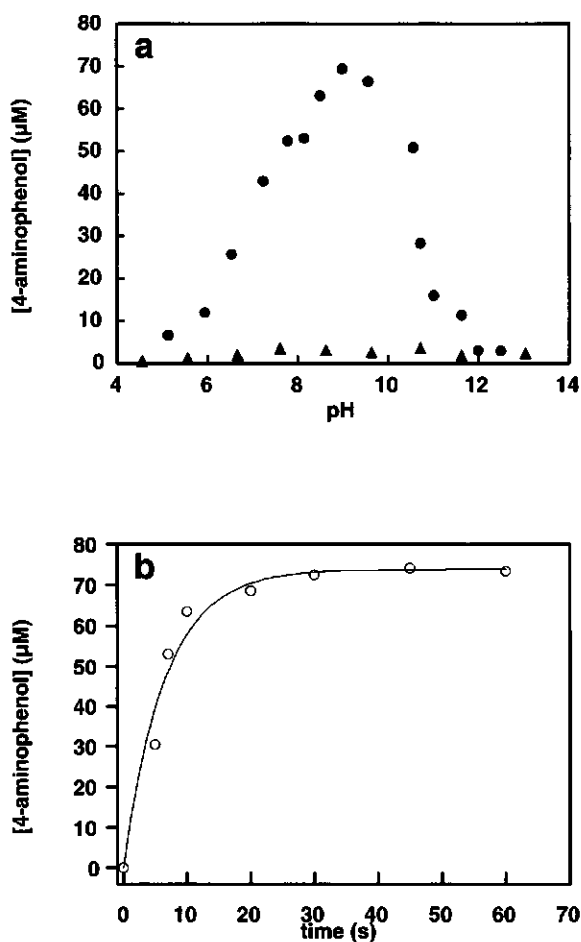


Figure 5.7. H_2O_2 (2.5 mM) driven conversion of aniline (10 mM) in the presence of 2 mM ascorbate by (a) Fe(III)MP-8 (7.5 μM) (closed circles) and Mn(III)MP-8 (closed triangles) (7.5 μM) at different pHs for 1 min incubation time, (b) Fe(III)MP-8 (7.5 μM) at pH 9.0 at increasing incubation time. Data were fitted according to the equation specified in the Results section.

presence of ascorbate. Clearly the data show that Mn(III)MP-8 has almost no activity in aniline *para*-hydroxylation even over a wide pH range, whereas the optimal pH for Fe(III)MP-8 catalysed aniline *para*-hydroxylation is 9. In the presence of ascorbate the amount of 4-aminophenol formed after 1 min with Mn(III)MP-8 is around 3 % of the amount formed with Fe(III)MP-8. As a consequence, operational stability of the mini-catalyst for this assay was only determined for Fe(III)MP-8 at its optimum pH. Figure 5.7b depicts the time-dependent 4-aminophenol formation at 10 mM aniline concentration for Fe(III)MP-8 in the presence of ascorbate. Data were fitted using the same equation as for the peroxidase type of conversion. Kinetic parameters for Fe(III)MP-8 were found as follows: $k_i=0.153 \pm 0.020s^{-1}$ and $k_{cat}=1.51 \pm 0.17s^{-1}$. Comparison to the 2-methoxyphenol oxidation by Fe(III)MP-8 shows a 14 times lower rate of *para*-hydroxylation and a 50 % higher inactivation rate.

5.4 Discussion

The present study deals with the effect of Fe to Mn substitution on the catalytic activity and operational stability of microperoxidase-8. The approach used for the synthesis of Mn(III)MP-8 was based on routine methods from the field of porphyrin chemistry. However, one of the challenges when working with heme-peptides instead of model porphyrins, is to avoid hydrolysis or chemical modification of the octapeptide chain during the de- and remetallation processes. The demetallation method described here (Falk, 64; Fuhrhop and Smith, 75; Espenson and Christensen, 77; Hasegawa *et al.*, 91) is a safer alternative for heme-peptide or hemoprotein demetallation than the hazardous HF method for the demetallation of MP-8 (Low *et al.*, 98). Comparison of the demetallated MP-8 when prepared by both methods, shows the formation of identical products of similar purity. However on HPLC the side-products formed by the present method appeared to be better resolved from the main demetallated MP-8, providing increased resolution during purification.

The ability of Fe(III)MP-8 to act as a peroxidase has been well documented (Kraehenbuhl *et al.*, 74; Baldwin *et al.*, 85; Baldwin *et al.*, 87; Adams, 90; Cunningham *et al.*, 91; Cunningham *et al.*, 92; Cunningham *et al.*, 94). More recently, it was also shown that Fe(III)MP's are capable of catalysing cytochrome P450 type of conversions (Rusvai *et*

al., 88; Mashino *et al.*, 90; Nakamura *et al.*, 92; Okochi et Mochizuki, 95; Osman *et al.*, 96; Dorovska-Taran *et al.*, 98). In the present study the *para*-hydroxylation of aniline was chosen as the model reaction for cytochrome P450 type of oxygen transfer. This choice was motivated by the previous demonstration that the addition of ascorbate blocks the H₂O₂ driven Fe(III)MP-8 catalysed formation of peroxidase-type of dimerization and polymerisation products from aniline, and increases the amount of *para*-hydroxylation (Osman *et al.*, 96) which has been confirmed in this study. This indicates that Fe(III)MP-8/H₂O₂ driven aniline conversion in the presence of ascorbate, provides a model system for studying oxygen transfer reactions instead of peroxidase type of reaction chemistry. The fact that ¹⁸O labelling studies demonstrated 100 % ¹⁸O incorporation into 4-aminophenol in the ascorbate containing Fe(III)MP-8/H₂¹⁸O₂ incubation (Osman *et al.*, 96) further supports this conclusion. Finally, previous studies (Osman *et al.*, 96; Dorovska-Taran *et al.*, 98; van Haandel *et al.*, 98) have eliminated the involvement of Fenton chemistry in reactions catalysed by Fe(III)MP-8. Thus in the present study it can be ignored.

The present results demonstrate that not only the Fe(III)MP-8 catalysed peroxidase reactions are inhibited by 2 mM ascorbate but also the Mn(III)MP-8 catalysed conversion of both 2-methoxyphenol and 3,3'-dimethoxybenzidine. To explain the differential effect of ascorbate on either peroxidase reactions or cytochrome P450 type of oxygen transfer to aniline by Fe(III)MP-8 the working hypothesis depicted in Figure 5.8 and adapted from the literature (Dorovska-Taran *et al.*, 98) can be put forward. The effects of the Fe to Mn substitution observed in the present study may then also be explained on the basis of this scheme.

First the model suggests that for the Fe(III)MP-8 in the presence of ascorbate, the nature of the reactive intermediate involved in the oxygen transfer to aniline is not a Compound I or II type of intermediate. In the absence of ascorbate Compound I and II are responsible for peroxidase-type of conversion of 2-methoxyphenol and 3,3'-dimethoxybenzidine, for the formation of dimerization and polymerisation products from aniline and/or for (part of the) oxygen incorporation into aniline, generating 4-aminophenol (Osman *et al.*, 96). Ascorbate is a better substrate for Compound I and II than aromatic substrates, allowing both reactive species to be scavenged (Chance, 49; Chance 52). As a result, the addition of ascorbate prevents peroxidase type of substrate conversions as well as polymerisation product formation from aniline. In addition, ascorbate may inhibit peroxidase-type of product formation by scavenging the substrate radicals

formed, reducing them to the original substrate molecules and thus preventing the formation of peroxidase-type of products (Osman *et al.*, 96). In the Fe(III)MP-8 system the oxygen transfer to aniline, resulting in formation of 4-aminophenol, is not inhibited by 2 mM ascorbate because it is supposed to be formed by another type of heme-iron oxygen intermediate. This other type of electrophilic heme-iron oxygen intermediate could be the heme-iron-hydroperoxide anion formed in the catalytic cycle before heterolytic cleavage of the dioxygen bond and formation of Compound I (Figure 5.8).

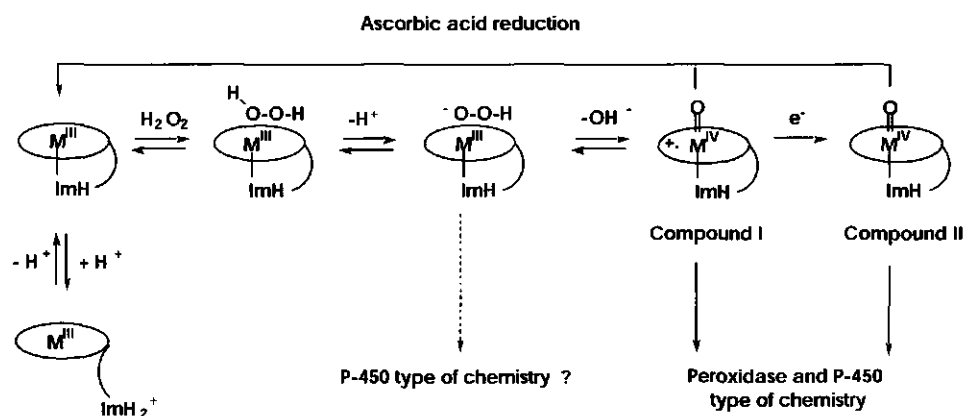


Figure 5.8. Supposed relation between the different possible intermediates involved in M(III)MP-8/ H₂O₂ driven oxidation of substrates. The end-on coordination geometry of the hydroperoxide anion is suggested to be the most probable in water solution (Loew and Dupuis, 96), side-on geometries have also been characterized for crystals of hydrophobic porphyrins (VanAtta *et al.*, 87). Key: ImH stands for the imidazole moiety of the coordinated histidine; M stands for both Fe and Mn. Adapted from literature (Dorovska-Taran *et al.*, 98).

Recently kinetic evidence for the existence of such an iron-hydroperoxide anion, formed prior to Compound I, has been reported using the horseradish peroxidase R38L mutant (Rodriguez-Lopez *et al.*, 96; Rodriguez-Lopez *et al.*, 97). The ability of peroxide intermediates to catalyse oxygen transfer reactions is supported by many chemical studies (for a review see Curci and Edwards, 91), as well as by the electrophilic monooxygenase activity of flavin based aromatic monooxygenases which use the C(4a)hydroperoxyflavin as the reactive species (Entsch *et al.*, 76; Maeda-Yorita and Massey, 93; Ridder *et al.*, 98). Such a monooxygenase activity of a supposed heme-iron-hydroperoxide anion intermediate

has been suggested before (Swinney and Mak, 94; Coon *et al.*, 96; Vaz *et al.*, 96; Lee and Nam, 97; Vaz and *al.*, 98; Dorovska-Taran *et al.*, 98; Lee *et al.*, 98) in, for example, the epoxidation of unactivated olefins (Vaz *et al.*, 98; Lee *et al.*, 98) or the deformylation of aldehydes (Vaz *et al.*, 96; Coon *et al.*, 96). Untill now, no involvement of a heme-iron-hydroperoxide intermediate has been suggested for the conversion of less reactive substrates such as alkanes for instance. It seems that the role of a heme-iron hydroperoxide intermediate would especially be relevant for the oxygen transfer to relatively reactive electron rich substrates, such as aniline, whereas for less reactive substrates Compound I and II would be involved. Alternatively, one might suggest that aniline could bind directly to the iron(III) centre, thereby activating it for hydroxylation by hydrogen peroxide.

The results of the present study for the Mn(III)MP-8 can best be explained on the basis of the lower oxidative potential of Mn as compared to Fe. The cyclic voltammetry results of the present study, as well as data from the literature (Harbury and Loach, 60a; Harbury and Loach, 60b; Low *et al.*, 98) are in line with this lower oxidative electron withdrawing nature of manganese as compared to iron. A lower oxidative potential of the metal centre would reduce the electrophilicity of the metal-oxo Compound I and II, thereby increasing their kinetic stability and decreasing their reactivity for electrophilic attack on substrates. This explains the decrease in peroxidase activity and the increase in operational stability upon Fe to Mn substitution. Furthermore, the lower oxidative potential of the Mn as compared to Fe reduces the electrophilicity of the metal(III)OOH MP-8 intermediate thereby lowering its reactivity in oxygen transfer to aniline and/or its possibility to activate aniline upon ligation for hydroxylation by hydrogen peroxide. Alternatively, the lower oxidative potential of Mn would increase the tendency of the metal(III)OOH MP-8 intermediate for heterolytic cleavage and Compound I formation. This reduces the chance for aniline *para*-hydroxylation by a metal(III)OOH species. Another effect of the Fe to Mn substitution would be the higher pH values necessary to induce the formation of the reactive metal-peroxo and metal-oxo (Compound I and II) complexes (Figure 5.8). Especially when it is assumed that the metal centre supports the initial deprotonation of the H₂O₂ in the MP-8/H₂O₂ complex. Due to its lower oxidative potential, Mn may lower the pK_a for H₂O₂ deprotonation (about 12 in solution (Jones and Dunford, 77; Baldwin *et al.*, 87) to a lesser extent than the Fe centre. This would explain why the Mn(III)MP-8 catalysed peroxidase reactions start to be observed at pH values 2-3 units higher than observed for the Fe(III)MP-8.

Thus, altogether, the data in the present study demonstrate that the lower oxidative power of Mn as compared to Fe, significantly affects the catalytic activity, the operational stability and also the pH dependent behaviour of Mn(III)MP-8 as compared to Fe(III)MP-8.

Acknowledgments

This work was supported by the Netherlands Foundation for Technical Research (STW), the National Centre for Scientific Research (CNRS) and by the Wageningen NMR Center, EU contract CHGE-CT94-0061. Financial aid from the Netherlands Organization for Scientific Research (NWO) is acknowledged.

6

Isolation and Characterisation of a Microperoxidase-8 with a Modified Histidine Axial Ligand; Implications for the Nature of Activated Heme-Oxo Intermediates.

Jean-Louis Primus, Sjef Boeren, Jacques Vervoort, Lucia Banci,
and Ivonne M.C.M. Rietjens.

Submitted

Abstract

Microperoxidase-8, Fe(III)MP-8, the heme octapeptide obtained by horse heart cytochrome c digestion, was studied in the presence of H₂O₂. A modified form of the catalyst was isolated by HPLC and showed a UV/visible spectrum similar to that of Fe(III)MP-8. ESI-MS measurements revealed a 16 Da increase in molecular mass for the modified catalyst when compared to Fe(III)MP-8, suggesting the insertion of an oxygen atom. ESI-MS² fragmentation measurements point at oxygen incorporation on the His18 residue of the octapeptide of the modified catalyst. Comparison of the ¹H NMR chemical shifts of the methyl protons of the porphyrin ring of Fe(III)MP-8 and the modified catalyst shows a large shift for especially the 3-methyl and 5-methyl resonances whereas the other ¹H NMR chemical shifts are almost unaffected. These observations can best be ascribed to a reorientation of the histidine axial ligand. The latter is suggested to be the consequence of an oxygen insertion on the imidazole ring of the His18 thereby corroborating the data obtained by ESI-MS². ¹H NMR NOE difference measurements on Fe(III)MP-8 and on the modified catalyst allowed to assign the H δ 2 and H ϵ 1 protons of the imidazole ring but not the H δ 1 proton in both forms of the catalyst. For Fe(III)MP-8 this absence of the H δ 1 resonance can be ascribed to fast H/D exchange whereas in the modified catalyst the NMR data are consistent with an oxygen insertion on position δ 1 of the His18 imidazole ring or – alternatively- with fast H/D exchange. Together these data identify the H₂O₂ modified catalyst as Fe(III)MP-8 with a hydroxylated His18 axial ligand. Analysis of the mechanism that could underlie Fe(III)MP-8 axial histidine hydroxylation and consequences for the nature of the Fe(III)MP-8 reactive catalytic intermediates are further discussed.

6.1 Introduction

The comprehension of the mechanisms underlying peroxidase and cytochrome P450 supported catalysis (Ortiz de Montellano, 92; Colonna *et al.*, 99; Guengerich and MacDonald, 84; Mansuy and Battioni, 2000) has been aided by the use of biomimetic models in order to understand the very details of their catalytic cycle (Mansuy, 87; Traylor, 91; Meunier, 92; Groves, 97; Weiss *et al.*, 2000).

Microperoxidase-8, Fe(III)MP-8, is a hydrosoluble biomimic obtained by controlled proteolytic digestion of horse heart cytochrome c retaining the axial histidine 18 as proximal ligand. Fe(III)MP-8, consists of an iron protoporphyrin IX connected to an octapeptide *via* two thioether bonds (Aron *et al.*, 86). The distal heme ligand can be easily exchanged for an oxygen donor such as H₂O₂, leading to the formation of reactive intermediates able to act in both peroxidase and cytochrome P450 model reactions (Aron *et al.*, 86; Osman *et al.*, 96; Primus *et al.*, 99 and references therein). This makes Fe(III)MP-8 an appealing model for studying peroxidase- and cytochrome P450-type of catalysis.

For peroxidase enzymes, a high-valent iron-oxo porphyrin radical cation, Compound I, having two equivalents of oxidation above the resting oxidation state of the enzyme, and the one electron reduced form, Compound II, are generally accepted as reactive intermediates (Ortiz de Montellano, 92). For Compound I, one oxidation equivalent is localised on the iron centre, like for Compound II. The second oxidation equivalent is delocalised as a radical on an organic moiety, generally the porphyrin macrocycle (Dolphin *et al.*, 71; Pond *et al.*, 98) or a protein residue (Yonetani and Ray, 65; Davies and Puppo, 92; Su *et al.*, 98). For cytochromes P450 the involvement of an isoelectronic form of peroxidase Compound I is postulated in most of the reactions (Sono *et al.*, 96; Coon *et al.*, 98; Mansuy and Renaud, 95), but involvement of a porphyrin iron-hydroperoxo intermediate or a porphyrin iron-peroxo intermediate is also proposed (Swinney and Mak, 94; Vaz *et al.*, 96; Coon *et al.*, 96; Lee and Nam, 97; Lee *et al.*, 98; Vaz *et al.*, 98; Dorovska-Taran *et al.*, 98; Primus *et al.*, 99).

The operational stability of Fe(III)MP-8 is closely related to the reactivity of the oxygen activated intermediates. Studies performed on a series of microperoxidases revealed that substrate, human serum albumin or antibody addition can protect the catalyst against inactivation, increasing its half-life in the presence of H₂O₂ (Spee *et al.*, 96; Metelitzka *et al.*, 94). This substrate/additive mediated protection is best ascribed to a competition between substrate/additive and the catalyst itself for oxidation by the high-valent iron-oxo (porphyrin radical cation) and/or porphyrin iron-(hydro)peroxo intermediates (Brown, 76; Traylor, 91). For hemoproteins, an intramolecular reaction of the reactive iron-(hydro)peroxo is probably involved in their catabolism (Brown *et al.*, 78; Wilks and Ortiz de Montellano, 93; Wilks *et al.*, 94; Takahashi *et al.*, 94; Ortiz de Montellano, 98). In addition to intramolecular reactions, intermolecular oxidative inactivation pathways may occur, although for peroxidase-enzymes with shielded porphyrin active sites, the chances for such intermolecular reactions seem to be much lower. The involvement of heme-oxo or heme-(hydro)peroxo intermediates is postulated in porphyrin ring opening (Bonnett and McDonagh, 73; Brown *et al.*, 78; Florence, 85) starting with oxidation at one of the carbon *meso* positions (Bonnett and Dimsdale, 72; Wilks and Ortiz de Montellano, 93; Wilks *et al.*, 94; Torpey and Ortiz de Montellano, 96; Torpey and Ortiz de Montellano, 97) and/or by other inactivation/heme degradation reactions including: non-*meso* ring hydroxylation (Sugiyama *et al.*, 97), modification of the porphyrin macrocycle through substrate suicide inhibition (Wiseman *et al.*, 82; Ator and Ortiz de Montellano 87a; Ator and Ortiz de Montellano 87b; Dexter and Hager, 95; Tian *et al.*, 95; Raner *et al.*, 97), adduct formation between the porphyrin ring and an oxidised protein residue(s) (Fox *et al.*, 74; Ortiz de Montellano, 87; Catalano *et al.*, 89; Osawa and Korzekwa, 91).

In the present work, the nature of a H₂O₂-dependent derivative of Fe(III)MP-8 is characterised by ¹H NMR and ESI MS² as a hydroxylated His18 Fe(III)MP-8. A possible mechanism for the formation of this modified intermediate proceeds by mesomerism resulting in partial delocalisation of the second oxidation equivalent of the postulated Fe(III)MP-8 Compound I analogue on the axial histidine ligand of the heme-peptide.

6.2 Materials and methods

Chemicals

Cytochrome c from horse heart was obtained from Boehringer (Mannheim, Germany). Fe(III)MP-8 was prepared by proteolytic digestion of horse heart cytochrome c essentially as described previously (Aron *et al.*, 86; Low *et al.*, 96). Sodium cyanide was purchased from Fluka (Buchs, Switzerland). L-Ascorbic acid and unlabelled H₂O₂ (30%) were from Merck (Darmstadt, Germany). Hydrogen peroxide was diluted in water to obtain a concentrated stock solution. The concentration of the latter solution was always checked spectrophotometrically using the molar extinction coefficient at $\epsilon_{240} = 39.4 \pm 0.2 \text{ M}^{-1} \cdot \text{cm}^{-1}$ (Nelson and Kiesow, 72). All HPLC solvents were of chromatographic grade. All other reagents used were of analytical grade.

Preparation of H₂O₂-driven intermediate

A typical incubation consisted of (final concentration) 100 μM of Fe(III)MP-8 in the presence of a 2-fold excess of H₂O₂, unless indicated otherwise, incubated for 1 min at 37 °C in a total volume of 0.2-20 mL, depending on the amount of intermediate required, 0.1 M potassium phosphate pH 7.6. The reaction was quenched by directly injecting a 10 μL aliquot on a HPLC column for analysis or by freezing the sample in liquid nitrogen followed by lyophilisation.

Isolation of the intermediate

Separation of the intermediate was performed by semi-preparative HPLC using two Isco Model 2300 HPLC pumps equipped with a Pye Unicam LC-UV Detector. The lyophilised preparation was dissolved in eluent A under vigorous stirring, followed by centrifugation. The supernatant, typically 300 μL , was loaded on a Waters Delta-Pak C18 column (25 \times 200 mm, 300 Å pore size, 10 μm particle size). Elution was performed with a gradient of 0.1 % trifluoroacetic acid/H₂O (eluent A) and 0.1 % trifluoroacetic acid /CH₃CN (eluent B) at 8 mL.min⁻¹. For semi-preparative purification of the intermediate, 5 % of B were first applied for 3 min then the percentage of B was increased to 31 % within 2 min followed by a linear gradient from 31 to 34 % B over 15 min. Care was taken to minimise exposure of the intermediate to room temperature and therefore the collected

fractions were stored on ice and once pooled, immediately frozen for lyophilisation. The intermediate was stable as a powder for a couple of months at 4 °C.

HPLC analysis

Analytical HPLC analysis of Fe(III)MP-8 H₂O₂ treated samples was performed using a Waters 600 pump equipped with a Waters 996 Photodiode Array Detector. Analysis was carried out on a Waters Delta-Pak C18 column (3.9 × 150 mm, 300 Å pore size, 5 µm particle size) and elution was carried out at a flow of 1 mL.min⁻¹ with 0.1 % trifluoroacetic acid/H₂O (eluent A) and 0.1 % trifluoroacetic acid/CH₃CN (eluent B) using a linear gradient from 20 to 38 % B over 18 min. Products were identified by comparison of observed peaks to the retention time and UV/visible spectrum of available standards combined with mass spectrometry and ¹H NMR spectroscopy.

Labelling experiments

Incubations in 95 % ¹⁸O-containing labelled water or with a 2-fold excess of 90 % ¹⁸O-containing labelled hydrogen peroxide were analysed by on-line ESI LC-MS. Typically, 50 µM Fe(III)MP-8 were incubated 1 min at 25 °C with a 2-fold excess labelled or non labelled hydrogen peroxide in 0.1 M potassium phosphate pH 7.6. The incubated samples were subsequently injected on a Waters Delta-Pak C18 column (2 × 150 mm, 300 Å pore size, 5 µm particle size) eluted isocratically at 1 mL.min⁻¹ with 26 % (eluent B). The mass analysed were performed as described in the next paragraph and were averaged out of 5 to 15 scans. The obtained mass isotopic distributions were compared with a linear combination of the non-labelled modified Fe(III)MP-8 and of the ¹⁸O-labelled modified Fe(III)MP-8. Consequently the ¹⁸O-labelling extent of the modified Fe(III)MP-8 could be estimated within 5 % variation.

Mass spectrometry analysis

Lyophilised samples of purified Fe(III)MP-8 or of the purified intermediate of Fe(III)MP-8 were dissolved in water and directly injected into the electrospray source. The mass spectrometry analysis (Finnigan MAT 95, San Jose, CA, USA) was performed in the positive electrospray mode using a spray voltage of 4.5 kV, a capillary voltage of 47 V and a capillary temperature of 180 °C with nitrogen as sheath and auxiliary gas. (MS)ⁿ

experiments were performed the same way with a separation width of 4 m/z, helium as the collision gas and relative collision energies between 23 and 28 %.

¹H NMR spectroscopy analysis

¹H NMR measurements were performed on a Bruker Avance 800 MHz spectrometer and on a Bruker AMX 500 spectrometer. Samples were dissolved in deuterated methanol CD₃OH to avoid aggregation and a 5-fold excess of solid sodium cyanide was added to the solution in the NMR tube to produce a low spin iron(III) species, which experiences narrower lines for nuclei close to the metal ion than the high spin species. Due to the instability of the intermediate, all measurements were carried out at 281 K. Typically acquisition of 1-D spectra was performed with a sweep width of 48 kHz at 800 MHz and 31.25 kHz at 500 MHz. Two-dimensional spectra were obtained with sweep widths varying from 16 to 32 kHz at 800 MHz and 24 kHz at 500 MHz in both dimensions, 4K points in F2, and 1K points in F1. Data were processed using the standard Bruker Software to a final size of 2K × 2K data points and multiplied by squared shift sine window functions prior to Fourier transform. For NOESY and TOCSY spectra the standard pulse sequences from the Bruker software were used. NOESY spectra were obtained with a mixing time of 250 ms to 350 ms, a pre-saturation time of 1 s and 96 scans per increment. TOCSY spectra were obtained using a DIPSI spinlock with a spinlock power of 7.8 W, a spinlock time of 80 ms, and 16 to 56 scans per increment. NOE differences experiments were performed on a Bruker AMX500 spectrometer operating at 500.14 MHz. For measurements of the NOE effect, the pulse sequence developed by Banci *et al.* (Banci *et al.*, 89) was used. A total of 16 K data points were collected over a 31.25 kHz band width. Selective saturation of the signal was performed by using a selective decoupling pulse of 0.016 W for the intermediate and 0.005 W for Fe(III)MP-8 kept on for 213 ms.

6.3 Results

HPLC analysis of the intermediate

Figure 6.1 shows the HPLC chromatogram of Fe(III)MP-8 incubated with a 2-fold excess of H₂O₂. Fe(III)MP-8 is eluting at 13.3 min. One modified heme product eluting at 11.9 min is observed which can be ascribed to a H₂O₂-driven intermediate. Both Fe(III)MP-8 and the intermediate have identical UV/visible spectra, with no decrease of intensity and no red-shift of the Soret band for the intermediate (data not shown) suggesting that the porphyrin ring of the intermediate is not altered (Wilks and Ortiz de Montellano, 93).

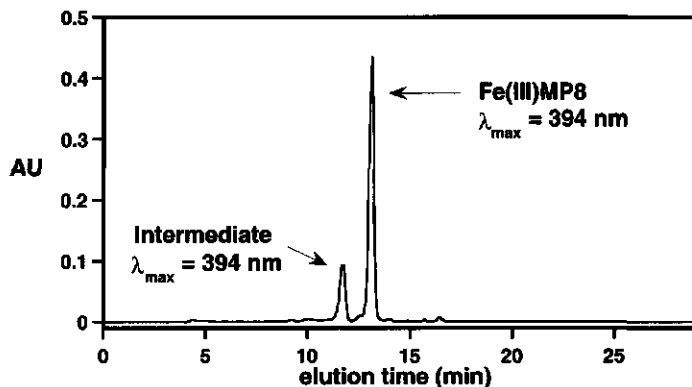


Figure 6.1 HPLC chromatogram, monitored at 395 nm, of 20 μM Fe(III)MP-8 incubated 1 min at 37°C with a 2-fold excess of H₂O₂. One product, eluting 1.4 min before Fe(III)MP-8 is detected. Both Fe(III)MP-8 and the H₂O₂-driven intermediate have a similar UV/visible spectrum.

ESI-mass spectrometry analysis of the isolated intermediate

The isolated intermediate was analysed by mass spectrometry. The intermediate ion peak is detected at m/z 1521.3 (Figure 6.2a). Comparison of the data presented in Figure 6.2a to the mass spectrum of Fe(III)MP-8 (m/z 1505.3) (spectrum not shown), reveals a 16 Da mass difference between both molecules. This increase of 16 Da for the intermediate when compared to Fe(III)MP-8 points at the insertion of an oxygen atom. The detection of a water elimination product in the ESI-mass spectrum of the intermediate (m/z 1503.3) (Figure 6.2a), but not in the ESI-mass spectrum of Fe(III)MP-8 (spectrum not shown),

further corroborates the hypothesis of the insertion of an oxygen atom on the intermediate molecule.

Two subsequent steps of MS-MS fragmentation, MS^2 and MS^3 , of the peak at m/z 1521.3 lead to the detection of ion peaks corresponding to N-terminal fragmentation at the octapeptide amide bonds; b ion fragments (Roepstorff and Fohlman, 84) (Figure 6.2b and 2c). Fragments b_8^* , b_7^* , b_6^* and b_5^* all lack 2 Da relative to the fragments expected for the CAQCHTVE sequence of the Fe(III)MP-8 octapeptide. In contrast fragments b_4 and b_3 perfectly match these expected values. Since the fragmentation is a recurrent process starting from the C-terminal end of the octapeptide and leading to b_8^* as the initial product, these results indicate that the b_5^* fragment is the last fragment in the series missing 2 Da. This implies that the C-terminal amino-acid in fragment b_5^* , i.e. His18, is the one actually lacking the 2 Da. Assuming these missing 2 Da can be assigned to 2 protons, this leads to the conclusion that these protons may be the ones accompanying the initial loss of the inserted oxygen atom as a water molecule from the intermediate (Figure 6.2a and 6.2b). This indicates that the extra oxygen atom inserted on the intermediate originates from the His18 residue. As a consequence, these ESI-mass spectrometry data indicate that the isolated Fe(III)MP-8 H_2O_2 -driven intermediate differs from Fe(III)MP-8 by the fact that it has an extra oxygen atom inserted on the histidine residue of the peptide.

1H NMR analysis of the isolated intermediate

Fe(III)MP-8 and the intermediate were analysed by 1H NMR spectroscopy. All resonances except for the ones of the peptide amide protons and of the histidine imidazole ring protons were assigned on the basis of 800 MHz 1-D, 2-D NOESY and 2-D TOCSY measurements performed at 281 K (Table 6.1). Assignments for Fe(III)MP-8 were slightly different from Low *et al.* (Low *et al.*, 97) probably due to temperature effects. Comparison of the C_α proton resonances for Fe(III)MP-8 and the intermediate shows a difference of at most 0.3 ppm between the corresponding resonances of the two molecules (Table 6.1). This suggests no differences between the peptide backbone of Fe(III)MP-8 and the peptide backbone of the modified Fe(III)MP-8. Assignments for the protons of the heme ring substituents of Fe(III)MP-8 and the intermediate are also compared in Table 6.1.

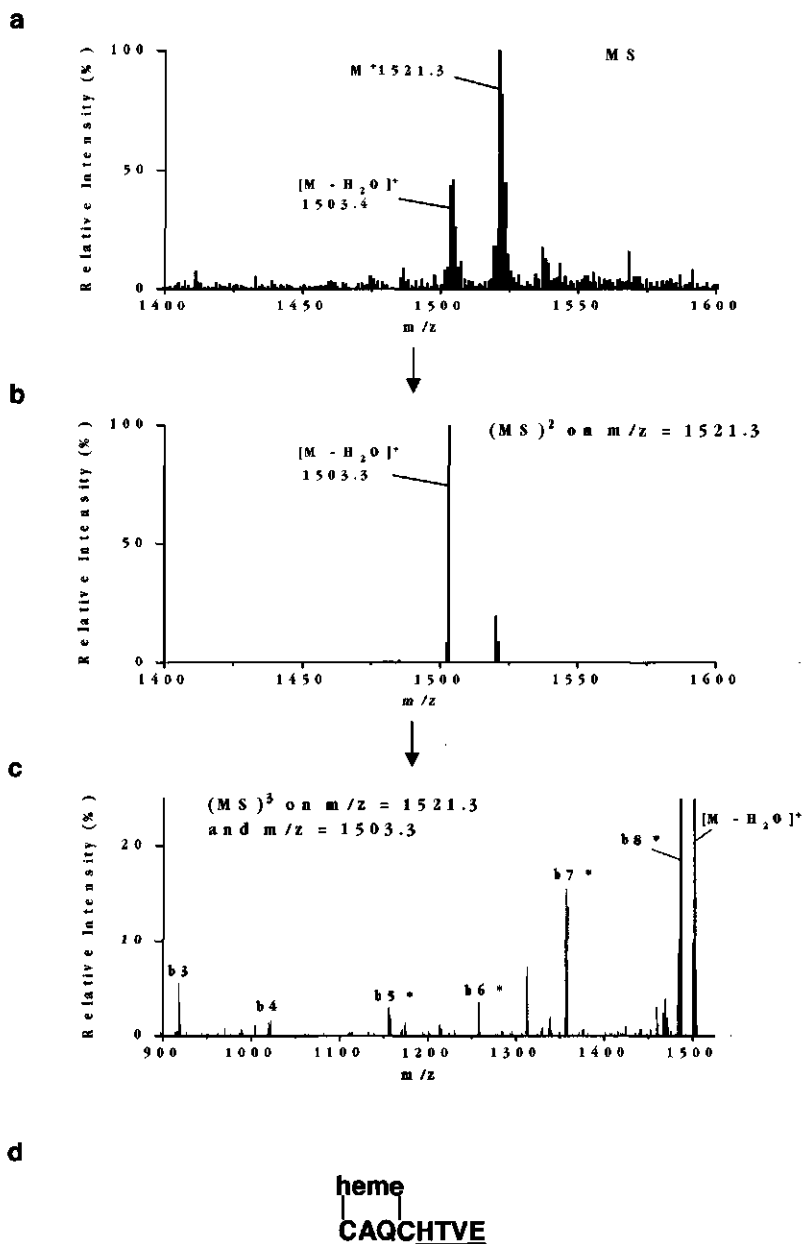


Figure 6.2 Detection of the localisation of the inserted oxygen atom by ESI mass spectrometry. (a) Mass spectrum of the isolated intermediate. The peak at m/z 1503.3 corresponds to a water elimination product. (b) MS^2 fragmentation of the peak at m/z 1521.3 in Figure 6.2a. The mass spectrum depicts the product resulting from water elimination already detected in Figure 6.2a at m/z 1503.4 (c) Mass spectrum obtained after MS^2 fragmentation of the peak at m/z 1503.3 in Figure 6.2b. The predicted N-terminal or b ion fragments (Roepstorff *et al.*, 84) of the octapeptide are labelled in the spectrum. Fragments marked with an asterisk, *i.e.* fragment b8* to fragment b5*, match the N-terminal fragments of the heme-peptide sequence (presented in d) minus 2 Da whereas fragments b4 and b3 perfectly match the corresponding fragments of the octapeptide.

Table 6.1 ^1H chemical shifts of the H_2O_2 driven intermediate compared to the corresponding Fe(III)MP-8 values the latter given between brackets. Measurements were carried out at 281 K.

(A) Peptide Resonances (ppm)				
residue	H α	H β	H γ	other
Cys 14	3.00 (-)	2.62 (-); 3.64 (-)		
Ala 15	5.77 (5.94)	2.04 (2.10)		
Gln 16	4.45 (4.55)	1.86 (1.97); 1.95 (2.13)	2.21 (2.35); (-) 2.43	7.41 (7.47), 7.61 (7.65)
Cys 17	5.29 (5.55)	1.29 (0.87); 2.74 (2.50)		
His 18	9.80 (9.63)	9.51 (10.12); 12.62 (12.96)		H δ 2 16.22 (16.32); H ϵ 1 -3.68 (-3.34)
Thr 19	5.70 (5.74)	5.13 (5.20)	2.04 (2.12)	
Val 20	5.07 (5.21)	2.80 (2.93)	1.62 (1.70); 1.59 (1.75)	
Glu 21	4.79 (5.08)	2.53 (2.68); 2.65 (2.82)	2.88 (3.04); 2.84 (3.08)	

(B) Heme Ring Resonances (ppm)			
substituent		substituent	
8-CH3	23.18 (23.88)	δ -meso	-1.56 (-2.83)
5-CH3	27.43 (22.71)	γ -meso	7.98 (7.74)
3-CH3	6.52 (10.77)	β -meso	-2.06 (-2.03)
1-CH3	18.06 (17.68)	α -meso	3.90 (4.31)
2- α H	1.17 (0.78)	6- α CH2	3.97 (2.95); 5.69 (4.50)
2- β CH3	1.24 (0.48)	6- β CH2	1.11 (0.71); (-) (-)
4- α H	-2.21 (-1.25)	7- α CH2	2.60 (3.78); 3.39 (4.38)
4- β CH3	-0.13 (0.12)	7- β CH2	0.63 (0.88); 0.63 (-)

Most of the resonances show only little variation between both molecules except for the 3-methyl and 5-methyl resonances which show a large difference of more than 4 ppm whereas the 1-methyl and 8-methyl resonances vary by only 0.4 ppm and 0.7 ppm respectively (Figure 6.3). Since the chemical shift values of the heme methyl substituents are determined by the electron density distribution on the heme moiety (Shulman *et al.*, 71; Turner, 95; Shokhirev and Ann Walker, 98; Kolczak *et al.*, 99) this observation indicates that there is a difference in the electron distribution on the heme moiety of the intermediate when compared to the electron distribution on the heme moiety of Fe(III)MP-8 (see Discussion).

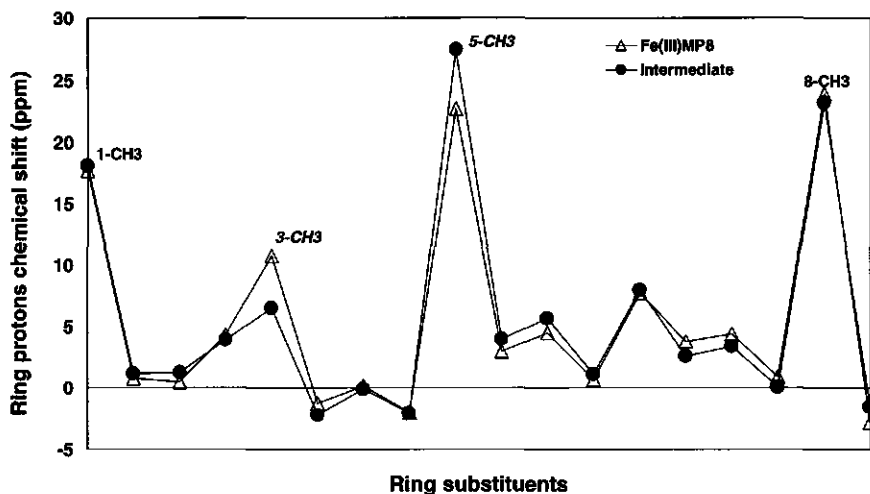


Figure 6.3 Plot of the chemical shifts of the ring substituents for both Fe(III)MP-8 and the intermediate. The graph shows a variation of especially the 3-methyl and 5-methyl heme resonances when comparing the intermediate to Fe(III)MP-8.

His18 imidazole ring resonances could not be derived from the acquired 2D-NOESY and TOCSY data sets because of fast relaxation and intrinsic large line widths of the corresponding protons (Louro *et al.*, 98). The assignment of the His18 imidazole ring protons for the intermediate was performed by 1-D ¹H NOE difference measurements (Figure 6.4) (Banci *et al.*, 89). Saturation of the broad signal at 16.2 ppm (Figure 6.4b) shows two NOE's from the saturated peak to respectively, the His18 H β 1 and the 8-methyl protons. Saturation of the broad signal at -3.7 ppm (Figure 6.4c) shows two NOE's from the saturated peak to respectively, the β -meso and the 4- α H protons. Based on these NOE's, the resonance at 16.2 ppm is found consistent with the assignment to the non-exchangeable proton H δ 2 of the axial histidine ligand. The His18 H δ 2 and H β 1 protons are about 2.7 Å away from each other according to the crystal structure of horse heart cytochrome c (Bushnell *et al.*, 94). The resonance at -3.7 ppm was deductively assigned to the non-exchangeable He1 proton of His18. These assignments for H δ 2 and He1 are consistent with literature values for Ala80cyt c-CN⁻ (H δ 2 = 16.1 ppm and He1 = -3.4 ppm) (Bren *et al.*, 95).

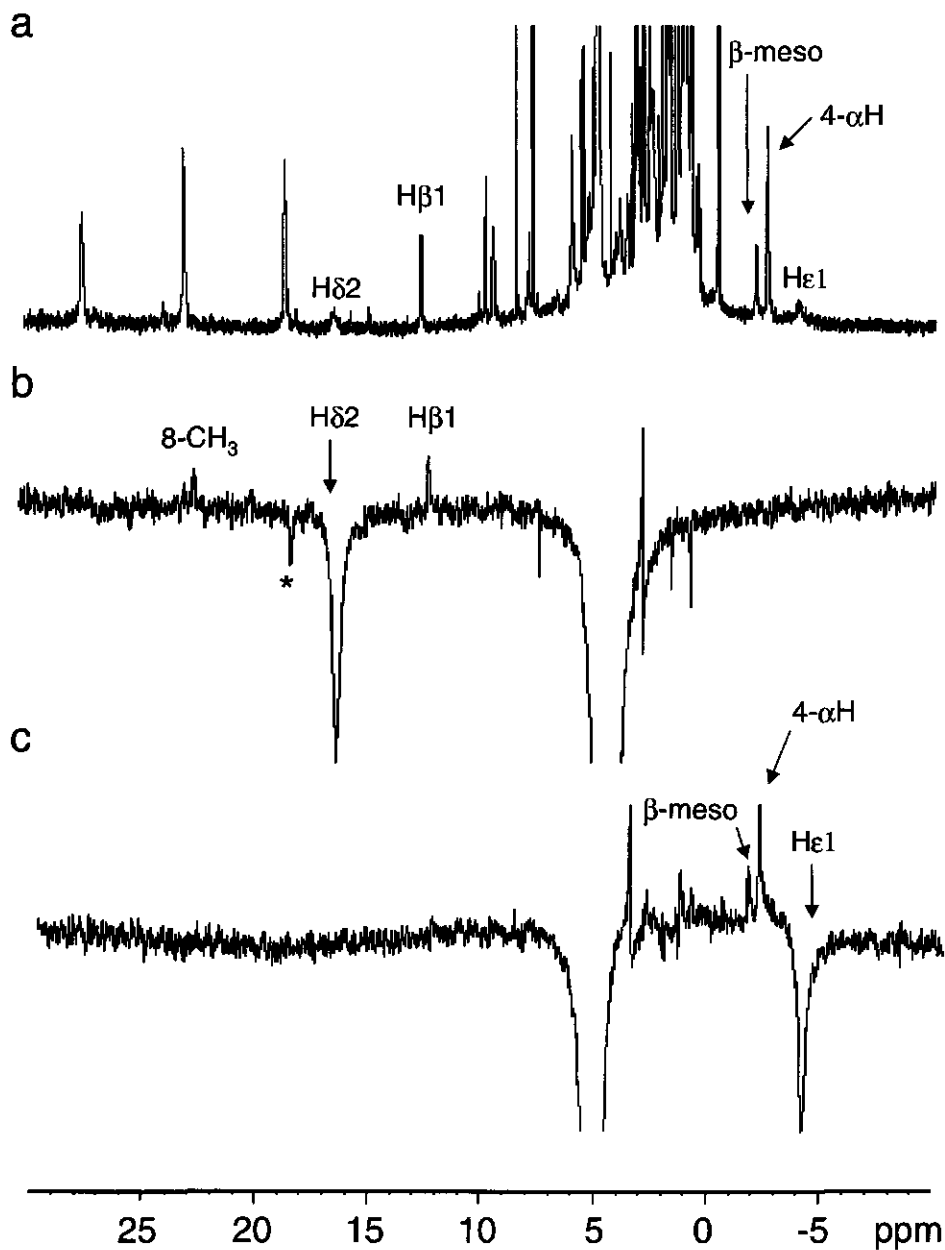


Figure 6.4 500 MHz ^1H NMR measurements of His18 hydroxylated Fe(III)MP-8 at 281 K: (a) 1-D spectrum; (b) NOE difference spectrum obtained on saturation of the His18 H δ 2 resonance at 16.2 ppm. The measurement show NOE's to the His18 H β 1 and 8-methyls protons. (c) NOE difference spectrum obtained on saturation of the His18 H ϵ 1 resonance at -3.68 ppm. The measurement show NOE's to the β -meso and the 4- α H protons. Saturated resonances in (b) and (c) are indicated by a downward arrow. Off-resonance saturated peaks are indicated by an asterisk.

Only slight differences were found when comparing the chemical shift values of His18 H δ 2 and H ϵ 1 for native and modified Fe(III)MP-8. Proton H δ 1 was not detected for the native molecule and the modified Fe(III)MP-8, in spectra recorded at various temperatures and with various CD₃OH/H₂O ratios, indicating fast H/D exchange of H δ 1 or alternatively suggesting a modification of the position δ 1 in the intermediate (see Discussion).

Labelling studies

ESI LC-MS on-line analysis performed on Fe(III)MP-8 incubated with a 2-fold excess of H₂O₂ dissolved in 95 % ¹⁸O containing labelled water showed a molecular cluster ion for the intermediate exhibiting an isotopic distribution consistent with the presence of 95 \pm 5 % ¹⁸O atoms in the hydroxylated product. A similar incubation performed on Fe(III)MP-8 incubated with a 2-fold excess of 90% ¹⁸O labelled H₂O₂ showed no significant presence of ¹⁸O atoms in the hydroxylated product. This suggests the inserted oxygen to originate from the solvent.

6.4 Discussion

The present study describes the characterisation of a modified Fe(III)MP-8 having an oxygenated His18 residue. The use of a comprehensive set of analytical methods for its characterisation leads to the conclusion that the His18 residue is modified by oxygen insertion presumably leading to a hydroxylated His18 at H δ 1. This conclusion is based on: i) data obtained by ESI mass spectrometry, which demonstrate the insertion of an oxygen atom on the His18 of the Fe(III)MP-8 octapeptide; ii) ¹H NMR 2-D TOCSY experiments in which the C α and C β protons of His18 were assigned; iii) results from ¹H NMR NOE difference spectroscopy which support the assignment for His18 H δ 2 and H ϵ 1. However, for Fe(III)MP-8, as well as for the modified Fe(III)MP-8, proton H δ 1 could not be detected. For Fe(III)MP-8 this might be due to fast H/D exchange. An exchange rate of 1700 s⁻¹ was measured in water at 309 K and pH 7 for proton H δ 1 of equine cytochrome c (Banci *et al.*, 98) and the fact that Fe(III)MP-8 lacks most of the polypeptide chain of the parent molecule will result in an even higher exchange rate. Based on ESI-MS and ¹H NMR, the absence of a signal for the H δ 1 proton in the 1-D spectra of the modified Fe(III)MP-8 and the absence of a NOE to a putative H δ 1 resonance in the 1-D NOE

difference experiments (Figure 6.4) can alternatively be assigned to the loss of this proton because of oxygen insertion at the position $\delta 1$ of the His18 imidazole ring. Oxygen insertion at one of the amide backbone nitrogens can be ruled out since in this case some of the C_{α} proton resonances would certainly be influenced, which is not observed (Table 6.1). C_{α} proton resonances of each residue can be directly related to the secondary structure of the peptide *i.e.* to changes in the backbone conformation. Therefore the similarity in the C_{α} proton resonances of native and modified Fe(III)MP-8 implies that both the peptide of modified Fe(III)MP-8 and the one of native Fe(III)MP-8 have a similar overall secondary structure. Thus, the oxygen insertion on the intermediate does not have a significant effect on the secondary structure of the peptide. The chemical shift of H $\delta 2$ is comparable to literature data (Bren *et al.*, 95) and the modified Fe(III)MP-8 is suggested to have a hydroxylated His18 on position $\delta 1$.

Additional evidence supporting the hypothesis of an imidazole hydroxylation on position $\delta 1$ can be found in the following. The difference observed for the 3-methyl and 5-methyl resonances between Fe(III)MP-8 and the modified Fe(III)MP-8 (Figure 6.3) must be related to changes in the electron density distribution on the heme moiety. Electron density distribution can be affected either by a change in the properties of the pyrrole substituents (Kolczak *et al.*, 99) or determined by the orientation of the iron axial ligand(s) (Shulman *et al.*, 71, Turner, 95, Shokhirev and Ann Walker, 98). Indeed the orientation of the axial ligand is an important parameter in determining the magnetic rhombic axes x and y for c type of hemes which orientation will influence the paramagnetic shifts of heme substituents (Bren *et al.*, 95; Banci *et al.*, 99; Bertini *et al.*, 99). Using a recently published heuristic equation to fit the experimental heme methyl chemical shifts (Bertini *et al.*, 99), the angle between the projection of the axial ligand on the heme plane and the direction of the iron-pyrrole II-IV nitrogen axis was estimated. Values of $51 \pm 6^{\circ}$ for Fe(III)MP-8 and of $42 \pm 10^{\circ}$ for the hydroxylated Fe(III)MP-8 were obtained. Both values are almost equal within experimental error. The angle value for Fe(III)MP-8 is found close to the literature value of 45° corresponding to horse heart cytochrome c (Shokhirev *et al.*, 98). The data support a small reorientation of the axial His18 for the hydroxylated biocatalyst. Such a reorientation of the axial ligand could be the result of the creation of a H-bond between the formed hydroxyl group on the imidazole ring of the modified Fe(III)MP-8 and one backbone donor or acceptor group.

Altogether these considerations are in favour of the hydroxylation of the position $\delta 1$ of the His18 imidazole ring of Fe(III)MP-8. The formation of a hydroxylated Fe(III)MP-8 can be related to the participation of heme-(hydro)peroxo or heme-oxo intermediates in H₂O₂-driven Fe(III)MP-8 supported chemistry. Incubation in the presence of 2 mM of ascorbate (Table 6.2) almost completely quenched the formation of the modified Fe(III)MP-8 indicating the involvement of a porphyrin high-valent iron-oxo (radical cation) intermediate in its formation since ascorbate acts as a scavenger for peroxidase Compound I or II (Chance, 49; Primus *et al.*, 99). The mechanism of hydroxylation of the His18 of Fe(III)MP-8 can be a direct oxygen transfer from the postulated Fe(III)MP-8 Compound I, or an initial electron transfer to the iron porphyrin axial ligand followed by water addition. The results of ESI LC-MS analysis of modified Fe(III)MP-8 formed in incubations with ¹⁸O labelled water and ¹⁸O labelled peroxide have shown the inserted oxygen to come from the solvent. Consequently, the hydroxylated Fe(III)MP-8 is probably not formed by direct transfer of the oxygen atom from the postulated Fe(III)MP-8 Compound I, but is the result of an initial internal oxidation of the histidine ring followed by an oxygen insertion from the solvent. Such type of mechanism has already been proposed for the oxidation of the porphyrin ring of metmyoglobin by hydrogen peroxide (Sugiyama *et al.*, 97). Moreover, incubation in the presence of radical scavengers (Table 6.2), also eliminates an oxidation mechanism being the result of an intermolecular oxidation process by Compound II or the postulated Fe(III)MP-8 Compound I. In that case, other products would be expected since there are other sites on Fe(III)MP-8 much more sensitive to oxidation than the His18 axial ligand, such as the carbon *meso* positions of the porphyrin ring (Wilks and Ortiz de Montellano, 93; Wilks *et al.*, 94; Torpey and Ortiz de Montellano 96; Torpey and Ortiz de Montellano, 97), other ring positions (Sugiyama *et al.*, 97) or the sulphur atom of the thioether bridges. None of these oxidation products were observed (Figure 6.1). Therefore the data of the present study suggest that the first step of the modified Fe(III)MP-8 formation is an intramolecular oxidation of the histidine 18 imidazole ring, induced by mesomerism within the high-valent iron-oxo porphyrin radical cation (Figure 6.5) (Poulos *et al.*, 96; Banci *et al.*, 96; Gross *et al.*, 96; Rietjens *et al.*, 96; Weiss *et al.*, 96). The mechanism of the subsequent water addition to the imidazole ring could be visualised as a water addition to a putative Fe(III)MP-8 "Compound I histidyl radical cation" (Figure 6.5). A similar intermediate may play a role in the transfer of the second oxidation equivalent to the Trp191 of cytochrome c peroxidase.

Table 6.2 Effects of various radical scavengers on the formation of the modified Fe(III)MP-8 in the presence of a 2-fold excess of H₂O₂.

Scavengers (final concentration)	2-fold excess H ₂ O ₂	Modified Fe(III)MP-8 (%) ^a
-	-	0
-	+	100
+ ascorbate (2 mM)	+	6
+ mannitol (10 mM ; 100 mM) ^b	+	108.3 ; 103.5
+ ethanol (10 mM ; 100 mM) ^b	+	99.4 ; 112.6

^a 100 % modified Fe(III)MP-8 formed = in the presence of a 2-fold excess of H₂O₂, without scavenger.

^b hydroxyl radical scavenger

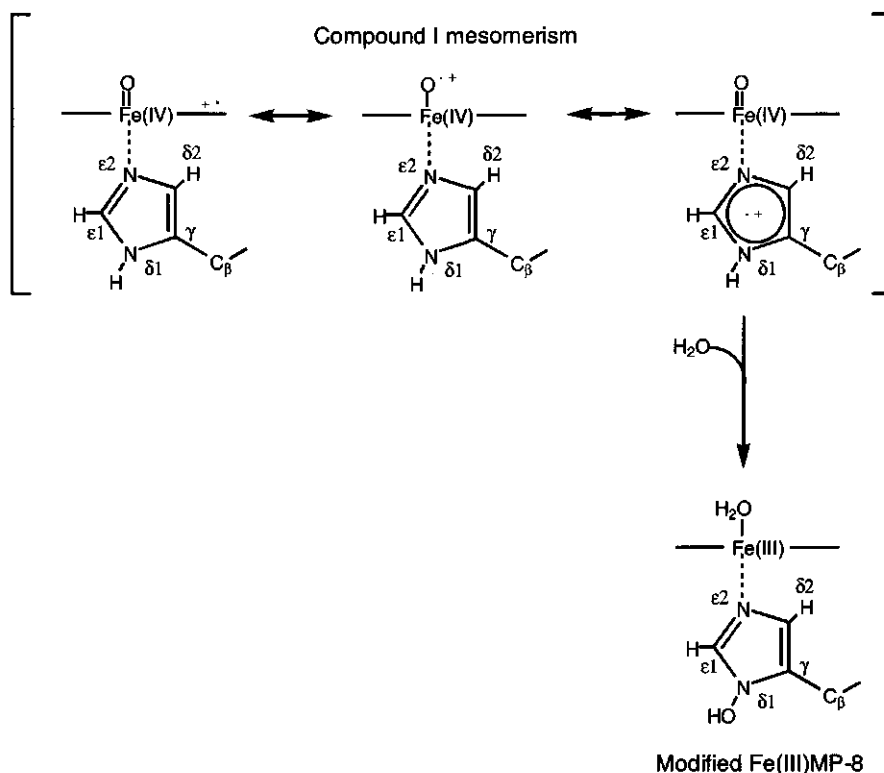


Figure 5. Mechanism showing the mesomerism of the second oxidation equivalent of the putative Fe(III)MP-8 Compound I on the porphyrin macrocycle, the oxo group and the axial ligand. The formation of the His18 hydroxylated Fe(III)MP-8 is proposed to proceed through water addition to the His18 imidazole ring.

This hypothesis implies that the second oxidation equivalent of the postulated Fe(III)MP-8 Compound I is majorly delocalised on the axial ligand instead of the porphyrin ligand, since no oxygen insertion is observed on the porphyrin ring. A NMR investigation on horseradish peroxidase (HRP) also has shown the radical of HRP Compound I to be delocalised on the histidine axial ligand which is in line with the present set of data for Fe(III)MP-8 (Thanabal *et al.*, 88).

Acknowledgements

The authors gratefully acknowledge support from the EU large scale NMR facility of the Florence Center for Paramagnetic NMR (contract number HPRI CT1999 00009) and from the Wageningen NMR center (WNMRc). The EU project Heamworks (contract number ERB FMRX-CT 98 0218) is also acknowledged. The authors are also indebted to the Dutch Foundation for Technical Research (CW/STW project number 349-3710), and to the EU project (contract number FMGE-CT 98 107) for financial support.

The nature of the intermediates in the reactions of Fe(III)- and Mn(III)-microperoxidase-8 with H₂O₂; A rapid kinetics study.

Jean-Louis Primus, Sylvie Grunenwald, Peter-Leon Hagedoorn, Anne-Marie Albrecht-Gary, Dominique Mandon, Ivonne M.C.M. Rietjens and Cees Veeger

Submitted

Abstract

The mechanism of formation of the reactive metal-oxo and metal-hydroperoxo intermediates of M(III)MP-8 upon reaction of H₂O₂ with Fe(III)MP-8 and Mn(III)MP-8 was investigated by rapid-scan stopped-flow spectroscopy and transient EPR. Two steps (k_{obs1} and k_{obs2}) were observed and analysed for the reaction of hydrogen peroxide with both catalysts. The plots of k_{obs1} as function of [H₂O₂] at pH 8.0 and pH 9.1 for Fe(III)MP-8, and at pH 10.2 and pH 10.9 for Mn(III)MP-8, exhibit saturation kinetics, which reveal the accumulation of an intermediate. Double reciprocal plots of $1/k_{\text{obs1}}$ as function of $1/[\text{H}_2\text{O}_2]$ at different pH-values, reveal a competitive effect of protons in the oxidation of M(III)MP-8. This effect of protons is confirmed by the linear dependence of $1/k_{\text{obs1}}$ on $[\text{H}^+]$ showing that k_{obs1} increases with the pH. The UV/visible spectra of the intermediates formed at the end of the first step (k_{obs1}) exhibit a spectrum characteristic of a high-valent metal-oxo intermediate for both catalysts. Transient EPR of Mn(III)MP-8 incubated with an excess of H₂O₂, at pH 11.5, shows the detection of a free radical signal at $g \approx 2$ and resonances at $g \approx 4$ and $g \approx 2$ characteristic of a Mn(IV) species. On the basis of these results the following mechanism is proposed: i) M(III)MP-8-OH₂ is deprotonated to M(III)MP-8-OH in a rapid pre-equilibrium step, with a $\text{p}K_{\text{a}} = 9.2 \pm 0.9$ for Fe(III)MP-8 and a $\text{p}K_{\text{a}} = 11.0 \pm 0.8$ for Mn(III)MP-8; ii) M(III)MP-8-OH reacts with H₂O₂ to form Compound 0, M(III)MP8-OOH, with a second-order rate constant $k_1 = (1.3 \pm 0.6) \times 10^6 \text{ M}^{-1} \cdot \text{s}^{-1}$ for Fe(III)MP-8 and $k_1 = (1.1 \pm 0.5) \times 10^5 \text{ M}^{-1} \cdot \text{s}^{-1}$ for Mn(III)MP-8. iii) This metal-hydroperoxo intermediate is subsequently converted to a high-valent metal-oxo species, M(IV)MP-8=O, with a free radical on the peptide (R[•]). The first order rate constants for the cleavage of the hydroperoxo group are $k_2 = 165 \pm 8 \text{ s}^{-1}$ for Fe(III)MP-8 and $k_2 = 145 \pm 7 \text{ s}^{-1}$ for Mn(III)MP-8 and iv) the proposed M(IV)MP-8=O(R[•]) intermediate slowly decays (k_{obs2}) with a rate constant of $k_{\text{obs2}} = 13.1 \pm 1.1 \text{ s}^{-1}$ for Fe(III)MP-8 and $k_{\text{obs2}} = 5.2 \pm 1.2 \text{ s}^{-1}$ for Mn(III)MP-8. The results show that Compound 0 is formed *prior* to what is analysed as a high-valent metal-oxo peptide radical intermediate.

7.1 Introduction

Protons play a fundamental role in the formation of the catalytic reactive species for both peroxidases and cytochromes P450 (P450s)¹. But, whereas the influence of protons in the distal heme active site starts to be better understood for peroxidases like horseradish peroxidase (HRP), (Mukai *et al.*, 97; Banci, 97) it remains less well defined for P450s (Poulos and Raag, 92). Reactivity studies have shown that residues of the heme distal active site of peroxidases act as acid/base catalysts to facilitate the deprotonation of the hydroperoxide substrate and the subsequent heterolytic cleavage of the O-O peroxide bond (Ortiz de Montellano, 92; Savenkova *et al.*, 98; Smith and Veitch, 98). This leads to the formation of Compound I, a high-valent iron-oxo porphyrin radical cation, $\text{Por}^{\bullet}\text{Fe(IV)=O}$, (Dolphin *et al.*, 71; Rutter *et al.*, 83; Pond *et al.*, 98) which upon reduction by substrate is converted into Compound II, PorFe(IV)=O , (Chance, 52; Dunford, 91). The porphyrin iron-hydroperoxo, PorFe(III)-OOH or Compound 0, was detected for HRP (Baek and van Wart, 89; Baek and van Wart, 92) at low temperature in 50 % MeOH, in the presence of a high concentration of hydroperoxide. Also the transient formation of a porphyrin iron-hydroperoxo was detected for the Arg38Leu HRP mutant (Rodriguez-Lopez *et al.*, 96). Indirect evidence for the existence of PorFe(III)-OOH in the reaction cycle of HRP comes from ¹⁸O-exchange studies (Dorovska-Taran *et al.*, 98; van Haandel *et al.*, 98). Compound 0 and its deprotonated form, $\text{PorFe(III)-O-O}^{\cdot-}$ are species encountered in the P450 chemistry and precede an isoelectronic analogue of Compound I in the reaction cycle (Coon *et al.*, 98).

The comprehension of the acid/base catalysis and the formation of the high-valent iron-oxo or of the iron-peroxo intermediates for peroxidase and P450 chemistry has benefit from the use of synthetic metalloporphyrin models (Groves *et al.*, 88; Bell *et al.*, 91; Meunier, 92; Groves *et al.*, 94). Non μ -oxo dimer forming water-soluble model porphyrins

¹ Abbreviations used : M(III)MP-8-OOH, Fe(III)MP-8-OOH or Mn(III)MP-8-OOH: metal-, iron- or manganese-hydroperoxo microperoxidase-8 respectively; Fe(IV)MP-8=O or Mn(IV)MP-8=O, high-valent iron- or manganese-oxo microperoxidase-8 respectively; Fe(IV)MP-8=O(R^{•+}) or Mn(IV)MP-8=O(R^{•+}): high-valent iron- or manganese-oxo peptide radical cation respectively, (Compound I-like); PorFe(III): iron porphyrin, the same nomenclature as for MP-8 is further used for the oxidised iron porphyrin intermediates; HRP: horseradish peroxidase, P450(s): cytochrome(s) P450. FeTDCPPS or MnTDCPPS: (meso-tetrakis-(2,6-dichloro-3-sulfonatophenyl)-porphinato)iron or manganese.

such as FeTDCPPS and MnTDCPPS were used to study the influence of the pH on the formation of manganese- and iron-hydroperoxo intermediates and on the formation of high-valent manganese- and iron-oxo intermediates (Murata *et al.*, 90; Arasasingham and Bruce, 91). However, these models all lack a proximal ligand, even though studies were performed in the presence of imidazole in order to mimic a proximal histidine ligand (Arasasingham and Bruce, 91). The influence of the proximal ligand is an important parameter to consider in the formation of reactive intermediates in oxidation catalysis. Microperoxidase-8, Fe(III)MP-8, is a water-soluble biomimic consisting of an iron protoporphyrin IX covalently attached to an octapeptide *via* two thioether bonds and one axial co-ordination bond between the iron and the histidine 18 residue of the peptide. Fe(III)MP-8 is obtained by controlled proteolytic digestion of horse heart cytochrome c and corresponds to residues 14 to 21 of the parent protein (Aron *et al.*, 86) The fact that Fe(III)MP-8 can be used as a model for both peroxidase chemistry and P450 chemistry (Aron *et al.*, 86; Osman *et al.*, 96 and references therein) makes it an attractive mimic for studying the influence of the pH on the formation of iron-(hydro)peroxo and high-valent iron-oxo intermediates.

Several studies on possible reactive heme-oxygen species formed by microperoxidase biomimics exists (Low *et al.*, 98; Primus *et al.*, 99; Clore *et al.*, 81; Low *et al.*, 96; Wang *et al.*, 91). The manganese complex of MP-8 was prepared to compare its reactivity with the iron complex of MP-8 (Low *et al.*, 98) and catalytic studies pointed at the involvement of Compound 0 in MP-8-catalysed oxygen transfer reactions (Primus *et al.*, 99). Stopped-flow kinetic studies performed on Fe(III)MP-11 in the presence of H₂O₂ at pH 7 and pH 10.4 showed the formation of a species tentatively assigned to Compound I (Clore *et al.*, 81). Investigations by UV/visible spectroscopy on Fe(III)MP-8 oxidised by photo-induced single-electron transfer showed the formation of an iron-hydroxo porphyrin radical cation, Por^{•+}Fe(III)MP-8-OH, converting into Compound II, PorFe(IV)MP-8=O, when the pH was increased (Low *et al.*, 96). Oxidation of Mn(III)MP-8 by H₂O₂ showed the formation of a manganese MP-8 analogue of Compound II, Mn(IV)MP-8=O, characterised by UV/visible and Raman spectroscopy (Low *et al.*, 98). Low-temperature stopped-flow kinetic studies performed in 50 % MeOH on N-Acetyl-Fe(III)MP-8 in the presence of H₂O₂ have postulated the formation of Fe(III)MP-8-OOH *prior* to the formation of Fe(III)MP-8 Compound I and Compound II (Wang *et al.*, 91). However, MeOH is a chaotropic and reducing agent, which influences the measurements.

The goal of the present work was to study the oxidation chemistry of Fe(III)MP-8 and Mn(III)MP-8 in water at ambient temperature with particular attention to the role played by protons in the formation of iron-hydroperoxo and high-valent iron-oxo intermediates. The reactivity of Fe(III)MP-8 with H₂O₂ is compared to the reactivity of Mn(III)MP-8 with H₂O₂ using rapid kinetics and EPR. The influence of the nature of the axial sixth ligand, aquo or hydroxo, on the formation of iron- or manganese-(hydro)peroxo intermediates is investigated. The consequences, for the formation and for the nature, of the high-valent iron- or manganese-oxo intermediates, are studied.

7.2 Materials and methods

Chemicals

Cytochrome c from horse heart was obtained from Boehringer (Mannheim, Germany). Fe(III)MP-8 was prepared by proteolytic digestion of horse heart cytochrome c essentially as described previously (Aron *et al.*, 86; Low *et al.*, 96). Anhydrous iron(II) chloride was obtained from Strem Chemicals (Newburyport MA, USA). Manganese(II) sulfate tetrahydrate, L-ascorbic acid and H₂O₂ 30 % v/v were from Merck (Darmstadt, Germany). The concentration of the diluted H₂O₂ solutions was always checked spectrophotometrically using the molar extinction coefficient at 240 nm, $\epsilon_{240} = 39.4 \pm 0.2 \text{ M}^{-1} \cdot \text{cm}^{-1}$ (Nelson and Kiesow, 72). All water solutions were prepared with de-ionised or nanopure water (mixed-bed of ion exchanger, Millipore) and the pH was measured using a combined glass micro-electrode (Ingold, High Alkalinity). The reference electrode (Ag/AgCl) was filled with a saturated solution of NaCl (Merck, Darmstadt, Germany) containing traces of silver chloride (Merck, Darmstadt, Germany) and the pH-meter was calibrated using buffer solutions (Prolabo, Normadose). All HPLC solvents were of chromatographic grade. All others reagents used were of analytical grade.

Synthesis of Mn(III)MP8

Manganese substituted MP-8 was prepared by metalation of MP-8 free base. Demetalation was essentially performed using an improved published method (Primus *et al.*, 99). During all the preparation, the reaction medium was protected from light. A solution of Fe(III)MP-8 (206 mg, 137 μmol) in 200 mL of ice cold acetic acid was made oxygen free by three cycles of vacuum/argon ; 410 μL of a 0.5 mg/mL argon saturated Fe(II)Cl₂ water

solution (12-fold excess, 1.64 mmol) were introduced together with 1.7 mL 36 % aqueous HCl (100 mM). Another three cycles of vacuum/argon was applied to the reaction mixture before it was allowed to stir for 5 min at ambient temperature in a light protected glass bottle. The reaction mixture was first evaporated (20 mm Hg/40 °C) to dryness, washed with water and re-evaporated to dryness (20 mm Hg/40 °C). The demetalated material was dissolved in a minimal volume of 0.05 M ammonium hydrogenocarbonate pH 7 and loaded on a Sephadex LH-20 column eluted with MeOH at 0.2 mL/min. Fractions free from iron salts were pooled and evaporated to dryness (20 mm Hg/40 °C). The remaining red material stuck to the column was discarded by washing with MeOH/AcOH/H₂O : 5/1/4.

Metalation was essentially performed using an adapted literature procedure (Low *et al.*, 98). The demetalated material was dissolved in 60 mL of 0.05 M ammonium acetate pH 5.5 giving a roughly 1-2 mM concentrated solution. The solution was saturated with argon by three cycles of vacuum/argon and 135 mg of Mn(II)SO₄ tetrahydrate (600 μmol) were added to the reaction mixture which was stirred at 40 °C in a light protected glass bottle. After 37 hours, another 135 mg of Mn(II)SO₄ tetrahydrate (600 μmol) were added to the reaction mixture which was made argon saturated by three cycles of vacuum/argon. The amount of Mn(III)MP-8 formed was regularly checked by HPLC. Usually after about 60 hours of reaction, the mixture contained 90 % Mn(III)MP-8 and 10 % MP-8 free base determined by UV detection at 220 nm. The reaction was stopped at that point and the mixture subsequently concentrated and washed to remove inorganic salts using an Amicon ultra-filtration cell with a YC05 membrane. The metalated material was further purified by semi-preparative HPLC.

Purification of crude Mn(III)MP8 was performed using two Isco Model 2300 HPLC pumps equipped with a Pye Unicam LC-UV Detector. The Mn(III)MP-8 solution was filtered and the filtrate, typically 5 mL, was loaded on a Waters Delta-Pak C18 column (25 mm × 200 mm, 300 Å pore size, 10 μm particle size). Elution was performed with a gradient of TEAP pH 7 (eluent A) and CH₃CN (eluent B) (Primus *et al.*, 99). For semi-preparative purification of the intermediate, 26 % of B were first applied for 3 min and simultaneously the flow was increased from 4 mL.min⁻¹ to 8 mL.min⁻¹. Elution was achieved by applying a linear gradient of B from 26 % to 37 % over 11 min followed by further increase to 41 % within 30 s at 8 mL.min⁻¹. The collected fractions were pooled, concentrated by evaporation (20 mm Hg, 35 °C) and finally lyophilised. Mn(III)MP-8 was checked for purity on analytical HPLC and dialysed against a 10 mM pH 9 carbonate buffer.

Stopped-flow measurements

Solutions of Fe(III)MP-8 and corresponding H₂O₂ solutions were both buffered with either 0.1 M potassium phosphate (pH 8.0), 0.1 M tricine (from pH 8.1 till pH 9) or 0.1 M potassium carbonate (from pH 9.1 till pH 10). For Fe(III)MP-8, concentrations of the oxygen donor, H₂O₂, were varied between 0.1 mM and 1.2 mM. Concentrations of Fe(III)MP-8 were chosen between 8.7 μ M and 13.1 μ M and were calculated using $\epsilon_{397} = 1.57 \times 10^5 \text{ M}^{-1} \cdot \text{cm}^{-1}$ for Fe(III)MP-8 at pH 7 (Aron *et al.*, 86). Solutions of Mn(III)MP-8 and corresponding H₂O₂ solutions were both buffered with either 0.1 M potassium carbonate (from pH 10 till pH 11) or 0.1 M potassium phosphate (from pH 11.1 till pH 13). For the manganese complex, Mn(III)MP-8, concentrations of the oxygen donor, H₂O₂, were varied between 0.6 mM and 50 mM. Concentrations of Mn(III)MP-8 were chosen between 6 μ M and 7.9 μ M and were calculated using the value of ϵ_{463} determined to be $2.82 \times 10^4 \pm 3.36 \times 10^3 \text{ M}^{-1} \cdot \text{cm}^{-1}$ for Mn(III)MP-8 at pH 7. Indicated concentrations are the final concentrations after mixing. All measurements were performed under pseudo-first order conditions with at least a 10-fold excess of H₂O₂ with respect to [Fe(III)MP-8] or [Mn(III)MP-8] and at a temperature of 25 ± 0.2 °C.

Time resolved spectra were recorded on an Applied Photophysics SX-18 MV stopped-flow spectrophotometer (Leatherhead, UK) using the photodiode array rapid-scan mode. The spectral resolution was around 1 nm with a mixing time of 3 ms. For the current study, no spectral information was lost during the mixing time. Reaction profiles were collected in the monochromatic mode of an Applied Photophysics (Leatherhead, UK) stopped-flow spectrophotometer. No kinetic information was lost during the 3 ms mixing time and currently 1000 data points per trace were acquired. The length of the light path was 1 cm for both type of measurements. The data sets, average out of three independent measurements, were recorded at 410 nm for Fe(III)MP-8 (Low *et al.*, 96) and 400 nm for Mn(III)MP-8 (Low *et al.*, 98) both strong absorbances in the spectrum of the oxidised products. Traces were processed on-line with commercial softwares based on the Marquardt algorithm (SpectraKinetic Software, Applied Photophysics Ltd., Leatherhead UK 1992) or the Simplex algorithm (Biokine v. 3.14, Bio-logic Co, Echirolles France 1991).

Rapid-freeze and EPR measurements

Rapid-freeze experiments were performed on a home-built apparatus following the method described by Duyvis (Duyvis, 97). EPR samples were prepared by mixing solutions of 1 mM Mn(III)MP-8 in 0.1 M carbonate at pH 11.5 with a 25-fold excess of H₂O₂ in the same buffer. After mixing, solutions were incubated in the ageing hose for 27 ms based on the analysis performed with the stopped-flow instrument. Samples were immediately frozen by spraying them into a funnel, connected with a rubber to the EPR tube. Both the funnel and the EPR tube were immersed and filled with cold isopentane cooled down with liquid nitrogen (around -140 °C). EPR experiments were performed on a Varian spectrometer. For Mn(III)MP-8, experiments were performed at the frequency of the X-band, 9.227 GHz, using the following conditions: modulation amplitude, 1 mT; microwave power, 12.6 mW; gain, 6.3×10^3 ; scan time, 4 min; time constant, 0.1 s and temperature 16 K. The center of the field was set at 250 mT, spectra were recorded over a 400 mT range and corrected for the absorption of non reacted samples.

7.3 Results

The rate of formation of the oxidised intermediates of Fe(III)MP-8 and Mn(III)MP-8 upon reaction with H₂O₂ were analysed within the pH range corresponding to the optimal activity of Fe(III)MP-8 ($8 < \text{pH} < 10$) and Mn(III)MP-8 ($10 < \text{pH} < 13$) for peroxidase- and P450-type of conversions (Primus *et al.*, 99). The time-dependent changes in the UV/visible spectrum of both catalysts upon oxidation by H₂O₂ are depicted in Figure 7.1a for Fe(III)MP-8 and in Figure 7.1b for Mn(III)MP-8. A sample of the recorded transient traces at 410 nm for Fe(III)MP-8 incubated at pH 9.1, and at 400 nm for Mn(III)MP-8 incubated at pH 10.9 is depicted in the inset of Figure 7.1a and 7.1b respectively. The transient traces obtained under varying pH and [H₂O₂] conditions were observed and analysed using a bi-exponential fitting of the absorbance changes with time. Subsequent degradation steps of the catalysts were not considered in the present study.

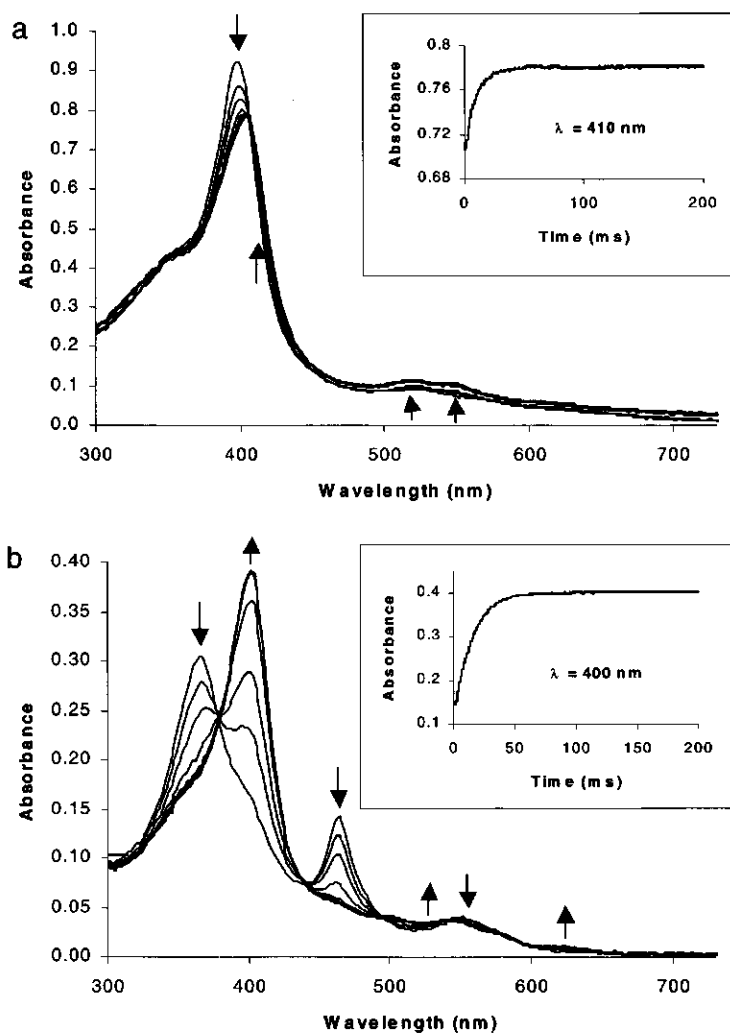


Figure 7.1 Time-resolved UV/visible spectra of the reaction of (a) 13.1 μM Fe(III)MP-8 with 1 mM H_2O_2 at pH 9.1 (100 scans in 300 ms, 3 ms integration time for the photodiode array; scans shown correspond to 1.3 ms, 6.4 ms, 11.5 ms, 24.3 ms and further every tenth scan is shown for clarity); in the inset a single-wavelength transient absorption spectra of 13.1 μM Fe(III)MP-8 mixed with 1 mM H_2O_2 at pH 9.1 is shown. Typically 1000 data points were acquired at $\lambda = 410$ nm. Time-resolved UV/visible spectra of the reaction of (b) 8 μM Mn(III)MP-8 with 2.5 mM H_2O_2 at pH 10.9 (100 scans in 300 ms, 3 ms integration time for the photodiode array; scans shown correspond to 1.3 ms, 6.4 ms, 11.5 ms, 24.3 ms and further every tenth scan is shown for clarity); in the inset a single-wavelength transient absorption spectra of 6.0 μM Mn(III)MP-8 mixed with 2.5 mM of H_2O_2 at pH 10.9 is shown. Arrows indicate the time-dependent directions for the spectral variations of both Fe(III)MP-8 and Mn(III)MP-8 samples.

The variations of the pseudo-first order rate constants k_{obs1} and k_{obs2} for Fe(III)MP-8 at pH 8 and 9.1 and for Mn(III)MP-8 at pH 10.2 and 10.9 were plotted as function of $[\text{H}_2\text{O}_2]$. The plot of k_{obs1} as function of $[\text{H}_2\text{O}_2]$ were fitted with a rectangular hyperbola in agreement with saturation kinetics for both catalysts (Figure 7.2a and 7.2c). The values of k_{obs2} at pH 8 and pH 9.1 for Fe(III)MP-8 and pH 10.2 and 10.9 for Mn(III)MP-8 were found to be independent of $[\text{H}_2\text{O}_2]$ for both catalysts.

The double reciprocal plots of $1/k_{\text{obs1}}$ as function of $1/[\text{H}_2\text{O}_2]$ show that the data can be fitted with a linear equation for the oxidation of Fe(III)MP-8 at pH 8 and 9.1 (Figure 7.2b) and the oxidation of Mn(III)MP-8 at pH 10.2 and 10.9 (Figure 7.2d). The fact that, for both catalysts, the linear fits of $1/k_{\text{obs1}}$ at different pH values have a different slope but a common intercept on the vertical axis indicates a competitive role played by protons in the formation of the oxidised species of M(III)MP-8.

The effect of the protons was further confirmed by studying the variation of k_{obs1} as function of the proton concentration for a specific hydrogen peroxide concentration. The pH was varied from pH 8 to pH 10, using a series of complementary buffers, for Fe(III)MP-8 in the presence of 1 mM H_2O_2 ; from pH 9.9 to pH 13 for Mn(III)MP-8 in the presence of 2.5 mM H_2O_2 . The values of $1/k_{\text{obs1}}$ as function of $[\text{H}^+]$ could be fitted with a linear equation (Figure 7.3a and 7.3b). For both catalysts the values of k_{obs1} are shown to increase with the pH. The variations of k_{obs2} in the presence of 1 mM H_2O_2 for Fe(III)MP-8 and in the presence of 2.5 mM H_2O_2 for Mn(III)MP-8 were plotted as function of $[\text{H}^+]$ and were found to be independent of $[\text{H}^+]$. Observed rate constants of $k_{\text{obs2}} = 13.1 \pm 1.0 \text{ s}^{-1}$ and $k_{\text{obs2}} = 5.2 \pm 1.2 \text{ s}^{-1}$ were measured for Fe(III)MP-8 and Mn(III)MP-8 respectively.

The UV/visible spectra of the resting state of the catalysts show a Soret band at 396 nm and Q bands at 510 nm and 623 nm for Fe(III)MP-8 (Figure 7.1a) (Low *et al.*, 96) and a split Soret band at 368 nm and 460 nm with Q band at 552 nm for Mn(III)MP-8 (Figure 7.1b) (Low *et al.*, 98). Simulations of the reaction of Fe(III)MP-8 with H_2O_2 show the spectrum of the final product of the first exponential step (k_{obs1}) to be typical of a high-valent iron-oxo intermediate, Fe(IV)MP-8=O, isoelectronic to a peroxidase Compound II species (see also Figure 7.1a). The spectrum depicts a red-shifted Soret band at 406 nm and characteristic Q bands at 519 nm and 548 nm (Wang *et al.*, 91; Low *et al.*, 96).

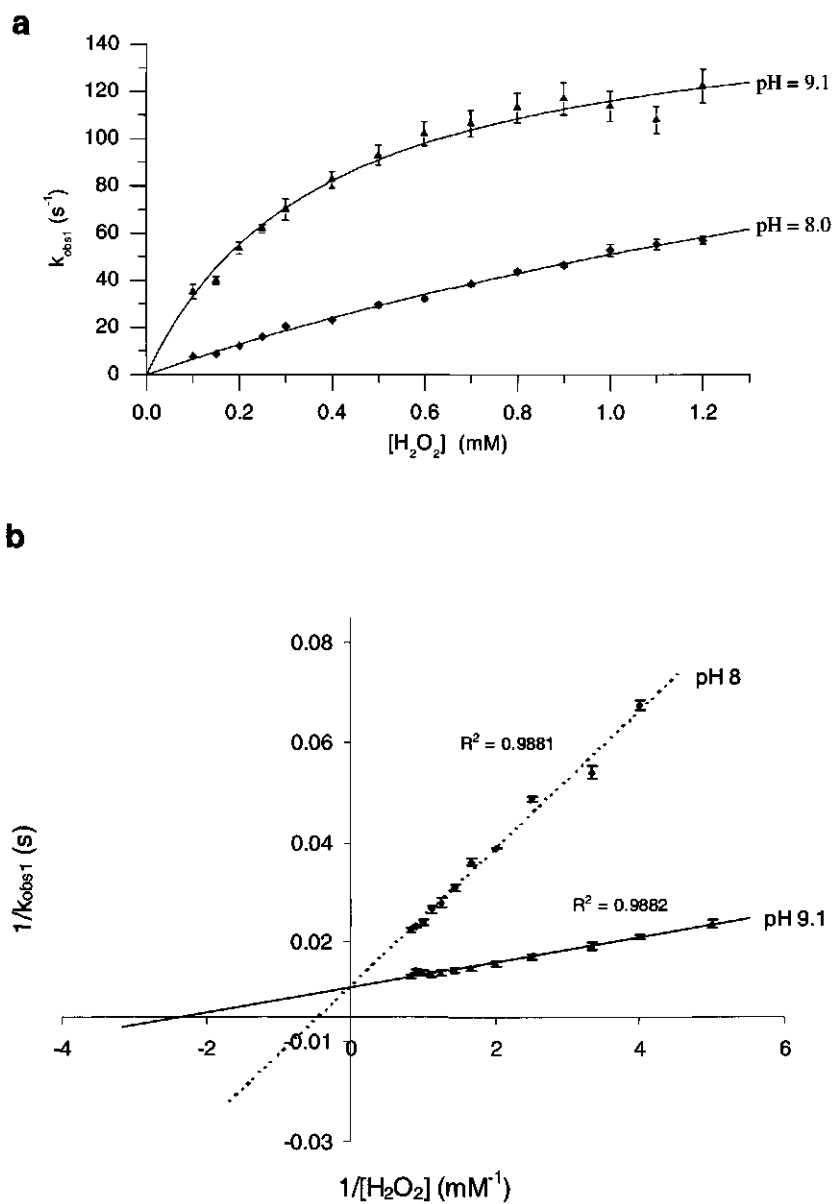


Figure 7.2 (a and b) Variation of the pseudo-first order rate constant of the first step k_{obs1} for (a) Fe(III)MP-8 at pH 8.0 and 9.1 as a function of $[\text{H}_2\text{O}_2]$, (b) is the double reciprocal plots of (a). For Fe(III)MP-8, the values of k_{obs1} follow saturation kinetics and least-square linear fitting of the data in (b) reveals a competitive role played by protons in the reaction of M(III)MP-8 with H_2O_2 . $[\text{Fe(III)MP-8}] = 8.7 \mu\text{M}$ at pH 9.1; $13.1 \mu\text{M}$ at pH 8.0.

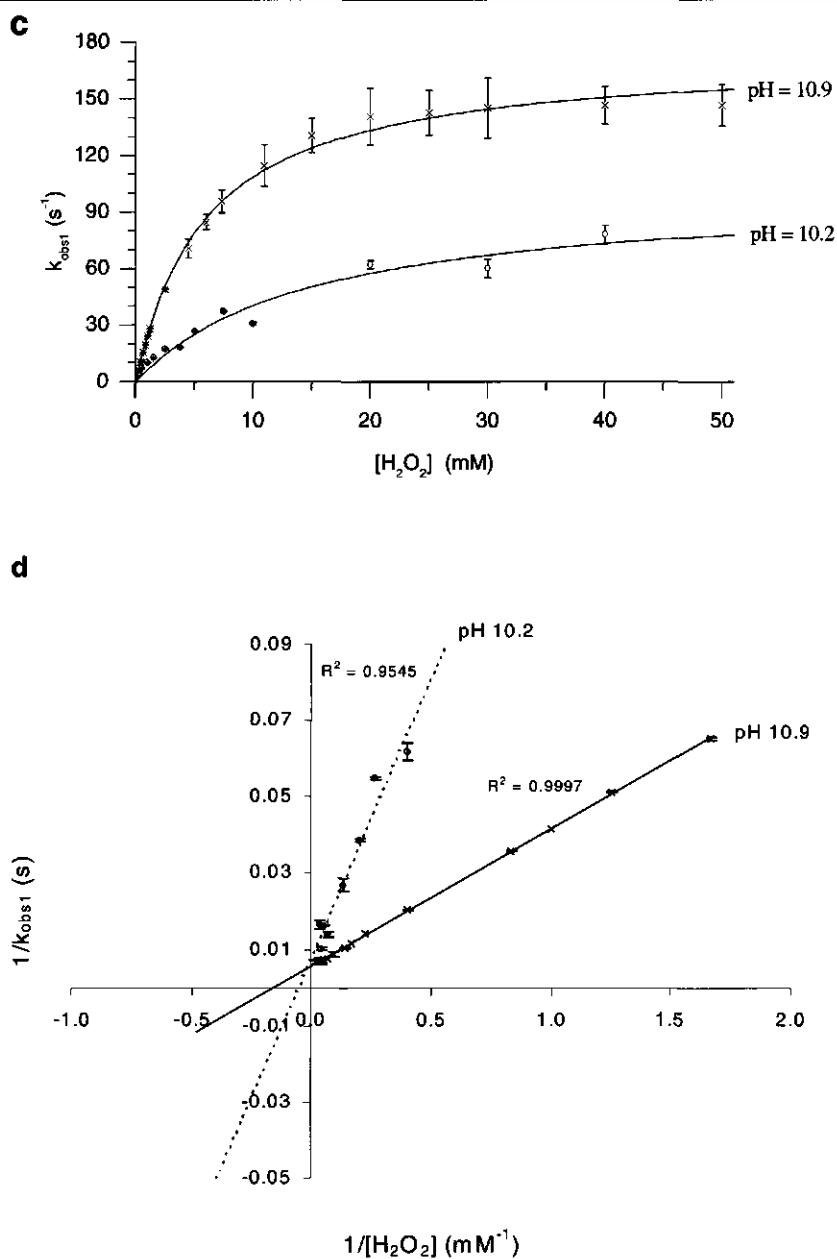


Figure 7.2 (c and d) Variation of the pseudo-first order rate constant of the first step k_{obs1} for (c) Mn(III)MP-8 at pH 10.2 and 10.9 as a function of $[\text{H}_2\text{O}_2]$, (d) is the double reciprocal plots of respectively (c). For Mn(III)MP-8, the values of k_{obs1} follow saturation kinetics and least-square linear fitting of the data in (d) reveals a competitive role played by protons in the reaction of M(III)MP-8 with H_2O_2 . $[\text{Mn(III)MP-8}] = 6.0 \mu\text{M}$ at pH 10.9; $7.9 \mu\text{M}$ at pH 10.2.

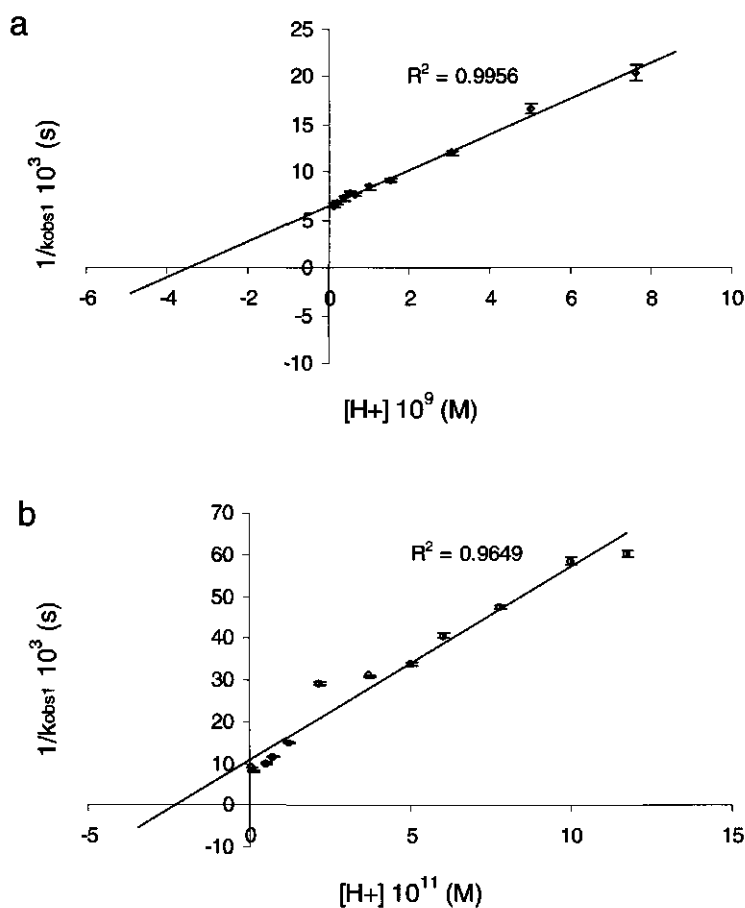


Figure 7.3 Variations of $1/k_{\text{obs1}}$ as function of $[H^+]$ for (a) $[\text{Fe(III)MP-8}] = 8.7 \mu\text{M}$; $[\text{H}_2\text{O}_2] = 1 \text{ mM}$ and for (b) $[\text{Mn(III)MP-8}] = 7.9 \mu\text{M}$; $[\text{H}_2\text{O}_2] = 2.5 \text{ mM}$ showing that k_{obs1} increases at higher pH-values. Data were fitted with a linear least-square procedure.

For the reaction of Mn(III)MP-8 , with H_2O_2 , simulations of the spectrum of the final product of the first exponential step (k_{obs1}) shows a spectrum typical of a high-valent manganese-oxo intermediate, Mn(IV)MP-8=O , showing a strong Soret band at 401 nm and shifted Q bands at 541 nm and 623 nm (see also Figure 7.1b) (Ayougou *et al.*, 95; Low *et al.*, 98). Figure 7.4 depicts the X-band transient EPR spectra of Mn(III)MP-8 incubated with an excess of H_2O_2 , at pH 11.5. The occurrence of a broad resonance at $g \approx 4$ is compatible with a high spin ($S = 3/2$) monomeric Mn(IV) species as shown by the spectrum

simulation. This species could be assigned to a high-valent manganese-oxo intermediate (Czernuszewicz *et al.*, 88; Ayougou *et al.*, 95). The second characteristic resonance of Mn(IV) ($S = 3/2$), is a broad signal occurring at $g \approx 2$. A free radical signal at $g \approx 2$ is also detected, suggesting the formation of a protein radical on the peptide part of Mn(III)MP-8 concomitantly with the Mn(IV)MP-8=O species.

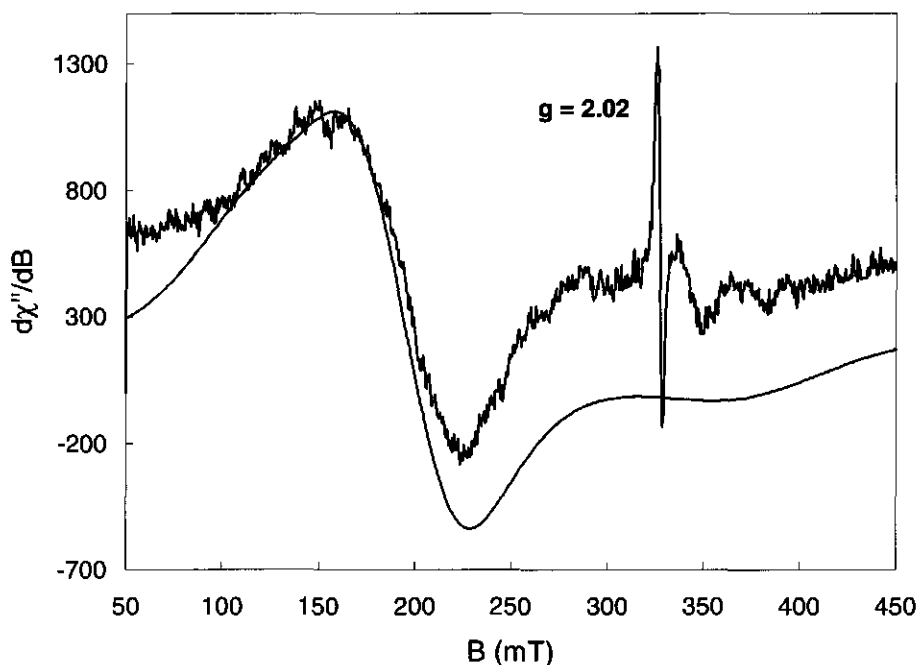


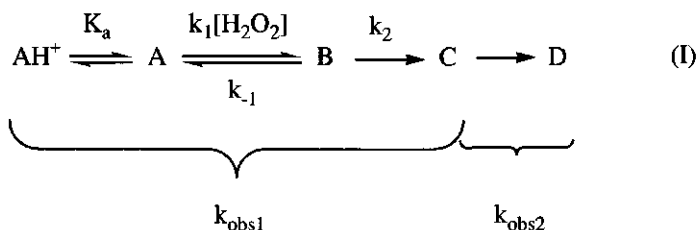
Figure 7.4 EPR X-band, 9.227 GHz, transient spectrum of 1 mM Mn(III)MP-8 incubated with 25-fold excess of H_2O_2 in 0.1 M carbonate pH 11.5 and simulated trace for a Mn(IV) ($S = 3/2$) system (thin line). A resonance assigned to a Mn(IV) ($S = 3/2$) species is visible at $g \approx 4$ and a free radical signal is indicated at $g \approx 2.02$.

7.4 Discussion

Kinetic analysis

The present study describes rapid kinetics for the formation of oxidised Fe(III)MP-8 and Mn(III)MP-8 upon reaction with H_2O_2 as function of $[H^+]$. The system is experimentally described by two observed mono-exponential steps (k_{obs1} and k_{obs2}) for Fe(III)MP-8 and Mn(III)MP-8 pointing at the fact that there is an intermediate C which is formed between the two steps. The analysis of the data, for the first observed mono-

exponential step k_{obs1} , is based on the following reactions sequence which shows one non-reversible elementary step preceded by two reversible elementary steps (see later for justification) (Scheme I).



The observation of saturation kinetics for both Fe(III)MP-8 and Mn(III)MP-8 (Figure 7.2) strongly suggests the formation of an intermediate B during the observed step k_{obs1} . Also, inspection of the saturation plots indicate that the conversion of B to C, is a non-reversible process. Finally, the competitive effect of the protons observed during the first step k_{obs1} (Figure 7.3) can be interpreted as the deprotonation step of a protonated precursor of A, denoted AH^+ . The following rate law can be derived to describe the formation of C in Scheme I (see Appendix eq 7.A6) :

$$v = \frac{d[\text{C}]}{dt} = k_{\text{obs1}} [\text{A}]_t = k_2 [\text{B}] \quad (7.1)$$

and consecutively an hyperbolic equation for k_{obs1} (eq 7.A8) :

$$k_{\text{obs1}} = \frac{k_2 [\text{H}_2\text{O}_2]}{\left(1 + \frac{[\text{H}^+]}{K_a}\right) \left(\frac{k_{-1} + k_2}{k_1}\right) + [\text{H}_2\text{O}_2]} \quad (7.2)$$

Using the double reciprocal form of equation (7.2), (see eq 7.A9), the values of the first order rate constant k_2 could be calculated from the double reciprocal plots of Figure 7.2. And $k_2 = 165 \pm 8 \text{ s}^{-1}$ for Fe(III)MP-8 and $k_2 = 145 \pm 7 \text{ s}^{-1}$ for Mn(III)MP-8 (from Figure 7.2b and 7.2d respectively).

When $[H_2O_2]$ is kept constant equation (7.A9) can be rewritten as follows :

$$\frac{1}{k_{obs1}} = \frac{1}{k'_{obs1}} + \frac{[H^+]}{K_a k'_{obs1}} \quad (7.3)$$

where k'_{obs1} is a theoretical pseudo-first order rate constant independent of the protons and dependent of $[H_2O_2]$. As proposed in the results section, the plots of Figure 7.2 and 7.3 point at a competitive effect of the protons for the formation of intermediate B. The inhibition constant K_a is calculated from the plots of Figure 7.3 using equation (7.3) and gives $pK_a = 9.5 \pm 0.5$ for Fe(III)MP-8 and $pK_a = 11.3 \pm 0.5$ for Mn(III)MP-8. Both values are in good agreement with the pH-optimum values for respectively Fe(III)MP-8 and Mn(III)MP-8 supported peroxidase-catalysis, and Fe(III)MP-8 supported P450-catalysis (Primus *et al.*, 99). The pK_a values can also be calculated from the saturation plots of Figure 7.2a and 7.2c using the non-double reciprocal form of equation (7.3) at a similar $[H_2O_2]$ for each of the two pH values. The values calculated are, $pK_a = 8.9 \pm 0.5$ for Fe(III)MP-8 and $pK_a = 10.8 \pm 0.5$ for Mn(III)MP-8 in agreement with the ones obtained from Figure 7.3.

At low $[H_2O_2]$ and assuming $k_1 \ll k_2$, equation (7.2) becomes (eq 7.A11) :

$$k_{obs1} = \frac{k_1 [H_2O_2]}{\left(1 + \frac{[H^+]}{K_a} \right)} \quad (7.4)$$

The second order rate constant k_1 can be determined from the tangent of the initial slope of the $[H_2O_2]$ -saturation plots in Figure 7.2a and 7.2c using equation (7.4). For Fe(III)MP-8, $k_1 = (1.1 \pm 0.1) \times 10^6 \text{ M}^{-1} \cdot \text{s}^{-1}$ at pH 8 and $k_1 = (1.2 \pm 0.1) \times 10^6 \text{ M}^{-1} \cdot \text{s}^{-1}$ at pH 9.1; for Mn(III)MP-8, $k_1 = (1.3 \pm 0.1) \times 10^5 \text{ M}^{-1} \cdot \text{s}^{-1}$ at pH 10.2 and $k_1 = (0.9 \pm 0.1) \times 10^5 \text{ M}^{-1} \cdot \text{s}^{-1}$ at pH 10.9. Consecutively, using the double reciprocal form of equation (7.2) (eq 7.A9), k_1 can be determined from the plots of Figure 7.2b and 7.2d. For Fe(III)MP-8, $k_1 = 0.8 \pm 0.01 \text{ s}^{-1}$ at pH 8 and $k_1 = 14.3 \pm 1.4 \text{ s}^{-1}$ at pH 9.1; for Mn(III)MP-8, $k_1 = 15.0 \pm 1.5 \text{ s}^{-1}$ at pH 10.2 and $k_1 = 16.2 \pm 1.6 \text{ s}^{-1}$ at pH 10.9. The obtained values of k_1 confirm that the assumption

made for deriving equation (7.4) is correct. Moreover with $k_{-1} \ll k'_1$ (see equation 7.A14) the rate constant k_{-1} can be ignored in Scheme I and it becomes possible to simulate the first step of the transient kinetics traces, k_{obs1} , using an equation describing the variation of [C] as function of time (eq 7.A12). The value of k_1 can be determined from the simulation with good confidence, considering that the time-dependent transient absorbance changes, recorded at 410 nm for Fe(III)MP-8 and 400 nm for MnMP-8, almost exclusively account for the formation of C. Simulation of selected traces give for Fe(III)MP-8, $k_1 = (1.6 \pm 0.2) \times 10^6 \text{ M}^{-1} \cdot \text{s}^{-1}$ and for Mn(III)MP-8, $k_1 = (1.1 \pm 0.1) \times 10^5 \text{ M}^{-1} \cdot \text{s}^{-1}$. The good agreement of these values with the ones estimated from the saturation plots of Figure 7.2 again confirms that the assumption of ignoring k_{-1} for determining k_1 , using equation (7.4) is correct. The average values of the kinetics and thermodynamic parameters obtained for both catalysts are given in Table 7.1.

Nature of the intermediates

The determination of the nature of the different intermediates A, B, C and D is based on the following facts. i) The transient UV/visible spectra of C and D are similar (see Figure 7.1) and can be assigned to a high-valent metal-oxo MP-8 species; ii) The transient EPR of Mn(III)MP-8 reacted with H_2O_2 during 27 ms indicates that a free radical species is formed concomitantly to a high-valent manganese-oxo species. iii) The conversion of C into D is independent of $[\text{H}^+]$ and $[\text{H}_2\text{O}_2]$; iv) The conversion of B into C is rate limiting, except at very low $[\text{H}_2\text{O}_2]$, and leads to the accumulation of B; v) The observed rate of formation of C increases at higher pH-values.

In consequence two species, C and D, depict the same UV/visible fingerprint but are kinetically well defined as two separated intermediates. For MnMP-8, using equation (7.A12), a calculation of the concentration of C after 27 ms reaction time in the conditions of the EPR measurement shows that the reaction mixture mainly contains 70 % of intermediate C. It is therefore reasonable to identify C as a possible high-valent manganese-oxo MP-8 with a free radical species not located on the porphyrin macrocycle. Intermediate D would represent the decaying species of C with no more free radical character but still regarded as a high-valent manganese-oxo species based on the UV/visible spectra.

For the reaction of Fe(III)MP-8 with H₂O₂, there is no evidence of a free radical character on the peptide of the molecule for intermediate C. However, the mechanism of oxidation common to Mn(III)MP-8 and Fe(III)MP-8, suggests an assignment, similar to the one made for Mn(III)MP-8, for intermediates C and D of Fe(III)MP-8. Additionally, for Fe(III)MP-8, a solvent modified Fe(III)MP-8 having a hydroxylated histidine axial ligand was isolated in the presence of H₂O₂. It has been proposed that this modified product would account for a delocalised second oxidation equivalent of a putative Fe(III)MP-8 high-valent iron-oxo and peptide radical intermediate (Primus *et al.*, 2000). Moreover, the formation of intermediate C follows saturation kinetics. Consequently, intermediate B can be assigned to the Compound 0 of MP-8, M(III)MP-8-OOH (Baek *et al.*, 89; Wang *et al.*, 91). In the reaction cycle of peroxidases, Compound 0 is preceding the formation of an intermediate consisting of a high-valent iron-oxo species and a radical species.

Table 7.1 Mean values of the kinetic and thermodynamic constants determined in this study, for the reaction of H₂O₂ with Fe(III)MP-8 and Mn(III)MP-8. The pK_a corresponds to the deprotonation of metal-bound water for both catalysts, k₁ to the second order rate constant for the formation of M(III)MP-8-OOH, k₋₁ to the corresponding first order reverse rate constant, k₂ to the first order rate constant for the cleavage of M(III)MP-8-OOH and k₋₂ to the corresponding reverse second order rate constant. The pseudo-first order rate constant k_{obs2} corresponds to the decaying phase of the postulated high-valent metal-oxo peptide radical intermediate. See discussion for the calculation of these parameters.

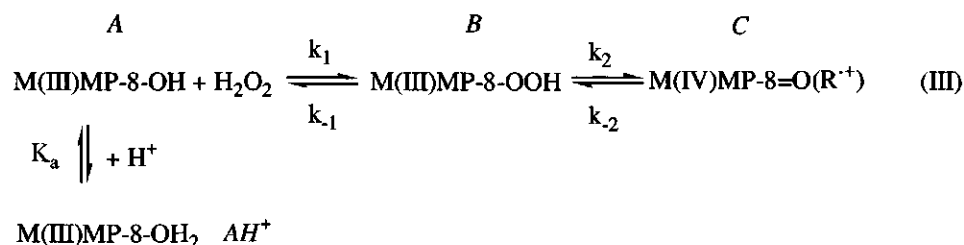
	pK _a ± 3σ ^a	k ₁ ± 3σ (M ⁻¹ .s ⁻¹) ^b	k ₋₁ ± 2σ (s ⁻¹)	k ₂ (s ⁻¹)	k ₋₂ (M ⁻¹ .s ⁻¹)	k _{obs2} (s ⁻¹)
Fe(III)MP-8	9.2 ± 0.9	(1.3 ± 0.6) × 10 ⁶	7.5 ± 12	165 ± 8	0.03 ± 0.01 ^c	13.1 ± 1.1
Mn(III)MP-8	11.0 ± 0.8	(1.1 ± 0.5) × 10 ⁵	15.6 ± 1.8	145 ± 7	nd	5.2 ± 1.2

^a the mean pK_a value was used to calculate k₁ and k₋₁, ^b the mean value of k₁ was used to calculate k₋₁, ^c calculated from van Haandel *et al.* (van Haandel *et al.*, 98)

A reasonable structure for intermediate C would therefore be a high-valent metal-oxo MP-8 peptide radical, M(IV)MP-8=O(R^{•+}), and for intermediate D a high-valent metal-oxo MP-8, M(IV)MP-8=O. Recently, based on rapid-freeze EPR and Mössbauer spectroscopy, such a structure has been proposed for the peroxy acetic acid oxidised product of cytochrome P450_{cam}. The accompanying radical is proposed to be localised on a tyrosine residue localised in the proximal heme active site (Schünemann *et al.*, 2000). Finally, the pK_a value measured in this study for Fe(III)MP-8 is found in good agreement

with the pK_a of Fe(III)MP-8 iron bound water deprotonation ($pK_a = 9.6$) (Baldwin *et al.*, 86; Wang *et al.*, 92). The two units higher pK_a value measured for Mn(III)MP-8 (Table 7.1) is consistent with the lower reduction potential of the manganese catalyst (Primus *et al.*, 99) and can be assigned to manganese bound water deprotonation. The rapid deprotonation of the aquo ligand is a prerequisite to form a species, M(III)MP-8-OH (intermediate A), able to react with H_2O_2 and to form Compound 0.

In conclusion, the reaction sequence describing k_{obs1} in Scheme I can now be written in the following way with the reverse rate constant k_{-2} estimated from oxygen exchange experiments (van Haandel *et al.*, 98) (Scheme III; intermediates AH^+ , A, B and C are indicated in italics) :



7.5 Conclusion

This study provides a comprehensive explanation for the pH-dependent reactivity of Fe(III)MP-8 and Mn(III)MP-8 with H_2O_2 . In contrast to HRP, the absence of a real active site pocket for MP-8, with a distal basic residue participating in the peroxide deprotonation and favouring the O-O peroxide bond cleavage could somehow be responsible for the low reactivity of MP-8 at low pH. Increase of the pH induces metal-bound water deprotonation, which subsequently, either assists concerted hydrogen peroxide deprotonation and coordination of the hydroperoxo group to the metal center, or is directly oxidised by hydrogen peroxide into a metal-hydroperoxo MP-8. For HRP, His42 could deprotonate the iron-bound water and promote a similar mechanism as the one suggested for MP-8. Compound 0 is subsequently converted into what can best be described as a high-valent metal-oxo intermediate and a peptide free radical. This latter intermediate slowly decays into a high-valent metal-oxo species, which may have been altered by the solvent.

7.6 Appendix

(1) Derivation of a common rate law for the reaction of Fe(III)MP-8 and Mn(III)MP-8 with H_2O_2 ; expression of k_{obs1} .

Considering the mechanism depicted in Scheme I, the rate of formation of intermediate B can be written as follows :

$$\frac{d[B]}{dt} = k_1 [H_2O_2][A]_t - k_2 [B] - k_{-1}[B] \quad (7.A1)$$

$$\text{also : } [A]_t = [AH^+] + [A] + [B] \quad (7.A2)$$

$$\text{and } K_a = \frac{[A][H^+]}{[AH^+]} \quad (7.A3)$$

Substitution of (7.A2) and (7.A3) in (7.A1) gives :

$$\frac{d[B]}{dt} = \frac{K_a k_1 [H_2O_2][A]_t}{K_a + [H^+]} - k_2 [B] - k_{-1}[B] - \frac{K_a k_1 [H_2O_2][B]}{K_a + [H^+]} \quad (7.A4)$$

which integrated leads to the following time-dependent expression for the concentration of intermediate B (Laidler, 55) :

$$[B] = \frac{[A]_t [H_2O_2] \left(1 - \exp \left(- \left(\frac{K_a k_1 [H_2O_2]}{K_a + [H^+]} + k_{-1} + k_2 \right) t \right) \right)}{\left(1 + \frac{[H^+]}{K_a} \right) \left(\frac{k_{-1} + k_2}{k_1} \right) + [H_2O_2]} \quad (7.A5)$$

The rate law for the formation of intermediate C is proposed as followed :

$$v = \frac{d[C]}{dt} = k_{obs1} [A]_t = k_2 [B] \quad (7.A6)$$

and substitution of (7.A5) in (7.A6) gives the following expression for k_{obs1} :

$$k_{obs1} = \frac{k_2 [H_2O_2] \left(1 - \exp \left(- \left(\frac{K_a k_1 [H_2O_2]}{K_a + [H^+]} + k_{-1} + k_2 \right) t \right) \right)}{\left(1 + \frac{[H^+]}{K_a} \right) \left(\frac{k_{-1} + k_2}{k_1} \right) + [H_2O_2]} \quad (7.A7)$$

For the present analysis of k_{obs1} , the exponential term of (7.A7) can be considered far below 1 when the reaction time of the system is taken higher than 10 ms and consequently (7.A7) simplifies to (7.A8) :

$$k_{\text{obs1}} = \frac{k_2 [\text{H}_2\text{O}_2]}{\left(1 + \frac{[\text{H}^+]}{K_a}\right) \left(\frac{k_1 + k_2}{k_1}\right) + [\text{H}_2\text{O}_2]} \quad (7.A8)$$

Equation (7.A8) can also be written in a double reciprocal form :

$$\frac{1}{k_{\text{obs1}}} = \frac{(K_a + [\text{H}^+])(k_2 + k_1)}{K_a k_2 k_1} \frac{1}{[\text{H}_2\text{O}_2]} + \frac{1}{k_2} \quad (7.A9)$$

Or when the concentration of H_2O_2 is low such as :

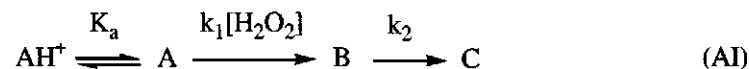
$$\left(1 + \frac{[\text{H}^+]}{K_a}\right) \left(\frac{k_1 + k_2}{k_1}\right) \gg [\text{H}_2\text{O}_2] \quad (7.A10)$$

and considering $k_1 \ll k_2$, equation (7.A8) becomes :

$$k_{\text{obs1}} = \frac{k_1 [\text{H}_2\text{O}_2]}{\left(1 + \frac{[\text{H}^+]}{K_a}\right)} \quad (7.A11)$$

(2) Expression of the variation of [C] as function of time for a consecutive non-reversible reaction sequence (Scheme AI).

Ignoring k_1 in Scheme I, the following consecutive non-reversible elementary two-steps reaction sequence preceded by a rapid pre-equilibrium is used to describe k_{obs1} :



The expression of the variation of [C] as function of time is adapted from Moore and Pearson (Moore and Pearson, 80) leading to :

$$[\text{C}] = \frac{[\text{A}]_0 K_a}{(K_a + [\text{H}^+])} \left[1 + \frac{1}{(k_1' - k_2)} (k_2 \exp(-k_1' t) - k_1' \exp(-k_2 t)) \right] \quad (7.A12)$$

with
$$[A]_0 = [A] \frac{(K_a + [H^+])}{K_a} \quad (7.A13)$$

and
$$k_1' = \frac{K_a k_1 [H_2O_2]}{K_a + [H^+]} \quad (7.A14)$$

The apparent first order rate constant k_1' can be simulated using equation (7.A12) and k_1 is consecutively obtained by using equation (7.A14).

Acknowledgements The authors gratefully acknowledge dr. Huub Haaker for help with the rapid-freeze experiments and prof. dr. R. Weiss for constant support. The EU Copernicus programme (grant no. ERBIC15-CT961004), the Dutch Foundation for Technical Research (CW/STW project no. 349-3710) and the Centre National pour la Recherche Scientifique (CNRS, France) are also acknowledged.

8

Summary and Discussion

Microperoxidase-8: from a heme-peroxidase biomimic to cytochrome P450 chemistry

Inspection of the chemical structure of $\text{Fe}^{\text{III}}\text{MP-8}$ which resembles an open peroxidase active site, suggests that it can be used as a model for peroxidase catalysis. Numerous publications have already appeared on the peroxidase activity of $\text{Fe}^{\text{III}}\text{MP-8}$ but also on the description of the monooxygenase activity of $\text{Fe}^{\text{III}}\text{MP-8}$, which is typical of cytochrome P450 enzymes. In this thesis, $\text{Fe}^{\text{III}}\text{MP-8}$ and the manganese variant $\text{Mn}^{\text{III}}\text{MP-8}$, were studied for their mechanism of oxygen exchange between the oxo group of porphyrin high-valent metal-oxo species and solvent, their P450 and peroxidase catalytic reactivity and the formation of their catalytic reactive intermediates.

Determinants of the peroxidase and P450 chemistry for $\text{Fe}^{\text{III}}\text{MP-8}$ and $\text{Mn}^{\text{III}}\text{MP-8}$ (Chapter 1)

In the Chapter 1 of this thesis, peroxidase and P450 enzymes were compared in order to understand the major differences between both types of enzymes underlying the differences in their chemistry. It was shown that peroxidases and P450s share similar intermediates in their catalytic cycles but that both types of enzymes were structurally different. Two major reasons for the differences between peroxidase and P450 chemistry can be derived from the analysis of the structure and the reactivity of both types of enzyme. Differences in the distal environment of the heme and in the nature of the axial ligand can be regarded as having an influence on their chemistry.

1. Differences in the heme distal environment

A comparison of the distal heme cavity for peroxidase and P450 enzymes shows that peroxidases do not have a clearly defined hydrophobic distal pocket allowing the binding of organic substrates near the heme iron centre. With the exception of hydroperoxides which bind to the heme iron centre and are subsequently reduced by the heme group to generate catalytic reactive intermediates, the organic substrate is proposed to bind on the δ -meso heme edge thereby allowing electrons transfer to the heme prosthetic group. The fact that organic substrates cannot bind to the distal part of the peroxidase active site near the oxo group of Compound I, explains why these enzymes do not support oxygen transfer reactions. Moreover the fact that only for peroxidase mutants where some "extra space" has been created on the distal part of the active site, monooxygenases reactions are observed but catalysed at a lower rate than for heme-thiolate enzymes, corroborates the assumption that substrate binding near the heme iron favours oxygen transfer. Evolutionary speaking, peroxidases are well designed to reduce small oxygen containing molecules, hydroperoxides, and to convert them into oxidative power which may be beneficial to the cell because of the formation of useful compounds such as polymers. P450s, however, have a distal active site pocket which allows substrate binding near the heme iron center. From an evolutionary point, P450s are well designed to convert harmful xenobiotics or modifying membrane lipid components in the cell. The fact that the substrate binds close to the site where the reactive catalytic intermediates are generated favours *in-situ* conversion and direct oxygen transfer to the substrate. Moreover this oxygen transfer can be mediated by the various catalytic intermediates of the reaction cycle preceding the Compound I analogue and not only by the Compound I analogue (Figure 8.1). The physical proximity of the substrate and the reactive intermediates favours a reaction of the catalytic intermediates with the substrate over a transformation of a given catalytic intermediate into the following catalytic intermediate of the reaction cycle of the enzyme.

2. Differences in the nature of the proximal axial ligand

Peroxidases and P450s differ by the nature of their proximal axial ligand. The negative charge of the cysteinate ligand of P450s is proposed to lower the oxidation potential of the Compound I analogue intermediate thereby favouring oxygen transfer *to substrate* over electron abstraction *from substrate*. The negative charge of the sulphur atom is somewhat reinforced by the involvement of a network of hydrogen bonds from the

residues of the heme proximal active site to the sulphur of the thiolate group. Theoretical MO-calculations also have shown that the sulphur orbitals of the cysteinate mix with the a_{2u} cationic state of the porphyrin high-valent iron-oxo intermediate along the reaction pathway. This is not observed for the proximal histidine ligand of peroxidases. In peroxidases, the neutral histidine ligand is proposed to favour electron abstraction *from substrate* over oxygen transfer *to substrate*.

Compound I oxo exchange: implications for oxygen transfer (Chapters 2 and 3)

In the field of heme-based catalysis, labelling studies are used to discriminate between peroxidase-type of chemistry and P450-type of chemistry. Tracing of the oxygen donor atoms in the product allows to differentiate between *true oxygen transfer*, where the oxygen atom inserted in the substrate originates from the primary oxygen donor, P450 chemistry, and *apparent oxygen transfer* where the oxygen atom inserted in the substrate originates from the solvent, peroxidase chemistry. However, heme-enzymes and the corresponding models were shown to exchange the oxo group of their Compound I intermediate, or Compound I analogue, with bulk solvent. Chapters 2 and 3 of this thesis are oriented on the mechanistic aspects of the exchangeability of the oxo group of Compound I with bulk solvent. In Chapter 2, HRP and the labelled oxygen donor are left incubating during an exchange step of variable time length before the substrate, aniline, is added. The conversion of aniline results in the insertion of one oxygen atom in the substrate by *para*-hydroxylation. The *para*-hydroxylated aniline formed during the conversion step subsequent to the exchange step was analysed by MS. This reveals an increasing percentage of the incorporation of oxygen atoms originating from the solvent when the duration of the exchange step is increased. When catalase was added between the two steps of the experiment, no product was formed. This shows that the heme catalyst induces oxygen exchange between bulk water and H_2O_2 , to form H_2O_2 containing oxygen atoms issued from the solvent. A mechanism explaining this oxygen exchange for an axially coordinated heme has been suggested including the reversibility of the formation of Compound I for HRP, but also for Fe^{III} MP-8, hemin and hematin. Actually, water becomes a substrate for the porphyrin high-valent iron-oxo intermediate and competes with the organic substrate, when present, for being oxidised. In the study presented in Chapter 2, substrate oxidation and water oxidation were decoupled thereby emphasising the water oxidation step. Moreover

this study indirectly suggests that oxidised heme-based systems can catalyse the formation of peroxide bonds at the (modest) apparent rate of $\approx 1 \text{ s}^{-1}$. This is a relevant outcome of this study, since the design of molecules containing a peroxide bond is of fundamental importance for oxidation chemistry and is of particularly interest for the chemical industry.

In Chapter 3, the same argumentation as proposed in Chapter 2 is supported by additional exchange experiments with iron and manganese water-soluble porphyrins. This chapter is an attempt to unify the views on porphyrin high-valent metal-oxo/solvent exchange processes. Direct oxygen exchange of the oxo group of Compound I, for a solvent oxygen atom is not found to account for the regeneration of H_2O_2 during the exchange step. Also a mechanism such as oxo/hydroxo tautomerism where the transfer of two protons from the *trans* water axial ligand to the oxygen of the oxo group results in an exchange of the oxo oxygen cannot explain Fe^{III} MP-8 supported oxygen exchange. The fact that Fe^{III} MP-8 has an axial histidine ligand prevents solvent binding *trans* to the oxo group, which would be a prerequisite for proton transfer resulting in oxygen exchange between both axial ligands. Obviously this cannot explain oxygen exchange catalysed by axially ligated heme or metalloporphyrins like Fe^{III} MP-8. The reversible formation of Compound I, proposed in Chapter 2, explains the results in a clear way.

Catalytic reactivity of Fe^{III} MP-8 and Mn^{III} MP-8 (Chapter 4 and 5)

The heme-peptide model, Fe^{III} MP-8, shows peroxidase activity and can also be used as a heme-enzyme model for studying P450 chemistry based on the fact that, upon addition of ascorbate, the reactive species which are responsible for peroxidase chemistry are scavenged. As a consequence Fe^{III} MP-8 can be active in two modes: the peroxidase mode where the catalysis is dominated by porphyrin high-valent iron-oxo intermediates and the P450 mode where the porphyrin high-valent iron-oxo intermediates are (partially) scavenged and catalysis is mainly performed by intermediates appearing *prior* to Compound I in the reaction cycle. The switch between the two modes is provided by the addition of ascorbate to the system in the case of P450 chemistry, which acts as scavenger for porphyrin high-valent iron-oxo intermediates.

In Chapter 4 the reactivity of Fe^{III} MP-8 for H_2O_2 supported O- and N-dealkylation, a peroxidase/P450 type of reaction, has been investigated. In the peroxidase mode, *i.e.* without ascorbate addition, the rate of conversion of the substrates is correlated with their

quantum mechanically calculated first ionisation potential. This indicates that their conversion proceeds *via* an initial electron abstraction from the substrate. This is corroborated by the observation of a large amount of polymerisation products together with the formation of small amounts of N-dealkylated products. In contrast however O-dealkylation was not observed. This observation that O-alkylated substrates are not dealkylated in the peroxidase mode can be related to the fact that their first ionisation potential is too low. In the P450 mode, *i.e.* in the presence of ascorbate, O- and N-alkylated substrates are both converted and a correlation with the calculated first ionisation potential of the substrates no longer exists. This suggests that O- and N-dealkylations in the P450 mode proceed *via* a non-radical type of mechanism and thus through other intermediates than Compound I and Compound II, since ascorbate is a scavenger of Compound I and II. As an alternative reactive species the non-radical type $\text{PorFe}^{\text{III}}\text{-(hydro)peroxo}$ intermediate, may be the species involved in the P450 mode of $\text{Fe}^{\text{III}}\text{MP-8}$ supported O- and N-dealkylation. The $\text{PorFe}^{\text{III}}\text{(hydro)peroxo}$ intermediate is known as Compound 0 and appears before Compound I in the catalytic cycle. Mechanisms for Compound 0 supported O- and N-dealkylations are discussed in detail.

The aim of the investigations described in Chapter 5 was to gain information on the nature of the different reactive species involved in MP-8 supported catalysis comparing again peroxidase and P450 reactions. For this purpose the manganese variant of Fe(III)MP-8 , Mn(III)MP-8 was synthesised. Iron and manganese porphyrin complexes have a similar chemistry but differ in their reaction kinetics providing information concerning which type of intermediate is involved in catalysis. The conversion of guaiacol (2-methoxyphenol), *ortho*-dianisidine (3,3'-dimethoxybenzidine) and aniline catalysed by $\text{Fe}^{\text{III}}\text{MP-8}$ and $\text{Mn}^{\text{III}}\text{MP-8}$ was studied. The first two substrates are models for the peroxidase reactivity of heme-enzymes and the third one is a model for the P450 reactivity of heme-enzymes. The pH-dependence of the rate of conversion, k_{cat} , of each substrate was studied for $\text{Fe}^{\text{III}}\text{MP-8}$ and $\text{Mn}^{\text{III}}\text{MP-8}$ supported conversions, using H_2O_2 as oxygen donor. For the peroxidase mode it was shown that the optimal pH for $\text{Mn}^{\text{III}}\text{MP-8}$ supported conversions is pH 11, about 2 units higher than for $\text{Fe}^{\text{III}}\text{MP-8}$ which has an optimal pH of 9. This can be correlated to the lower reduction potential of the $\text{Mn}^{\text{III}}\text{MP-8}/\text{Mn}^{\text{II}}\text{MP-8}$ transition when compared to the iron complex. The iron atom is proposed to better stabilise the deprotonated coordinated hydroperoxide molecule than the manganese centre due to its

higher electron withdrawing effect on the proximal oxygen of the (hydro)peroxy group. For the cytochrome P450 mode, *i.e.* in the presence of ascorbate, it was found that $\text{Mn}^{\text{III}}\text{MP-8}$ was not able to catalyse the *para*-hydroxylation of aniline whereas it was possible for $\text{Fe}^{\text{III}}\text{MP-8}$ under the same conditions. These results are in line with the conclusions of Chapter 4 and indicate that the MP-8 supported cytochrome P450 chemistry proceeds *via* a $\text{PorFe}^{\text{III}}$ -hydroperoxy intermediate. This also explains the absence of aniline hydroxylation activity for $\text{Mn}^{\text{III}}\text{MP-8}$ based catalysis because the Mn^{III} -(hydro)peroxy intermediate is much less reactive toward electrophilic hydroxylation than the corresponding iron intermediate. As a consequence the hydroxylation of aniline by $\text{Fe}^{\text{III}}\text{MP-8}$ may be performed by Compound 0. However, as stressed also in Chapter 4, Compound I and II, typical of the peroxidase mode, may also play a role in the P450 mode since ascorbate competes with aniline for oxidation by Compound I and II.

Characterisation of peroxidase and P450 intermediates (Chapter 6 and 7)

One of the major drawbacks of MP-8 is the high inactivation rate observed for the catalyst under operational conditions in both the P450 and the peroxidase mode. In an effort aiming at understanding the reasons for the fast inactivation of $\text{Fe}^{\text{III}}\text{MP-8}$, the fate of the catalyst was studied under turnover conditions in the absence of substrate. Chapter 6 presents the characterisation of a modified $\text{Fe}^{\text{III}}\text{MP-8}$ with a hydroxylated His18. The modified catalyst was isolated under operational conditions in the presence of H_2O_2 . The structure of the native and the modified $\text{Fe}^{\text{III}}\text{MP-8}$ were compared by HPLC, UV/visible, ESI-MS² and ¹H-NMR. Analysis showed the formation of a product more hydrophilic than $\text{Fe}^{\text{III}}\text{MP-8}$, with an intact heme ring and having an extra oxygen inserted on the peptide. ESI-MS² and ¹H-NMR suggest the extra oxygen atom to be inserted on the N δ 1 of the imidazole ring of the His18. The formation of the modified intermediate is inhibited by ascorbate and labelling studies have shown that the inserted oxygen originates from the solvent. This suggests the modified $\text{Fe}^{\text{III}}\text{MP-8}$ to derive from a Compound I analogue of $\text{Fe}^{\text{III}}\text{MP-8}$. The fact that the solvent-assisted hydroxylation occurs on the proximal histidine ligand suggests the second oxidation equivalent of the analogue of $\text{Fe}^{\text{III}}\text{MP-8}$ Compound I to be majorly delocalised on the His18 axial ligand by mesomerism.

The characterisation and the analysis of the kinetics of formation of the heme-intermediates competent in MP-8-supported peroxidase and P450 catalysis is the subject of Chapter 7. The kinetics for the formation of Compound 0, Compound I analogue and Compound II were compared for $\text{Fe}^{\text{III}}\text{MP-8}$ and $\text{Mn}^{\text{III}}\text{MP-8}$. Analysis reveals a one order of magnitude higher rate of formation of $\text{PorFe}^{\text{III}}\text{-OOH}$ ($k = 1.3 \times 10^6 \text{ M}^{-1} \cdot \text{s}^{-1}$) when compared to the rate of formation of $\text{PorMn}^{\text{III}}\text{-OOH}$ ($k = 1.1 \times 10^5 \text{ M}^{-1} \cdot \text{s}^{-1}$). The overall rate of the reaction for both complexes with H_2O_2 , increases with higher pH-values. The corresponding pK_a values which were found to explain this pH-dependency are in complete agreement with the optimal values for $\text{Fe}^{\text{III}}\text{MP-8}$ (pH 9.2) and $\text{Mn}^{\text{III}}\text{MP-8}$ (pH 11.0) supported catalysis (Chapter 5) and were found to correspond to the deprotonation of metal-bound water for $\text{Fe}^{\text{III}}\text{MP-8}$. This explains how heme-peptide models which lack a distal histidine, acting as an acid/base catalyst for the deprotonation of H_2O_2 and for the subsequent cleavage of the O-O peroxide bond, facilitate the deprotonation of H_2O_2 . For MP-8, the peroxide deprotonation may proceed through a concerted mechanism which results in the replacement of the hydroxyl ligand by a hydroperoxo ligand. It is not sure, however, how MP-8 catalyses the cleavage of the O-O peroxide bond, since no residue or group able to deliver protons to the distal oxygen in order to facilitate bond cleavage are present on the distal site. An eventual participation of the N δ 1 of the imidazole ring of the His18 of a second molecule of MP-8 as proton donor cannot be excluded. The manganese Compound 0 is proposed to be heterolytically cleaved into a Compound I type of intermediate, $\text{Mn}^{\text{IV}}\text{MP-8}=\text{O}(\text{R}^+)$, where the second oxidation equivalent seems to be localised on the peptide part of the molecule. This is suggested by the analysis of the transient UV/visible and EPR spectra of oxidised $\text{Mn}^{\text{III}}\text{MP-8}$. Based on the kinetic analysis and on the results of Chapter 6, iron Compound 0 is also proposed to be heterolytically cleaved into a similar Compound I type of intermediate, $\text{Fe}^{\text{IV}}\text{MP-8}=\text{O}(\text{R}^+)$, with a cleavage rate analogue to the one of the manganese complex ($k \approx 150 \text{ s}^{-1}$).

To summarise, in peroxidases, the hydroperoxo intermediate is rapidly converted, during the reaction cycle, into Compound I catalysed by the residues of the distal heme pocket. In P450s the corresponding hydroperoxo or peroxo intermediates may react with the substrate bound in the active site before they are converted into a Compound I analogue. In other words, P450 chemistry is not only based on the catalytic reactivity of Compound I but also on the reactivity of Compound 0 and the deprotonated form of Compound 0 respectively the $\text{PorFe}^{\text{III}}$ -hydroperoxo and the $\text{PorFe}^{\text{III}}$ -peroxo intermediates.

Whereas the isoelectronic analogue of Compound I can be seen as an intermediate in electrophilic reactions such as Compound 0, the deprotonated Compound 0 is proposed to be active in both electrophilic and nucleophilic reactions (Figure 8.1).

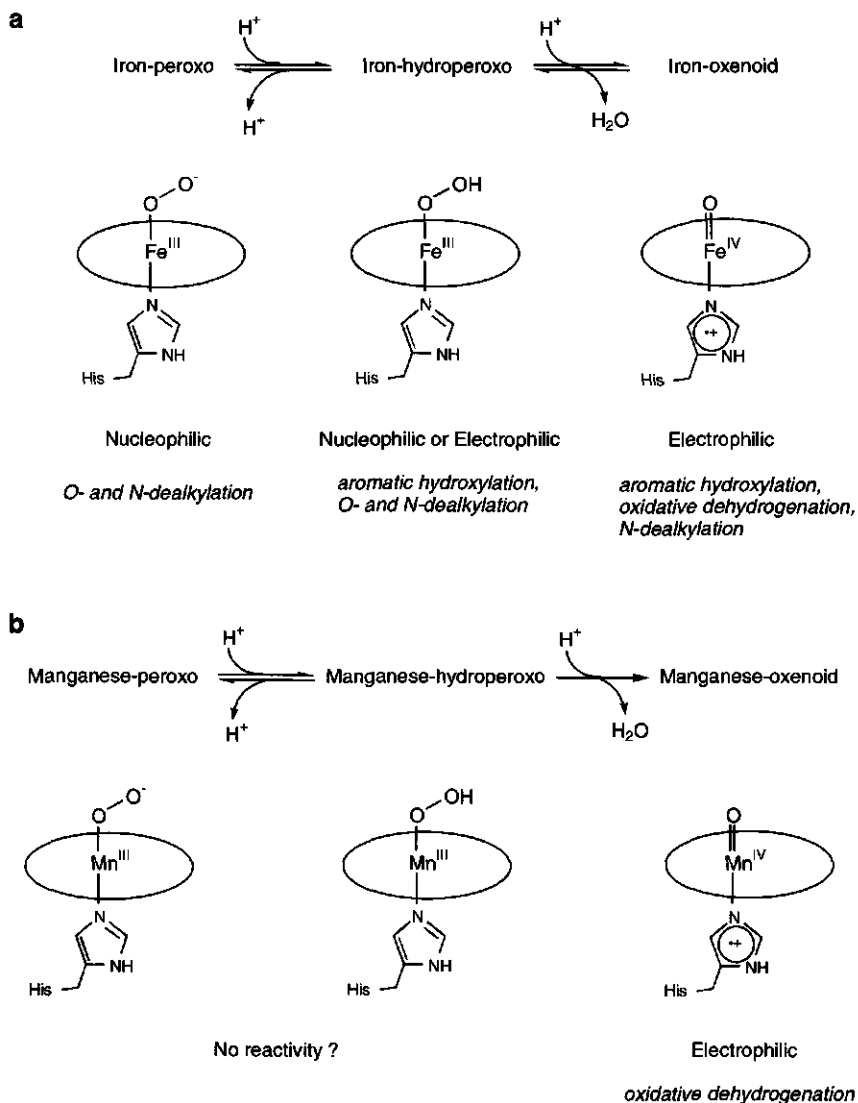


Figure 8.1 Reactive intermediates encountered in the (a) Fe^{III} MP-8, and (b) Mn^{III} MP-8 P450-type and peroxidase-type of chemistry and corresponding catalysed conversions described in Chapter 4 and 5 of this thesis. The structure of the iron-oxenoid and manganese-oxenoid intermediate is based on the conclusions of Chapter 7. Adapted from Coon *et al.* (Coon *et al.*, 98) and from the Chapter 5 of the present thesis.

As a consequence, one might conclude that designing a biomimic for the P450 chemistry requires two major conditions: i) the presence of an open active site and ii) the stabilisation of the catalytic reactive intermediates preceding the formation of the porphyrin high-valent iron-oxo intermediate in the reaction cycle. Fe^{III}MP-8 and Mn^{III}MP-8 resemble an open peroxidase active site having no distal environment. It has been shown that for both MP-8 models the co-ordination of a molecule of hydrogen peroxide on the metal is facilitated by bound water, providing the pH in the medium is high (Chapter 7). This questions the role played by the distal histidine ligand in peroxidases. Generally the hydroperoxide substrate is proposed to be deprotonated by the distal histidine ligand before it displaces metal bound water. But the preliminary deprotonation of the bound water by the distal histidine, followed by concerted deprotonation of the hydroperoxide and displacement of the hydroxyl ligand might be considered as a relevant alternative mechanism. In order to mimic P450 catalysis, the porphyrin iron-hydroperoxo and the porphyrin iron-peroxo intermediates should be stabilised with respect to the porphyrin high-valent metal-oxo intermediate. This is rendered possible by partially scavenging the porphyrin high-valent metal-oxo intermediates species analogue of Compound I using ascorbate, regenerating the native MP-8. The reductant competes with the substrate for the oxidation by the porphyrin high-valent metal-oxo intermediate and does almost not affect porphyrin iron-(hydro)peroxo-based intermediates. Therefore in the presence of ascorbate, *i.e.* in the P450 mode, MP-8 can be considered as a model for P450 chemistry and without ascorbate, *i.e.* in the peroxidase mode, MP-8 can be considered as a model for peroxidase chemistry.

As a conclusion, the present work has contributed to the better understanding of the chemistry of metalloporphyrin hydroperoxo and metalloporphyrin peroxo intermediates both relevant active species of the P450 chemistry. Furthermore the peroxidase mimic, MP-8, can efficiently be used as a model for the P450 chemistry.

Résumé

La microperoxydase-8, Fe(III)MP-8, est un modèle biomimétique d'enzyme héminique. Fe(III)MP-8 catalyse principalement deux types de réactions d'oxydation. En absence d'ascorbate, le modèle fonctionne en mode cytochrome P450 et permet l'étude des transferts d'oxygène *réels* catalysés par des intermédiaires fer-hydroperoxo ou fer-peroxo ainsi que fer(IV)-oxo porphyrine radical cation. En présence d'ascorbate, le modèle fonctionne en mode peroxydase et permet l'étude des transferts d'oxygène *apparents* catalysés par des intermédiaires fer(IV)-oxo ou fer(IV)-oxo porphyrine radical cation.

Le suivi du transfert d'oxygène, par un marquage à l'oxygène 18, permet de discriminer entre les deux types de réactions catalysées par Fe(III)MP-8. Toutefois, il a pu être montré que lors de la catalyse, les atomes d'oxygène du solvant peuvent également être échangés avec l'espèce réactive fer(IV)-oxo porphyrine radical cation.

L'O- et la N-déalkylation des substrats catalysée par Fe(III)MP-8 en présence et en absence d'ascorbate, l'oxydation catalytique du guaiacol et de l'*ortho*-dianisidine (mode peroxydase) par Fe(III)MP-8 et Mn(III)MP-8, ainsi que l'hydroxylation de l'aniline (mode cytochrome P450) par Fe(III)MP-8 ont été ensuite étudiés. Les résultats suggèrent que l'intermédiaire fer-(hydro)peroxo est l'espèce réactive majeure pour la *para*-hydroxylation de l'aniline et pour les réactions de O- et N-déalkylation en mode cytochrome P450.

Une forme modifiée de Fe(III)MP-8 ayant le cycle imidazole de son histidine hydroxylé a été isolée en présence de H₂O₂. L'importance de l'étape de déprotonation du ligand axial aquo dans la formation de l'intermédiaire fer-hydroperoxo a été démontrée. La délocalisation, par effet mésomère, du second équivalent d'oxydation de l'intermédiaire fer-oxo radical cation de MP-8 sur le cycle imidazole de l'histidine est proposée.

Ce travail de thèse démontre l'importance des espèces fer-peroxo et fer-hydroperoxo comme intermédiaires réactionnels de la chimie de type cytochrome P450.

Samenvatting

Microperoxidase-8, Fe(III)MP-8, is een biomimetisch model voor heem enzymen. Fe(III)MP-8 katalyseert twee verschillende types van oxidatie. Omzettingen in de cytochroom P450-modus komen voor in aanwezigheid van ascorbate. In deze modus is het mogelijk *ware* zuurstofoverdracht te bestuderen, die gekatalyseerd wordt door een ijzer-hydroperoxo-, ijzer-peroxo- en/of hoge-valentie-ijzer-oxo porfyrin radicaal kation-vorm van de heem katalysator. Omzettingen in de peroxidase-modus komen voor in afwezigheid van ascorbate. In deze modus is het mogelijk *schijnbare* zuurstofoverdracht te bestuderen, die door een hoge-valentie-ijzer-oxo en/of een hoge-valentie-ijzer-oxo porphyrine radicaal kation gekatalyseerd wordt.

De zuurstofoverdracht kan gevolgd worden door middel van het gebruik van een oxiderende stof (H_2O_2) gelabeld met zuurstof 18. Dit maakt het mogelijk onderscheid te maken tussen de twee types van oxidering gekatalyseerd door Fe(III)MP-8. Toch bleek dat tijdens katalyse zuurstofatomen vanuit het oplosmiddel met de ijzer-oxo porfyrin radicaal kation vorm van MP-8 uitgewisseld kunnen worden.

De O- en N-dealkylering van substraten gekatalyseerd door Fe(III)MP-8 in aanwezigheid of afwezigheid van ascorbate; de door Fe(III)MP-8 en Mn(III)MP-8 gekatalyseerde oxidering van guaiacol en *ortho*-dianisidine (peroxidase modus); de hydroxylering van aniline (cytochroom P450 modus) gekatalyseerd door Fe(III)MP-8 zijn ook bestudeerd. Resultaten tonen aan dat de ijzer-(hydro)peroxo, de actieve vorm is voor de *para*-hydroxylering van aniline en voor de O- en N-dealkylering van substraten in de cytochroom P450-modus.

Een gemodificeerde vorm van Fe(III)MP-8, met een gehydroxyleerde imidazol ring, is geïsoleerd in aanwezigheid van H_2O_2 . De snelheden van de vorming van ijzer-hydroperoxo en mangaan-hydroperoxo complexen nemen toe met de pH en dit toont aan dat de deprotonering van de aquo axiale-ligand belangrijk is voor de vorming van deze actieve vorm van de twee modellen. Uit de studies blijkt ook dat het tweede oxidatie-equivalent van het hoge-valentie-ijzer-oxo radicaal kation van MP-8 is gedelocaliseerd op de imidazolring van de histidine.

Dit proefschrift toont het belang van de ijzer-peroxo en ijzer-hydroperoxo als reactieve intermediären voor de cytochroom P450 chemie.

Abbreviations

Å	Ångström (10^{-10} m)
AM ₁	Austin Model 1
ARP	<i>Arthromyces ramosus</i> peroxidase
B	magnetic field
CcP	cytochrome c peroxidase
PorFe ^{III} -O-O [•]	porphyrin iron-peroxo
PorFe ^{III} -OOH	porphyrin iron-hydroperoxo, peroxidase Compound 0
Por ^{•+} Fe ^{IV} =O	high-valent iron-oxo porphyrin radical cation, iron-oxenoid, peroxidase Compound I
PorFe ^{IV} =O	porphyrin high-valent iron-oxo, peroxidase Compound II
CPO	chloroperoxidase
Cyt c	cytochrome c
ϵ_x	molar extinction coefficient at x nm
EPR	electron paramagnetic resonance
ESI LC-MS	electrospray ionisation liquid chromatography mass spectrometry
ESI-MS	electrospray ionisation mass spectrometry
ESI-MS ²	tandem electrospray ionisation mass spectrometry
Fe ^{III} MP-8	iron microperoxidase-8
Fe ^{III} (F ₂₀ TPP)Cl	(<i>meso</i> -tetrakis-(pentafluorophenyl)-porphinato)iron(III)
Fe ^{III} TDCPPS	(<i>meso</i> -tetrakis-(2,6-dichloro-3-sulfonatophenyl)-porphinato)iron(III)
¹ H-NMR	proton nuclear magnetic resonance spectroscopy
HPLC	high pressure liquid chromatography
HRP	horseradish peroxidase
HAS	human albumin serum
k	kinetic rate constant
k _{cat}	first-order rate constant of catalytic/enzymatic conversion
K	thermodynamic equilibrium constant

K_m	Michaelis and Menten constant
LC	liquid chromatography
LiP	lignin peroxidase
MALDI-TOF	Matrix-Assisted Laser Desorption Spectroscopy
$Mn^{III}MP-8$	manganese microperoxidase-8
$Mn^{III}TDCPPS$	(<i>meso</i> -tetrakis-(2,6-dichloro-3-sulfonatophenyl)-porphinato) manganese(III)
$Mn^{III}TMP$	(<i>meso</i> -tetrakis-(mesityl)-porphinato)manganese(III)
$Mn^{III}TMPyP$	(<i>meso</i> -tetrakis-(4- <i>N</i> -methylpyridiniumyl)-porphinato) manganese(III)
$Mn^{III}TPP$	(<i>meso</i> -(tetrakis-(phenyl)-porphinato)manganese(III)
MO	molecular orbitals
MP's	microperoxidases
MP-8	microperoxidase-8
MS	mass spectrometry
MS-MS	tandem mass spectrometry
nd	not determined
NOE	nuclear overhauser effect
NAD(P)H	nicotinamide adenine dinucleotide (phosphate) reduced
1-D NOESY	one- dimensional nuclear overhauser effect spectroscopy
2-D NOESY	two-dimensional nuclear overhauser effect spectroscopy
P450	cytochrome P450
ppm	parts per million
$t_{1/2}$	half reaction time
SSE	saturated silver electrode
SCE	saturated calomel electrode
TOCSY	time correlated spectroscopy
UV/visible	UV/visible spectroscopy

References

A

- Adams, P.A. (1990) The peroxidasic activity of the haem octapeptide microperoxidase-8 (MP-8): the kinetic mechanism of the catalytic reduction of H_2O_2 by MP-8 using 2,2'-azino-bis-(3-ethylbenzothiazoline-6-sulphonate) (ABTS) as reducing substrate. *J. Chem. Soc. Perkin Trans. 2*, 1407-1414.
- Akhtar, M., Calder, M.R., Corina, D.L., Wright, J.N. (1982) Mechanistic studies on C-19 demethylation in oestrogen biosynthesis. *Biochem. J.* **201**, 569-580.
- Arasasingham, R.D, Bruice, T.C. (1991) The dynamics of the reactions of methyl diphenylhydroperoxyacetate with [*meso*-tetrakis(2,6-dimethyl-3-sulfonatophenyl)-porphinato]-manganese(III) hydrate and [*meso*-tetrakis(2,6-dimethyl-3-sulfonatophenyl)porphinato]-manganese(III) hydrate and imidazole complexes. Comparison of the reactions of manganese(III) and iron(III) porphyrins. *J. Am. Chem. Soc.* **113**, 6095-6103.
- Arnao, M.B., Acosta, M., del Rio, J.A., Varon, R., Garcia-Canovas, F. (1990) A kinetic study on the suicide inactivation of peroxidase by hydrogen peroxide. *Biochim. Biophys. Acta* **1041**, 43-47.
- Aron, J., Baldwin, D.A., Marques, H.M., Pratt, J.M., Adams, P.A. (1986) Hemes and hemoproteins. 1: Preparation and analysis of the heme-containing octapeptide (microperoxidase-8) and identification of the monomeric form in aqueous solution. *J. Inorg. Biochem.* **27**, 227-243.
- Atkinson, J.K., Hollenberg, P., Ingold, K.U., Johnson, C.C., Le Tadic, M.-H., Newcomb, M., Putt, D.A. (1994) Cytochrome P450-catalysed hydroxylation of hydrocarbons: kinetic deuterium isotope effects for the hydroxylation of an ultrafast radical clock. *Biochemistry* **33**, 10630-10637.

- Ator, M.A., Ortiz de Montellano, P.R. (1987a) Protein control of the heme reactivity. Reaction of substrates with the heme edge of horseradish peroxidase. *J. Biol. Chem.* **262**, 1542-1551.
- Ator, M. A., Ortiz de Montellano, P. R. (1987b) Structure and catalytic mechanism of horseradish peroxidase. Regiospecific meso alkylation of the prosthetic heme group by alkylhydrazines. *J. Biol. Chem.* **262**, 14954-14960.
- Ayougou, K., Bill, E., Charnock, J.M., Garner, C.D., Mandon, D., Trautwein, A.X., Weiss, R., Winkler, H. (1995) Characterization of an oxo(porphyrinato)manganese(IV) complex by X-ray absorption spectroscopy. *Angew. Chem. Int. Ed. Engl.* **34**, 343-346.

B

- Bach, R.D., Su, M.-D., Andrés, J.L., Schlegel, H.B. (1993) Structure and reactivity of diamidoiron(III) hydroperoxide. The mechanism of oxygen atom transfer to ammonia. *J. Am. Chem. Soc.* **115**, 8763-8769.
- Baek, H.K., van Wart, H.E. (1989) Elementary steps in the formation of horseradish peroxidase compound I: Direct observation of compound O, a new intermediate with a hyperporphyrin spectrum. *Biochemistry* **28**, 5714-5719.
- Baek, H.K., van Wart, H.E. (1992) Elementary steps in the reaction of horseradish peroxidase with several peroxides: Kinetics and thermodynamics of formation of compound O and compound I. *J. Am. Chem. Soc.* **114**, 718-725.
- Baldwin, D.A., Marques, H.M., Pratt, J.M. (1985) Mechanism of activation of H₂O₂ by peroxidases: kinetic studies on a model system. *FEBS Lett.* **183**, 309-312.
- Baldwin, D.A., Marques, H.M., Pratt, J.M. (1986) Hemes and hemoproteins. 2: The pH-dependent equilibria of microperoxidase-8 and characterization of the coordination sphere of Fe(III). *J. Inorg. Biochem.* **27**, 245-254.
- Baldwin, D.A., Marques, H.M., Pratt, J.M. (1987) Hemes and hemoproteins. 5: Kinetics of the peroxidatic activity of microperoxidase-8: model for the peroxidases enzymes. *J. Inorg. Biochem.* **30**, 203-217.
- Banci, L., Bertini, I., Luchinat, C., Piccioli, M., Scozzafava, A., Turano, P. (1989) ¹H-NOE studies on dicopper(II) dicobalt(II) superoxide dismutase. *Inorg. Chem.* **28**, 4650-4656.
- Banci, L., Rosato, A., Turano, P. (1996) Can the axial ligand strength be monitored through spectroscopic measurements. *J. Biol. Inorg. Chem.* **1**, 364-367.
- Banci, L. (1997) Structural properties of peroxidases. *J. Biotech.* **53**, 253-263.
- Banci, L., Berners-Price, S.J., Bertini, I., Clementi, V., Luchinat, C., Spyroulias, G.A., Turano, P. (1998) Water-protein interaction in native and partially unfolded equine cytochrome c. *Mol. Phys.* **95**, 797-808.
- Banci, L.; Bertini, I.; Luchinat, C., Pierattelli, R., Shokhirev, N.V., Ann Walker, F. (1998) Analysis of the temperature dependence of the ¹H and ¹³C isotropic shifts of horse heart ferricytochrome c: Explanation of curie and anti-curie temperature dependence and nonlinear pseudocontact shifts in a common two-level framework. *J. Am. Chem. Soc.* **120**, 8472-8479.
- Bell, S.E.J., Cooke, P.R., Inchley, P., Leanord, D.R., Lindsay Smith, J.R., Robbins, A., (1991) Oxoiron(IV) porphyrins derived from charged iron(III) tetraarylporphyrins and chemical oxidants in aqueous and methanolic solutions. *J. Chem. Perkin Trans. 2*, 549-559.
- Benson, D.E., Suslick, K.S., Sligar, S.G. (1997) Reduced oxy intermediate observed in D251N cytochrome P450cam. *Biochemistry* **36**, 5104-5107.

- Bernadou, J., Pratviel, G., Bennis, F., Girardet, M., Meunier, B. (1989) Potassium monopersulfate and a water-soluble manganese porphyrin complex, [Mn(TMPyP)](OAc)₅, as an efficient reagent for the oxidative cleavage of DNA. *Biochemistry* **28**, 7268-7275.
- Bernadou, J., Fabiano, A.-S., Robert, A., Meunier, B. (1994) "Redox tautomerism" in high-valent metal-oxo-aquo complexes. Origin of the oxygen atom in epoxidation reactions catalyzed by water-soluble metalloporphyrins. *J. Am. Chem. Soc.* **116**, 9375-9376.
- Bernadou, J., Meunier, B. (1998) "Oxo-hydroxo tautomerism" as useful mechanistic tool in oxygenation catalysed by water-soluble metalloporphyrins. *Chem. Soc. Chem. Commun.* 2167-2173.
- Bertini, I., Banci, L., Luchinat, C. (1989) Proton magnetic resonance of paramagnetic metalloproteins. *Methods Enzymol.* **177**, 246-263.
- Bertini, I., Luchinat, C., Parigi, G., Ann Walker, F. (1999) Heme methyl ¹H chemical shifts as structural parameters in some low-spin ferriheme proteins. *J. Biol. Inorg. Chem.* **4**, 515-519.
- Bhattacharyya, D.Kr., Bandyopadhyay, U., Banerjee, R.K. (1992) Chemical and kinetic evidence for an essential histidine in horseradish peroxidase for iodide oxidation. *J. Biol. Chem.* **267**, 9800-9804.
- Boersma, M.G., Cnubben, N.H.P., van Berkel, W.J.H., Blom, M., Vervoort, J., Rietjens, I.M.C.M. (1993) Role of cytochromes P450 and flavin-containing monooxygenase in the biotransformation of 4-fluoro-N-methylaniline. *Drug Met. Disp.* **21**, 218-230.
- Bonagura, C.A., Sunaramoorthy, M., Pappa, H.S., Patterson, W.R., Poulos, T.L. (1996) An engineered cation site in cytochrome c peroxidase alters the reactivity of the redox active tryptophan. *Biochemistry* **35**, 6107-6115.
- Bonnett, R., Dimsdale, M. (1972) The *meso*-reactivity of porphyrins and related compounds. Part V. The *meso*-oxidation of metalloporphyrins. *J. Chem. Soc. Perkin Trans. 1*, 2540-2548.
- Bonnett, R., McDonagh, A. (1973) The *meso*-reactivity of porphyrins and related compounds. Part VI: Oxidative cleavage of the haem system. The four isomeric biliverdins of the IX series. *J. Chem. Soc. Perkin. Trans. 1*, 881-888.
- Boucher, L. (1968) Manganese porphyrin complexes. I: Synthesis and spectroscopy of manganese(III) protoporphyrin IX dimethyl ester halides. *J. Am. Chem. Soc.* **90**, 6640-6645.
- Boucher, L. (1969) Manganese porphyrin complexes. III: Spectroscopy of chloro-aquo complexes of several porphyrins. *J. Am. Chem. Soc.* **92**, 2725-2730.
- Bren, K. L., Gray, H. B., Banci, L., Bertini, I., Turano, P. (1995) Paramagnetic ¹H-NMR spectroscopy of the cyanide derivative of Met80Ala-iso-1-cytochrome c. *J. Am. Chem. Soc.* **117**, 8067-8073.
- Brodie, B.B., Axelrod, J. (1948) The estimation of acetanilide and its metabolic products, aniline, *N*-acetyl *p*-aminophenol and *p*-aminophenol (free and total conjugated) in biological fluids and tissues. *J. Pharmacol. Exp. Ther.* **94**, 22-28.
- Brown, S.B. (1976) Stereospecific haem cleavage: A model for the formation of bile-pigment isomers *in vivo* and *in vitro*. *Biochem. J.* **159**, 23-27.
- Brown, S.P., Hatzikonstantinou, H., Herries, D.G. (1978) The role of peroxide in Haem degradation. A study of the oxidation of ferrihaems by hydrogen peroxide. *Biochem. J.* **174**, 901-907.
- Bushnell, G.W., Louie, G.V., Brayer, G.D. (1990) High-resolution three-dimensional structure of horse heart cytochrome c. *J. Mol. Biol.* **214**, 585-595.

C

- Campestrini, S., Meunier, B. (1992) Olefin epoxidation and alkane hydroxylation catalyzed by robust sulfonated manganese and iron porphyrins supported on cationic ion-exchange resins. *Inorg. Chem.* **31**, 1999-2006.
- Catalano, C.E., Choe, Y.S., Ortiz de Montellano, P.R. (1989) Reactions of the protein radical in peroxide-treated myoglobin. Formation of a heme-protein cross-link. *J. Biol. Chem.* **18**, 10534-10541.
- Cederbaum, A.I., Dicker, E., Cohen, G. (1978) Effect of hydroxyl radical scavengers on microsomal oxidation of alcohols and associated microsomal reactions. *Biochemistry* **17**, 3058-3064.
- Cederbaum, A.I., Cohen, G. (1984) Microsomal oxidant radical production and ethanol oxidation. *Meth. in Enzymol.* **105**, 516-522.
- Champion, P.M. (1989) Elementary electronic excitations and the mechanism of cytochrome P450. *J. Am Chem. Soc.* **111**, 3433-3434.
- Chance, B. (1943) The kinetics of the enzyme-substrate compound of peroxidase. *J. Biol. Chem.* **151**, 553-577.
- Chance, B. (1949a) The enzyme-substrate compounds of horseradish peroxidases and peroxides. II. Kinetics of the formation and decomposition of the primary and secondary complexes. *Arch. Biochem. Biophys.* **22**, 224-252.
- Chance, B. (1949b) The properties of the enzyme-substrate compounds of horseradish peroxidase and peroxides. III: the reaction of complex II with ascorbic acid. *Arch. Biochem. Biophys.* **24**, 389-409.
- Chance, B. (1949c) The properties of the enzyme-substrate compounds of horseradish peroxidase and peroxides. IV. The effect of pH upon the rate of reaction complex II with several acceptors and its relation to their oxidation- reduction potential. *Arch. Biochem. Biophys.* **24**, 410-421.
- Chance, B. (1952) The kinetics and stoichiometry of the transition from the primary to the secondary peroxidase peroxide complexes. *Arch. Biochem. Biophys.* **41**, 416-424.
- Chapman, S.K., Daff, S., Munro, A.W. (1997) Heme: The most versatile redox centre in biology. *Structure and Bonding* **88**, 39-70.
- Chorghade, M.S., Hill, D.R., Lee, E.C., Pariza, R.J., Dolphin, D.H., Hino, F., Zhang, L.-Y. (1996) Metalloporphyrins as chemical mimics of cytochrome P450 systems. *Pure & Appl. Chem.* **68**, 753-756.
- Chuang, W.-J., Chang, Y.-D., Jeng, W.-Y. (1999) Kinetic and structural studies of N-acetyl-microperoxidase-5 and -microperoxidase-8. *J. Inorg. Biochem.* **75**, 93-97.
- Clore, G.M., Hollaway, M.R., Orengo, C., Peterson, J., Wilson, M.T. (1981) The kinetics of the reactions of low spin ferric haem undecapeptide with hydrogen peroxide. *Inorg. Chim. Acta* **56**, 143-148.
- Cnubben, N.H.P., Vervoort, J., Boersma, M.G., Rietjens, I.M.C.M. (1995) The effect of varying halogen substituent patterns on the cytochrome P450-catalyzed dehalogenation of 4-halogenated anilines to 4-aminophenol metabolites. *Biochem. Pharmacol.* **49**, 1235-1248.
- Colonna, S., Gaggero, N., Richelmi, C., Pasta, P. (1999) Recent biotechnological developments in the use of peroxidases. *Trends in Biotech.* **17**, 163-168.

- Conroy, C.W., Tyma, P., Daum, P.H., Erman, J.E. (1978) Oxidation-reduction potential measurements of cytochrome c peroxidase and pH dependent spectra transitions in the ferrous enzyme. *Biochim. Biophys. Acta* **537**, 62-69.
- Coon, M.J., Vaz, A.D.N., Bestervelt, L.L. (1996) Peroxidative reactions of diversozymes. *FASEB J.* **10**, 428-434.
- Coon, M.J., Vaz, A.D.N., McGinnity, D.F., Peng, H.-M. (1998) Multiple activated oxygen species in P450 catalysis. *Drug. Meta. Disp.* **26**, 1190-1193.
- Cunningham, I.D., Bachelor, J.L., Pratt, J.M. (1991) Kinetic study of the H₂O₂ oxidation of phenols, naphthols and anilines catalysed by the haem octapeptide microperoxidase-8. *J. Chem. Soc. Perkin. Trans 2*, 1839-1843.
- Cunningham, I.D., Snare, G.R. (1992) Identification of catalytic pathways in the peroxidatic reactions of the haem octapeptide microperoxidase-8. *J. Chem. Soc. Perkin Trans 2*, 2019-2023.
- Cunningham, I.D., Bachelor, J.L., Pratt, J.M. (1994) Peroxidatic of haem octapeptide complexes with anilines, naphthols and phenols. *J. Chem. Soc. Perkin Trans 2*, 1347-1350.
- Curci, R., Edwards, J.M. (1991). *Catalysis by metal complexes*. G. Strukul (Eds), Kluwer Academic Publishers, Dordrecht, p 45-95.
- Czapski, G. (1984) Reaction of $\cdot\text{OH}$. *Meth. in Enzymol.* **105**, 209-215.
- Czernuszewicz, R.S., Su, O.Y., Stern, M.K. Macor, K.A., Kim, D., Groves, J.T., Spiro, T.G. (1988) Oxomanganese(IV) porphyrins identified by resonance Raman and infrared spectroscopy: weak bonds and the stability of the half-filled t_{2g} subshell. *J. Am. Chem. Soc.* **110**, 4158-4165.

D

- D'Auria, G., Maglio, O., Nastri, F., Lombardi, A., Mazzeo, M., Morelli, G., Paolillo, L., Pedone, C., Pavone, V. (1997) Hemoprotein models based on a covalent helix-heme-helix sandwich: 2. Structural characterisation of Co^{III} mimochrome I Δ and Λ isomers. *Chem. Eur. J.* **3**, 350-362.
- Davies, M.J., Puppo, A. (1992) Direct detection of a globin-derived radical in leghaemoglobin treated with peroxides. *Biochem. J.* **281**, 197-201.
- Dawson, J.H. (1988) Probing structure-function relations in heme-containing oxygenases and peroxidases. *Science* **240**, 433-439
- Dexter, A.F., Hager, L.P. (1995) Transient heme N-alkylation of chloroperoxidase by terminal alkenes and alkynes. *J. Am. Chem. Soc.* **117**, 817-818.
- Dolphin, D., Forman, A., Borg, D.C., Fajer, J., Felton, R.H. (1971) Compounds I of catalase and horseradish peroxidase: π -cation radicals. *Proc. Nat. Acad. Sci. U.S.A.* **68**, 614-618.
- Dorovska-Taran, V., Posthumus, M.A., Boeren, S., Boersma, M.G., Teunis, C.J., Rietjens, I.M.C.M., Veeger, C. (1998) Oxygen exchange with water in heme-oxo intermediates during H₂O₂-driven oxygen incorporation in aromatic hydrocarbons catalysed by microperoxidase-8. *Eur. J. Biochem.* **253**, 659-668.

- Dunford, H.B., Adeniran, A.J. (1986) Hammett rho sigma correlation for reactions of horseradish peroxidase Compound-II with phenols. *Arch. Biochem. Biophys.* **251**, 536-542.
- Dunford, H.B. (1991) *Peroxidases in Chemistry and Biology*, J. Everse, K.E. Everse, M.B. Grisham (Eds), CRC Press, Boca Raton, vol. II, p 1-24.
- Duyvis, M.G. (1997) Kinetics of nitrogenase from *Azotobacter vinelandii*. Doctorate dissertation, Wageningen University, Wageningen, The Netherlands, pp 90.

E

- Egawa, T., Miki, H., Ogura, T., Makino, R., Ishimura, Y., Kitagawa, T., (1992) Observation of the $\text{Fe}^{\text{IV}}=\text{O}$ stretching Raman band for a thiolate-ligated heme protein. *FEBS Letters* **305**, 206-208.
- Entsch, B., Ballou, D.P., Massey, V. (1976) Flavin-oxygen derivatives involved in hydroxylation by *p*-Hydroxybenzoate hydroxylase. *J. Biol. Chem.* **251**, 2550-2563.
- Erecińska, M., Vanderkooi, J.M. (1978) Modification of cytochrome c: modification of aromatic amino acids, photoaffinity labels, and metal substitution. *Methods. Enzymol.* **53**, 165-181.
- Espenson, J.H., Christensen, R. (1977) Kinetics and mechanism of the demetalation of iron(III) porphyrins catalyzed by iron(II). *J. Inorg. Chem.* **16**, 2561-2564.

F

- Falk, J.E. (1964) *Porphyrins and Metalloporphyrins*. J.E. Falk (Ed), Elsevier, New-York, Insertion and removal of iron, pp129-135.
- Finzel, B.C., Poulos, T.L., Kraut, J. (1984) Crystal structure of yeast cytochrome c peroxidase refined at 1,7-Å resolution. *J. Biol. Chem.* **21**, 13027-13036.
- Fleischer, E.B., Palmer, J.M., Srivastava, T.S., Chatterjee, A. (1971) Thermodynamic and kinetic properties of an iron-porphyrin system. *J. Am. Chem. Soc.* **93**, 3162-3167.
- Florence, T.M. (1985) The degradation of cytochrome c by hydrogen peroxide. *J. Inorg. Biochem.* **23**, 131-141.
- Fox, J. B., Nicholas, R. A., Ackerman, S. A., Swift, C. E. (1974) A multiple wavelength analysis of the reaction between hydrogen peroxide and metmyoglobin. *Biochemistry* **13**, 5178-5186.
- Fujii, H. (1993) Effects of the electron-withdrawing power of substituents on the electronic structure and reactivity in oxoiron(IV) porphyrin π -cation radical complexes. *J. Am. Chem. Soc.* **115**, 4641-4648.
- Fuhrhop, J-H., Smith, K.M. (1975) *Porphyrins and Metalloporphyrins*. K.M. Smith (Ed), Elsevier, New-York, p 800-803.

G

- Gajhede, M., Schuller, D.J., Henriksen, A., Smith, A.T., Poulos, T.L. (1997) Crystal structure determination of classical horseradish peroxidase at 2.15 Å resolution. *Nat. Struct. Biol.* **4**, 1032-1038.
- Gelb, M.H., Toscano, W.A., Sligar, S.G. (1982) Chemical mechanisms for cytochrome P450 oxidation: Spectral and catalytic properties of a manganese-substituted protein. *Proc. Natl. Acad. Sci. USA* **79**, 5758-5762.
- George, P. (1953) The chemical nature of the second hydrogen peroxide compound formed by cytochrome c peroxidase and horseradish peroxidase. I. Titration with reducing agents. *Biochem. J.* **54**, 267-276.
- Gerber, N.C., Sligar, S.G. (1992) Catalytic mechanism of cytochrome P450: evidence for a distal charge relay. *J. Am. Chem. Soc.* **114**, 8742-8743.
- Goh, Y.M., Nam, W. (1999) Significant electronic effect of porphyrin ligand on the reactivities of high-valent iron(IV) oxo porphyrin cation radical complexes. *Inorg. Chem.* **38**, 914-920.
- Gross, Z. (1996) The effect of axial ligands on the reactivity and stability of the oxoferryl moiety in model complexes of Compound-I of heme-dependent enzymes. *J. Biol. Inorg. Chem.* **1**, 368-371.
- Groves, J.T., McClusky, G.A. (1978) Aliphatic hydroxylation by highly purified liver microsomal cytochrome P450. Evidence for a carbon radical intermediate. *Biochem. Biophys. Res. Commun.* **81**, 154-160.
- Groves, J.T., Kruper, W.J.Jr. (1979) Preparation and characterization of an oxoporphinatochromium(V) complex. *J. Am. Chem. Soc.* **101**, 7613-7615.
- Groves, J.T., Kruper, W.J.Jr., Haushalter, R.C. (1980) Hydrocarbons oxidations with oxometalloporphinates. Isolation and reactions of a (porphinato)-manganese(V) complex. *J. Am. Chem. Soc.* **102**, 6375-6377.
- Groves, J.T., Haushalter, R.C., Nakamura, M., Nemo, T.E., Evans, B.J. (1981) High-valent iron-porphyrin complexes related to peroxidases and cytochromes P450. *J. Am. Chem. Soc.* **103**, 2884-2886.
- Groves, J.T. (1985) Key elements of the chemistry of cytochrome P450. The oxygen rebound mechanism. *J. Chem. Educ.* **62**, 928-931.
- Groves, J.T., Stern, M.K. (1987) Olefin epoxidation by manganese(IV) porphyrins: evidence for two reaction pathways. *J. Am. Chem. Soc.* **109**, 3812-3814.
- Groves, J.T., Stern, M.K. (1988) Synthesis, characterisation, and reactivity of oxomanganese(IV) porphyrin complexes. *J. Am. Chem. Soc.* **110**, 8628-8638.
- Groves, J.T., Watanabe, Y. (1988) Reactive iron porphyrin derivatives related to the catalytic cycles of cytochrome P450 and peroxidase. Studies of the mechanism of oxygen activation. *J. Am. Chem. Soc.* **110**, 8443-8452.
- Groves, J.T., Gross, Z., Stern, M.K. (1994) Preparation and reactivity of oxoiron(IV) porphyrins. *Inorg. Chem.* **33**, 5065-5072.
- Groves, J.T., Lee, J., Marla, S.S. (1997) Detection and characterization of an oxomanganese(V) porphyrin complex by rapid-mixing stopped-flow spectrophotometry. *J. Am. Chem. Soc.* **119**, 6269-6273.
- Groves, J.T. (1997) The importance of being selective. *Nature* **389**, 329-330.

- Guengerich, F.P., MacDonald, T.L. (1984) Chemical mechanisms of catalysis by cytochromes P450: A unified view. *Acc. Chem. Res.* **17**, 9-16.
- Guengerich, F.P., MacDonald, T.L. (1990) Mechanisms of cytochrome P450 catalysis. *FASEB J.* **4**, 2453-2459.
- Guengerich, F.P., Yun, C.-H., Macdonald, T.L. (1996) Evidence for a 1-electron oxidation mechanism in N-dealkylation of N,N-dialkylanilines by cytochrome P450 2B1. *J. Biol. Chem.* **271**, 27321-27329.

H

- van Haandel, M.J.H., Primus, J.-L., Teunis, C., Boersma, M.G., Osman, A.M., Veeger, C., and Rietjens, I.M.C.M. (1998) Reversible formation of high-valent-iron-oxo porphyrin intermediates in heme-based catalysis: revisiting the kinetic model for horseradish peroxidase. *Inorg. Chim. Acta* **275-276**, 98-105.
- Hagen, W.R. (1989) Direct electron transfert of redox proteins at the bare glassy carbon electrode. *Eur. J. Biochem.* **182**, 523-530.
- Haim, N., Nemeč, J., Roman, J., Sinha, B.K. (1987) Peroxidase-catalyzed metabolism of etoposide (VP-16-213) and covalent binding of reactive intermediates to cellular macromolecules. *Cancer Res.* **47**, 5835-5840.
- Hamza, M.S.A., Pratt, J.M. (1994) Hemes and hemoproteins. Part 10. Co-ordination of imidazole and other azoles by the iron(III) porphyrin microperoxidase-8. *J. Chem. Soc. Dalton Trans.*, 1367-1371.
- Harbury, H.A., Loach, P.A. (1960a) Oxidation-linked proton functions in heme octa- and undecapeptides from mammalian cytochrome c. *J. Biol. Chem.* **235**, 3640-3645.
- Harbury, H.A., Loach, P.A. (1960b) Interaction of nitrogenous ligands with heme peptides from mammalian cytochrome c. *J. Biol. Chem.* **235**, 3646-3653.
- Harbury, H.A., Cronin, J.R., Fanger, M.W., Hettinger, T.P., Murphy, A.J., Myer, Y.P., Vinogradov, S.N. (1965) Complex formation between methionine and a heme peptide from cytochrome c. *Proc. Natl. Acad. Sci. USA* **54**, 1658-1664.
- Harris, D.L., Loew, G.H. (1996) Identification of putative peroxide intermediates of peroxidases by electronic structure and spectra calculations. *J. Am. Chem. Soc.* **118**, 10588-10594.
- Hasegawa, E., Matsubuchi, E., Tsuchida, E. (1991) Demetalation of (5,10,15,20-Tetraphenylporphyrinato)iron complexes: Effect of substituents at the *o*-positions of phenyl groups. *Bull. Chem. Soc. Jpn.* **64**, 2289-2291.
- Hashimoto, S., Tatsuno, Y., Kitagawa, T. (1986a) Resonance Raman evidence for oxygen exchange between the Fe^{IV}=O heme and bulk water during enzymic catalysis of horseradish peroxidase and its relation with heme-linked ionisation. *Proc. Natl. Acad. Sci. USA* **83**, 2417-2421.
- Hashimoto, S., Teraoka, J., Inubushi, T., Yonetani, T., Kitagawa, T. (1986b) Resonance Raman study on cytochrome c peroxidase and its intermediate. *J. Biol. Chem.* **261**, 11110-11118.
- Heimbrook, D.C., Sligar, S.G. (1981) Multiple mechanisms of cytochrome P450-catalyzed substrate hydroxylations. *Biochem. Biophys. Res. Commun.* **99**, 530-535.
- Hoffman, B.M., Gibson, Q.H., Bull, C., Crepeau, R.H., Edelstein, S.J., Fisher, R.G., McDonald, M.J. (1975) Manganese-substituted hemoglobin and myoglobin. *Ann. NY Acad. Sci.* **244**, 174-185.

- Hoffman, B.M., Roberts, J.E., Brown, T.G., Kaug, C.H., Margoliash, E. (1979) Electron-nuclear double resonance of the hydrogen peroxide compound of cytochrome c peroxidase: Identification of the free radical site with a methionyl cluster. *Proc. Natl. Acad. Sci. U.S.A.* **76**, 6132-6136.
- Hori, H., Ikeda-Saito, M., Yonetani, T., (1987) Electron paramagnetic resonance and spectrophotometric studies of the peroxide compounds of manganese-substituted horseradish peroxidase, cytochrome-c peroxidase and manganese-porphyrin model complexes. *Biophys. Biochem. Acta* **912**, 74-81.
- Huang, Y.-Y., Hara, T., Sligar, S., Coon, M.J., Kimura, T. (1986) Thermodynamic properties of oxidation-reduction reactions of bacterial, microsomal, and mitochondrial cytochrome P450: An entropy-enthalpy compensation effect. *Biochemistry* **25**, 1390-1394.
- Husain, M., Entsch, B., Ballou, D., Massey, V., Chapman, P.J. (1980) Fluoride elimination from substrates in hydroxylation reactions catalyzed by p-hydroxybenzoate hydroxylase. *J. Biol. Chem.* **255**, 4189-4197.
- Huyett, J.E., Doan, P.E., Gurbiel, R., Houseman, A.L.P., Sivaraja, M., Goodin, D.B., Hoffman, B.M. (1995) Compound ES of cytochrome c peroxidase contains a Trp π -cation radical: Characterization by CW and pulsed Q-band ENDOR spectroscopy. *J. Am. Chem. Soc.* **117**, 9033-9041.

IJ

- Jiménez, H.R., Momenteau, M. (1994) Synthesis and characterization of water soluble superstructured porphyrins and their iron complexes. *New J. Chem.* **18**, 569-574.
- Job, D., Dunford, H.B. (1976) Substituent effect on the oxidation of phenols and aromatic amines by horseradish peroxidase compound I. *Eur. J. Biochem.* **66**, 607-614.
- Jones, P., Suggett, A. (1968a) The catalase-hydrogen peroxide system. Kinetics of catalytic action at high substrate concentrations. *Biochem. J.* **110**, 617-620.
- Jones, P., Suggett, A. (1968b) The catalase-hydrogen peroxide system. A theoretical appraisal of the mechanism of catalase action. *Biochem. J.* **110**, 621-629.
- Jones, P., Dunford, H.B. (1977) On the mechanism of compound-I formation from peroxidases and catalases. *J. Theor. Biol.* **69**, 457-470.

K

- Kedders, G.L., Hollenberg, P.F. (1984) Peroxidase-catalyzed N-demethylation reactions. Substrate deuterium isotopes effects. *J. Biol. Chem.* **259**, 3663-3668.
- King, E.L., Altman, C. (1956) A schematic method of deriving the rate laws for enzyme-catalyzed reactions. *J. Phys. Chem.* **60**, 1375-1378.
- Kobayashi, S., Nakano, M., Goto, T., Kimura, T., Schaap, A.P. (1986) An evidence of the peroxidase-dependent oxygen transfer from hydrogen peroxide to sulfides. *Biochem. Biophys. Res. Commun.* **135**, 166-171.
- Kobayashi, S., Nakano, M., Kimura, T., Schaap, A.P. (1987) On the mechanism of the peroxidase-catalysed oxygen-transfer reaction. *Biochemistry* **26**, 5019-5022.

- Kolczak, U., Hauksson, J.B., Davis, N.L., Pande, U., de Ropp, J.S., Langry, K.C., Smith, K.M., La Mar, G.N. (1999) $^1\text{H-NMR}$ investigation of the role of intrinsic heme versus protein-induced rhombic perturbations on the electronic structure of low-spin ferrihemoproteins: Effect of heme substituents on heme orientation in myoglobin. *J. Am. Chem. Soc.* **121**, 835-843.
- Kraehenbuhl, J.P., Galardy, R.E., Jamieson, J.D. (1974) Preparation and characterisation of an immuno-electron microscope tracer consisting of a heme-octapeptide coupled to Fab. *J. Exp. Med.* **139**, 208-223.

L

- Laidler, K.J. (1955) Theory of the transient phase in kinetics, with special reference to enzyme systems. *Can. J. Chem.* **33**, 1614-1624.
- Lau, S.M.C., Harder, P.A., O-Keefe, P.D. (1993) Low carbon monoxide affinity allene oxide synthase is the predominant cytochrome P450 in many plant tissues. *Biochemistry* **32**, 1945-1950.
- Lee, K.A., Nam, W. (1997) Determination of reactive intermediates in iron porphyrin complex-catalyzed oxygenations of hydrocarbons using isotopically labeled water: Mechanistic insights. *J. Am. Chem. Soc.* **119**, 1916-1922.
- Lee, Y.J., Goh, Y.M., Han, S-Y., Kim, C., Nam, W. (1998) Epoxidation of olefins with H_2O_2 catalyzed by an electronegatively-substituted iron porphyrin complex in aprotic solvent. *Chem. Lett.*, 837-838.
- Loew, G., Dupuis, M. (1996) Structure of a model transient peroxide intermediate of peroxidases by ab initio methods. *J. Am. Chem. Soc.* **118**, 10584-10587.
- Longo, F.R., Griffith Finarelli, M., Kim, J.B. (1969) The synthesis and some physical properties of *ms*-tetra(pentafluorophenyl)-porphin and *ms*-tetra(pentachlorophenyl)porphin. *J. Heterocyclic Chem.* **6**, 927-931.
- Louro, R.O., Correia, I.J., Brennan, L., Coutinho, I.B., Xavier, A.V., Turner, D.L. (1998) Electronic structure of low-spin ferric porphyrins: $^{13}\text{C-NMR}$ studies of the influence of axial ligand orientation. *J. Am. Chem. Soc.* **120**, 13240-13247.
- Low, D.W., Winkler, J.R., Gray, H.B. (1996) Photoinduced oxidation of microperoxidase-8: Generation of ferryl and cation-radical porphyrins. *J. Am. Chem. Soc.* **118**, 117-120.
- Low, D.W., Gray, H.B., Duus, J.Ø. (1997) Paramagnetic NMR spectroscopy of Microperoxidase-8. *J. Am. Chem. Soc.* **119**, 1-5.
- Low, D.W., Abedin, S., Yang, G., Winkler, J.R., Gray, H.B. (1998) Manganese microperoxidase-8. *Inorg. Chem.* **37**, 1841-1843.

M

- MacDonald, T.L., Burka, L.T., Wright, S.T., Guengerich, F.P. (1982) Mechanisms of hydroxylation by cytochrome P450: exchange of iron-oxygen intermediates with water. *Biochem. Biophys. Res. Commun.* **104**, 620-625.
- Maeda-Yorita, K., Massey, V. (1993) On the reaction mechanism of phenol hydroxylase. New information obtained by correlation of fluorescence and absorbance stopped flow studies. *J. Biol. Chem.* **268**, 4134-4144.

- Mansuy, D. (1987) Cytochrome P450 and synthetic models. *Pure & Appl. Chem.* **59**, 759-770.
- Mansuy, D., Battioni, P., Battioni, J.P. (1989) Chemical model systems for drug-metabolizing cytochrome-P450-dependent monooxygenases. *Eur. J. Biochem.* **184**, 267-285.
- Mansuy, D., Renaud, J.-P. (1995) *Cytochrome P450: Structure, Mechanism and Biochemistry*, P.R. Ortiz de Montellano (Eds), Plenum Publishing: New-York, p 537-574.
- Mansuy, D., Battioni, P. (2000) *The Porphyrin Handbook*, K.M. Kadish, K.M. Smith, R. Guilard (Eds), Academic Press, Volume 4/Biochemistry and Binding: 'Activation of Small Molecules', pp 1-15.
- Marques, H.M. (1990) Cyclic voltammetry of imidazolemicroperoxidase-8: modeling the control of the redox potential of the cytochromes. *Inorg. Chem.* **29**, 1597-1599.
- Mashino, T., Nakamura, S., Hirobe, M. (1990) Sulfide oxidation, amine N-demethylation, and olefin oxidation by heme-undecapeptide, microperoxidase-11, in the presence of hydrogen peroxide. *Tetrahedron Lett.* **31**, 3163-3166.
- Mauro, J.M., Fishel, L.A., Hazzard, J.T., Meyer, T.E., Tollin, G., Cusanovich, M.A., Kraut, J. (1988) Tryptophan¹⁹¹ → Phenylalanine, a proximal-side mutation in yeast cytochrome c peroxidase that strongly affects the kinetics of ferrocyclochrome c oxidation. *Biochemistry* **27**, 6243-6256.
- Metelitzka, D.I., Arapova, G.S., Vidžiunaite, R.A., Demcheva, M.V., Litvinchuk, A.V., Razumas, V.I. (1994) Co-oxidation of phenol and 4-aminoantipyrine catalyzed by microperoxidases and microperoxidase-protein complexes. *Biochemistry (Moscow)* **59**, 949-958.
- Meunier, B., Guilmet, E., De Carvalho, M.-E., Poilblanc, R. (1984) Sodium hypochlorite: A convenient oxygen source for olefin epoxidation catalyzed by (porphyrinato)-manganese complexes. *J. Am. Chem. Soc.* **106**, 6668-6676.
- Meunier, B. (1992) Metalloporphyrins as versatile catalysts for oxidation reactions and oxidative DNA cleavage. *Chem. Rev.* **92**, 1411-1456.
- Meunier, G., Meunier, B. (1985) Evidences for an efficient demethylation of methoxy ellipticine catalyzed by a peroxidase. *J. Am. Chem. Soc.* **107**, 2558-2560.
- Miller, C., Rivier, J. (1996) Peptide Chemistry: Development of high performance liquid chromatography and capillary zone electrophoresis. *Biopolymers (Peptide Science)* **40**, 265-317.
- Millis, C.D., Cai, D., Stankovic, M.T., Tien, M. (1989) Oxidation-reduction potentials and ionization states of extracellular peroxidases from the lignin-degrading fungus *Phanerochaete chrysosporium*. *Biochemistry* **28**, 8484-8489.
- Moore, J.W., Pearson, R.G. (1980) *Kinetics and Mechanism*, John Wiley and Sons (Eds), pp 290-296.
- Mukai, M., Nagano, S., Tanaka, M., Ishimori, K., Morishima, I., Ogura, T., Watanabe, Y., Kitagawa, T. (1997) Effects of concerted hydrogen bonding of distal histidine on active site structures of horseradish peroxidase. Resonance Raman studies with Asn70 mutants. *J. Am. Chem. Soc.* **119**, 1758-1766.
- Murata, K., Panicucci, R., Gopinath, E., Bruice, T.C. (1990) The reaction of 5,10,15,20-tetrakis(2,6-dichloro-3-sulphonatophenyl)porphinato-iron(III) hydrate with alkyl and acyl hydroperoxides. The dynamics of reaction of water-soluble and non μ -oxo dimer forming iron(III) porphyrins in aqueous solutions. *J. Am. Chem. Soc.* **112**, 6072-6083.
- Munro, A.W., Malarkey, K., Lindsay, J.G., Coggins, J.R., Price, N.C., Kelly, S.M., McKnight, J., Thomson, A.J., Miles, J.S. (1994) The role of Tryptophane 97 of

cytochrome P450 BM3 from bacillus megaterium in catalytic function. Evidence against the 'covalent switching' hypothesis of P450 electron transfer. *Biochem. J.* **303**, 423-428.

N

- Nagano, S., Tanaka, M., Ishimori, K., Watanabe, Y., Morishima, I. (1996) Catalytic roles of the distal site asparagine-histidine couple in peroxidases. *Biochemistry* **35**, 14251-14258.
- Nakajima, R., Yamazaki, I. (1987) The mechanism of oxyperoxidase formation from ferryl peroxidase and hydrogen peroxide. *J. Biol. Chem.* **262**, 2576-2581.
- Nakamura, S., Mashino, T., Hirobe, M. (1992) ^{18}O incorporation from $\text{H}_2^{18}\text{O}_2$ in the oxidation of N-methylcarbazole and sulfides catalysed by microperoxidase-11. *Tetrahedron. Lett.* **33**, 5409-5412.
- Nam, W., Valentine, J.S. (1993) Reevaluation of the significance of ^{18}O incorporation in metal complex-catalyzed oxygenation reactions carried out in the presence of H_2^{18}O . *J. Am. Chem. Soc.* **115**, 1772-1778.
- Nastri, F., Lombardi, A., Morelli, G., Maglio, O., D'Auria, G., Pedone, C., Pavone, V. (1997) Hemoprotein models based on a covalent helix-heme-helix sandwich: 1. Design, synthesis and characterisation. *Chem. Eur. J.* **3**, 340-349.
- Nastri, F., Lombardi, A., D'Andrea, L.D., Sanseverino, M., Maglio, O., Pavone, V. (1998) Miniaturised hemoproteins. *Biopoly.* **47**, 5-22.
- Nelson, D.P., Kiesow, L.A. (1972) Enthalpy of decomposition of hydrogen peroxide by catalase at 25°C (with molar extinction coefficients of H_2O_2 solutions in the UV). *Anal. Biochem.* **49**, 474-478.
- Newmyer, S.L., Ortiz de Montellano, P.R., (1996) Rescue of the catalytic activity of an H42A mutant of horseradish peroxidase by exogenous imidazoles. *J. Biol. Chem.* **271**, 14891-14896.
- Nicholls, P (1962). *Oxygenase*. O. Hayaishi (Ed), Academic Press, Chapter 7: Peroxidase as an Oxygenase, pp 273-305.
- Nordblom G.D., White R.E., Coon M.J. (1976) Studies on hydroperoxide-dependent substrate hydroxylation by purified liver microsomal cytochrome P450. *Arch. Biochem. Biophys.* **175**, 524-533.

O

- O'Carra, P. (1975) *Porphyryns and Metalloporphyryns*. K.M. Smith (Ed), Elsevier, New-York, pp124-153.
- Ohe, T., Mashino, T., Hirobe, M. (1995) Novel oxidative pathway of para-substituted in cytochrome P450 chemical model: substituent elimination accompanied by *ipso*-substitution by the oxygen atom of the active species. *Tetrahedron Lett.* **36**, 7681-7684.
- Okochi E., Mochizuki, M. (1995) Dealkylation of N-Nitrosodibenzylamine by metalloporphyrin/oxidant model systems for cytochrome P450. *Chem. Pharm. Bull.* **45**, 2173-2176.
- Ortiz de Montellano, P.R. (1987) Control of the catalytic activity of prosthetic heme by the structure of hemoproteins. *Acc. Chem. Res.* **20**, 289-294.

- Ortiz de Montellano, P.R. (1992) Catalytic sites of hemoprotein peroxidases. *Ann. Rev. Pharmacol. Toxicol.* **32**, 89-107.
- Ortiz de Montellano, P.R. (1998) Heme oxygenase mechanism: Evidence for an electrophilic ferric peroxide species. *Acc. Chem. Res.* **31**, 543-549.
- Osawa, Y., Korzekwa, K. (1991) Oxidative modification by low levels of HOOH can transform myoglobin to an oxidase. *Proc. Natl. Acad. Sci. USA* **88**, 7081-7085.
- Osman, A.M., Koerts, J., Boersma, M.G., Boeren, S., Veeger, C., Rietjens, I.M.C.M. (1996) Microperoxidase/H₂O₂-catalyzed aromatic hydroxylation proceeds by a cytochrome-P450-type oxygen-transfer reaction mechanism. *Eur. J. Biochem.* **240**, 232-238.
- Osman, A.M., Boeren, S., Boersma, M.G., Veeger, C., Rietjens, I.M.C.M. (1997a) Microperoxidase/H₂O₂-mediated alkoxylating dehalogenation of halophenol derivatives in alcoholic media. *Proc. Natl. Acad. Sci. USA* **94**, 4295-4299.
- Osman, A.M., Boeren, S., Veeger, C., Rietjens, I.M.C.M. (1997b) MP-8 dependent oxidative dehalogenation: evidence for the direct formation of 1,4-benzoquinone from 4-fluorophenol by a peroxidatic-type of reaction pathway. *Chem-Biol. Interactions* **104**, 147-164.
- Owens, J.W., O'Connor, C.J., (1988) Comparison of the electronic and vibrational spectra of complexes of protoporphyrin-IX, hemeoctapeptide, and heme proteins. *Coord. Chem. Rev.* **84**, 1-45.
- Ozaki, S., Ortiz de Montellano, P.R. (1995) Molecular engineering of horseradish peroxidase: Thioether sulfoxidation and styrene epoxidation by Phe-41 Leucine and Threonine mutants. *J. Am. Chem. Soc.* **117**, 7056-7064.
- Ozette, K., Leduc, P., Palacio, M., Bartoli, J.-F., Barkigia, K.M., Fajer, J., Battioni, P., Mansuy, D. (1997) New metalloporphyrins with extremely altered redox properties: synthesis, structure, and facile reduction to air-stable π -anion radicals of zinc and nickel β -heptanitroporphyrins. *J. Am. Chem. Soc.* **119**, 6642-6643.

P

- Palcic, M.M., Rutter, R., Raiso, T., Hager, L.P., Dunford, H.B. (1980) Spectrum of chloroperoxidase compound I. *Biochem. Biophys. Res. Commun.* **94**, 1123-1127.
- Panicucci, R., Bruce, T.C. (1990) Dynamics of the reaction of hydrogen peroxide with a water soluble non μ -oxo dimer forming iron(III) tetraphenylporphyrin. 2. The reaction of hydrogen peroxide with 5,10,15,20-tetrakis(2,6-dichloro-3-sulfonatophenyl)porphyrinatoiron(III) in aqueous solution. *J. Am. Chem. Soc.* **112**, 6063-6071.
- Patel, P.K., Mondal, M.S., Modi, S., Behere, D.V. (1997) Kinetic studies on the oxidation of phenols by the horseradish peroxidase Compound-II. *Biochim. Biophys. Acta* **1339**, 79-87.
- Pitié, M., Bernadou, J., Meunier, B. (1995) Oxidation at carbon-1' of DNA deoxyriboses by the Mn-TMPyP/KHSO₅ system results from a cytochrome P450-type hydroxylation reaction. *J. Am. Chem. Soc.* **117**, 2935-2936.
- Pond, A.E., Bruce, G.S., English, A.M., Sono, M., Dawson, J.H. (1998) Spectroscopic study of the compound ES and the oxoferryl compound II states of cytochrome c peroxidase: comparison with the compound II of horseradish peroxidase. *Inorg. Chim. Acta* **275-276**, 250-255.

- Poulos, T.L., Kraut, J. (1980a) The stereochemistry of peroxidase catalysis. *J. Biol. Chem.* **255**, 8199-8205.
- Poulos, T.L., Kraut, J. (1980b) A hypothetical model of the cytochrome c peroxidase-cytochrome c electron transfer complex. *J. Biol. Chem.* **255**, 10322-10330.
- Poulos, T.L., Finzel, B.C., Gunsalus, I.C. Wagner, G.C. (1985) The 2.6 Å crystal structure of pseudomonas 2 CCP. *J. Biol. Chem.* **260**, 16122-16130.
- Poulos, T.L., Raag, R. (1992) Cytochrome P450_{cam}: crystallography, oxygen activation, and electron transfer. *FASEB J.* **6**, 674-679.
- Poulos, T.L. (1996) The role of the proximal ligand in heme enzymes. *J. Biol. Inorg. Chem.* **1**, 356-359.
- Poulos, T.L., (2000) *The Porphyrin Handbook*, K.M. Kadish, K.M. Smith, R. Guilard (Eds), Academic Press, Volume 4/Biochemistry and Binding: Activation of Small Molecules, pp 189-218.
- Primus, J.-L., Boersma, M.G., Mandon, D., Boeren, S., Veeger, C., Weiss, R., Rietjens, I.M.C.M. (1999) The effect of iron to manganese substitution on microperoxidase 8 catalysed peroxidase and cytochrome P450 catalysis. *J. Biol. Inorg. Chem.* **4**, 274-283.
- Primus, J.-L., Boeren, S., Banci, L., Vervoort, J., Rietjens I.M.C.M. (2000) Isolation and characterisation of a microperoxidase-8 with a modified histidine axial ligand: Implications for the nature of activated heme-oxo intermediates. *Chapter 6 of this thesis.*
- Proshlyakov, D.A., Paeng, I.R., Paeng, K.-J., Kitagawa, T. (1996) Resonance Raman studies of Compounds I and II of *Arthromyces ramosus* peroxidase: close similarities in their Raman spectra but distinct oxygen exchangeability of the Fe=O heme. *Biospectroscopy* **2**, 317-329.

QR

- Raag, R., Martinis, S.A., Sligar, S.G., Poulos, T.L. (1991) Crystal structure of the cytochrome P-450_{cam} active site mutant Thr252Ala. *Biochemistry* **30**, 11420-11429.
- Raner, G.M., Chiang, E.W., Vaz, A.D.N., Coon, M.J. (1997) Mechanism-based inactivation of cytochrome P450 2B4 by aldehydes: Relationship to aldehyde deformylation via a peroxyhemiacetal intermediate. *Biochemistry* **36**, 4895-4902.
- Raphael, A.L., Gray, H.B. (1989) Axial ligand replacement in horse heart cytochrome c by semisynthesis. *Proteins: Struct., Funct., Genet.* **6**, 338-340.
- Raphael, A.L., Gray, H.B. (1991) Semisynthesis of axial-ligand (position 80) mutants of cytochrome c. *J. Am. Chem. Soc.* **113**, 1038-1040.
- Ridder, L., Mulholland, A.J., Vervoort, J., Rietjens, I.M.C.M. (1998) Correlation of calculated activation energies with experimental rate constants for an enzyme catalyzed aromatic hydroxylation. *J. Am. Chem. Soc.* **120**, 7641-7642.
- Rietjens, I.M.C.M., Vervoort, J. (1991) Bioactivation of 4-fluorinated anilines to benzoquinoneimines as primary reaction product. *Chem.-Biol. Interactions* **77**, 263-281.
- Rietjens, I.M.C.M., Osman, A.M., Veeger, C., Zakharieva, O., Antony, J., Grodzicki, M., Trautwein, A.X. (1996) On the role of the axial ligand in heme-based catalysis of the peroxidase and P450 type. *J. Biol. Inorg. Chem.* **1**, 372-376.
- Robert, A., Meunier, B. (1988) Oxygenation of hydrocarbons by KHSO₅ catalyzed by manganese porphyrin complexes. *New J. Chem.* **12**, 885-896.

- Roberts, E.S., Vaz, A.D.N., Coon, M.J. (1991) Catalysis by cytochrome P450 of an oxidative reaction in xenobiotic aldehyde metabolism: Deformylation with olefin formation. *Proc. Natl. Acad. Sci.* **88**, 8963-8966.
- Rodriguez-Lopez, J.N., Smith, A.T., Thorneley, R.N.F. (1996) Role of arginine 38 in horseradish peroxidase. A critical residue for substrate binding and catalysis. *J. Biol. Chem.* **271**, 4023-4030.
- Rodriguez-Lopez, J.N., Smith, A.T., Thorneley, R.N.F. (1996) Recombinant horseradish peroxidase isoenzyme C: the effect of distal haem cavity mutations (His42-Leu and Arg38-Leu) on compound I formation and substrate binding. *J. Biol. Inorg. Chem.* **1**, 136-142.
- Rodriguez-Lopez, J.N., Smith, A.T., Thorneley, R.N.F. (1997) Effect of distal cavity mutations on the binding and activation of oxygen by ferrous horseradish peroxidase. *J. Biol. Chem.* **272**, 389-395.
- Roepstorff, P., Fohlman, J. (1984) Proposal for a common nomenclature for sequence ions in mass spectra of peptides. *Mass. Spectrom.* **11**, 601.
- Ross, D., Larsson, R., Norbeck, K., Ryhage, R., Moldéus, P. (1985) Characterization and mechanism of formation of reactive products formed during peroxidase-catalyzed oxidation of p-phenetidine. Trapping of reactive species by reduced glutathione and butylated hydroxyanisole. *Molec. Pharmacol.* **27**, 277-286.
- Rusvai, E., Vegh, M., Kramer, M., Horvath, I. (1988) Hydroxylation of aniline mediated by heme-bound oxy-radicals in a heme peptide model system. *Biochem. Pharmacol.* **37**, 4574-4577.
- Rutter, R., Valentine, M., Hendrich, M.P., Hager, L.P., Debrunner, P.G. (1983) Chemical nature of the porphyrin π cation radical in horseradish peroxidase Compound I. *Biochemistry* **22**, 4769-4774.

S

- Sakurada, J., Sekiguchi, R., Sato, K., Hosoya, T. (1990) Kinetic and molecular orbital studies on the rate of oxidation of monosubstituted phenol and anilines by horseradish peroxidase Compound-II. *Biochemistry* **29**, 4093-4098.
- Santucci, R., Picciau, A., Antonini, G., Campanella, L. (1995) A complex of microperoxidase with a synthetic peptide: structural and functional characterisation. *Biochim. Biophys. Acta* **1250**, 183-188.
- Savenkova, M.I., Newmyer, S.L., Ortiz de Montellano, P.R. (1996) Rescue of His42-Ala horseradish peroxidase by a Phe41-His mutation. Engineering of a surrogate catalytic histidine. *J. Biol. Chem.* **271**, 24598-24603.
- Savenkova, M.I., Kuo, J.M., Ortiz de Montellano, P.R. (1998) Improvement of peroxygenase activity by relocation of a catalytic histidine within the active site of horseradish peroxidase. *Biochemistry* **37**, 10828-10836.
- Schünemann, V., Jung, C., Trautwein, A.X., Mandon, D., Weiss, R. (2000) Intermediates in the reaction of substrate-free cytochrome P450_{cam} with peroxy acetic acid. *FEBS Lett.* **179**, 149-154.
- Shokhirev, N.V., Ann Walker, F. (1998) The effect of axial ligand plane orientation on the contact and pseudocontact shifts of low-spin ferriheme proteins. *J. Biol. Inorg. Chem.* **3**, 581-594.

- Shulman, R.G., Glarum, S.H., Karplus, M. (1971) Electronic structure of cyanide complexes of hemes and heme proteins. *J. Mol. Biol.* **57**, 93-115.
- Sligar, S.G., Lipscomb, J.D., Debrunner, J.D., Gunsalus, I.C. (1974) Superoxide anion production by the autoxidation of cytochrome P450_{cam}. *Biochem. Biophys. Res. Commun.* **61**, 290-296.
- Sligar, S.G. (1976) Coupling of spin, substrate, and redox equilibria in cytochrome P450. *Biochemistry* **15**, 5399-5406.
- Sligar, S.G., Filipovic, D., Stayton, P.S. (1991) Mutagenesis of cytochrome P450_{cam} and b5. *Methods Enzymol.* **206**, 31-49.
- Smith, A.T., Veitch, N. (1998) Substrate binding and catalysis in heme peroxidases. *Curr. Op. Chem. Biol.* **2**, 269-278.
- Smith, K.M. (1975) *Porphyrins and Metalloporphyrins*. K.M. Smith (Eds), Elsevier, New-York, pp24.
- Song, W.C., Brash, A.R. (1991) Purification of an allene oxide synthase and identification of the enzyme as cytochrome P450. *Science* **253**, 781-784.
- Sono, M., Roach, M.P., Coulter, E.D., Dawson, J.H. (1996) Heme-containing oxygenases. *Chem. Rev.* **96**, 2841-2887
- Sorokin, A., Meunier, B. (1994) Efficient H₂O₂ oxidation of chlorinated phenols catalysed by supported phthalocyanins. *J. Chem. Soc. Commun.*, 1799-1800.
- Spee, J.H., Boersma, M.G., Veeger, C., Samyn, B., van Beeumen, J., Warmerdam, G., Canters, G.W., van Dongen, W.M.A.M., Rietjens, I.M.C.M. (1996) The influence of the peptide chain on the kinetics and stability of microperoxidases. *Eur. J. Biochem.* **241**, 215-220.
- Stoll, V.C., Blanchard, J.S. (1990) Buffers: Principles and practice. *Methods Enzymol.* **182**, 24-38.
- Su, C., Sahlin, M., Oliw, E.H. (1998) A protein radical and ferryl intermediates are generated by linoleate diol synthase, a ferric hemeprotein with dioxygenase and hydroperoxide isomerase activities. *J. Biol. Chem.* **273**, 20744-20751.
- Sugiyama, K., Highet, R.J., Woods, A., Cotter, R.J., Osawa, Y. (1997) Hydrogen peroxide-mediated alteration of the heme prosthetic group of metmyoglobin to an iron chlorin product: Evidence for a novel oxidative pathway. *Proc. Natl. Acad. Sci. USA* **94**, 796-801.
- Sundaramoorthy, M., Terner, J., Poulos, T.L. (1995) The crystal structure of chloroperoxidase: a heme peroxidase-cytochrome P450 functional hybrid. *Structure* **3**, 1367-1377.
- Swinney, D.C., Mak, A.Y. (1994) Androgen formation by cytochrome P450 CYP17. Solvent isotope effect and pL studies suggest a role for protons in the regulation of oxene versus peroxide chemistry. *Biochemistry* **33**, 2185-2190.

T

- Takahashi, S., Wang, J., Rousseau, D.L., Ishikawa, K., Yoshida, T., Host, J.R., Ikeda-Saito, M. (1994) Heme-heme oxygenase complex. Structure of the catalytic site and its implication for oxygen activation. *J. Biol. Chem.* **269**, 1010-1014.
- Tanaka, M., Ishimori, K., Mukai, M., Kitagawa, T. Morishima, I. (1997) Catalytic activities and structural properties of horseradish peroxidase distal His42-Glu or Gln mutant. *Biochemistry* **36**, 9889-9898.

- Taniguchi, V.T., Ellis, W.R.Jr., Cammarata, V., Webb, J. Anson, F.C., Gray, H.B. (1982) *Adv. Chem. Ser.* **201**, 51-68.
- Thanabal, V., La Mar, G.N., de Ropp, J.S. (1988) A nuclear overhauser effect study of the heme crevice in the resting state and compound I of horseradish peroxidase: Evidence for cation radical delocalization to the proximal histidine. *Biochemistry* **27**, 5400-5407.
- Thomas, J.A., Morris, D.R., Hager, L.P. (1970) Chloroperoxidase. VIII. Formation of peroxide and halide complexes and their relation to the mechanism of the halogenation reaction. *J. Biol. Chem.* **245**, 3135-3142.
- Tian, Z.-Q., Richards, J.L., Traylor, T.G. (1995) Formation of both primary and secondary N-alkylhemins during heme-catalyzed epoxidation of terminal alkenes. *J. Am. Chem. Soc.* **117**, 21-29.
- Torpey, J., Ortiz de Montellano, P.R. (1996) Oxidation of the *meso*-methylmesoheme regioisomers by heme oxygenase. Electronic control of the reaction regioselectivity. *J. Biol. Chem.* **271**, 26067-26073.
- Torpey, J., Ortiz de Montellano, P.R. (1997) Oxidation of α -*meso*-formylmesoheme by heme oxygenase. Electronic control of the reaction regioselectivity. *J. Biol. Chem.* **272**, 22008-22014.
- Traylor, T.G. (1991) Kinetics and mechanism studies in biomimetic chemistry: Metalloenzyme model systems. *Pure & Appl. Chem.* **63**, 265-274.
- Tsou, C.L. (1951) Cytochrome c modified by digestion with proteolytic enzymes. 1: Digestion. *Biochem. J.* **49**, 362-367.
- Tsou, C.L. (1951) Cytochrome c modified by digestion with proteolytic enzymes. 2: Properties of pepsin-modified cytochrome c. *Biochem. J.* **49**, 367-374.
- Turner, D.L. (1995) Determination of haem electronic structure in His-Met cytochrome c by ^{13}C -NMR. The effect of the axial ligands. *Eur. J. Biochem.* **227**, 829-837.

U

- Ueyama, N., Nishikawa, N., Yamada, Y., Okamura, T., Nakamura, A. (1996) Cytochrome P450 model (porphinato)(thiolato)iron(III) complexes with single and double $\text{NH}\cdots\text{S}$ hydrogen bonds at the thiolate site. *J. Am. Chem. Soc.* **118**, 12826-12827.
- Urano, Y., Higuchi, T., Hirobe, M., Nagano, T. (1997) Pronounced axial thiolate ligand effect on the reactivity of high-valent oxo-iron porphyrin intermediate. *J. Am. Chem. Soc.* **119**, 12008-12009.

V

- VanAtta, R.B., Strouse, C.E., Hanson, L.K., Valentine, J.S. (1987) [Peroxotetraphenylporphinato]manganese(III) and [Chlorotetraphenylporphinato]manganese(II) anions. Syntheses, crystal structures, and electronic structures. *J. Am. Chem. Soc.* **109**, 1425-1434.
- Vaz, A.D.N., Roberts, E.S., Coon, M.J. (1991) Olefin formation in oxidative deformylation of aldehydes by cytochrome P450: Mechanistic implications for catalysis by oxygen-derived peroxide. *J. Am. Chem. Soc.* **113**, 5886-5887.

- Vaz, A.D.N., Kessel, K.S., Coon, M.J. (1994) Aromatization of a bicyclic analog 3-oxodecalin-4ene-10carboxaldehyde by liver cytochrome P450 2B4. *Biochemistry* **33**, 13651-13661.
- Vaz, A.D.N., Pernecky, S.J., Raner, G.M., Coon, M.J. (1996) Peroxo-iron and oxenoid-iron species as alternative oxygenating agents in cytochrome P450-catalyzed reaction: Swiching by Threonine-302 to Alanine mutagenesis of cytochrome P450 2B4. *Proc. Natl. Acad. Sci. USA* **93**, 4644-4648.
- Vaz, A.D.N., McGinnity, D.F., Coon, M.J. (1998) Epoxidation of olefins by cytochrome P450: Evidence from site-specific mutagenesis for hydroperoxo-iron as an electrophilic oxidant. *Proc. Natl. Acad. Sci. USA* **95**, 3555-3560.
- Veeger, C., Rietjens, I.M.C.M., van Dongen, W., Canters, G.W. (1995) Development of a new generation of heme-based mini-enzymes for cytochrome P450- and peroxidase-type of conversions. *Projectvoorstel SON-ronde Stichting Technische Wetenschappen (SON-STW)*.
- Volz, H., Holzbecher, M. (1997) A bridged porphyrinato(thiolato)iron(III) complex as a model of the active center of the cytochrome P450 isozyme. *Angew. Chem. Int. Ed. Engl.* **36**, 1442-1445.

W

- Wagenknecht, H.-A., Woggon, W.-D. (1997) New active-site analogs of chloroperoxidase -syntheses and catalytic reactions. *Angew. Chem. Int. Ed. Engl.* **36**, 390-392.
- Wang, J.S., van Wart, H.E. (1989) Resonance Raman Characterization of the heme c group in N-acetyl microperoxidase-8: A thermal intermediate spin-high spin state mixture *J. Phys. Chem.* **93**, 7925-7931.
- Wang, J.S., Baek, H.K., van Wart, H.E. (1991) High-valent intermediates in the reaction of N^α-acetyl microperoxidase-8 with hydrogen peroxide: models for compounds O, I and II of horse radish peroxidase. *Biochem. Biophys. Res. Commun.* **179**, 1320-1324.
- Wang, J.S., Tsai, A.-L., Heldt, J., Palmer, G., van Wart, H.E. (1992) Temperature- and pH-dependent changes in the coordination sphere of the heme c group in the model peroxidase N^α-acetyl microperoxidase-8. *J. Biol. Chem.* **267**, 15310-15318.
- Waterman, M.R., Yonetani, T. (1970) Studies on modified hemoglobins. I. Properties of hybrid hemoglobins containing manganese protoporphyrin IX. *J. Biol. Chem.* **245**, 5847-5852.
- Weiss, R., Mandon, D., Wolter, T., Trautwein, A.X., Mütter, M., Bill, E., Gold, A., Jayaraj, K., Terner, J. (1996) Delocalisation over the heme and the axial ligands of one of the two oxidising equivalents stored above the ferric state in the peroxidase and catalase Compound-I intermediates: indirect participation of the proximal axial ligand of iron in the oxidation reactions catalysed by heme-based peroxidases and catalases ? *J. Biol. Inorg. Chem.* **1**, 377-383.
- Weiss, R., Gold, A., Trautwein, A.X., Terner, J. (2000) *The Porphyrin Handbook*, K.M. Kadish, K.M. Smith, R. Guilard (Eds), Academic Press, Volume 4/Biochemistry and Binding: Activation of Small Molecules, pp 63-95.
- White, R.E., McCarthy, M.B. (1984) Aliphatic hydroxylation by cytochrome P450. Evidence for rapid hydrolysis of an intermediate iron-nitrene complex. *J. Am. Chem. Soc.* **106**, 4922-4926.
- Wilks, A., Ortiz de Montellano, P.R. (1993) Rat liver heme oxygenase: High level expression of truncated soluble form and nature of the *meso*-hydroxylating species. *J. Biol. Chem.* **268**, 22357-22362.

- Wilks, A., Torpey, J., Ortiz de Montellano, P.R. (1994) Heme oxygenase (HO-1). Evidence for electrophilic oxygen addition to the porphyrin ring in the formation of α -meso-hydroxyheme. *J. Biol. Chem.* **269**, 29553-29556.
- Wiseman, J.S., Nichols, J.S., Kolpak, M.X. (1982) Mechanism of inhibition of horseradish peroxidase by cyclopropanone hydrate. *J. Biol. Chem.* **257**, 6328-6332.

XY

- Yamada, H., Makino, R., Yamazaki, I. (1975) Effects of 2,4-substituents of deuteropheme upon redox potentials of horseradish peroxidase. *Arch. Biochim. Biophys.* **169**, 344-353.
- Yamaguchi, K., Watanabe, Y., Morishima, I. (1993) Direct observation of the push effect on the O-O bond cleavage of acylperoxoiron(III) porphyrin complexes. *J. Am. Chem. Soc.* **115**, 4058-4065.
- Yamazaki, I., Tamura, M., Nakajima, R. (1981) Horseradish peroxidase c. *Mol. Cell. Biochem.* **40**, 143-153.
- Yang, S.J., Nam, W. (1998) Water-soluble iron porphyrin complex-catalysed epoxidation of olefins with hydrogen peroxide and *tert*-butyl hydroperoxide in aqueous solution. *Inorg. Chem.* **37**, 606-607.
- Yonetani, T. (1965) Studies on cytochrome c peroxidase. II. Stoichiometry between enzyme, H₂O₂, and ferrocytochrome c and enzymic determination of extinction coefficients of cytochrome c. *J. Biol. Chem.* **240**, 4509-4514.
- Yonetani, T., Asakura, T. (1969) Studies on cytochrome c peroxidase. XV: Comparison of manganese porphyrin-containing cytochrome c peroxidase, horseradish peroxidase, and myoglobin. *J. Biol. Chem.* **244**, 4580-4588.
- Yonetani, T. (1970) Electromagnetic properties of hemoproteins. III. Electron paramagnetic resonance characteristics of iron (III) and manganese (II) protoporphyrins IX and their apohemoprotein complexes in high spin states. *J. Biol. Chem.* **245**, 2998-3003.
- Yonetani, T. (1976) *The Enzymes*. P.D. Boyer (Ed), Academic Press, volume 13/Oxidation-Reduction, Part C Dehydrogenases (II), Oxidases(II), Hydrogen Peroxide Cleavage, pp 345-361.

Z

- Zakharieva, O., Grodzicki, M., Trautwein, A.X., Veeger, C., Rietjens, I.M.C.M. (1996) Molecular orbital study of the hydroxylation of benzene and monofluorobenzene catalysed by iron-oxo porphyrin π cation radical complexes. *J. Biol. Inorg. Chem.* **1**, 192-204.
- Zakharieva, O., Trautwein, A.X., Veeger, C. (2000) Porphyrin-Fe(III)-hydroperoxide and porphyrin-Fe(III)-peroxide anion as catalytic intermediates in cytochrome P450-catalysed hydroxylation reactions; a molecular orbital study. *Biophys. Chem.* **88**, 11-34.
- Zipplies, M.F., Lee, W.A., Bruce, T.C. (1986) Influence of hydrogen ion activity and general acid-base catalysis on the rate of decomposition of hydrogen peroxide by a novel nonaggregating water-soluble iron(III) tetraphenylporphyrin derivative. *J. Am. Chem. Soc.* **108**, 4433-4445.

List of publications

- van Haandel, M.J.H., Primus, J.-L., Teunis, C., Boersma, M.G., Osman, A.M., Veeger, C., Rietjens, I.M.C.M. (1998) Reversible formation of high-valent-iron-oxo porphyrin intermediates in heme-based catalysis: Revisiting the kinetic model for horseradish peroxidase. *Inorg. Chim. Acta* **275-276**, 98-105.
- Primus, J.-L., Boersma, M.G., Mandon, D., Boeren, S., Veeger, C., Weiss, R., Rietjens, I.M.C.M. (1999) The effect of iron to manganese substitution on microperoxidase-8 catalysed peroxidase and cytochrome P450 type of catalysis. *J. Biol. Inorg. Chem.* **3**, 274-283.
- Primus, J.-L., Teunis, C., Mandon, D., Veeger, C., Rietjens, I.M.C.M. (2000) A mechanism for oxygen exchange between ligated oxometalloporphyrins and bulk water. *Biochem. Biophys. Res. Comm.* **272**, 551-556.
- Boersma, M.G., Primus, J.-L., Koerts, J., Rietjens, I.M.C.M., Veeger, C. (2000) Heme-(hydro)peroxide catalysed O- and N-dealkylation; A study with microperoxidase. *Eur. J. Biochem.* **267**, 6673-6678.
- Primus, J.-L., Boeren, S., Banci, L., Vervoort, J., Rietjens, I.M.C.M. Isolation and characterisation of microperoxidase-8 with a modified histidine axial ligand: Implications for the nature of activated the heme-oxo intermediates. *Submitted*.
- Primus, J.-L., Grünenwald, S., Hagedoorn, P.-L., Albrecht-Gary, A.-M., Mandon, D., Veeger, C., Rietjens, I.M.C.M. The nature of the intermediates in the reactions of Fe(III)- and Mn(III)-microperoxidases with H₂O₂; A rapid kinetics study. *Submitted*.

Acknowledgements

This book would not exist without the help and the contribution of many people I wish to acknowledge here.

Raymond Weiss is acknowledged for his support since my pre-doctoral year and for being one of my promotor. Raymond, your curiosity and accuracy in science were an important milestone in my scientific education. I thank you for having supported me in applying for this PhD project.

I am grateful to Cees Veeger for proposing me this PhD project, being one of my promotor and supporting me. Cees, your input during the final phase of my PhD thesis was of great help. I must say that your enthusiasm in dealing with kinetics is communicative.

I would like to thank Ivonne Rietjens for her daily supervision and being one of my promotor. Ivonne, you always were in state to propose clever and efficient solutions. Thank you for the freedom you gave me and the trust you have put in me.

I also would like to thank Colja Laane, head of the Department of Biochemie, during the last four years.

My PhD project was shared between laboratories in Strasbourg and Wageningen which made me meeting two different worlds. My thanks go to Dominique Mandon in Strasbourg. You learned me a lot concerning good laboratory practice in inorganic chemistry. The Chapter 7 of this book would not exist without your initial input and the hospitality of Anne-Marie Albrecht-Gary in Strasbourg. There, I have appreciated the heavy laboratory work and kinetic considerations with Sylvie Grünenwald and the good atmosphere with the people during the day and sometimes the evening. My acknowledgements also goes to Fred Hagen and to Peter-Leon Hagedoorn in Delft for exciting measurements at the EPR spectrometer.

Chapter 6 is the result of a collaboration with Lucia Banci from Florence. She has introduced me to the world of paramagnetic NMR. Everybody on the third floor of Biochemistry, connect Jacques to the NMR. I would like to thank him for his continuous interest on the Chapter 6 of my thesis, constantly suggesting new ideas and also performing measurements. Sjef is unavoidable for what concerns HPLC and MS. Besides crucial experiments he learned me chromatography. Staying in the field of MS, Kees Teunis is also unavoidable. He was always willing to perform new measurements for Chapter 2 and 3. Chapter 4 would not be part of this book without the active involvement of Janneke and Marelle and I am really grateful to them. Marelle has helped a lot in measuring but also in introducing me to the underwater world of scuba-diving. I do not forget my roommates, Marjon, Lars, Hanem and Kees-Jan for the excellent atmosphere and among other the discussions in Dutch... My labmates of lab 10 Harrold, Henno and Marco, for the very cool working spirit. Rein, my student, is acknowledged for the very intense and fruitful (scientific) exchanges we had. I also would like to thank our different visitors and foreign fellows at the Laboratory of Biochemistry in Wageningen. Tatiana, Ahmed, Žilvinas, Kasia and Rigo. You made me travel the world without leaving my office. I have learned a lot from you. At last, I would like to thank all other people from Biochemistry and particularly the AIO's for the dinners and week-ends and also Laura the secretary.

My thanks also go to the people from the lab in Strasbourg, the X-Rays team, Nathalie, André De Cian and Jean Fischer, Marie-André Woehrlé the secretary and the former chemists, Sylvain and Hugo for the many discussions we had.

I would like to thank my mother for leaving me free of choosing my own path whatever she has experienced in her personal life. To my father, I guess he would be proud of his son today ! Also to friends and family, thanks for their support. Anne-Sophie you were on the first row during these four and a half years. Your love and support have filled my life everyday. Well, it is now achieved, the second Doctor of our little family just got his title ! But let us not forget the essential.

Jean-Louis

Curriculum Vitae

Jean-Louis Primus was born on 6 April 1971 in Colmar (France). Early attracted by science, he began turning his interest into reality in 1989 when he obtained his high school diploma in Mathematics and Physics. He studied general aspects of Biology, Physics and Chemistry for two years at the Université Louis Pasteur in Strasbourg (France) before entering the Magistère of Chemical-Biology at the Université Louis Pasteur of Strasbourg (France) in 1993. He graduated both in Chemical-Biology and in Chemistry of the Transition Metal Series and Molecular Engineering in 1995. The practical part of his Master degree was obtained at the Laboratory of Cristallogenesis and Structural Chemistry under the supervision of prof. dr. R. Weiss. From February 1996 till September 2000, he carried out his European PhD study, which research was shared between the Laboratory of Cristallogenesis and Structural Chemistry of the University Louis Pasteur in Strasbourg, and the Department of Biochemistry of the Wageningen University in Wageningen (The Netherlands). Since november 1999, he has become a member of the first promotion of the European Doctorate College of Strasbourg. The research part of his PhD project was performed under the supervision of prof. dr. R. Weiss, prof. dr. C. Veeger and prof. dr. I.M.C.M. Rietjens and financed by the Dutch Organisation for Scientific Research (NWO).